



Advances in
Molecular Toxicology

Volume 5



VOLUME FIVE

ADVANCES IN MOLECULAR TOXICOLOGY

This page intentionally left blank

VOLUME FIVE

ADVANCES IN MOLECULAR TOXICOLOGY

Editor

JAMES C. FISHBEIN

Department of Chemistry and Biochemistry
University of Maryland, Baltimore County
Baltimore, Maryland, USA



ELSEVIER

AMSTERDAM • BOSTON • HEIDELBERG • LONDON
NEW YORK • OXFORD • PARIS • SAN DIEGO
SAN FRANCISCO • SINGAPORE • SYDNEY • TOKYO

Elsevier

Linacre House, Jordan Hill, Oxford OX2 8DP, UK

Radarweg 29, PO Box 211, 1000 AE Amsterdam, The Netherlands

First edition 2011

Copyright © 2011 Elsevier B.V. All rights reserved

No part of this publication may be reproduced, stored in a retrieval system, or transmitted in any form or by any means, electronic, mechanical, photocopying, recording, or otherwise, without the prior written permission of the publisher.

Permissions may be sought directly from Elsevier's Science & Technology Rights Department in Oxford, UK: phone (+44) (0) 1865 843830; fax (+44) (0) 1865 853333; email: permissions@elsevier.com. Alternatively you can submit your request online by visiting the Elsevier web site at <http://elsevier.com/locate/permissions>, and selecting *Obtaining permission to use Elsevier material*

Notice

No responsibility is assumed by the publisher for any injury and/or damage to persons or property as a matter of products liability, negligence or otherwise, or from any use or operation of any methods, products, instructions or ideas contained in the material herein. Because of rapid advances in the medical sciences, in particular, independent verification of diagnoses and drug dosages should be made.

British Library Cataloguing-in-Publication Data

A catalogue record for this book is available from the British Library

Library of Congress Cataloging-in-Publication Data

A catalog record for this book is available from the Library of Congress

ISBN: 978-0-444-53864-2

ISSN: 1872-0854

For information on all Elsevier publications visit our website at www.elsevierdirect.com

This book has been manufactured using Print On Demand technology. Each copy is produced to order and is limited to black ink. The online version of this book will show color figures where appropriate.

11 12 13 14 10 9 8 7 6 5 4 3 2 1

Working together to grow
libraries in developing countries

www.elsevier.com | www.bookaid.org | www.sabrc.org

ELSEVIER

BOOK AID
International

Sabre Foundation

CONTENTS

<i>Contributors</i>	<i>ix</i>
<i>Preface</i>	<i>xi</i>
1. Metal-Independent Pathways of Chlorinated Phenol/Quinone Toxicity	1
Ben-Zhan Zhu, Jun-Ge Zhu, Rui-Mei Fan, and Li Mao	
1. Introduction	2
2. Pentachlorophenol	6
3. Mechanism of Protection by the “Specific” Iron-Chelating Agent Desferrioxamine Against TCHQ-Induced DNA Damage	13
4. Molecular Mechanism of PCP Quinoid Metabolite-Induced Genotoxicity	17
5. Detoxifying Carcinogenic Polyhalogenated Quinones by Hydroxamic Acids via an Unusually Mild and Facile Double Lossen Rearrangement Mechanism	31
6. Conclusions and Future Research	36
Acknowledgments	37
References	37
2. The Use of Proteomics in the Study of Molecular Responses and Toxicity Pathways in Biological Systems	45
Gian Paolo Rossini, Gian Luca Sala, Giuseppe Ronzitti, and Mirella Bellocchi	
1. Introduction	46
2. Proteomics in the Study of Biological Systems Exposed to Toxins	47
3. From Receptor-Driven to Response-Driven Investigations into the Mechanisms of Action of Algal Toxins	51
4. Proteomic Studies Aimed at the Characterization of Modes of Action of Algal Toxins	55
5. Proteomic Analyses for Predictive Toxicology and the Detection of Algal Toxin Contaminations	75
6. Preliminary Considerations on Strengths and Weaknesses of Proteomic Approaches in Investigations onto Toxicity Pathways	81
7. Conclusions and Perspectives	97
Acknowledgments	98
References	98

3. The Molecular Toxicology of Chemical Warfare Nerve Agents	111
Kimberly D. Spradling and James F. Dillman III	
1. Introduction	112
2. Nerve Agent Toxicity	114
3. Current Medical Countermeasures to Nerve Agent Toxicity	116
4. Global Molecular Screening Approaches Enable the Identification of Molecular Mechanisms of Toxicant Exposure	117
5. Global Molecular Techniques Support the Three-Phase Model of Nerve Agent Toxicity	121
6. Global Molecular Techniques Provide Evidence for Non-AChE Mechanisms of OP Nerve Agent Toxicity and Reveal Secondary Effects of Exposure	123
7. Future Directions in the Molecular Toxicology of Nerve Agents	134
8. Conclusions	135
Acknowledgments	138
References	138
4. Toxicity of Metal Oxides Nanoparticles	145
Masanori Horie and Katsuhide Fujita	
1. Introduction	146
2. Oxidative Stress	147
3. Apoptosis	152
4. Inflammation Response	153
5. Long-Term Effects	154
6. Biological Effect Factors Due to Metal Oxide Nanoparticles	155
7. Methods of Evaluating Biological Effects of Metal Oxide Nanoparticles	162
8. Gene Expression Profiling for Evaluating the Biologic Effects of Manufactured Nanomaterials	165
9. Summary	169
References	171
5. Toxicity of Silver Nanomaterials in Higher Eukaryotes	179
Marcin Kruszewski, Kamil Brzoska, Gunnar Brunborg, Nana Asare, Małgorzata Dobrzyńska, Mária Dušinská, Lise M. Fjellsbø, Anastasia Georgantzopoulou, Joanna Gromadzka-Ostrowska, Arno C. Gutleb, Anna Lankoff, Zuzana Magdolenová, Elise R. Pran, Alessandra Rinna, Christine Instanes, Wiggo J. Sandberg, Per Schwarze, Tomasz Stępkowski, Maria Wojewódzka, and Magne Refsnes	
1. Introduction	180
2. Cellular Uptake	181
3. Toxicity of AgNPs	184

4. Inflammatory Response	205
5. The Role of Oxidative Stress in AgNP-Induced Toxicity and DNA Damage	206
6. Summary	211
Acknowledgments	212
References	212
6. Carboxymethylation of DNA Induced by <i>N</i>-Nitroso Compounds and Its Biological Implications	219
Jianshuang Wang and Yinsheng Wang	
1. Introduction	220
2. The Chemistry of DNA Carboxymethylation	221
3. Detection of Carboxymethylated DNA Adducts	227
4. Chemical Synthesis of Carboxymethylated Nucleosides and Their Incorporation into DNA	230
5. Biological Implications	236
References	239
Subject Index	245

This page intentionally left blank

CONTRIBUTORS

Nana Asare	179
Mirella Bellocci	45
Gunnar Brunborg	179
Kamil Brzoska	179
James F. Dillman III	111
Małgorzata Dobrzyńska	179
Mária Dušinská	179
Lise M. Fjellsbø	179
Katsuhide Fujita	145
Anastasia Georgantzopoulou	179
Jun-Ge Zhu	1
Joanna Gromadzka-Ostrowska	179
Arno C. Gutleb	179
Masanori Horie	145
Christine Instanes	179
Marcin Kruszewski	179
Anna Lankoff	179
Zuzana Magdolenová	179
Li Mao	1
Rui-Mei Fan	1
Elise R. Pran	179
Magne Refsnes	179
Alessandra Rinna	179
Giuseppe Ronzitti	45
Gian Paolo Rossini	45
Gian Luca Sala	45
Wiggo J. Sandberg	179
Per Schwarze	179
Kimberly D. Spradling	111
Tomasz Stępkowski	179
Jianshuang Wang	219
Yinsheng Wang	219
Maria Wojewódzka	179
Ben-Zhan Zhu	1

This page intentionally left blank

PREFACE

This fifth volume continues the tradition of showcasing the rich diversity of topics and approaches to understanding toxicity at a truly molecular level, bearing in mind the diverse interpretations of the term “molecular.”

Polychlorinated phenols have been widely employed industrially as wood preservatives and pesticides. Though they are now banned in many countries, they are highly persistent in the human environment. Recent work has unveiled novel mechanisms of toxicity, and this is the focus of Chapter 1 by Zhu and Mao.

“Omics” approaches to characterize and understand cellular responses to toxins have found increasing application. Human exposure to algal toxins occurs through recreation, the potable water supply, and consumption of fish and shellfish. Characterization of the proteomic responses to various algal toxins elucidates mechanism and biomarkers of exposure. Rossini and colleagues document recent advances in this area in Chapter 2. Complementarily, in Chapter 3, Spradling and Dillman outline the elaborate systemic response, beyond the immediate effects of cholinesterase blockage, that is effected by organophosphate chemical warfare agents. Here, an array of “omics” approaches has been brought to bear on the manifestations of exposure.

Genomic profiling has also been applied to the toxicology of nanomaterials and this is discussed by Horie and Fujita in Chapter 4 in the case of metal oxide nanomaterials. Varied responses to a spectrum of agents have been characterized, and this has begun to allow sorting out of various properties that manifest toxic responses and prospective biomarkers of nanoparticle toxicity.

Nanoparticles of silver are among those that have found widest application on the basis of their antibacterial properties. But the toxicology of silver nanomaterials is relatively sparse. The number of variables between types of such materials that contribute to toxicity are also not well documented. Kruszewski and colleagues survey the status of this rapidly evolving field in Chapter 5.

In Chapter 6, Wang and Wang explore the chemistry and biochemical consequences of DNA carboxymethylation. This modification is the product of a variety of agents, particularly *N*-nitroso compounds, a class of compounds that is a favorite of the editor. Sources, lesion variety, biochemical and mutagenic consequences, as well as analytical methodologies are reviewed.

It is hoped that the reader will enjoy these timely and varied contributions.

This page intentionally left blank

METAL-INDEPENDENT PATHWAYS OF CHLORINATED PHENOL/QUINONE TOXICITY

Ben-Zhan Zhu,* Jun-Ge Zhu, Rui-Mei Fan, and Li Mao

Contents

1. Introduction	2
1.1. Chlorinated phenols	2
1.2. Carcinogenesis of chlorinated phenols	5
2. Pentachlorophenol	6
2.1. PCP and its major carcinogenic quinoid metabolites	6
2.2. Molecular mechanisms of PCP quinoid metabolite-induced DNA damage	9
2.3. The pro-oxidant versus antioxidant equilibrium	12
3. Mechanism of Protection by the “Specific” Iron-Chelating Agent Desferrioxamine Against TCHQ-Induced DNA Damage	13
3.1. The protection by desferrioxamine against TCHQ-induced DNA damage was not due to its classic iron-chelating property, but rather to its scavenging of the reactive TCSQ •	13
3.2. Protection by DFO against TCHQ-induced cyto- and genotoxicity in human fibroblasts	16
4. Molecular Mechanism of PCP Quinoid Metabolite-Induced Genotoxicity	17
4.1. Metal-independent production of •OH by PCP quinoid metabolite and H ₂ O ₂	17
4.2. Molecular mechanism of metal-independent production of •OH by PCP quinoid metabolites and H ₂ O ₂	19
4.3. Metal-independent decomposition of organic hydroperoxides and formation of alkoxyl radicals by halogenated quinones	24
4.4. Detection and identification of a key quinone ketoxy radical intermediate	26

State Key Laboratory of Environmental Chemistry and Ecotoxicology, Research Center for Eco-Environmental Sciences, Chinese Academy of Sciences, Beijing, People's Republic of China

*Corresponding author. Tel.: +86-010-62849030; Fax: +86-010-62923563

E-mail address: bzhu@rcees.ac.cn

5. Detoxifying Carcinogenic Polyhalogenated Quinones by Hydroxamic Acids via an Unusually Mild and Facile Double Lossen Rearrangement Mechanism	31
6. Conclusions and Future Research	36
Acknowledgments	37
References	37

Abstract

Pentachlorophenol (PCP) was the most widely used chlorinated phenols, primarily for wood preservation. The genotoxicity of PCP has been attributed to its two major quinoid metabolites: tetrachlorohydroquinone and tetrachloro-1,4-benzoquinone (TCBQ). Although the redox cycling of PCP quinoid metabolites to generate reactive oxygen species is believed to play an important role, the exact molecular mechanism underlying PCP genotoxicity is not clear. Hydroxyl radical is one of the most highly reactive oxygen species produced in biological systems. Frequently, hydroxyl radical formation from hydrogen peroxide has been ascribed to the transition metal-catalyzed Fenton reaction. We found, however, that $\cdot\text{OH}$ can be produced by PCP quinoid metabolite TCBQ and H_2O_2 , but it is not dependent on the presence of either transition metal ions or its corresponding semiquinone radical. We propose that $\cdot\text{OH}$ production by TCBQ and H_2O_2 is through a novel nucleophilic substitution coupled with homolytical decomposition pathway, which may partly explain the potential genotoxicity of PCP and other widely used polyhalogenated aromatic biocides.

1. INTRODUCTION

1.1. Chlorinated phenols

Chlorinated phenols constitute a series of 19 compounds composed of mono-, di-, tri-, and tetrachloroisomers and one pentachlorophenol (PCP). Although all of the possible structural isomers are available commercially, only four polychlorinated phenols (2,4-dichloro-, 2,4,5-trichloro-, 2,4,6-trichloro-, and PCP) have been of major industrial significance (Figure 1), primarily

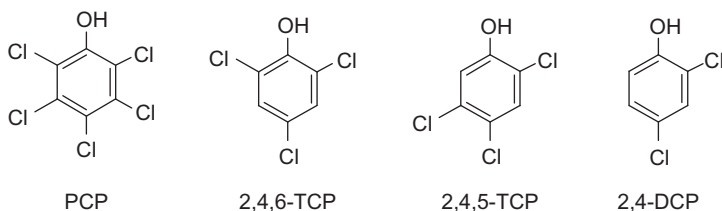


Figure 1 Chemical structures of the four representative chlorinated phenols.

as pesticides and as intermediates in the synthesis of the widely used chlorophenoxy herbicides such as 2,4-dichlorophenoxyacetic acid (2,4-D) and 2,4,5-trichlorophenoxyacetic acid (2,4,5-T), the two major components of Agent Orange (1–7). The annual worldwide production of chlorinated phenols has been estimated to be about 200,000 tons, while PCP represents about 90,000 tons of that [1,2].

Chlorinated phenols have found wide use in pesticides, disinfectants, wood preservatives, personal care formulations, and many other products. Residues of chlorinated phenols have been found worldwide in soil, water, and air samples; food products; and human and animal tissues and body fluids. Environmental contamination with these chemicals occurs from industrial effluents, agricultural runoff, breakdown of chlorophenoxyacetic acid herbicides, and hexachlorobenzene, and also from spontaneous formation following chlorination of water for disinfection and deodorization during wood pulp bleaching with chlorine [1–3]. Chlorinated phenols are poorly biodegradable with a half-life in aerobic waters that can exceed 3 months and can exceed some years in organic sediments. The existing guidelines set the permissible chlorinated phenol level (depending on Cl content) in surface water at 0.06–4.4 mg/L and the permissible concentration in drinking water at 10 µg/L [4].

However, growing knowledge about the toxicities and environmental fates of specific chlorinated phenols has caused governments to regulate these compounds. Chlorinated phenols have been found in at least 166 of the 1467 National Priorities List sites, and 5 of them are listed by the U.S. Environmental Protection Agency (EPA) as priority pollutants, including the four chlorinated phenols mentioned above and 2-chlorophenol (2-CP), which are present in the environment in significant quantities [5]. For example, chlorinated phenols were recently found to occur at relatively high concentrations in some Chinese waters. 2,4-DCP and 2,4,6-TCP were more frequently detected at higher concentrations in the rivers of North China compared with those of South China. High-concentration sites of 2,4-DCP and 2,4,6-TCP mainly occurred in the Yellow River watershed, while PCP contamination mainly occurred in the Yangtze River watershed. PCP was the most ubiquitous chlorinated phenols being detected in 85.4% of samples; 2,4-DCP and 2,4,6-TCP were detected in 51.3% and 54.4%, respectively [6]. Thus, the ubiquitous nature of these substances coupled with their carcinogenicity in animal models has raised public awareness of the potential health risks posed by these chlorinated phenols.

It is known that toxicity of simple chlorinated phenols depends on the number and position of chlorine substitutions [7]. Some chlorinated phenols, such as PCP, are regarded as classic examples of oxidative uncoupling agents due to their hydrophobic ($\log K_{ow} = 5.02$) and weakly acidic nature ($pK_a = 4.74$) [8]. PCP is still used to protect timber from fungal

rot and wood-boring insects. PCP concentrations in groundwater can be 3–23 mg/L in wood-treatment areas and concentrations in milligram per liter can be found near industrial discharges.

The toxicity and bioaccumulation of chlorinated phenols increase with the degree of chlorine substitution [7]. The pK_a values of chlorinated phenols decrease with the number of chlorine substitutions. *Ortho*-chlorinated phenols are more acidic than other isomers because of the large inductive effect of chlorine on the hydroxyl group in close proximity [9]. Increased chlorine substitution also increases the octanol–water partition coefficient (K_{ow}) [10], which is positively correlated to the bioaccumulation potential of chlorinated phenols [11]. Thus, PCP with the largest K_{ow} value is the most hydrophobic chlorinated phenol, which allows it to diffuse through cellular membranes. Highly chlorinated phenols undergo oxidation into the phenoxyl radicals readily at physiological pH because the oxidation step involves the concerted loss of an electron and a proton and these chlorinated phenols exist as the phenolate form under physiological conditions.

Despite being banned in many countries and having its use severely restricted in others, PCP remains an important pesticide from a toxicological perspective [12]. It is a stable and persistent compound. In humans, it is readily absorbed by ingestion and inhalation but is less well absorbed dermally. Assessment of the toxicity of PCP is confounded by the presence of contaminants known to cause effects identical to those attributed to PCP. However, severe exposure by any route may result in an acute and occasionally fatal illness that bears all the hallmarks of being mediated by uncoupling of oxidative phosphorylation. Tachycardia, tachypnea, sweating, altered consciousness, hyperthermia, convulsions, and early onset of marked rigor (if death occurs) are the most notable features. Pulmonary edema, intravascular hemolysis, pancreatitis, jaundice, and acute renal failure have been reported. There are no antidote and no adequate data available to support the use of repeat-dose oral cholestyramine, forced diuresis, or urine alkalinization as effective methods of enhancing PCP elimination in poisoned humans. Supportive care and vigorous management of hyperthermia should produce a satisfactory outcome. Chronic occupational exposure to PCP may produce a syndrome similar to acute systemic poisoning, together with conjunctivitis and irritation of the upper respiratory and oral mucosae. Long-term exposure has also been reported to result in chronic fatigue or neuropsychiatric features in combination with skin infections (including chloracne), chronic respiratory symptoms, neuralgic pains in the legs, and impaired fertility and hypothyroidism secondary to endocrine disruption [13]. In a cross-sectional study on former sawmill workers exposed to PCP in New Zealand, McLean *et al.* found that PCP exposure was associated with a number of physical and neuropsychological health effects that persisted long after exposure had ceased [14].

1.2. Carcinogenesis of chlorinated phenols

It has been suggested that there might be an association between chlorinated phenols and Hodgkin's disease, soft-tissue sarcoma, and acute leukemia [15]. Carcinogenicity of orally administered PCP has been tested in rats and mice. The purity of PCP has been considered as an important factor, since PCP is usually contaminated with chlorinated dibenzo-*p*-dioxins, some of which (2,3,7,8-tetrachlorodibenzo-*p*-dioxin, TCDD) are known animal carcinogens. Technical-grade PCP (90% pure) was tested in mice by The National Toxicology Program (NTP) [16]. Groups of male and female B6C3F1 mice were given diets containing 0, 100, or 200 parts per million (ppm) PCP. A significant increase over the male control incidence in tumors of the adrenal medulla and liver was found in PCP-treated males. Treated females displayed a significant increase over female controls with regard to the incidence of hemangiosarcomas of the spleen and liver. The occurrence of rare hemangiosarcomas was considered a carcinogenic response due to PCP exposure, although this study was limited because of the unusually low survival in the male control group [16]. Pure PCP (99% pure) was also tested by NTP for carcinogenicity in rats [17]. Groups of male and female F344 rats were given diets containing 0, 200, 400, or 600 ppm PCP for 105 days. Some evidence that purified PCP is carcinogenic to rats was detected in 2 years with malignant mesotheliomas and nasal squamous cell carcinomas being noted in some of the rats with high dose regimes that actually exceed the maximum tolerable dose. However, hepatocellular adenomas and carcinomas were not detected [17], which is different from the study with mice [16]. Overall, these choric animal bioassays suggested that the liver is a target organ for carcinogenesis in mice, but not in the rat. Based on the NTP data, a cancer potency factor of 0.12 mg/kg/day was calculated by the Integrated Risk Information Systems (IRIS) [18], which translates to an upper-bound unit risk level of 9×10^{-3} mg/kg/day for a cancer risk of 1 in 1000.

Cooper and Jones [19] reviewed currently available data to determine the extent to which recent studies assist in distinguishing the effect of PCP from that of its contaminants (e.g., dioxins and other chlorinated phenols). They performed a systematic review of published studies pertaining to cancer risk in relation to PCP exposure, focusing on results pertaining specifically to all cancer sites and specific hematopoietic cancers, and data pertaining to risks associated with other types of chlorinated phenols, dioxins, or furans. They found that the PCP studies presented considerable evidence pertaining to hematopoietic cancers, with strong associations seen in multiple studies, in different locations, and using different designs. There is little evidence of an association between these cancers and chlorinated phenols that contain fewer than four chlorines. The extension of a large cohort study of sawmill workers, with follow-up to 1995, provided

information about risks of relatively rare cancers (e.g., non-Hodgkin lymphoma, multiple myeloma), using a validated exposure assessment procedure that distinguishes between exposures to PCP and tetrachlorophenol. In contrast with dioxin, PCP exposure has not been associated with total cancer incidence or mortality. They concluded that the updated cohort study focusing on PCP provides increased statistical power and precision and demonstrates associations between hematopoietic cancer and PCP exposure not observed in earlier evaluations of this cohort. Contaminant confounding is an unlikely explanation for the risks seen with PCP exposure.

Since PCP was the most well-studied chlorinated phenol, therefore, PCP will be used as an example for further review. We will focus on a novel mechanism for metal-independent decomposition of hydroperoxides by PCP quinoid metabolites and production of hydroxyl/alkoxyl radicals, which has been suggested as a potential mechanism for PCP-induced carcinogenicity.



2. PENTACHLOROPHENOL

2.1. PCP and its major carcinogenic quinoid metabolites

PCP is a major industrial and agricultural biocide that has been used primarily as a wood preservative [20,21]. The annual production of PCP has been estimated to be about 46 million pounds in the United States. Because of its efficiency, broad spectrum, and low cost, PCP has also been used as algaecide, bactericide, fungicide, herbicide, insecticide, and molluscicide [20–23]. In the USA, ~97% of PCP was used as a wood preservative [20,21]. The majority of U.S. use of PCP has been to preserve wooden poles for power transmission lines and other utilities. In China and other developing countries, PCP has also been used to kill snails to prevent snail fever (*Schistosomiasis*). Its worldwide usage and relative stability make PCP a ubiquitous environmental pollutant [20–23]. In fact, PCP has been detected in body fluids, such as human urine, serum, and milk, and tissues of people who are not occupationally exposed to it [20–23]. Extensive studies of PCP concentrations in body fluids (plasma or urine) of nonoccupationally exposed individuals have found average PCP concentrations of 40 parts per billion (ppb) (range: 0–1840 ppb). In contrast, in blood of occupationally exposed workers, the median level of PCP was found to be as high as 19,580 ppb (range: 6000–45,200 ppb). Postmortem analysis of serum, tissue, and urine samples from individuals who died from PCP intoxication showed tissue PCP concentrations of 20–140 ppm and urine concentrations of 28–96 ppm. The most likely source of exposure is PCP-treated wood products by way of the food chain. In groups of individuals who are not specifically exposed to PCP, net daily intake estimated in eight countries

varied from 5 to 37 μg . Net intake was between 51 and 157 $\mu\text{g}/\text{day}$ in residents of homes made of PCP-treated logs [20]. In individuals occupationally exposed to PCP, net daily intake varied widely, from 35 to about 24,000 μg , depending on the type of work [20–23]. Human exposure to PCP can also originate, albeit to a minor extent, through metabolic formation from hexachlorobenzene or hexachlorocyclohexane, which are also ubiquitous environmental contaminants [20–23].

PCP is a potent carcinogen. Following chronic exposure of B6C3F1 mice to PCP, hepatocellular carcinomas or adenomas, hemangiosarcomas, and pheochromocytomas were observed [24]. In a recent report, malignant mesothelioma and nasal squamous cell carcinomas were induced in F334/N rats [25]. In humans, malignant lymphoma and leukemia have been associated with occupational exposure to PCP [20–23]. PCP has been found in at least 313 of the 1585 National Priorities List sites, listed as a priority pollutant by the U.S. EPA, and classified as a group 2B (possibly carcinogenic to humans) environmental carcinogen by the International Association for Research on Cancer (IARC) [12,20,21]. While the precise mechanism of PCP's genotoxicity remains to be elucidated, it has been suggested that its quinone and semiquinone metabolites play an important role (Figure 2).

PCP is oxidatively dechlorinated to produce tetrachlorohydroquinone (TCHQ) by liver microsomal cytochrome P450s from rats and humans *in vitro* [23,26] and by rodents *in vivo* [27–30]. About 20% of PCP was recovered in urine of PCP-treated B6C3F1 mice as TCHQ and its glucuronide and sulfate conjugates [28]. TCHQ can be further oxidized to tetrachloro-1,4-benzoquinone (TCBQ) via its corresponding semiquinone,

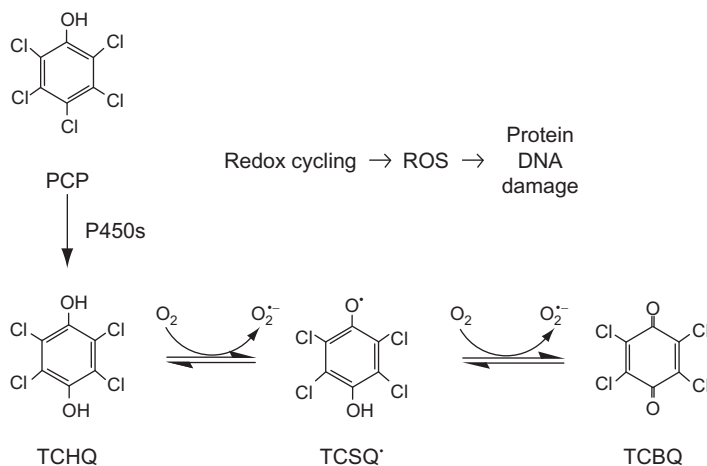
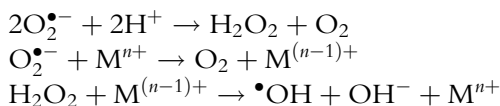


Figure 2 PCP and its carcinogenic quinoid metabolites: TCHQ, tetrachlorohydroquinone; TCSQ[•], tetrachlorosemiquinone radical; TCBQ, tetrachloro-1,4-benzoquinone.

the tetrachlorosemiquinone radical (TCSQ \bullet) [31]. TCBQ and its thiol and glucuronide conjugates were also found in animals and humans [26–30]. TCBQ has also been observed as a reactive oxidation intermediate or product in processes used to oxidize or destroy PCP and other polychlorinated persistent organic pollutants (POPs) in various chemical and enzymatic systems [23,32–35]. TCBQ itself has been widely used as a fungicide (Sperguson) for treatment of seeds and foliage, and as an oxidizing or dehydrating agent in organic synthesis (often called *p*-chloranil [23]).

The Rappaport laboratory has developed an assay to simultaneously quantify protein adducts of quinones and semiquinones following PCP administration to rats and mice [36]. They found that TCBQ is a Michael acceptor and forms adducts with cysteinyl residues of proteins both *in vitro* and *in vivo* [36]. TCBQ was found to retain its oxidized quinone structure following covalent attachment of cysteinyl residues with chloride displacement. The mono-adduct continues to react with additional sulfhydryls leading to di- and tri-substituted adducts. This assay employs Raney nickel to selectively cleave the cysteinyl adducts, which generates quinones or tetrachlorophenols from semiquinone-derived adducts, and the latter products were only detected *in vivo* [36]. Therefore, this assay can be used to measure the extent of quinone versus semiquinone adduct formation during PCP metabolism. In this regard, administration of a single oral dose of PCP to Sprague–Dawley rats and B6C3F1 mice generated proportionally greater amounts of tetrachloro-1,2-semiquinone adducts in the livers of the rodents at low doses of PCP (<4–10 mg/kg body weight) that was 40-fold greater in rats than in mice. Production of TCBQ adducts was proportionally greater at high doses of PCP (460–230 mg/kg body weight) that was 2- to 11-fold greater in mice than in rats over the entire range of doses [36]. These results suggested that species differences in the metabolism of PCP to semiquinones and quinones were, in part, responsible for the production of liver tumors in mice but not in rats [36].

Redox cycling of compounds with a quinoid structure is a well-known phenomenon [37,38]. The cyclic (auto)oxidation and reduction reactions with the intermediary formation of semiquinone radicals can produce large amounts of reactive oxygen species (ROS) by reducing molecular oxygen to superoxide (O $_2^{\bullet-}$), which in turn can induce oxidative stress [37,38]. However, it is generally accepted that O $_2^{\bullet-}$ itself is not directly attacking DNA, but only after its dismutation to hydrogen peroxide (H $_2$ O $_2$) and subsequent metal-mediated cleavage to hydroxyl radical (\bullet OH). This reaction sequence is called the Haber–Weiss reaction, or superoxide-driven Fenton reaction (M represents transition metals, especially iron and copper) [39]:



While PCP itself does not show any reactivity toward DNA, TCHQ was found to induce single-strand breaks in isolated DNA [30], a variety of cell lines [31,40–42], and liver of mice [43,44]. TCHQ also induced micronuclei and mutations at the HPRT locus of V79 cells [45,46], and the formation of 8-hydroxy-2'-deoxyguanosine (8-OH-dG) in V79 cells [47] and B6C3F1 mice [43]. At low concentrations, TCHQ reduced colony-forming ability of human fibroblasts [40], and inhibited cell growth in CHO cells [42]. Recently, TCHQ was found to induce formation of direct adducts, apurinic/apyrimidinic (AP) sites, and oxidized bases in human HeLa S3 cells [48].

2.2. Molecular mechanisms of PCP quinoid metabolite-induced DNA damage

Both oxidative DNA damage and direct DNA adducts have been implicated in PCP-induced mouse liver carcinogenesis [23,42,44,48]. The most commonly analyzed biomarker of oxidative DNA damage, 8-OH-dG, was detected in the livers of B6C3F1 mice that received acute and subacute doses of PCP and TCHQ, and the levels were increased significantly over the corresponding controls [42]. Recent findings in Fischer 344 rats that had been administered PCP for 27 weeks also revealed a statistically significant increase in 8-OH-dG in hepatic DNA over control [49]. In addition to oxidized bases, it is likely that other types of oxidative DNA lesions are involved. Redox cycling of PCP quinoid metabolites to generate ROS is believed to play an important role in PCP genotoxicity.

Among ROS, $\bullet\text{OH}$ is regarded as the most reactive one produced in biological systems. DNA damage resulting from attack by $\bullet\text{OH}$ includes base oxidation, deoxyribose damage, strand breaks, and AP sites [39]. $\bullet\text{OH}$ can induce AP sites by direct hydrogen abstraction from the sugar moiety of DNA, resulting in 5'-nicked oxidized AP sites formation [50–52]. Another pathway for AP sites formation may involve depurination/depyrimidination of quinone–DNA adducts. TCBQ and its corresponding semiquinone radical are reactive electrophiles and therefore are also capable of alkylating DNA and forming DNA adducts [49,53,54]. Recently, Lin *et al.* [53] showed that low degree of oxidative and direct DNA damage was produced by high concentrations of TCBQ.

Comparison of the genotoxicity of TCHQ to H_2O_2 in human fibroblasts also revealed a greater genotoxic potential for TCHQ than for H_2O_2 [46]. DNA damage was determined after 1 h treatment with TCHQ or H_2O_2 by the comet assay (also called single cell gel electrophoresis assay). A distinct tail moment was noted for TCHQ at concentrations of 10 μM , whereas 60 μM H_2O_2 was required to produce the same extent of DNA damage. By monitoring the incorporation of [^3H]-thymidine into DNA of nonreplicating cells (UDS), the extent of DNA repair was measured and

25 μM TCHQ was found to inhibit repair, while H_2O_2 continuously induced DNA repair up to 60 μM . In contrast to H_2O_2 , TCHQ was also mutagenic in the HPRT locus of V79 cells with a mutant frequency of 75 and 151 mutants per 10^6 cloneable cells at nontoxic concentrations of 5 and 7 μM . It was suggested [46] that the TCSQ radical may react with DNA directly and cause AP sites which are transformed to strand breaks either by endonucleases or under the alkaline conditions of the comet assay. This would explain the ineffectiveness of dimethyl sulfoxide (DMSO) to quench TCHQ-induced damage in cellular DNA. However, an alternative explanation may stem from TCHQ-induced $\bullet\text{OH}$ production by a metal-independent process (see below) that takes place close to the DNA surface, precluding effective $\bullet\text{OH}$ scavenging by DMSO. The fact that TCHQ also inhibits DNA repair enzymes would provide a rationale for its potent genotoxicity and mutagenicity. In contrast, DNA damage by H_2O_2 would require transition metal ions for catalysis and DNA repair enzymes are not inhibited by H_2O_2 [46].

While little is known about direct interactions of TCSQ radical with DNA, the fully oxidized PCP quinoid metabolite TCBQ is known to react covalently with DNA to generate DNA adducts, as evidenced by the ^{32}P -postlabeling assay [49,52]. Treatment of calf thymus (CT) DNA with 5 mM TCBQ generated four major and several minor adducts (3.5 adducts per 10^5 total nucleotides) [53]. These adducts were chemically stable and do not generate AP sites. In addition, increases in 8-oxo-dG and AP sites were observed that were ascribed to oxidative damage. These results demonstrated that PCP quinone and hydroquinone metabolites induce direct and oxidative base modifications as well as the formation of 5'-cleaved AP sites in genomic DNA [53]. Cell culture and *in vivo* studies have shown that PCP itself causes direct genotoxicity under certain conditions. Treatment of rat hepatocytes with a single dose of PCP (50 μM) generated 17 adducts per 10^9 total nucleotides. Chronic (60 mg/kg/day for 27 weeks), but not acute (60 mg/kg/day for 1 or 5 days), exposure of rat to PCP induced a twofold increase in 8-oxo-dG (1.8 vs. 0.91×10^6 in controls) and generated two major adducts, one derived from TCBQ, with relative ^{32}P -postlabeling of 0.78 adducts per 10^7 total nucleotides [49]. The TCBQ-derived DNA adduct was also detected in mouse liver DNA following exposure to PCP at 8 adducts per 10^7 nucleotides which is 10-fold greater compared with the rat. The greater amounts of both oxidative and direct DNA damage, together with increased hepatotoxicity and cell proliferation, may provide the critical events necessary for hepatic carcinogenesis in the mouse. In contrast, the decreased amount of DNA damage and the lack of hepatotoxicity and cell proliferation in the rat do not result in such critical changes [49].

As mentioned above, DNA adducts attributable to TCBQ have been observed previously *in vitro* and detected *in vivo*. In addition, an unidentified adduct in these studies co-eluted with the product of the reaction of

deoxyguanosine (dG) and TCBQ. Sturla's group [55] have synthesized, isolated, purified, and characterized the predominant adduct formed from the reaction of dG and TCBQ. They proposed that the adduct is a dichlorobenzoquinone nucleoside in which two chlorine atoms in TCBQ have been displaced by reaction at the 1 and N^2 positions of dG. Their results suggest that direct reactions between chlorophenols and DNA may play a role in the toxic effects of chlorinated phenols and indicate a potential difference in reactivity and biological influence between PCP and other less substituted chlorinated phenols. They further elucidated the structure of new agent-specific DNA adducts resulting from the reaction of dGuo, dCyd, and Thd with TCBQ [56]. Two dGuo adducts and one dCyd adduct resulting from the reaction of double-stranded DNA with TCBQ were identified. The results indicate that, in the structural context of DNA, TCBQ reacts most readily with dGuo compared to the other DNA bases and that the mode of TCBQ reactivity is dependent on the base structure, that is, multiple types of adducts are formed. DNA adducts consistent with TCBQ reactions were also observed when DNA or dGuo was treated with PCP and a peroxidase-based bioactivating system.

The association of chlorinated phenols to incidences of leukemia was also found to be consistent with the leukemogen activity of phenolic xenobiotics such as phenol and the phenolic anticancer drug etoposide [5]. Phenolic compounds are substrates for myeloperoxidase present in bone marrow and could be converted into phenoxyl radicals. Direct reactions of phenoxyl radicals and thiyl radicals with biomolecules could also contribute to peroxidase-driven toxic effects of phenolic xenobiotics. With regard to direct reactions of phenoxyl radicals with DNA, an *in vitro* study by the Turesky's group demonstrated that adduct levels ($3679/10^5$ nucleotides) by 0.1 mM PCP following activation by horseradish peroxidase (HRP)/ H_2O_2 are 30-fold higher than levels induced by CYP450-containing microsomes and 10-fold higher than levels induced by TCBQ (5 mM) itself [57]. This suggested the possibility that the pentachlorophenoxyl radical generated by HRP/ H_2O_2 -mediated PCP oxidation might contribute to DNA adduct formation. Manderville's group [58] found that treatment of PCP (0.1 mM) with HRP/ H_2O_2 or myeloperoxidase (MPO/ H_2O_2) with excess dG (2 mM) led to the isolation and identification of the oxygen-bonded C8-dG nucleoside adduct. The reaction was absolutely specific for dG; no detectable adduct(s) was observed from HRP/ H_2O_2 and PCP in the presence of deoxyadenosine, deoxycytidine, or thymidine. Formation of the oxygen-bonded C8-dG nucleoside adduct was also specific for peroxidase activation that is known to oxidize PCP into its phenoxyl radical. Treatment of PCP/dG with rat liver microsomes (RLM) failed to generate the adduct; instead, an adduct derived from the benzoquinone electrophile TCBQ was observed in the extracted ion chromatogram from the RLM/NADPH-treated PCP/dG sample. The oxygen-bonded

C8-dG nucleoside adduct is the first structurally characterized O-bonded phenolic DNA nucleoside adduct and highlights the ambident electrophilicity of phenoxyl radicals (O vs. C) in reaction at C8 of dG. Given that PCP is known to induce DNA adduct formation *in vivo* and human exposure has been linked to incidences of leukemia, the adduct could play a key role in PCP-mediated carcinogenesis [58].

Then they expand their investigations on a wider range of chlorinated phenol substrates to establish their reactivity toward dG and duplex DNA (CT) following activation by HRP/H₂O₂, as a representative peroxidase system [59]. Their data showed that chlorophenoxyl radicals may either react directly with dG and CT-DNA to form C8-dG O-adducts in an irreversible process or couple to yield 1,4-BQ electrophiles that react with dG to afford adducts of the benzetheno variety. These results established the *in vitro* relevance of C8-dG O-adducts of phenolic toxins. The ¹H NMR chemical shifts and reactivity of the benzetheno adducts favor 4''-hydroxy-1,N²-benzetheno-dG adduct assignment, which is in contrast to the other literature which has assigned the 1,4-BQ-dG adduct as 3''-hydroxy-1,N²-benzetheno-dG. Overall, their study has provided new insights into peroxidase-mediated activation of chlorinated phenol substrates and has strengthened the hypothesis that direct reactions of chlorophenoxyl radicals with DNA contribute to peroxidase-driven toxic effects of chlorophenolic xenobiotics.

2.3. The pro-oxidant versus antioxidant equilibrium

The pro-oxidant potential of biological systems and their antioxidant capacity usually are in an approximate equilibrium [39]. In normal cells, a primary defense against oxidative damage is provided by small molecule antioxidants such as glutathione (GSH) and ascorbate, which are present in millimolar concentrations. However, these defense mechanisms can be overwhelmed by xenobiotics such as PCP and its metabolites that induce the production of excessive ROS, which can result in damage to biological macromolecules such as DNA [37–39]. It should be noted that the concentration of ROS, including H₂O₂, in cells under normal physiological conditions is low, but ROS concentration may be significantly increased in cells that are subjected to oxidative stress conditions such as exposure to PCP metabolites, as we showed recently in NIH 3T3 cells [60]. TCHQ treatment was shown to cause more than 60% GSH depletion in liver tissues of mice, possibly by forming GSH-conjugates [30,37,38,44]. It was suggested that depletion of GSH and other antioxidants by PCP metabolites could abolish the protective ability of the cell against ROS and lead to DNA damage [45]. It is thus reasonable to hypothesize that PCP metabolite-induced DNA damage could be prevented if the levels of intracellular antioxidants were raised through supplementation of dietary antioxidants. Indeed, it has been demonstrated recently [61] that oral administration of

antioxidant vitamin E and diallyl sulfide 3 h before each PCP challenge significantly protected against elevation of hepatic 8-OH-dG levels in male B6C3F1 mice, while vitamin C, epigallocatechin gallate, and ellagic acid showed partial protection. These findings indicate that PCP-induced oxidative DNA damage in the target organ liver can be blocked by a number of dietary antioxidants.

3. MECHANISM OF PROTECTION BY THE “SPECIFIC” IRON-CHELATING AGENT DESFERRIOXAMINE AGAINST TCHQ-INDUCED DNA DAMAGE

3.1. The protection by desferrioxamine against TCHQ-induced DNA damage was not due to its classic iron-chelating property, but rather to its scavenging of the reactive TCSQ[•]

As discussed above, TCHQ has been identified as one of the main toxic metabolites of PCP. TCHQ can induce DNA single-strand breaks and has also been implicated in PCP-associated genotoxicity. The ability of TCHQ to induce DNA damage has been previously attributed to its ability to form [•]OH through the classic metal-dependent Fenton reaction (see above). This notion was based on the fact that TCHQ-induced DNA damage was completely prevented by desferrioxamine (DFO, also called Desferal[®] and deferoxamine). DFO has been used as an iron-chelating agent for the treatment of iron overload. This includes clinical cases of individuals who have ingested toxic oral doses of iron salts or require multiple blood transfusions, such as in the treatment of β -thalassemia. DFO is a linear trihydroxamic acid siderophore that forms a kinetically and thermodynamically stable complex with ferric iron, ferrioxamine (Figure 3). Its high binding constant ($\log \beta = 31$) and its redox properties ($E^\circ = -0.45$ V) render the bound iron unreactive for the catalysis of oxygen radical production as has been implicated in a variety of biological processes. It has been classically assessed that prevention of damage by DFO was a sufficient proof for the role of loosely bound iron in the injurious processes. Although DFO has been repeatedly used to probe metal-catalyzed hydroxyl radical formation in biological systems, recent studies demonstrated the ability of this trihydroxamate compound to act as radical scavenger, in addition to and independent of its iron-binding properties. Diethylenetriaminepentaacetic acid (DTPA) is an analog of the widely used chelating agent ethylenediaminetetraacetic acid (EDTA). DTPA could also form a kinetically and thermodynamically stable complex with ferric iron (Figure 4; $\log \beta = 28$; $E^\circ = +0.03$ V). Both DFO and DTPA have been widely used to study the role of iron in various chemical and biological systems, and therefore

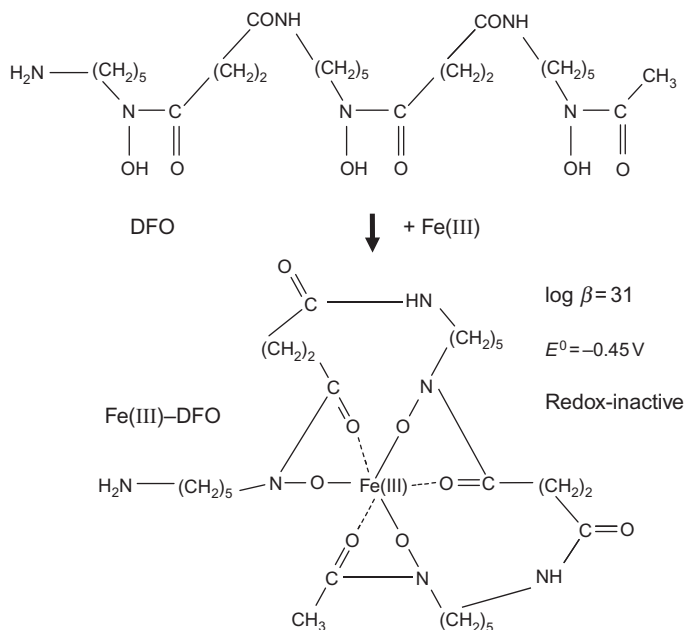


Figure 3 Chemical structures of desferrioxamine (DFO) and its Fe(III) complex.

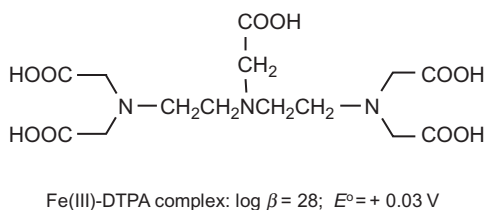


Figure 4 Chemical structure of DTPA (diethylenetriaminepentaacetic acid).

we employed these two structurally different but relatively specific iron-chelating agents to probe whether iron played any role in TCHQ-induced DNA damage. We found [62] that DFO protected against TCHQ-induced DNA single-strand breaks in isolated DNA, while other iron chelators such as DTPA did not. To better understand its underlying molecular mechanism, the auto-oxidation process of TCHQ yielding TCSQ^\bullet intermediate was studied in the presence and absence of these two iron-chelating agents.

We found that DFO led to a marked reduction in both the concentration and half-life of TCSQ^\bullet . Interestingly, the decay of TCSQ^\bullet was accompanied by concurrent formation of DFO–nitroxide radicals (DFO^\bullet), which contains the structural component $-\text{CH}_2-\text{NO}^\bullet-\text{CO}-$ and gives a characteristic nine-line spectrum as a result of splitting of the nitroxide nitrogen coupling ($a^{\text{N}} = 7.9 \text{ G}$) by two protons [$a(2)^{\text{H}} = 6.3 \text{ G}$] from the neighboring CH_2 group (Figure 5). These effects have been demonstrated both by UV–visible and electron spin resonance (ESR) spectral methods. In contrast, DTPA had no detectable effect on TCHQ auto-oxidation. These results suggest that the protection by DFO against TCHQ-induced DNA damage was not due to its binding of iron, but rather due to its scavenging of the reactive TCSQ^\bullet [62].

Interestingly, we found that DFO could also dramatically enhance the hydrolysis (dechlorination) of TCHQ (and TCBQ) to form chloranilic acid (2,5-dichloro-3,6-dihydroxy-1,4-benzoquinone, DDBQ) [62]. The exact underlying molecular mechanism has recently been investigated in our lab, and to our surprise, a novel double Lossen rearrangement reaction was found to be involved in this process (see Section 5). Compared to TCBQ, the DDBQ molecule was considered to be more stable, less reactive, and much less toxic; therefore, the enhanced formation of DDBQ from TCBQ catalyzed by DFO also contributed to its reduction of the toxicity of TCHQ. Further, the enhanced conversion of TCHQ to DDBQ reduced the possibility of redox cycling between TCBQ and TCHQ in the cell, whereby repeatedly producing TCSQ^\bullet .

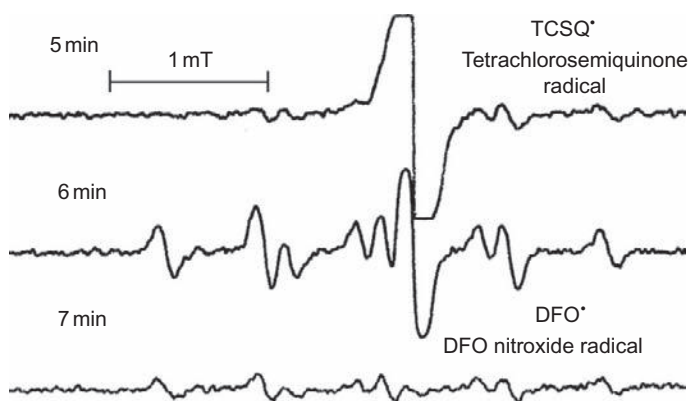


Figure 5 The decay of tetrachlorosemiquinone radical (TCSQ^\bullet) was accompanied by the concurrent formation of desferrioxamine (DFO) nitroxide radical, DFO^\bullet (modified based on Ref. [62]).

3.2. Protection by DFO against TCHQ-induced cyto- and genotoxicity in human fibroblasts

Then we extended our study from isolated DNA to human fibroblasts, and from DFO to other hydroxamic acids. Cyto- and genotoxic effects of PCP metabolites were evaluated, respectively, by the MTT and “comet” assay (also called single cell gel electrophoresis). We found [63] that co-incubation of DFO provided marked protection against both the cyto- and genotoxicity induced by TCHQ. Pretreatment of the cells with DFO followed by washing also provided protection, although less efficiently compared to the simultaneous treatment. Similar patterns of protection were also observed for three other hydroxamic acids: aceto-, benzo-, and salicyl-hydroxamic acid (AHA, BHA, and SHA). Spectral studies showed that the three hydroxamic acids tested other than DFO also effectively scavenged the reactive TCSQ[•] and enhanced the formation of the less reactive and less toxic chloranilic acid (Figure 6). DMSO, an efficient [•]OH scavenger, provided partial protection only at high concentrations. The results of this study demonstrated that the protection provided by DFO and other hydroxamic acids against TCHQ-induced cyto- and genotoxicity

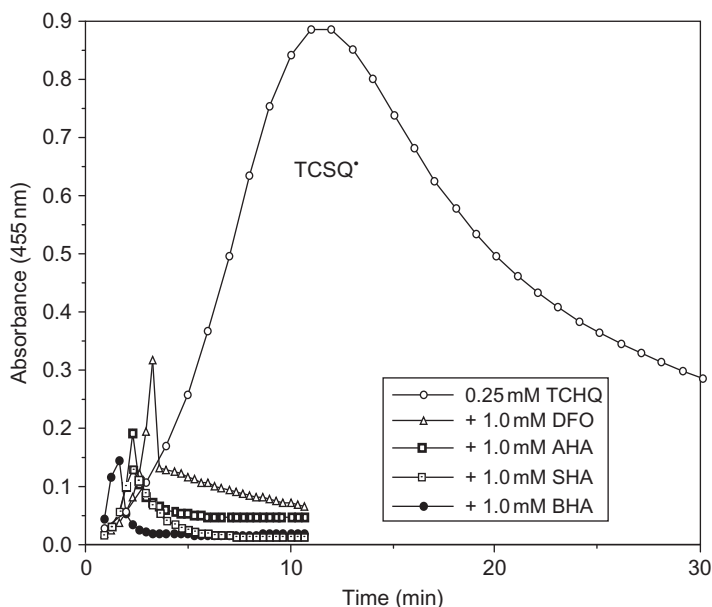


Figure 6 Inhibition of tetrachlorosemiquinone radical (TCSQ[•]) formation by desferrioxamine (DFO) and other hydroxamic acids monitored at 455 nm. AHA, aceto-hydroxamic acid; SHA, salicyl-hydroxamic acid; and BHA, benzohydroxamic acid (modified based on Ref. [63]).

in human fibroblasts is mainly through scavenging of the observed reactive TCSQ \cdot and not through prevention of the Fenton reaction by the binding of iron in a redox-inactive form [63].

4. MOLECULAR MECHANISM OF PCP QUINOID METABOLITE-INDUCED GENOTOXICITY

4.1. Metal-independent production of $\cdot\text{OH}$ by PCP quinoid metabolite and H_2O_2

The above findings suggest that iron was not involved in TCHQ-induced DNA damage. In another word, TCHQ-induced DNA damage may not be due to the iron-mediated $\cdot\text{OH}$ production through the classic Fenton reaction. Then the question became what was the underlying molecular mechanism for PCP metabolites-mediated $\cdot\text{OH}$ production? To test whether $\cdot\text{OH}$ can be produced by PCP metabolites, we first employed the well-known salicylate hydroxylation method. HPLC with electrochemical detection was used to measure the levels of 2,3- and 2,5-dihydroxybenzoic acid (DHBA) formed when $\cdot\text{OH}$ reacts with salicylate. We found [64] that TCHQ and H_2O_2 could produce both 2,3- and 2,5-DHBA when incubated with salicylate. Their production was markedly inhibited by the $\cdot\text{OH}$ scavenging agents DMSO and ethanol. In contrast, their production was not affected by the nonhydroxamate iron chelators and the copper-specific chelator. Similar effects were also observed with TCBQ and H_2O_2 . Based on these results, we suggested that $\cdot\text{OH}$ was produced by TCHQ and H_2O_2 , possibly through a metal-independent Fenton-like reaction [64].

Since the salicylate hydroxylation method cannot provide direct evidence for $\cdot\text{OH}$ formation, a more specific method, such as secondary radical ESR spin trapping with 5, 5-dimethyl-1-pyrroline *N*-oxide (DMPO), is needed to further substantiate and extend our previous observations. A typical DMPO/ $\cdot\text{OH}$ signal, and DMPO/ $\cdot\text{CH}_3$ signal derived from $\cdot\text{OH}$ attack on DMSO, will be more conclusive evidence for $\cdot\text{OH}$ production from H_2O_2 and TCHQ or TCBQ [40] (Figure 7). We found [65] that when incubated with DMPO, TCBQ and H_2O_2 produced the DMPO/ $\cdot\text{OH}$ adduct. In contrast, incubation of either compound alone did not cause $\cdot\text{OH}$ formation. The formation of DMPO/ $\cdot\text{OH}$ was markedly inhibited by the $\cdot\text{OH}$ scavenging agents DMSO and formate, with the concomitant formation of the characteristic DMPO adducts with $\cdot\text{CH}_3$ and $\cdot\text{COO}^-$, respectively (Figure 8). These secondary radical ESR spin-trapping results provided definitive evidence that $\cdot\text{OH}$ could indeed be produced by TCBQ and H_2O_2 .

Then a critical question arose: Was the production of $\cdot\text{OH}$ by TCBQ and H_2O_2 metal-dependent or -independent? To answer this question, the

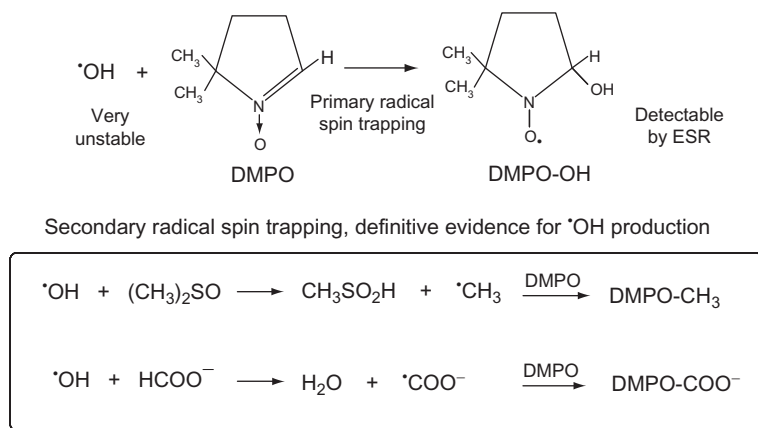


Figure 7 $\cdot\text{OH}$ detection and identification by primary and secondary ESR spin-trapping methods.

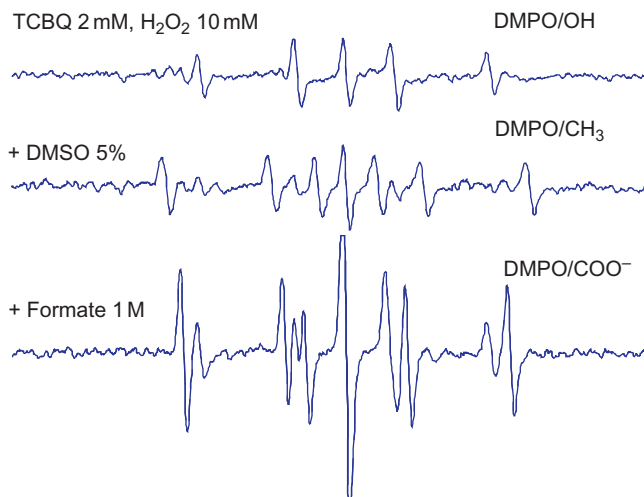


Figure 8 Definitive evidence for $\cdot\text{OH}$ production by TCBQ and H_2O_2 as demonstrated by secondary ESR spin-trapping method (modified based on Ref. [64]).

potential role of catalytic transition metals contaminating the DMPO/TCBQ/ H_2O_2 reaction system was carefully examined by using several structurally different and relatively specific metal chelating agents for iron and copper [66–68]. Neither the DMPO/ $\cdot\text{OH}$ signal nor the DMPO/ $\cdot\text{CH}_3$ signal produced by the DMPO/TCBQ/ H_2O_2 system in the absence and presence, respectively, of DMSO was affected by the

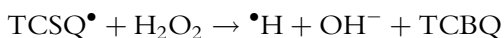
addition of various nonhydroxamate iron-chelating agents, viz., bathophenanthroline disulfonate (BPS), ferrozine, and ferene, as well as the copper-specific chelating agent bathocuproine disulfonate (BCS). In addition, no significant decrease in the DMPO/ $\bullet\text{OH}$ and DMPO/ $\bullet\text{CH}_3$ signal was observed by low concentrations ($\leq 10\ \mu\text{M}$) of the trihydroxamate iron-chelating agent DFO. These DFO concentrations should be sufficient to chelate any trace amounts of iron contaminating the chelex-pretreated buffer. However, the formation of DMPO/ $\bullet\text{OH}$ and DMPO/ $\bullet\text{CH}_3$ was abolished by high concentrations of DFO ($\geq 1\ \text{mM}$), with the concurrent formation of the DFO \bullet . As discussed before, the inhibition of $\bullet\text{OH}$ production by DFO was not due to its iron-binding capacity, but rather due to its ability to scavenge TCSQ \bullet . Similar marked inhibition of DMPO/ $\bullet\text{OH}$ and DMPO/ $\bullet\text{CH}_3$ formation was observed with another TCSQ \bullet scavenger, BHA. In addition, even when trace amounts of iron (Fe (II), $0.5\ \mu\text{M}$) were added to the DMPO/TCBQ/ H_2O_2 system, no increase in $\bullet\text{OH}$ production was observed.

In contrast, the formation of both DMPO/ $\bullet\text{OH}$ and DMPO/ $\bullet\text{CH}_3$ by the DMPO/Fe(II)/ H_2O_2 system in the absence and presence, respectively, of DMSO was almost completely inhibited by the nonhydroxamate iron-chelating agents BPS, ferrozine, and ferene, as well as the hydroxamate iron-chelating agent DFO. No concurrent formation of the DFO \bullet was detected, indicating that DFO acted by chelating iron in this classic Fenton system. These results clearly demonstrated that the production of $\bullet\text{OH}$ by TCBQ and H_2O_2 is *independent* of transition metal ions.

It should be noted that the metal-independent production of $\bullet\text{OH}$ was not limited to TCBQ and H_2O_2 , but was also observed in the presence of other halogenated quinones, that is, 2-chloro-, 2,5-dichloro-, 2,6-dichloro-, trichloro-, tetrafluoro-, and tetrabromo-1,4-benzoquinone (Figure 9). In contrast, no $\bullet\text{OH}$ production was detected from H_2O_2 and the nonhalogenated quinone, 1,4-benzoquinone, and the methyl-substituted quinones 2,6-dimethyl- and tetramethyl-1,4-benzoquinone [65].

4.2. Molecular mechanism of metal-independent production of $\bullet\text{OH}$ by PCP quinoid metabolites and H_2O_2

Based on the above experimental results, we first proposed [64,65] that the production of $\bullet\text{OH}$ by TCBQ and H_2O_2 might be through a metal-independent semiquinone-mediated organic Fenton reaction:



where TCSQ \bullet substitutes for ferrous iron in the classic, metal-dependent Fenton reaction. This type of reaction between semiquinone radicals and

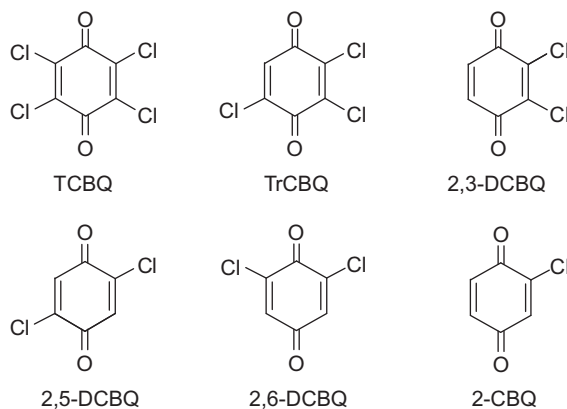


Figure 9 Chemical structures of the chlorinated quinones.

H_2O_2 has been previously proposed by Koppenol and Butler [69], who suggested that if a quinone/semiquinone couple has a reduction potential of between -330 and $+460$ mV, it can theoretically bring about a metal-independent Fenton reaction. It was suggested that such reactions are thermodynamically feasible and do not require metal ions for catalysis [69,70], which might be the case in this study, where the reduction potentials of the quinone/semiquinone couples for 2-chloro-, 2,5-dichloro-, tetrafluoro-, tetrabromo-, and tetrachloro-1,4-benzoquinone are -100 , $+60$, $+200$, $+240$, and $+250$ mV, respectively [71]. These values are within the suggested range of -330 to $+460$ mV. In contrast, the reduction potentials for 2,6-dimethyl-1,4-benzoquinone and tetramethyl-1,4-benzoquinone of -430 and -600 mV, respectively [71], are outside this range, and indeed, no $\cdot\text{OH}$ formation could be detected.

If the above mechanism was correct, then the production of $\cdot\text{OH}$ from H_2O_2 and TCBQ should be dependent on the concentration of $\text{TCSQ}\cdot$, that is, the higher the concentration of $\text{TCSQ}\cdot$, the more $\cdot\text{OH}$ should be produced. Further, the main product of this reaction should be TCBQ. Using secondary radical ESR spin-trapping method, we found that $\text{DMPO}/\cdot\text{CH}_3$ and $\text{DMPO}/\cdot\text{OH}$ adducts can be produced by H_2O_2 and TCBQ in the presence of the spin-trapping agent DMPO and $\cdot\text{OH}$ scavenger DMSO. However, no $\text{DMPO}/\cdot\text{CH}_3$ and $\text{DMPO}/\cdot\text{OH}$ adducts were detected from H_2O_2 and TCHQ (the reduced form of TCBQ), although high concentrations of $\text{TCSQ}\cdot$ could be produced during the auto-oxidation of TCHQ. Interestingly, if TCHQ was quickly oxidized to TCBQ with MPO, $\text{DMPO}/\cdot\text{CH}_3$ and $\text{DMPO}/\cdot\text{OH}$ adducts could be detected again, similar to that produced by TCBQ (Figure 10). Further, the formation of $\text{DMPO}/\cdot\text{CH}_3$ and $\text{DMPO}/\cdot\text{OH}$ was found to be directly dependent on the concentrations of TCBQ and H_2O_2 . These

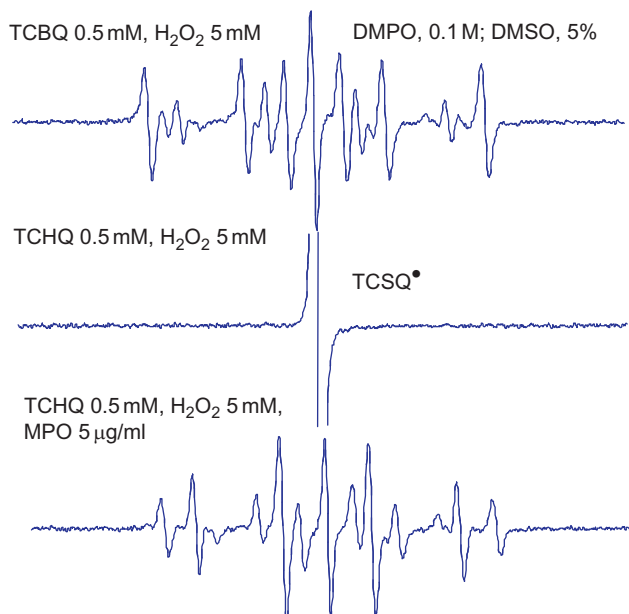


Figure 10 Tetrachlorosemiquinone radical (TCSQ•) is not essential for •OH production by TCBQ and H₂O₂. MPO, myeloperoxidase (modified based on Ref. [72]).

results strongly suggest that TCBQ, but not its corresponding semiquinone radical TCSQ•, is essential for •OH production. Therefore, the production of •OH by TCBQ and H₂O₂ appears not to occur through a semiquinone-dependent organic Fenton reaction.

To get more information on the mechanism of •OH production by TCBQ/H₂O₂, the time- and concentration-dependent production of DMPO/•OH by TCBQ/H₂O₂ was studied. Two distinct phases were observed: the first fast phase (about 30 s) and the second slower phase. This indicates that •OH may be produced by two-step reactions between TCBQ and H₂O₂. When TCBQ concentration was fixed at 0.1 mM, the rate of DMPO/•OH production was dependent on H₂O₂ concentration. It should be noted that DMPO/•OH could be detected at H₂O₂ concentration as low as 10 μM. When H₂O₂ concentration was fixed at 0.1 mM, DMPO/•OH could be detected at TCBQ concentration as low as 5 μM. Further, UV-visible spectral studies showed that there was a direct interaction between TCBQ and H₂O₂, with the reaction mixture changing quickly from the original yellow color ($\lambda_{\text{max}} = 292 \text{ nm}$) to a characteristic purple color ($\lambda_{\text{max}} = 295$ and 535 nm) in phosphate buffer (pH 7.4). The final reaction products between TCBQ and H₂O₂ were then identified by electrospray ionization quadrupole time-of-flight mass spectrometry (ESI-Q-TOF-MS). The mass spectrum of TCBQ is characterized by a

four-chlorine isotope cluster at m/z 246 and traces of a three-chlorine isotope cluster at m/z 227. The addition of H_2O_2 to TCBQ led to complete disappearance of the molecular ion peak clusters at m/z 246 and dramatic increase of the peak clusters at m/z 227. Tandem mass spectrometric analysis showed that the peak at m/z 227 could be fragmented to form the peak at m/z 197, which suggests that the peak at m/z 197 is solely derived from the peak at m/z 227. These results indicate that the major reaction product between TCBQ and H_2O_2 was probably the ionic form of trichloro-hydroxy-1,4-benzoquinone (TrCBQ-OH). This was further confirmed by comparing with the authentic TrCBQ-OH synthesized according to published method [73], which showed the same ESI-MS profile and the same retention time in HPLC.

To better understand the source and origin of the oxygen atom inserted into the reaction product TrCBQ-OH formed from the reaction between H_2O_2 and TCBQ, TCBQ was incubated with oxygen-18-enriched H_2O_2 ($[\text{O}^{18}]\text{-H}_2\text{O}_2$). The mass spectra of the molecular ion region of deprotonated TrCBQ-OH, obtained with unlabeled and labeled H_2O_2 , demonstrated the shift of the molecular ion isotope cluster peaks of the unlabeled compound with 2 mass units, as could be expected for the incorporation of ^{18}O . These results indicate that H_2O_2 is the source and origin of the oxygen atom inserted into the reaction product TrCBQ-OH.

It has also been shown [74] that both TCBQ and H_2O_2 were consumed with a stoichiometric ratio of about 1:1, and H_2O_2 accelerated the rate of TCBQ decomposition by two orders of magnitude with the loss of chloride. Thus, the metal-independent production of $\bullet\text{OH}$ by TCBQ and H_2O_2 may be not through a previously proposed semiquinone-mediated organic Fenton reaction. Based on the above experimental results and the fact that H_2O_2 is a better nucleophile than H_2O [75], we proposed a novel mechanism for $\bullet\text{OH}$ production by H_2O_2 and TCBQ [72] (Figure 11): a nucleophilic reaction may take place between TCBQ and H_2O_2 , forming an unstable trichloro-hydroperoxyl-1,4-benzoquinone (TrCBQ-OOH) intermediate, which can decompose homolytically to produce $\bullet\text{OH}$ and trichloro-hydroxy-1,4-benzoquinone radical (TrCBQ-O \bullet). TrCBQ-O \bullet then may disproportionate to form the ionic form of trichloro-hydroxy-1,4-benzoquinone (TrCBQ-O $^-$). In the presence of excess of H_2O_2 , TrCBQ-O $^-$ may further react with H_2O_2 via similar pathway to produce another $\bullet\text{OH}$ (Figure 11).

Recently, we employed a previously developed photoelectrochemical DNA sensor to investigate whether DNA damage could be induced by tetrahalogenated quinones and H_2O_2 through the above metal-independent mechanism [76]. The sensor surface was composed of a double-stranded DNA film assembled on a SnO_2 semiconductor electrode. A DNA intercalator, $\text{Ru}(\text{bpy})_2(\text{dppz})^{2+}$, was allowed to bind to the DNA film and produce photocurrent upon light irradiation. After the DNA film was

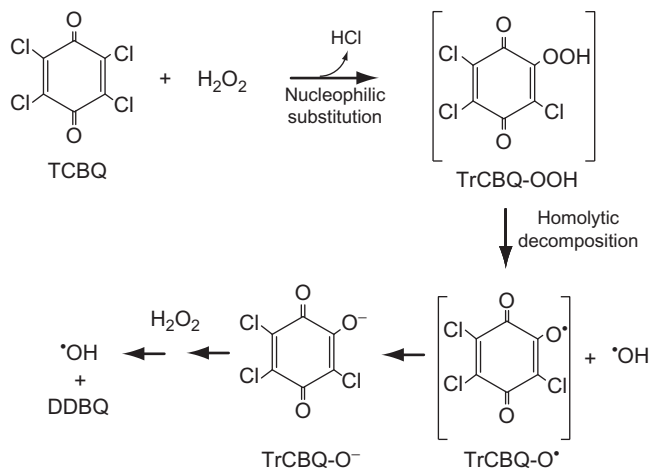


Figure 11 Proposed mechanism for metal-independent two-step $\bullet\text{OH}$ production by TCBQ and H_2O_2 (modified based on Ref. [72]).

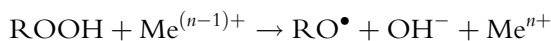
exposed to 0.30 mM tetrafluoro-1,4-benzoquinone (TFBQ), the photocurrent dropped by 20%. In a mixture of 0.30 mM TFBQ and 2 mM H_2O_2 , the signal dropped by 40%. The signal reduction indicates less binding of $\text{Ru}(\text{bpy})_2(\text{dppz})^{2+}$ due to structural damage of ds-DNA in the film. Similar results were obtained with TCBQ, although the signal was not reduced as much as TFBQ. Fluorescence measurement showed that TFBQ/ H_2O_2 generated more $\bullet\text{OH}$ than TCBQ/ H_2O_2 . Gel electrophoresis proved that the two halogenated quinones produced DNA strand breaks together with H_2O_2 , but not by themselves. These results indicate that DNA damage could be indeed induced by tetrahalogenated quinones and H_2O_2 through the above metal-independent mechanism for $\bullet\text{OH}$ production.

Direct evidence of $\bullet\text{OH}$ production in livers of *Carassius auratus* (one of the main economic fish species in Eastern China) exposed to PCP was found recently using ESR spin-trapping method [77]. A dose-effect relationship was obtained between $\bullet\text{OH}$ intensities and PCP exposure. It was observed that $\bullet\text{OH}$ was significantly induced by 0.001 mg/L (below the criteria for Chinese fishery water quality) of PCP exposure. A strong positive correlation ($r = 0.9581$, $p < 0.001$) was observed between PCP liver concentrations and $\bullet\text{OH}$ intensities within 7 days of PCP exposure, which suggests that $\bullet\text{OH}$ are mainly produced from PCP itself. However, no correlation was observed between PCP liver concentrations and $\bullet\text{OH}$ intensities after 7 days, and a higher intensity of OH could still be observed when the PCP liver concentrations decreased to a lower level, which suggests that other mechanisms may possibly contribute to $\bullet\text{OH}$ production after 7 days [77]. The glutathione/oxidized glutathione (GSH/GSSG)

ratio decreased below that of the control level during the entire period of PCP exposure (0.05 mg/L), which suggested oxidative stress occurred. It is not clear whether the production of $\bullet\text{OH}$ in this model system is metal independent or not. Further studies are needed to investigate this issue.

4.3. Metal-independent decomposition of organic hydroperoxides and formation of alkoxyl radicals by halogenated quinones

Organic hydroperoxides (ROOH) can be formed both nonenzymatically by reaction of free radicals with polyunsaturated fatty acids and enzymatically by lipoxygenase- or cyclooxygenase-catalyzed oxidation of linoleic acid and arachidonic acid [39,78,79]. It has been shown that organic hydroperoxides can undergo transition metal ion-catalyzed decomposition to alkoxyl radicals, which may initiate *de novo* lipid peroxidation or further decompose to α,β -unsaturated aldehydes that can react with and damage DNA and other biological macromolecules [39,78,79].



In previous studies, using the salicylate hydroxylation assay and ESR spin-trapping methods, we found that $\bullet\text{OH}$ can be produced from H_2O_2 by TCBQ and other halogenated quinones independent of transition metal ions [65,66]. However, it is not clear whether halogenated quinones react in a similar fashion with organic hydroperoxides to produce alkoxyl radicals independent of transition metal ions.

Using 2,5-dichloro-1,4-benzoquinone (DCBQ) as a model halogenated quinone, and *tert*-butylhydroperoxide (*t*-BuOOH) as a model short-chain organic hydroperoxide, we found [81] that DCBQ could markedly enhance the decomposition of *t*-BuOOH, leading to the formation of the DMPO adducts with *t*-butoxyl radicals (*t*-BuO \bullet) and methyl radicals ($\bullet\text{CH}_3$) (Figure 12). The formation of DMPO/*t*-BuO \bullet and DMPO/ $\bullet\text{CH}_3$ from DCBQ and *t*-BuOOH was dose dependent with respect to both DCBQ and *t*-BuOOH and was not affected by iron-specific or copper-specific metal chelators. Comparison of the data obtained with DCBQ and *t*-BuOOH with those obtained in a parallel study with ferrous iron and *t*-BuOOH strongly suggested that *t*-BuO \bullet was produced by DCBQ and *t*-BuOOH through a metal-independent mechanism. Other halogenated quinones such as TCBQ were also found to enhance the decomposition of *t*-BuOOH and other organic hydroperoxides such as cumene hydroperoxide, leading to the formation of the respective organic alkoxyl radicals in a metal-independent fashion.

UV-visible spectral studies showed that there was a direct interaction between DCBQ and *t*-BuOOH, with the reaction mixture changing

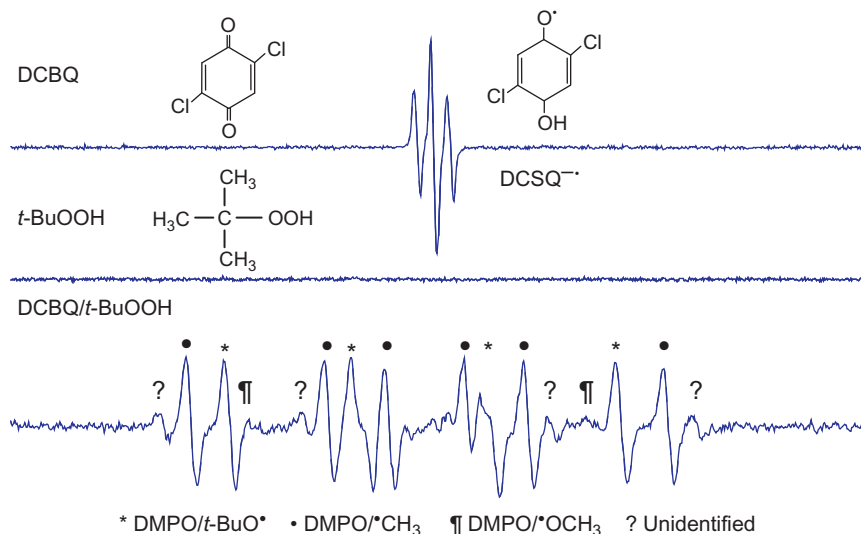


Figure 12 Metal-independent decomposition of *t*-butylhydroperoxide (*t*-BuOOH) and formation of alkoxyl radicals by 2,5-dichloro-1,4-benzoquinone (DCBQ) (modified based on Ref. [79]).

quickly from the original yellow color ($\lambda_{\text{max}} = 272 \text{ nm}$) to a characteristic purple color ($\lambda_{\text{max}} = 278$ and 515 nm) in phosphate buffer (pH 7.4). The reaction intermediate and final products between DCBQ and *t*-BuOOH were identified by ESI-MS. These MS results indicate that the major reaction intermediate between DCBQ and *t*-BuOOH was probably chloro-*t*-butylperoxyl-1,4-benzoquinone (CBQ-OO-*t*-Bu), and the major reaction product between DCBQ and *t*-BuOOH was probably the ionic form of 2-chloro-5-hydroxy-1,4-benzoquinone (CBQ-OH; peak clusters at m/z 157).

Based on the above experimental results, a novel mechanism can be proposed [79] for DCBQ-mediated *t*-BuOOH decomposition and formation of *t*-BuO \cdot and $\cdot\text{CH}_3$: a nucleophilic reaction may take place between DCBQ and *t*-BuOOH, forming a CBQ-OO-*t*-Bu intermediate, which can decompose homolytically to produce *t*-BuO \cdot and 2-chloro-5-hydroxy-1,4-benzoquinone radical (CBQ-O \cdot). CBQ-O \cdot then disproportionates to form the ionic form of 2-chloro-5-hydroxy-1,4-benzoquinone (CBQ-O $^-$), and $\cdot\text{CH}_3$ can be produced through β -scission of *t*-BuO \cdot (Figure 13). It should be noted that CBQ-O \cdot could not be detected under current experimental conditions. The reason may be that either its half-life span is too short, or its steady-state concentration is too low.

These findings suggest that the chlorinated quinones may react with lipid hydroperoxides and exert toxic effects through enhanced production of

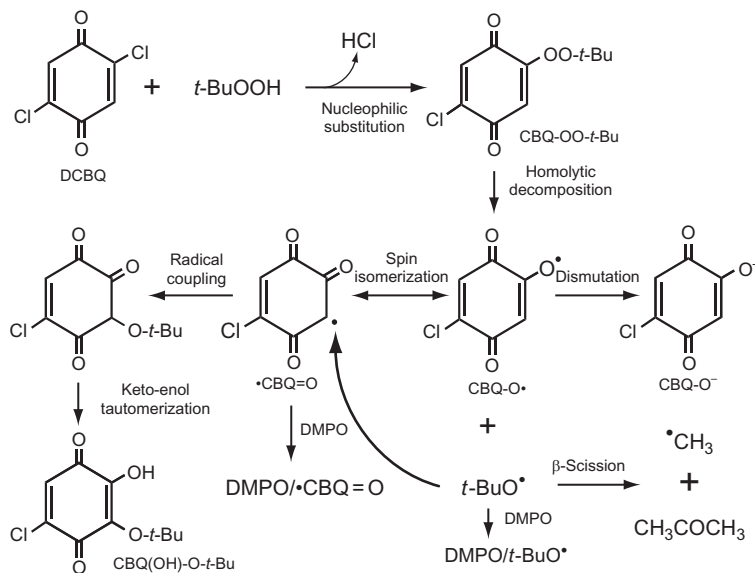


Figure 13 Proposed mechanism for DCBQ-mediated *t*-BuOOH decomposition and formation of the novel carbon-centered quinone ketoxy radical and the final reaction product CBQ(OH)-O-*t*-Bu (modified based on Ref. [80]).

alkoxyl radicals, and hence increased lipid peroxidation. Additional work is needed to investigate whether these reactions occur and are relevant under physiological conditions or *in vivo*.

4.4. Detection and identification of a key quinone ketoxy radical intermediate

In the above studies, we found that halogenated quinones could enhance the decomposition of hydroperoxides and formation of alkoxy/hydroxyl radicals through a metal-independent mechanism [72,79]. However, neither the major reaction products nor the proposed quinone-peroxide reaction intermediate CBQ-OO-*t*-Bu and quinone enoxy radical CBQ-O• were unambiguously identified.

Therefore, in the following study, we employed semi-preparative HPLC method in order to quickly isolate and purify the proposed unstable quinone-peroxide reaction intermediate and the major products from the reaction between DCBQ and *t*-BuOOH [80]. Two major compounds were isolated and purified. As expected, one of them was identified as CBQ-OH. The other compound was first assumed to be the quinone-peroxide reaction intermediate CBQ-OO-*t*-Bu (MW 230), since this compound was characterized by ESI-Q-TOF-MS with one-chlorine isotope clusters at *m/z* 229,

and tandem mass spectrometric analysis showed that this peak at m/z 229 could be readily fragmented to form a peak at m/z 172. Further, detailed studies on its chemical structure suggested, however, that this compound was not the expected quinone–peroxide reaction intermediate.

The NMR and IR spectral studies demonstrated that this compound may contain a hydroxyl group based on the following lines of evidence: (1) D_2O exchange experiment showed that the chemical shift at 10.74 vanished instantly after adding D_2O ; (2) its IR spectra showed one broad band at 3318 cm^{-1} , which is a distinct vibration mode for an O–H bond; and (3) it showed a characteristic purple color ($\lambda_{\text{max}} = 551\text{ nm}$) in phosphate buffer (pH 7.4), which is the typical color for hydroxylated quinones. In addition, this compound was found to be stable for at least 1 h in the reaction solution.

Based on the above analysis and other experimental data, this compound was finally identified, unexpectedly, as 2-hydroxy-3-*t*-butoxy-5-chloro-1,4-benzoquinone (CBQ(OH)-O-*t*-Bu), which is the rearranged isomer of the proposed unstable quinone–peroxide reaction intermediate CBQ-OO-*t*-Bu (for its chemical structure, see Figure 13).

This surprising finding raised two new questions: (1) Is the new reaction product CBQ(OH)-O-*t*-Bu derived directly from the unstable quinone–peroxide reaction intermediate CBQ-OO-*t*-Bu? (2) If so, what is the underlying molecular mechanism? To answer these questions, we hypothesized that the homolytical decomposition of the unstable reaction intermediate CBQ-OO-*t*-Bu could lead to the production of $t\text{-BuO}^\bullet$ and CBQ-O^\bullet . The oxygen-centered quinone enoxy radical CBQ-O^\bullet might be isomerized spontaneously to form its corresponding carbon-centered quinone ketoxy radical ($\bullet\text{CBQ} = \text{O}$), which might be more stable because it is stabilized by the resonant delocalization of the unpaired electron over the adjacent π system which contains two conjugated carbonyl groups [81]. $\bullet\text{CBQ} = \text{O}$ then may couple with $t\text{-BuO}^\bullet$ to produce the final reaction product CBQ(OH)-O-*t*-Bu via keto–enol tautomerization (Figure 13).

If the above hypothesis was correct, DMPO should compete with $\bullet\text{CBQ} = \text{O}$ to trap $t\text{-BuO}^\bullet$ since we have shown in our previous study that DMPO can trap alkoxyl radicals [79]. This will reduce the chance of $t\text{-BuO}^\bullet$ coupling to $\bullet\text{CBQ} = \text{O}$ and therefore inhibit the formation of CBQ(OH)-O-*t*-Bu accordingly. This was found to be exactly the case: The formation of CBQ(OH)-O-*t*-Bu was indeed inhibited by DMPO in a concentration-dependent manner.

Interestingly and unexpectedly, in the presence of DMPO, a new peak was observed from the reaction between DCBQ and $t\text{-BuOOH}$. This new compound was characterized by ESI-Q-TOF-MS with one-chlorine isotope peak clusters at m/z 268 (ESI negative) or at m/z 270 (ESI positive). These data indicate that the new compound might be a DMPO adduct with either the proposed quinone enoxy CBQ-O^\bullet or ketoxy $\bullet\text{CBQ} = \text{O}$ radical (MW 157) (for simplicity, this DMPO adduct was referred as DMPO-157).

To get more accurate molecular weight, elemental composition, and structural information of the DMPO radical adducts, Fourier transform ion cyclotron resonance (FTICR) mass spectrometry was used for further studies since it is one of the techniques that can provide high mass accuracy and high mass resolution [82,83]. DMPO-157 was characterized by FTICR/MS with one-chlorine isotope peak clusters at m/z 268.0383, which corresponds to the deprotonated molecule of the oxidized nitron form (theoretical mass 268.0377) of the DMPO-157 nitroxide radical adduct. The same DMPO-157 adduct was also observed when *t*-BuOOH was substituted by other hydroperoxides such as H_2O_2 and cumene hydroperoxide.

Interestingly, DMPO adducts with the corresponding quinone radical could also be detected by FTICR/MS when DCBQ was substituted by certain halogenated quinones such as 2,5-dibromo-1,4-benzoquinone (2,5-DBrBQ, characterized with one-bromine isotope peak clusters at m/z 312) and trichloro-1,4-benzoquinone (TrCBQ, characterized with two-chlorine isotope peak clusters at m/z 302), but not by other halogenated quinones such as 2,3-dichloro-, tetrachloro-, and tetrabromo-1,4-benzoquinone.

As mentioned above, the same DMPO-157 adduct could also be observed when *t*-BuOOH was substituted by H_2O_2 to react with DCBQ. According to the above hypothesis, the source and origin of the oxygen atom inserted into DMPO-157 adduct should be from hydroperoxide. To test whether this is the case, DCBQ was incubated with oxygen-17-labeled H_2O_2 ($[^{17}O]-H_2O_2$). The mass spectra of the molecular ion region of deprotonated DMPO-157, obtained with unlabeled and labeled H_2O_2 , demonstrated the shift of the molecular ion isotope cluster peaks of the unlabeled compound with 1 mass unit, as could be expected for the incorporation of ^{17}O . These results indicate that H_2O_2 is the source and origin of the oxygen atom inserted into DMPO-157 adduct.

In our previous study on DCBQ/*t*-BuOOH/DMPO system, beside the strong and predominant ESR signals for DMPO/*t*-BuO \cdot and DMPO/ \cdot CH $_3$, a minor DMPO/radical adduct with weak ESR signals was also observed, but remained unidentified [79] (Figure 12). With the new FTICR/MS data, we realized that this unidentified radical adduct might be the DMPO adduct either with the proposed oxygen-centered quinone enoxy radical CBQ-O \cdot or with its carbon-centered ketoxy spin isomer \cdot CBQ = O. However, due to the interference by the strong DMPO/*t*-BuO \cdot and DMPO/ \cdot CH $_3$ signals, only a weak four-line ESR signal with equal intensity could be observed. Thus, it is not clear just from these results whether the quinone radical trapped by DMPO is an oxygen-centered or a carbon-centered radical.

According to our previously proposed mechanism for halogenated quinone-enhanced decomposition of hydroperoxides and formation of alkoxy/hydroxyl radicals [72,79], we expect that, in the presence of DMPO, the reaction between DCBQ and H_2O_2 should produce the

same DMPO-157 radical adduct with the same FTICR/MS and ESR characteristics as from the reaction between DCBQ and *t*-BuOOH. To get rid of the interference of the strong ESR signals of DMPO/*t*-BuO \cdot and DMPO/ \cdot CH $_3$ and obtain more simple and clear ESR spectra for DMPO-157 radical adduct, we studied DCBQ/H $_2$ O $_2$ /DMPO system. As expected, a six-line ESR signal with equal intensity ($a^H = 28.8$ G; $a^N = 17.0$ G; $a^N/a^H = 0.59$) could be clearly observed in addition to the DMPO/ \cdot OH signal (Figure 14). These parameters are characteristic of the spin trapping of a carbon-centered quinone kexoxy radical \cdot CBQ = O, rather than an oxygen-centered enoxy radical CBQ-O \cdot [84]. It is interesting to note that the total width of the spectrum of DMPO-quinone kexoxy radical is unusually wide for a DMPO spin adduct. The larger a^N and a^H values of this novel spin adduct is probably due to an increase in spin density on nitrogen and a decrease in β -CH dihedral angle caused by intramolecular H-bonding from the hydroxyl hydrogen on the quinone ring to the nitroxide oxygen [85].

Similar six-line ESR signals for DMPO/carbon-centered quinone kexoxy radical adducts were also observed when DCBQ was substituted by 2,5-dibromo- and trichloro-1,4-benzoquinone, but not by 2,3-DCBQ, tetrachloro-, and tetrabromo-1,4-benzoquinone. These ESR spin-trapping results are in good agreement with the above FTICR/MS results, which suggest that in order to observe the carbon-centered quinone kexoxy radical, it is important for the halogenated quinone to contain one hydrogen atom at the *ortho*-position of halogen atom on the quinone ring.

To get more definitive evidence, the DMPO-157 nitron adduct was isolated and purified by semi-preparative HPLC, and characterized by 1 H NMR. The downfield signals at 6.26 and 6.82 ppm, corresponding to the single protons at the C3' position on CBQ-OH and C2 position on DMPO,

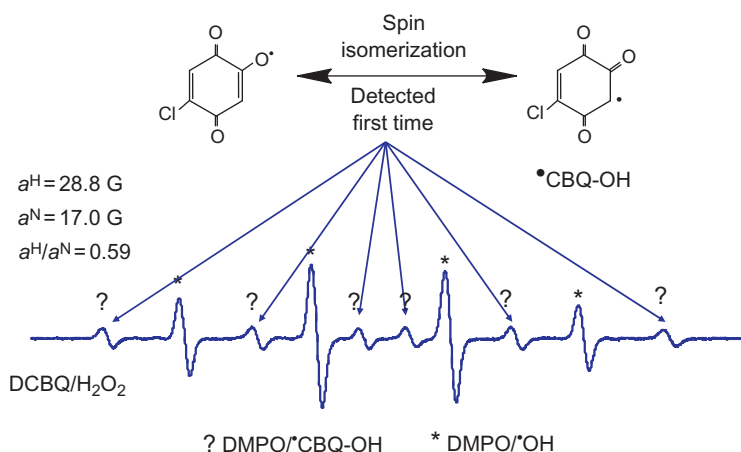


Figure 14 DMPO nitroxide adduct with the carbon-centered quinone kexoxy radical.

respectively, was clearly missing in the spectrum of DMPO-157 nitron adduct presumably due to the formation of a new covalent bond between DMPO and CBQ-OH. The formation of this covalent bond also caused significant chemical shift changes of the neighboring proton signals, namely, the protons at the C3 position, but had little or no effect on the proton signals farther away, that is, 5,5-dimethyl protons and the protons at the C4 and C6' positions. Therefore, our NMR data provide more direct evidence to support the structural assignments of the DMPO-157 nitron adduct. To the best of our knowledge, this is the first report that a carbon-centered quinone ketoxy radical was detected and identified by the complementary application of ESR spin trapping, NMR, and FTICR/MS methods.


It should be noted, however, that although we can isolate DMPO-157 adduct with semi-preparative HPLC, no corresponding six-line ESR signal was observed with the collected fraction. The reason might be that either the DMPO-157 nitron radical adduct may not be stable enough to pass through the HPLC column and decayed to its ESR-silent nitron form during the separation process, or the concentration of the radical adduct in the collected fraction was just too low to be detected by ESR.

The detection and identification of a carbon-centered quinone ketoxy radical as one of the major radical intermediates, together with the identification of CBQ(OH)-O-*t*-Bu as one of the major reaction products from the reaction between DCBQ and *t*-BuOOH, strongly support the possible existence of its corresponding isomer, the proposed quinone-peroxide reaction intermediate CBQ-OO-*t*-Bu. However, we could not isolate and purify its nature by traditional separation methods due to its unstable nature. These results together with the identification of CBQ-OH as another major reaction product also support the possible existence of the proposed oxygen-centered quinone enoxy radical CBQ-O \cdot , although we still could not detect it directly by ESR, either due to its short half-life or due to its low steady-state concentration.

Taken together, these new results provided direct experimental evidence for the involvement of the carbon-centered quinone ketoxy radicals during metal-independent decomposition of hydroperoxides and formation of alkoxyl/hydroxyl radicals by halogenated quinones. Therefore, the previously proposed molecular mechanism was further expanded to incorporate all of our new findings with previous experimental data [80]: A nucleophilic reaction may take place between DCBQ and *t*-BuOOH, forming a quinone-peroxide reaction intermediate CBQ-OO-*t*-Bu, which can decompose homolytically to produce *t*-BuO \cdot and CBQ-O \cdot . CBQ-O \cdot then either disproportionate to form one of the major reaction product CBQ-OH or isomerizes to form the carbon-centered quinone ketoxy radical \cdot CBQ = O, which then coupled with *t*-BuO \cdot to produce another major reaction product CBQ(OH)-O-*t*-Bu via keto-enol tautomerization (Figure 13).

Our observation that not only DCBQ but also other halogenated quinones can react with both organic hydroperoxides and hydrogen peroxide to produce carbon-centered quinone ketyl radicals in addition to alkoxy/hydroxyl radicals in a metal-independent manner may also have interesting biological implications. Our data suggest that these halogenated quinones may react with hydroperoxides and exert toxic effects not only through enhanced production of alkoxy/hydroxyl radicals but also through the formation of carbon-centered quinone ketyl radicals which may react directly with critical biological macromolecules such as DNA, protein, and lipids.

Recently, H_2O_2 has been increasingly favored as an environmentally safe oxidant for remediation of the environmental pollutants such as chlorinated phenols [33–35]. In these “environmentally green” systems, H_2O_2 is often used at millimolar levels. One recent study showed 2,6-DCBQ could be detected within the first minutes and then undergone further transformations during the oxidative mineralization of 2,4,6-TCP by H_2O_2 with the catalysis of iron complexes [35]. Another study showed [74] that H_2O_2 could accelerate the rate of TCBQ decomposition by two orders of magnitude, and the rate of this reaction was too fast to measure except at acidic pH. It was suggested that peroxide-dependent decomposition pathway for halogenated quinones may be important in systems where hydroperoxide is either used or produced. However, the exact molecular mechanisms underlying such further transformations are not clear. Our new findings may provide a new perspective to better understand such transformation mechanisms during wastewater treatment or remediation process in which halogenated quinones are formed.



5. DETOXIFYING CARCINOGENIC POLYHALOGENATED QUINONES BY HYDROXAMIC ACIDS VIA AN UNUSUALLY MILD AND FACILE DOUBLE LOSSEN REARRANGEMENT MECHANISM

Hydroxamic acids have attracted considerable interest recently because of their capacity to inhibit a variety of enzymes such as metalloproteases and lipoxygenase, and transition metal-mediated oxidative stress. Some hydroxamates, such as suberoylanilide hydroxamic acid and DFO, have been used clinically for the treatment of cancer or iron-overload diseases [86–89]. Much of the activities of these hydroxamic acids were thought to be due to their metal chelating properties.

In our previous work, we found that DFO and other hydroxamic acids, but not other classic iron chelators such as DTPA, provided strong protection against PCP quinoid metabolite-induced cyto- and genotoxicity in human fibroblasts [62,63]. During our recent studies on metal-independent

decomposition of hydroperoxides by halogenated quinones, we showed that these hydroxamic acids could also markedly inhibit TCBQ-mediated hydroperoxide decomposition and hydroxyl/alkoxyl radical formation [64,65,72,79,80]. Interestingly, we found that the protection or inhibition by these hydroxamic acids was not due to their iron-chelating properties, but possibly due to their effective scavenging of the reactive TCSQ[•] and (or) their remarkable acceleration of TCBQ hydrolysis to the much less reactive and almost nontoxic DDBQ (also called chloranilic acid) [62,63].

It was a great surprise for us to find that hydroxamic acids could markedly accelerate the conversion of TCBQ to DDBQ, since we could not find a reasonable explanation based on our chemical knowledge at the time. Although we first observed the above interesting phenomenon a decade ago [62], its underlying molecular mechanism remained a puzzle. Recently, the reactions between TCBQ and hydroxamic acids were carefully reexamined, and the reaction products were isolated, purified, and unambiguously identified by HPLC/ESI-MS, NMR, and oxygen-18 isotope-labeling methods. We found, unexpectedly, that a novel double Lossen rearrangement was responsible for this unusual reaction [90].

We found that hydroxamic acids could markedly accelerate TCBQ hydrolysis to the much less toxic DDBQ (also called chloranilic acid), and among the five hydroxamic acids tested, the most effective one was BHA, with rate accelerations of up to 150,000-fold (Figure 15). In contrast, no enhancing effect was observed with *O*-methyl BHA, which clearly indicates that the free benzohydroxamate anion is essential for the dramatic acceleration of TCBQ hydrolysis to occur [90].

Analogous results were observed when TCBQ was substituted with other tetrahalogenated quinones, including tetrabromo- and tetrafluoro-1,4-benzoquinones and their corresponding hydroquinone forms, as well as tetrabromo- and tetrachloro-1,2-benzoquinones, and when BHA was substituted with other hydroxamic acids such as suberoylanilide hydroxamic acid and DFO. These findings suggest that this is a general reaction between hydroxamic acids and tetrahalogenated quinoid compounds.

Since the rate of TCBQ hydrolysis in the presence of BHA is much faster than that of its spontaneous hydrolysis, it appeared that BHA could catalyze this process. However, we found that BHA was consumed during its reaction with TCBQ, with the concurrent formation of a new compound with *m/z* at 255. This suggested that the hydroxamic acid is not a true catalyst in the TCBQ hydrolysis reaction. To better understand the underlying molecular mechanism for this reaction, the final products of BHA after reacting with TCBQ were then isolated, purified, and identified by HPLC-ESI-MS and NMR. Interestingly, *O*-phenylcarbamyl benzo-hydroxamate (I) was identified as the major reaction product of BHA, while *N*, *N'*-diphenylurea (II) as a minor product.

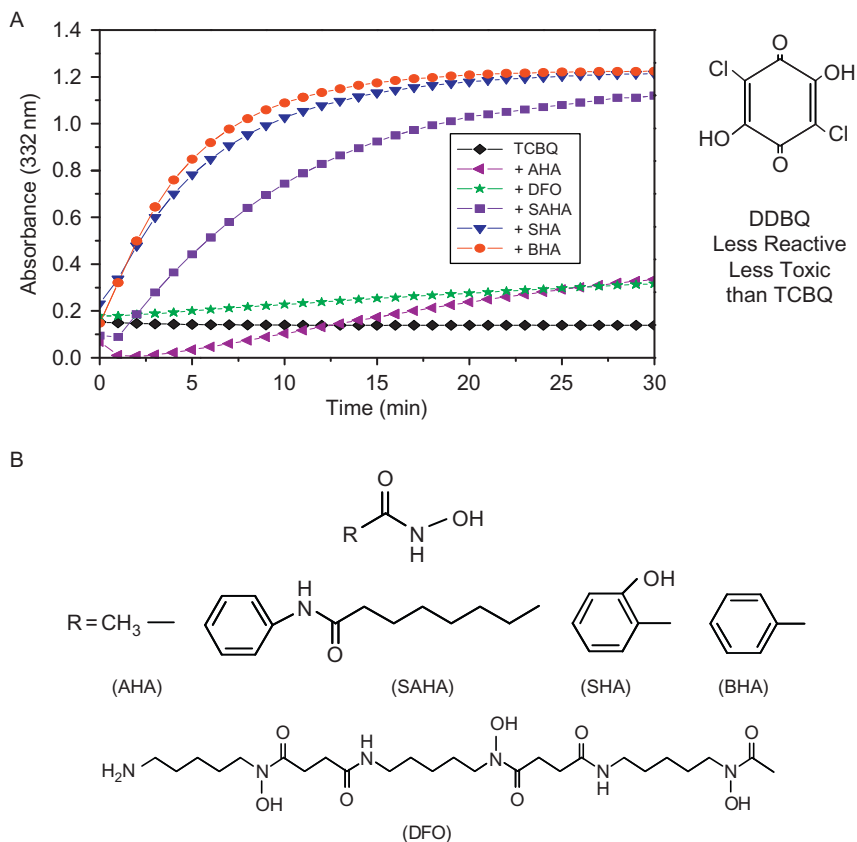


Figure 15 (A) TCBQ conversion to DDBQ was dramatically enhanced by benzohydroxamic acid (BHA) and other hydroxamic acids (HAs); (B) the chemical structures of HAs (modified based on Ref. [90]).

Then the question is: How are these products (I and II) formed? It has been shown [91,92] that product I could be formed through nucleophilic addition of phenyl isocyanate with a molecule of BHA and product II could be formed through the hydrolysis of phenyl isocyanate to aniline, followed by reaction of aniline with another molecule of phenyl isocyanate (Figure 16). The above analysis strongly suggests that phenyl isocyanate ($ArN=C=O$) should be formed as an initial unstable product during the reaction of BHA and TCBQ.

This leads to a new question: In what way could phenyl isocyanate be produced from BHA? It has been shown that one typical way could be through the classic Lossen rearrangement, a well-known reaction which describes the transformation of an *O*-activated hydroxamic acid ($RC(O)NHOX$) into the corresponding isocyanate [92,93]. The rate-limiting step

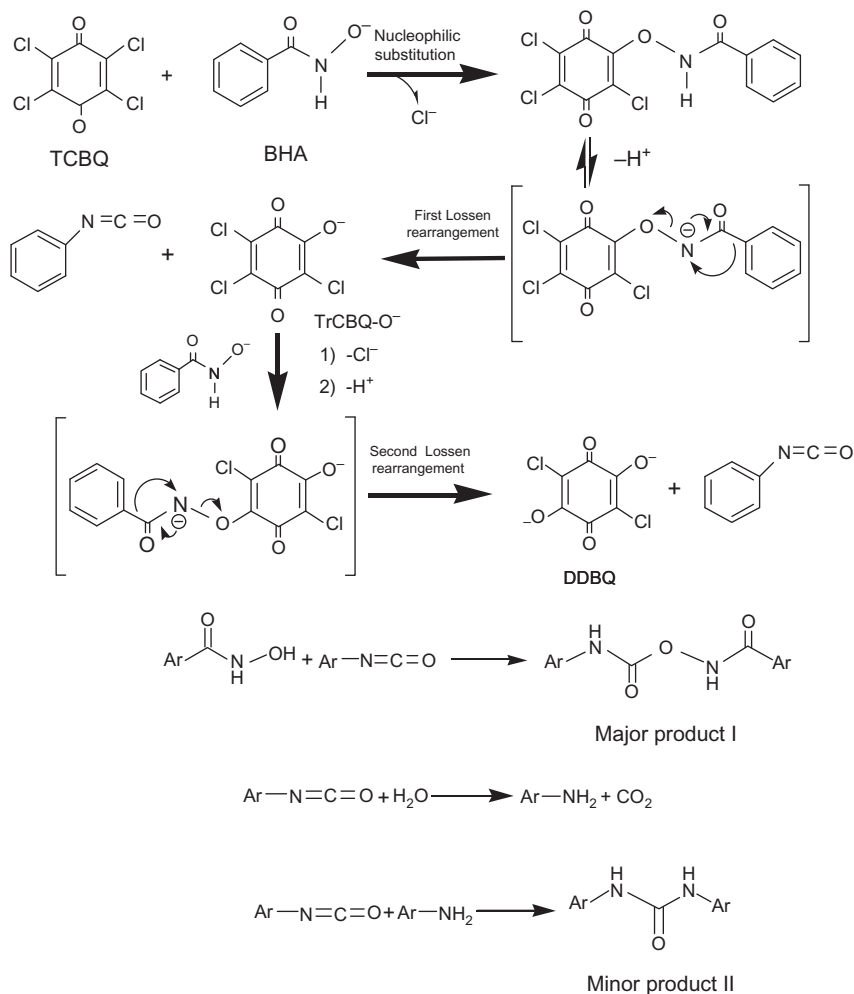
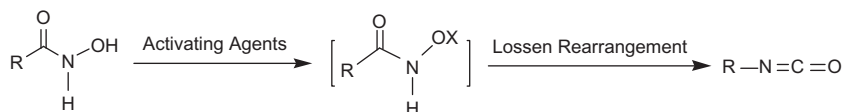


Figure 16 Proposed mechanism for the dramatic acceleration of TCBQ hydrolysis by BHA: suicidal nucleophilic attack coupled with an unusual double Lossen rearrangement (modified based on Ref. [90]).

of this reaction is the activation of the hydroxamic acid by various agents (i.e., sulfonyl and benzoyl chloride, etc.; X = SO₂R, C(O)R):



The above analysis suggested that the reaction between BHA and TCBQ might proceed through an analogous, but previously unknown Lossen-type rearrangement pathway.

Based on the above experimental results and earlier research on Lossen rearrangement [91–94], as well as the fact that the benzohydroxamate anion is a particularly effective α -nucleophile [91], a novel mechanism for BHA-accelerated TCBQ hydrolysis was proposed (Figure 16). According to the mechanism, a nucleophilic reaction takes place between the benzohydroxamate anion (ArC(O)NHO^-) and TCBQ, first forming an unstable transient intermediate ArC(O)NHOTrCBQ . Following loss of a proton from nitrogen to form the anionic $\text{ArC(O)N}^-\text{OTrCBQ}$ intermediate, a spontaneous Lossen-type rearrangement leads to the formation of TrCBQ-O^- (at low BHA/TCBQ molar ratios) and phenyl isocyanate. When BHA is in excess, TrCBQ-O^- further reacts with BHA, through a similar reaction intermediate, and a second-step spontaneous Lossen-type rearrangement reaction yields DDBQ and another molecule of phenyl isocyanate [90]. As mentioned above, phenyl isocyanate could react with another molecule of BHA to yield the major reaction product I.

If the above proposed double Lossen rearrangement mechanism is correct, then we expect that the source and origin of the oxygen atom in DDBQ and product I from the reaction of TCBQ (or TrCBQ-OH) with BHA should be from the hydroxyl group of BHA, not from water. To test whether this is the case, TCBQ (or TrCBQ-OH) was incubated with BHA in buffer solution prepared with oxygen-18-labeled H_2O ($[\text{}^{18}\text{O}]\text{-H}_2\text{O}$) as solvent. If water is the source of the oxygen atom in any of the products, the mass spectra of the molecular ion region of DDBQ and product I, obtained with unlabeled and labeled H_2O , should show the shift of the molecular ion isotope cluster peaks of the unlabeled compounds with 2 or 4 mass units, as could be expected for the incorporation of ^{18}O . However, no ^{18}O was found to be incorporated in any of these products. These isotope-labeling data provide strong experimental evidence to further support the above proposed mechanism.

Most of the previously reported Lossen rearrangement reactions take place only under alkaline conditions and/or through heating to a requisite temperature [91–94]. In the present study, we found that the reaction between BHA and TCBQ could occur at room temperature and under neutral or even weakly acidic pH. This is possibly due to the unusually rapid and facile rearrangement of the postulated reaction intermediate, the O-trichloroquinonated BHA.

We found that this unusual double rearrangement reaction mechanism is not only limited to TCBQ and BHA, but it is also a general mechanism for all tetrahalogenated quinonoid compounds and hydroxamic acids. Therefore, our findings may have interesting biological and environmental implications: Many widely used polyhalogenated aromatic compounds can be

metabolized *in vivo* [23,37,95–97], or dehalogenated chemically and enzymatically [33–35], to their corresponding quinones. Polychlorinated quinoid compounds were also found in discharges from pulp and paper mills [20–23]. More recently, several polyhalogenated quinones, which are suspected bladder carcinogens, were identified as new chlorination disinfection byproducts in drinking water [98]. These polyhalogenated quinones not only cause oxidative damage to DNA and other macromolecules but also form protein and DNA adducts both *in vitro* and *in vivo* [20–23,37]. Thus, these molecules are potential mammalian carcinogens, which render their destruction or remediation under mild conditions of critical importance.

Of particular interest in this regard is the fact that two hydroxamic acids are already approved for clinical applications, DFO for iron overload and suberoylanilide hydroxyamic acid (also called Vorinostat), recently approved for cutaneous T-cell lymphoma [86–89]. As demonstrated in the present and our previous studies [62–65,72,76,79,80], these compounds, in addition to BHA, might be especially suited for detoxication of polyhalogenated quinones. It is worth noting that hydroxamic acids can also efficiently inhibit hexachlorobenzene-induced porphyria [99] and detoxify chemical warfare agents such as the nerve gases Sarin and Soman (which are fluorinated organophosphonates) [92,93,100], as well as nitrogen mustard [101] in animal models, possibly through an analogous Lossen rearrangement mechanism. Therefore, suicidal nucleophilic attack coupled with spontaneous Lossen rearrangement may serve as a general, but previously unrecognized new detoxication mechanism for the widely used hydroxamic acids. Therefore, our findings may have broad chemical, biological, and environmental implications for future research on polyhalogenated aromatic pollutants and hydroxamic acids, which are two important classes of compounds of major environmental and biomedical concern that have been attracting the attention of both academic researchers, and the broader general public.

6. CONCLUSIONS AND FUTURE RESEARCH

The above findings represent a novel mechanism of $\bullet\text{OH}$ and alkoxy radical formation not requiring the involvement of redox-active transition metal ions, and may partly explain the potential carcinogenicity of not only PCP, but also other widely used polyhalogenated aromatic compounds such as 2,4,6- and 2,4,5-TCP, hexachlorobenzene, Agent Orange (the mixture of 2,4,5-T and 2,4-D) and the brominated flame-retardant 3,3',5,5'-tetrabromobisphenol A (TBBPA), since these compounds can be metabolized *in vivo* [20–23,95,99,102–105], or dechlorinated chemically to tetra-, di- or mono-halogenated quinones. Our data suggest that TCBQ and other

halogenated quinones may react with hydroperoxides and exert toxic effects through enhanced production of hydroxyl/alkoxyl radicals, and hence increased DNA, protein, and lipid oxidation. We also found that hydroxamic acids could detoxify TCBQ and other polyhalogenated quinoid carcinogens via a novel two-step Lossen rearrangement mechanism. The two clinically used hydroxyamic acids (DFO and suberoylanilide hydroxamic acid (Vorinostat)) might be used as prophylactics for the prevention or treatment of human diseases such as liver and bladder cancer associated with the toxicity of polyhalogenated quinoid carcinogens.

It should be noted, however, that many questions still need to be addressed, especially regarding the biological relevance of the reactions under study. For example, “How does the reaction of the quinone with H_2O_2 compare kinetically with reactions with other good nucleophiles such as GSH and other thiols which are present at high concentrations *in vivo*?” What is the rate constant for the reaction between TCBQ and H_2O_2 , and could it be able to compete with the classic Fenton reaction? Could $\bullet OH$ produced by this pathway be detected in cell culture or even in an animal model? Could a more stable carbon-centered quinone ketoxy radical adduct with the corresponding clean nitroxide ESR signal be isolated and purified using other spin-trapping agents? Could the proposed oxygen-centered quinone enoxy radical and the quinone–peroxide intermediate be detected by a freeze–quenching technique? Could the carbon-centered quinone ketoxy radical react with macromolecules such as DNA, protein, and lipids? Could hydroxamic acids provide protection against PCP-induced genotoxicity in animal models?

ACKNOWLEDGMENTS

The work in this chapter was supported by Project 973 (2008CB418106); Hundred-Talent Project, CAS; NSFC Grants (20925724, 20777080, 20877081, 20890112, and 20921063); Golda Meir Fellowships from The Hebrew University of Jerusalem; and NIH grants ES11497, RR01008, and ES00210.

REFERENCES

- [1] U.G. Ahlborg, T.M. Thunberg, Chlorinated phenols: Occurrence, toxicity, metabolism, and environmental impact, *Crit. Rev. Toxicol.* 7 (1980) 1–35.
- [2] IARC, IARC Monographs on the Evaluation of Carcinogenic Risks of Chemicals to Humans: Some Halogenated Hydrocarbons and Pesticide Exposure. Occupational Exposures Chlorophenols, vol. 41, IARC, Lyon, 1986, pp. 319–356.
- [3] S. Ramamoorthy, S. Ramamoorthy, Chlorinated Organic Compounds in the Environment, CRC Press, Boca Raton, FL, 1997.

- [4] M. Pera-Titus, V. Garcia-Molina, M.A. Banos, J. Gimenez, S. Esplugas, Degradation of chlorophenols by means of advanced oxidation processes: A general review, *Appl. Catal. B* 47 (2004) 219–256.
- [5] Agency for Toxic Substances and Disease Registry (ATSDR), Toxicological Profile for Chlorophenols, U.S. Department of Health and Human Services, Public Health Service, Atlanta, GA, 2010. Update.
- [6] J. Gao, L. Liu, X. Liu, H. Zhou, S. Huang, Z. Wang, Levels and spatial distribution of chlorophenols—2,4-Dichlorophenol, 2,4,6-trichlorophenol, and pentachlorophenol in surface water of China, *Chemosphere* 71 (2008) 1181–1187.
- [7] D.M. DeMarini, H.G. Brooks, D.G. Parks Jr., Induction of prophage lambda by chlorophenols, *Environ. Mol. Mutagen.* 15 (1990) 1–9.
- [8] G. Schuurmann, R.K. Somashekar, U. Kristen, Structure–activity relationships for chloro- and nitrophenol toxicity in the pollen tube growth test, *Environ. Toxicol. Chem.* 15 (1996) 1702–1708.
- [9] J. Han, R.L. Deming, F.-M. Tao, Theoretical study of molecular structures and properties of the complete series of chlorophenols, *J. Phys. Chem. A* 108 (2004) 7736–7743.
- [10] T. Kishino, K. Kobayashi, Relation between the chemical structures of chlorophenols and their dissociation constants and partition coefficients in several solvent–water systems, *Water Res.* 28 (1994) 1547–1552.
- [11] R.C. Loehr, R. Krishnamoorthy, Terrestrial bioaccumulation potential of phenolic compounds, *Hazard. Waste Hazard. Mater.* 5 (1988) 109–119.
- [12] Agency for Toxic Substances and Disease Registry (ATSDR), Toxicological Profile for Pentachlorophenol, U.S. Department of Health and Human Services, Public Health Service, Atlanta, GA, 2010. Update.
- [13] A.T. Proudfoot, Pentachlorophenol poisoning, *Toxicol. Rev.* 22 (2003) 3–11.
- [14] D. McLean, A. Eng, E. Dryson, C. Walls, E. Harding, K.C. Wong, S. Cheng, A. Mannetje, L. Ellison-Loschmann, T. Slater, P. Shoemack, N. Pearce, Morbidity in former sawmill workers exposed to pentachlorophenol (PCP): A cross-sectional study in New Zealand, *Am. J. Ind. Med.* 52 (2009) 271–281.
- [15] P.A. Scherr, G.B. Hutchison, R.S. Neiman, Non-Hodgkin's lymphoma and occupational exposure, *Cancer Res.* 52 (1992) 5503s–5509s.
- [16] NTP, NTP technical report on the toxicology and carcinogenesis studies of two pentachlorophenol technical grade mixtures (CAS no. 87-86-5) in B6C3F1 mice (feed studies). National Toxicology Program, Research Triangle Park, NC, 1989 NTP TR 349, NIH publication no. 89-2804.
- [17] NTP, Toxicology and Carcinogenesis Studies of Pentachlorophenol (CAS no. 87-86-5) in F344/N rats (Feed Studies). National Institutes of Health, Public Health Service, U.S. Department of Health and Human Services, National Toxicology Program, Research Triangle Park, NC, 1999 NTP TR 483, NIH publication no. 99-3973.
- [18] IRIS, Integrated risk information systems, Office of Health and Environmental Assessment, Environmental Criteria and Assessment Office, U.S. Environmental Protection Agency, Cincinnati, OH, 2001.
- [19] G.S. Cooper, S. Jones, Pentachlorophenol and cancer risk: Focusing the lens on specific chlorophenols and contaminants, *Environ. Health Perspect.* 116 (2008) 1001–1008.
- [20] K.R. Rao, Pentachlorophenol: Chemistry, Pharmacology, and Environmental Toxicology, Plenum, New York, 1987.
- [21] IARC, Pentachlorophenol. in: IARC Monographs on the Evaluation of Carcinogenic Risks to Humans: Occupational Exposures in Insecticide Application, and Some Pesticides, vol. 53, IARC, Lyon, 1991, pp. 371–402.
- [22] J.P. Seiler, Pentachlorophenol, *Mutat. Res.* 257 (1991) 27–47.

- [23] B.-Z. Zhu, G.-Q. Shan, Potential mechanism for pentachlorophenol-Induced carcinogenicity: A novel mechanism for metal-independent production of hydroxyl radicals, *Chem. Res. Toxicol.* 22 (2009) 969–977.
- [24] E.E. McConnell, J.E. Huff, M. Hejtmancik, A.C. Peters, R. Persing, Toxicology and carcinogenesis studies of two grades of pentachlorophenol in B6C3F1 mice, *Fundam. Appl. Toxicol.* 17 (1991) 519–532.
- [25] R.S. Chhabra, R.M. Maronpot, J.R. Bucher, J.K. Haseman, J.D. Toft, M.R. Hejtmancik, Toxicology and carcinogenesis studies of pentachlorophenol in rats, *Toxicol. Sci.* 48 (1999) 14–20.
- [26] G. Renner, W. Mucke, Transformations of pentachlorophenol. Part I: Metabolism in animals and man, *Toxicol. Environ. Chem.* 11 (1986) 9–29.
- [27] G. Renner, C. Hopfer, Metabolic studies of pentachlorophenol (PCP) in rats, *Xenobiotica* 20 (1990) 573–582.
- [28] B.G. Reigner, J.F. Rigod, T.N. Tozer, Disposition, bioavailability, and serum protein binding of pentachlorophenol in the B6C3F1 mouse, *Pharm. Res.* 9 (1992) 1053–1057.
- [29] P.H. Lin, S. Waidyanatha, G.M. Pollack, S.M. Rappaport, Dosimetry of chlorinated quinone metabolites of pentachlorophenol in the livers of rats and mice based upon measurement of protein adducts, *Toxicol. Appl. Pharmacol.* 145 (1997) 399–408.
- [30] C.H. Tsai, P.H. Lin, S. Waidyanatha, S.M. Rappaport, Fractionation of protein adducts in rats and mice dosed with [^{14}C]pentachlorophenol, *Arch. Toxicol.* 76 (2002) 628–633.
- [31] C.P. Carstens, J.K. Blum, I. Witte, The role of hydroxyl radicals in tetrachlorohydroquinone induced DNA strand break formation in PM2 DNA and human fibroblasts, *Chem. Biol. Interact.* 74 (1990) 305–314.
- [32] R.A. Manderville, A. Pfohl-Leszkowicz, Genotoxicity of chlorophenols and ochratoxin A, in: J.C. Fishbein (Ed.), *Advances Molecular Toxicology*, Elsevier, Amsterdam, 2006, pp. 85–138.
- [33] B. Meunier, Catalytic degradation of chlorinated phenols, *Science* 296 (2002) 270–271.
- [34] S.S. Gupta, M. Stadler, C.A. Noser, A. Ghosh, B. Steinhoff, D. Lenoir, C.P. Horwitz, K.W. Schramm, T.J. Collins, Rapid total destruction of chlorophenols by activated hydrogen peroxide, *Science* 296 (2002) 326–328.
- [35] A. Sorokin, J.L. Seris, B. Meunier, Efficient oxidative dechlorination and aromatic ring-cleavage of chlorinated phenols catalyzed by iron sulphophthalocyanine, *Science* 268 (1995) 1163–1166.
- [36] P.-H. Lin, S. Waidyanatha, G.M. Pollack, J.A. Swenberg, S.M. Rappaport, Dose specific production of chlorinated quinone and semiquinone adducts in rodent livers following administration of pentachlorophenol, *Toxicol. Sci.* 47 (1999) 126–133.
- [37] J.L. Bolton, M.A. Trush, T.M. Penning, G. Dryhurst, T.J. Monks, Role of quinones in toxicology, *Chem. Res. Toxicol.* 13 (2000) 135–160.
- [38] P.J. O'Brien, Molecular mechanisms of quinone cytotoxicity, *Chem. Biol. Interact.* 80 (1991) 1–41.
- [39] B. Halliwell, J.M.C. Gutteridge, *Free Radicals in Biology and Medicine*, Oxford University Press, New York, 2007.
- [40] I. Witte, U. Juhl, W. Butte, DNA-damaging properties and cytotoxicity in human fibroblasts of tetrachlorohydroquinone, a pentachlorophenol metabolite, *Mutat. Res.* 145 (1985) 71–75.
- [41] M. Dahlhaus, E. Almstadt, P. Henachke, S. Luttgert, K.E. Appel, Oxidative DNA lesions in V79 cells mediated by pentachlorophenol metabolites, *Arch. Toxicol.* 70 (1996) 457–460.

- [42] W. Ehrlich, The effect of pentachlorophenol and its metabolite tetrachlorohydroquinone on cell growth and the induction of DNA damage in Chinese hamster ovary cells, *Mutat. Res.* 244 (1990) 299–302.
- [43] M. Dahlhaus, E. Almstadt, K.E. Appel, The pentachlorophenol metabolite tetrachloro-*p*-hydroquinone induces the formation of 8-hydroxy-2-deoxyguanosine in liver DNA of male B6C3F1 mice, *Toxicol. Lett.* 74 (1994) 265–274.
- [44] Y.J. Wang, Y.S. Ho, S.W. Chu, H.J. Lien, T.H. Liu, J.K. Lin, Induction of glutathione depletion, p53 protein accumulation and cellular transformation by tetrachlorohydroquinone, a toxic metabolite of pentachlorophenol, *Chem. Biol. Interact.* 105 (1997) 1–16.
- [45] K. Jansson, V. Jansson, Induction of micronuclei in V79 Chinese hamster cells by tetrachlorohydroquinone, a metabolite of pentachlorophenol, *Mutat. Res.* 279 (1992) 205–208.
- [46] M. Purschke, H. Jacobi, I. Witte, Differences in genotoxicity of H₂O₂ and tetrachlorohydroquinone in human fibroblasts, *Mutat. Res.* 513 (2002) 159–167.
- [47] M. Dahlhaus, E. Almstadt, P. Henschke, S. Luttgert, K.E. Appel, Induction of 8-hydroxy-2-deoxyguanosine and single strand breaks in DNA of V79 cells by tetrachloro-*p*-hydroquinone, *Mutat. Res.* 329 (1995) 29–36.
- [48] P.H. Lin, J. Nakamura, S. Yamaguchi, D.K. La, P.B. Upton, J.A. Swenberg, Induction of direct adducts, apurinic/apyrimidinic sites and oxidized bases in nuclear DNA of human HeLa S3 tumor cells by tetrachlorohydroquinone, *Carcinogenesis* 22 (2001) 635–639.
- [49] P.H. Lin, D.K. La, P.B. Upton, J.A. Swenberg, Analysis of DNA adducts in rats exposed to pentachlorophenol, *Carcinogenesis* 23 (2002) 365–369.
- [50] A.P. Breen, J.A. Murphy, Reactions of oxyl radicals with DNA, *Free Radic. Biol. Med.* 18 (1995) 1033–1077.
- [51] B. Balasubramanian, W.K. Pogozelski, T.D. Tullius, DNA strand breaking by the hydroxyl radical is governed by the accessible surface areas of the hydrogen atoms of the DNA backbone, *Proc. Natl. Acad. Sci. USA* 95 (1998) 9738–9743.
- [52] J. Nakamura, D.K. La, J.A. Swenberg, 5'-Nicked apurinic/apyrimidinic sites are resistant to β -elimination by β -polymerase and are persistent in human cultured cells after oxidative stress, *J. Biol. Chem.* 275 (2000) 5323–5328.
- [53] P.H. Lin, J. Nakamura, S. Yamaguchi, D.K. La, P.B. Upton, J.A. Swenberg, Oxidative damage and direct adducts in calf thymus DNA induced by tetrachlorohydroquinone and tetrachloro-1,4-benzoquinone, *Carcinogenesis* 22 (2001) 627–634.
- [54] W.J. Bodell, Q. Ye, D.N. Pathak, K. Pongracz, Oxidation of eugenol to form DNA adducts and 8-hydroxy-2'-deoxyguanosine: Role of quinone methide derivative in DNA adduct formation, *Carcinogenesis* 19 (1998) 437–443.
- [55] T.N. Nguyen, A.B. Bertagnolli, P.W. Villalta, P. Buhlmann, S.J. Sturla, Characterization of a deoxyguanosine adduct of tetrachlorobenzoquinone: dichlorobenzoquinone-1, *N*'-etheno-2'-deoxyguanosine, *Chem. Res. Toxicol.* 18 (2005) 1770–1776.
- [56] V.G. Vaidyanathan, P.W. Villalta, S.J. Sturla, Nucleobase-dependent reactivity of a quinone metabolite of pentachlorophenol, *Chem. Res. Toxicol.* 20 (2007) 913–919.
- [57] J.-C. Gautier, J. Richoz, D.H. Welti, J. Markovik, E. Gremaud, F.P. Guengerich, R.J. Turesky, Metabolism of ochratoxin A: Absence of formation of genotoxic derivatives by human and rat enzymes, *Chem. Res. Toxicol.* 14 (2001) 34–45.
- [58] J. Dai, M.W. Wright, R.A. Manderville, An oxygen-bonded C8-deoxy-guanosine nucleoside adduct of pentachlorophenol by peroxidase activation: Evidence for ambident C8 reactivity by phenoxyl radicals, *Chem. Res. Toxicol.* 16 (2003) 817–821.
- [59] J. Dai, A.L. Sloat, M.W. Wright, R.A. Manderville, Role of phenoxyl radicals in DNA adduction by chlorophenol xenobiotics following peroxidase activation, *Chem. Res. Toxicol.* 18 (2005) 771–779.

- [60] Y.P. Lin, B.-Z. Zhu, M.C. Yang, B. Frei, M.S. Pan, J.K. Lin, Y.J. Wang, Bcl-2 over-expression inhibits pentachlorophenol metabolite-induced apoptosis in NIH3T3 cells: A possible mechanism for tumor promotion, *Mol. Carcinog.* 40 (2004) 24–33.
- [61] K. Sai-Kato, T. Umemura, A. Takagi, R. Hasegawa, A. Tanimura, Y. Kurokawa, Pentachlorophenol-induced oxidative DNA damage in mouse liver and protective effect of antioxidants, *Food Chem. Toxicol.* 33 (1995) 877–882.
- [62] B.-Z. Zhu, R. Har-El, N. Kitrossky, M. Chevion, New modes of action of desferrioxamine: scavenging of semiquinone radical and stimulation of hydrolysis of tetrachlorohydroquinone, *Free Radic. Biol. Med.* 24 (1998) 360–369.
- [63] I. Witte, B.-Z. Zhu, A. Lueken, D. Magnani, H. Stossberg, M. Chevion, Protection by desferrioxamine and other hydroxamic acids against tetrachlorohydroquinone-induced cyto- and genotoxicity in human fibroblasts, *Free Radic. Biol. Med.* 28 (2000) 693–700.
- [64] B.-Z. Zhu, N. Kitrossky, M. Chevion, Evidence for production of hydroxyl radicals by pentachlorophenol metabolites and hydrogen peroxide: A metal-independent organic Fenton reaction, *Biochem. Biophys. Res. Commun.* 270 (2000) 942–946.
- [65] B.-Z. Zhu, H.T. Zhao, B. Kalyanaraman, B. Frei, Metal-independent production of hydroxyl radicals by chlorinated quinones and hydrogen peroxide: An ESR spin-trapping study, *Free Radic. Biol. Med.* 32 (2002) 465–473.
- [66] A. Mohindru, J.M. Fisher, M. Rabinowitz, Bathocuproine sulphonate: A tissue culture-compatible indicator of copper-mediated toxicity, *Nature* 303 (1983) 64–65.
- [67] E. Graf, J.R. Mahoney, R.G. Bryant, J.W. Eaton, Iron-catalyzed hydroxyl radical formation. Stringent requirement for free iron coordination site, *J. Biol. Chem.* 259 (1984) 3620–3624.
- [68] R.T. Dean, P. Nicholson, The action of nine chelators on iron-dependent radical damage, *Free Radic. Res.* 20 (1994) 83–101.
- [69] W.H. Koppenol, J. Butler, Energetics in interconversion reactions of oxyradicals, *Adv. Free Radic. Biol. Med.* 1 (1985) 91–131.
- [70] H. Nohl, W. Jordan, The involvement of biological quinones in the formation of hydroxyl radicals via the Haber-Weiss reaction, *Bioorg. Chem.* 15 (1987) 374–382.
- [71] M.E. Peover, A polarographic investigation into the redox behavior of quinones: The role of electron affinity and solvent, *J. Chem. Soc.* (1962) 4540–4549, Part 3.
- [72] B.-Z. Zhu, B. Kalyanaraman, G. Jiang, Molecular mechanism for metal-independent production of hydroxyl radicals by hydrogen peroxide and halogenated quinones, *Proc. Natl. Acad. Sci. USA* 104 (2007) 17575–17578.
- [73] J.W. Hancock, C.E. Morrell, D. Rhum, Trichlorohydroquinone, *Tetrahedron Lett.* 22 (1962) 987–988.
- [74] D.H. Sarr, C. Kazunga, M.J. Charles, J.G. Pavlovich, M.D. Aitken, Decomposition of tetrachloro-1,4-benzoquinone (*P*-chloranil) in aqueous solution, *Environ. Sci. Technol.* 29 (1995) 2735–2740.
- [75] R. Curci, J.O. Edwards, Activation of hydrogen peroxide by organic compounds, in: G. Strukul (Ed.), *Catalytic Oxidations with Hydrogen Peroxide as Oxidant*, Kluwer Academic Publishers, Dordrecht, 1992, pp. 57–60.
- [76] S. Jia, B.-Z. Zhu, L.H. Guo, Detection and mechanistic investigation of halogenated benzoquinone induced DNA damage by photoelectrochemical DNA sensor, *Anal. Bioanal. Chem.* 397 (2010) 2395–2400.
- [77] Y. Luo, X.R. Wang, L.L. Ji, Y. Su, EPR detection of hydroxyl radical generation and its interaction with antioxidant system in *Carassius auratus* exposed to pentachlorophenol, *J. Hazard. Mater.* 171 (2009) 1096–1102.
- [78] L.J. Marnett, Oxyradicals and DNA damage, *Carcinogenesis* 21 (2000) 361–370.
- [79] B.-Z. Zhu, H.-T. Zhao, B. Kalyanaraman, J. Liu, G.-Q. Shan, Y.-G. Du, B. Frei, Mechanism of metal-independent decomposition of organic hydroperoxides and

- formation of alkoxy radicals by halogenated quinones, *Proc. Natl. Acad. Sci. USA* 104 (2007) 3698–3702.
- [80] B.-Z. Zhu, G.-Q. Shan, C.-H. Huang, B. Kalyanaraman, L. Mao, Y.-G. Du, Metal-independent decomposition of hydroperoxides by halogenated quinones: Detection and identification of a quinone ketoxy radical, *Proc. Natl. Acad. Sci. USA* 106 (2009) 11466–11471.
- [81] H. Zipse, in: A. Gansaeuer (Ed.), *Radical Stability- A Theoretical Perspective*, Topics in Current Chemistry, Springer-Verlag GmbH, Berlin Heidelberg, 2006, pp. 163–189.
- [82] D.A. Laude, *Electrospray Ionization/Fourier Transform Ion Cyclotron Resonance Mass Spectrometry*, *Electrospray Ionization Mass Spectrometry: Fundamentals, Instrumentation, and Applications*, John Wiley and Sons, Inc., New York, 1997, pp. 291–320.
- [83] L. Cui, M.A. Isbell, Y. Chawengsub, J.R. Falck, W.B. Campbell, K. Nithipatikom, Structural characterization of monohydroxyeicosatetraenoic acids and dihydroxy- and trihydroxyeicosatrienoic acids by ESI-FTICR, *J. Am. Soc. Mass Spectrom.* 19 (2008) 569–585.
- [84] A.S. Li, C.F.J. Chignell, The NoH value in EPR spin trapping: A new parameter for the identification of 5,5-dimethyl-1-pyrroline-N-oxide spin adducts, *Biochem. Biophys. Methods* 22 (1991) 83–87.
- [85] E.D. Janzen, J.I.P. Liu, Radical addition reactions of 5,5-dimethyl-1-pyrroline-1-oxide. ESR spin trapping with a cyclic nitron, *J. Magn. Reson.* 9 (1973) 510–512.
- [86] Y. Yu, J. Wong, D.B. Lovejoy, D.S. Kalinowski, D.R. Richardson, Chelators at the cancer coalface: Desferrioxamine to triapine and beyond, *Clin. Cancer Res.* 12 (2006) 6876–6883.
- [87] P.A. Marks, R. Breslow, Dimethyl sulfoxide to vorinostat: Development of this histone deacetylase inhibitor as an anticancer drug, *Nat. Biotechnol.* 25 (2007) 84–90.
- [88] N. Li, D. Zhao, M. Kirschbaum, C. Zhang, C.L. Lin, I. Todorov, F. Kandeel, S. Forman, D. Zeng, HDAC inhibitor reduces cytokine storm and facilitates induction of chimerism that reverses lupus in anti-CD3 conditioning regimen, *Proc. Natl. Acad. Sci. USA* 105 (2008) 4796–4801.
- [89] C. Choudhary, C. Kumar, F. Gnad, M.L. Nielsen, M. Rehman, T.C. Walther, J.V. Olsen, M. Mann, Lysine acetylation targets protein complexes and co-regulates major cellular functions, *Science* 325 (2009) 834–840.
- [90] B.-Z. Zhu, J.-G. Zhu, B. Kalyanaraman, L. Mao, G.Q. Shan, Detoxifying polyhalogenated quinones by hydroxamic acids via an unusual double Lossen rearrangement, *Proc. Natl. Acad. Sci. USA* 107 (2010) 20686–20690.
- [91] E.S. Orth, P.L. da Silva, R.S. Mello, C.A. Bunton, H.M. Milagre, M.N. Eberlin, H.D. Fiedler, F. Nome, Suicide nucleophilic attack: Reactions of benzohydroxamate anion with bis(2,4-dinitrophenyl) phosphate, *J. Org. Chem.* 74 (2009) 5011–5016.
- [92] L. Bauer, O. Exner, Chemistry of hydroxamic acids and *N*-hydroxyimides, *Angew. Chem. Int. Ed. Engl.* 13 (1974) 376–384.
- [93] M.M.A. Pereira, P.P. Santos, in: Z. Rappoport, J.F. Liebman (Eds.), *Rearrangements of Hydroxylamines, Oximes and Hydroxamic Acids*, *The Chemistry of Hydroxylamines, Oximes and Hydroxamic Acids*, John Wiley & Sons, Ltd, Chichester, 2009, pp. 343–499.
- [94] P. Dubé, N.F. Nathel, M. Vetelino, M. Couturier, C.L. Aboussafy, S. Pichette, M.L. Jorgensen, M. Hardink, Carbonyldiimidazole-mediated Lossen rearrangement, *Org. Lett.* 11 (2009) 5622–5625.
- [95] C.F. Chignell, S.K. Han, A. Mouithys-Mickalad, R.H. Sik, K. Stadler, M.B. Kadiiska, EPR studies of in vivo radical production by 3,3',5,5'-tetrabromobisphenol A (TBBPA) in the Sprague-Dawley rat, *Toxicol. Appl. Pharmacol.* 230 (2008) 17–22.
- [96] E.L. Teuten, L. Xu, C.M. Reddy, Two abundant bioaccumulated halogenated compounds are natural products, *Science* 307 (2005) 917–920.

- [97] B.C. Kelly, M.G. Ikononou, J.D. Blair, A.E. Morin, F.A. Gobas, Food web-specific biomagnification of persistent organic pollutants, *Science* 317 (2007) 236–239.
- [98] Y.L. Zhao, F. Qin, J.M. Boyd, J. Anichina, X.F. Li, Characterization and determination of chloro- and bromo-benzoquinones as new chlorination disinfection byproducts in drinking water, *Anal. Chem.* 82 (2010) 4599–4605.
- [99] R. Wainstock de Calmanovici, S.C. Billi, C.A. Aldonatti, L.C. San Martín de Viale, Effect of desferrioxamine on the development of hexachlorobenzene-induced porphyria, *Biochem. Pharmacol.* 35 (1986) 2399–2405.
- [100] L. Bromberg, H. Schreuder-Gibson, W.R. Creasy, D.J. McGarvey, R.A. Fry, T.A. Hatton, Degradation of chemical warfare agents by reactive polymers, *Ind. Eng. Chem. Res.* 48 (2009) 1650–1659.
- [101] Y. Morad, E. Banin, E. Averbukh, E. Berenshtein, A. Obolensky, M. Chevion, Treatment of ocular tissues exposed to nitrogen mustard: Beneficial effect of zinc desferrioxamine combined with steroids, *Invest. Ophthalmol. Vis. Sci.* 46 (2005) 1640–1646.
- [102] R.A. Haugland, D.J. Schlemm, R.P. Lyons 3rd, P.R. Sferri, A.M. Chakrabarty, Degradation of the chlorinated phenoxyacetate herbicides 2,4-dichlorophenoxyacetic acid and 2,4,5-trichlorophenoxyacetic acid by pure and mixed bacterial cultures, *Appl. Environ. Microbiol.* 56 (1990) 1357–1362.
- [103] G. Koss, M. Losekam, J. Seidel, K. Steinbach, W. Koransky, Inhibitory effect of tetrachloro-p-hydroquinone and other metabolites of hexachlorobenzene on hepatic uroporphyrinogen decarboxylase activity with reference to the role of glutathione, *Ann. N. Y. Acad. Sci.* 514 (1987) 148–159.
- [104] B. van Ommen, A.E. Adang, L. Brader, M.A. Posthumus, F. Müller, P.J. van Bladeren, The microsomal metabolism of hexachlorobenzene. Origin of the covalent binding to protein, *Biochem. Pharmacol.* 35 (1986) 3233–3238.
- [105] M. Czaplicka, Sources and transformations of chlorophenols in the natural environment, *Sci. Total Environ.* 322 (2004) 21–39.

This page intentionally left blank

THE USE OF PROTEOMICS IN THE STUDY OF MOLECULAR RESPONSES AND TOXICITY PATHWAYS IN BIOLOGICAL SYSTEMS

Gian Paolo Rossini,* Gian Luca Sala, Giuseppe Ronzitti,[†] and Mirella Bellocci

Contents

1. Introduction	46
2. Proteomics in the Study of Biological Systems Exposed to Toxins	47
3. From Receptor-Driven to Response-Driven Investigations into the Mechanisms of Action of Algal Toxins	51
4. Proteomic Studies Aimed at the Characterization of Modes of Action of Algal Toxins	55
4.1. Microcystins	56
4.2. Okadaic acid	60
4.3. Azaspiracids	64
4.4. Yessotoxins	67
4.5. Ciguatoxins	69
4.6. Gambierol	71
4.7. Palytoxin	71
4.8. Toxin mixtures	73
5. Proteomic Analyses for Predictive Toxicology and the Detection of Algal Toxin Contaminations	75
5.1. Microcystins	76
5.2. Okadaic acid	78
5.3. Azaspiracids	80
6. Preliminary Considerations on Strengths and Weaknesses of Proteomic Approaches in Investigations onto Toxicity Pathways	81
6.1. Quantitative issues in differential expression proteomics	81
6.2. Characterization of toxicity pathways	84

Dipartimento di Scienze Biomediche, Università di Modena e Reggio Emilia, Modena, Italy

* Corresponding author. Tel.: +39-059-205-5388; Fax: +39-059-205-5410

E-mail address: gianpaolo.rossini@unimore.it

[†] Present address: Italian Institute of Technology, Genova, Italy.

6.3. Distinguishing artifacts from biomarkers of toxicity	91
6.4. Experimental systems and variables which may affect mechanistic interpretations	94
6.5. Bioinformatic tools and databases in differential expression proteomics	95
7. Conclusions and Perspectives	97
Acknowledgments	98
References	98

Abstract

The characterization of the chains of events triggered by noxious agents in sensitive systems is mandatory for a full understanding of their mechanisms of toxicity and the advancement of mechanistic-based toxicity testing. The complexity inherent into the characterization of toxicity pathways and the identification of biomarkers representing nodes of altered cell functioning support the development of analyses at a system level. Proteomics is being increasingly used for the characterization of biological systems from a toxicological perspective. Differential expression proteomics has been employed in the area of microalgal toxins, and critical review of data indicates that system level analysis by this nonbiased approach allows identification of components of toxicity pathways. Still, the characterization of elements of the system has often involved targeted investigations, supporting the conclusion that the integration of systemic and reductionistic approaches will be essential to obtain quantitative, robust models of toxicity pathways and toxicity networks.

1. INTRODUCTION

A paradigm shift in toxicity testing is attracting increasing attention from the scientific community, stemming from concerns raised as to the efficacy of classical approaches based on analysis of apical endpoints of responses in whole animals, as opposed to a full characterization of mechanistic links in the sets of molecular events responsible for the action of toxicants [1–5]. Within this vision, some topics are becoming of particular importance. The first issue is related to the concept of *toxicity pathways* that would stem from the chains of reactions and mechanisms of control in normal cellular functioning (metabolic pathways and signaling pathways). When normal pathways are perturbed to an extent that may not be compensated for by ordinary homeostatic mechanisms, resulting in adverse effects, the process becomes a toxicity pathway, which is expression of a compromised biological condition [3,6].

A knowledge of molecular targets of individual toxicants may not necessarily suffice to fully characterize their mechanism of action, lending support to the notion that a detailed description of the toxicity pathways of

noxious agents is needed [3,4]. Thus, a complete account of the chains of events triggered by the interaction of a noxious agent with its cellular target, further down to the molecular effectors of the toxic response, is being viewed as an absolute need for a real understanding of the mechanisms of toxicity [3]. The characterization of toxicity pathways then becomes a major task of toxicity testing, to support evidence-based choices for the protection of human health and the environment [3].

A second issue relates to the recognition that detailed characterization of some elements of biological entities might not suffice to properly describe their state and make predictions on their evolution over time. Thus, knowledge of the entire system and mathematical *modeling of the system's behavior* are being sought [3]. Indeed, a characterization of *biological networks* [7] is part of this conceptual frame. A third issue contributes to the building-up of the proposed paradigm shift in toxicity testing [3], stemming from the recognition that the identification of a single biomarker of toxicity may not suffice to account for relevant mechanistic aspects of any toxic response in biological systems. Hence, the identification of *sets of biomarkers*, to represent critical nodes of specific toxicity pathways in appropriate cellular systems, is being sought, as major milestones in the development of mechanistic-based toxicity testing [1,3].

The classical targeted approaches of biological investigations, resting on the reductionistic view that the behavior of complex systems could be explained by breaking them down to their parts, and characterizing the mechanistic links existing among these parts, do not appear to suffice when approaching biological entities at a system level. Thus, systemic approaches are being increasingly used for the characterization of biological entities as well as the processes they participate in, from a toxicological perspective.



2. PROTEOMICS IN THE STUDY OF BIOLOGICAL SYSTEMS EXPOSED TO TOXINS

Analyses of biological entities at a system level have been developed with a battery of approaches that have stemmed from the sequencing of the human genome. This fundamental achievement has been a prerequisite to a full understanding of functioning of biological systems. An editorial in the Nature issue of February 15, 2001, publishing some of the papers reporting results of the Human Genome Project, clearly recorded the ongoing shift in researchers' attention to "...identifying the functions and expression patterns of proteins encoded by the genes." [8]. The development of transcriptomics, proteomics, and metabolomics then represented a shift in the attention of the scientific community from the potential characteristics of biological entities, as stored in their genomes, to real living entities, made of

billions of components existing in their phenotypes [9,10]. Investigating onto different molecular domains of living organisms by transcriptomics, proteomics, and metabolomics, in fact, aims at providing a proper account of biological entities at a system level, consisting of the full set of transcribed RNAs, the expressed proteins, and the produced metabolites, respectively. Owing to the wide scope of “omics” technologies, they are considered the best suited tools to approach the challenges posed by the characterization of toxicity pathways, the identification of relevant sets of biomarkers, and the modeling of the system, to yield a robust understanding of the modes of action of noxious agents [3,11–14].

Within this frame, we wish to stress some issues related to terminology, to avoid possible ambiguities in the presentation of materials and individual studies. The term “proteome” is often taken to indicate the entire set of proteins of a biological system, building on both established and recent methodologies to analyze large sets of proteins (see, for instance, Ref. [9] and references therein). Indeed, extensive efforts are being dedicated to increase the number of proteins that can be obtained, processed, identified, and properly quantified in biological samples, that in best cases have been close to 7000 different components [14]. If this figure is matched with the current estimates of over 10^5 different proteins existing in a eukaryotic cell [10,14], it is clear that proteomic analyses provide data on large sets of proteins in subproteomes, whose features largely depend on the experimental design chosen to obtain the samples used in any study. In keeping with this consideration, it must be recognized that a turn of attention to phenotypes certainly brings a biological entity of interest into focus with regard to the molecular components existing while it is living. Still, any transcriptomic, proteomic, and metabolomic analysis of a biological system cannot be truly comprehensive. Transcript, protein, or metabolic profiling of a biological system, in fact, yield data that are affected by the specific conditions of the system of interest and are related, for instance, to the times of sampling and the origin of analyzed materials. The experimental design, therefore, must be carefully considered both when planning investigations and in evaluating the significance of experimental data [1,10–14].

The relevance of experimental design will be considered in several sections of this contribution with specific reference to the use of proteomics. A detailed review of experimental designs and methodological settings that can be used in proteomics studies, however, is not in the scope of this contribution, and the interested reader is referred to the many excellent reviews that have been appearing in the last years on this topic (see, for instance, Ref. [14] and references therein).

The general setting of experiments exploiting proteomic approaches includes five steps, often referred to as the “proteomic pipeline” [9,14], comprising the preparation of protein samples, the separation and digestion

of proteins and/or peptides in the samples, a first analysis of peptides by mass spectrometry (MS), a second MS analysis of peptides of interest after their fragmentation. The process terminates with a final step comprising the analysis of MS data by bioinformatic tools, which allow the characterization of peptides and, hence, the identification of the protein from which they originated [14]. Although the specific features of the last three steps of the process do not greatly differ among separate experimental settings, the steps that yield the peptides to be subjected to MS analyses can show extreme changes, depending on the experimental design.

A classical organization of the first steps of proteomic analyses, for instance, has been used in most studies described in Sections 3 and 4 of this review, and its workflow is outlined in Figure 1. The samples prepared for proteome analyses are obtained by cell lysis with a buffer comprising urea, detergents, and inhibitors of different kinds of hydrolytic enzymes, and extracts are used after they have been subjected to clarification by centrifugation procedures, to remove residual particulate contamination that might have remained in the lysate. The second step of the procedure includes the separation of intact proteins, by the use of two-dimensional (2D) electrophoresis. The proteins in the clarified cell extracts are separated in the first

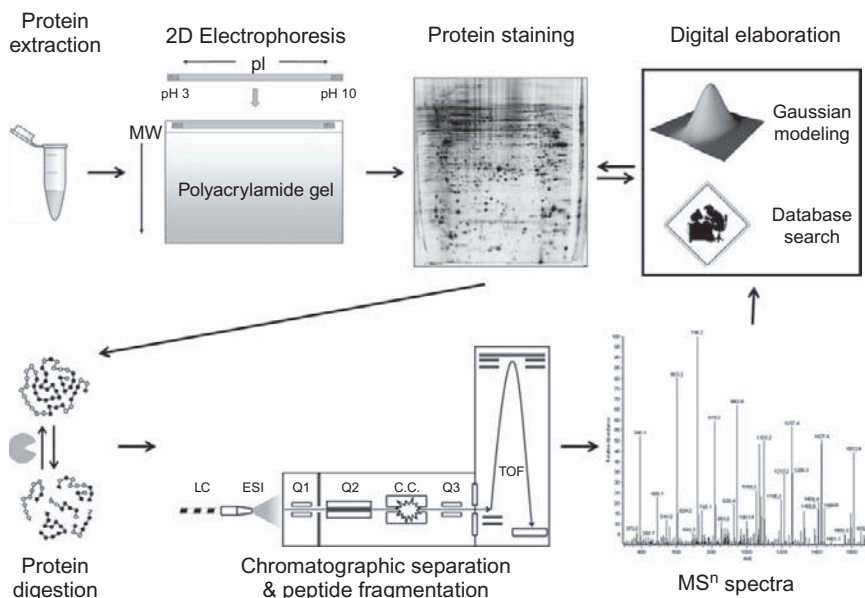


Figure 1 Major steps of a generic experiment for the characterization of proteomes. See text for explanation.

dimension according to their isoelectric point, using gels containing a pH gradient immobilized on an inert support. At the end of the isoelectrofocusing, the components are further separated in the second dimension according to their size, by inserting the strip with the immobilized gel containing the fractionated proteins orthogonal to a second polyacrylamide gel. At the end of the separation, proteins are distributed in the entire gel and are visualized by staining, yielding patterns of protein spots which are next subjected to image analysis, using densitometric scanning of stained gels, and their processing by a specific software (Figure 1, top). The analyses of the protein patterns by the software then lead to recognition of protein spots that show significant quantitative changes in extracts from cells of interest as compared to controls, thereby indicating the components worthy of identification by MS analysis. In keeping with this condition, relevant protein spots are subjected to trypsin digestion, to yield peptides that undergo the last steps of the proteomic pipeline. MS analyses of peptides and processing of spectrometric data by the use of databases then allow the identification of proteins of interest.

Considering the general structure of the experiments described above, and independently of differences that may characterize methodological settings in individual studies (see next sections), a specific feature of investigations based on the use of “omics” approaches is that they should be unbiased because they do not actually require any *a priori* assumption or specific hypothesis. Indeed, many proteomic studies have not been targeted to probe possible alterations of any particular function or molecular process in the biological system of interest. Thus, comparisons of protein profiles between samples from control and toxin-exposed living systems often represent a general feature of proteomic studies, an experimental setting that is termed “differential expression proteomics” [9,15,16]. By this term, it is then intended that analyses of proteomes are aimed at identification of qualitative and quantitative changes in the levels of proteins associated with distinct conditions of a biological system, independently of the fact that they might result from normal and/or pathological functioning, or else as a consequence of exogenous or endogenous perturbations of the system.

The very general nature of this kind of experimental strategy would make any attempt to review existing information on proteomics studies devoted to toxicants problematic. We will then focus our attention onto an area of toxicants, represented by nonproteinaceous components produced by some microalgae. The molecular processes targeted by this broad and heterogeneous family of toxicants include key biological and regulatory functions. A critical review of existing data, and some discussion regarding their potential implications in toxicology, would then allow a preliminary examination of the applicability of the toxicity pathway concept. Further, some issues that might demand particular efforts for the best possible efficacy of proteomics in toxicity testing will be discussed.



3. FROM RECEPTOR-DRIVEN TO RESPONSE-DRIVEN INVESTIGATIONS INTO THE MECHANISMS OF ACTION OF ALGAL TOXINS

Some taxa of marine microalgae are known to produce nonproteinaceous substances possessing very powerful biological activities in a variety of systems. Under some circumstances, humans and animals may become exposed to concentrations of toxins that are sufficiently high to cause intoxications and poisonings [17,18]. This might occur as a consequence of an increase in the cell population of a microalga producing toxins (the so-called harmful algal bloom, HAB), the accumulation of microalgal toxins in edible fish and shellfish due to their feeding behaviors, or else through the drinking water, when toxins are produced and released by toxic producers in freshwaters [17,18]. The complexity of issues linked to algal biotoxins has been attracting the interest of scientists from different areas, well beyond those related to the chemical characterization of natural compounds, the biology of microalgae and human toxicology. Indeed, a glimpse to two recent books, providing a comprehensive treatment of major aspects related to microalgal biotoxins [19,20], shows the wide impact of microalgal biotoxins on human activities, spanning from fishery to natural sciences, from recreation to human health.

The natural compounds we will be dealing with are classified according to their chemical characteristics into separate groups. Most of them are produced by microalgae, leading to the common use of the term microalgal toxins, which traditionally comprises some toxins synthesized in bacteria, such as the microcystins (MCs). The chemical, biological, and toxicological properties of microalgal toxins, as well as the description of the different types of intoxications caused by individual groups, will not be detailed here, but the interested reader can find relevant information in recent reviews and references therein (for instance, Refs. [18,21–30]). In turn, we will approach methodological and conceptual issues related to the understanding of the modes of action of toxins at a system level by proteomic approaches, aiming at supporting the investigations in this area.

In a biomolecular, mechanistic perspective, two aspects are of paramount importance when considering the major classes of toxins: their potency and molecular targets (Table 1). Although concentrations lower than 10^{-9} M are sufficient to cause significant responses in many cases, some toxins, such as palytoxin (PITX) and maitotoxin, can induce their effects at concentrations as low as 10^{-11} M (see the many examples reported in Refs. [31,32]). The different ranges of effective concentrations are related to the affinity displayed by distinct toxin groups for their specific molecular targets, which include ion channels and transporters on cellular membranes,

Table 1 The major groups of microalgal toxins and their molecular targets

Group	Molecular target	EC ₅₀
Dinophysistoxins	Phosphoprotein phosphatases (ser/thr)	10 ⁻¹⁰
Microcystins	Phosphoprotein phosphatases (ser/thr)	10 ⁻¹⁰
Saxitoxins	Voltage-dependent Na ⁺ channel	10 ⁻⁹
Palytoxin	Na ⁺ ,K ⁺ -ATPase	10 ⁻¹¹
Yessotoxins	Unknown	10 ⁻¹⁰
Azaspiracids	Unknown	10 ⁻¹⁰
Brevetoxins	Voltage-dependent Na ⁺ channel	10 ⁻⁹
Ciguatoxins	Voltage-dependent Na ⁺ channel	10 ⁻¹⁰
Domoic acid	Glutamate receptors (non-NMDA)	10 ⁻⁹
Maitotoxin	Ca ²⁺ channel (plasma membrane)	10 ⁻¹⁰
Gambierol	Voltage-dependent K ⁺ channel	10 ⁻⁹
Pectenotoxins	Actin filaments	10 ⁻⁸

enzymes, and cytoskeletal components (Refs. [18,21–30] and references therein). These toxins, therefore, perturb cellular homeostasis of Na⁺, K⁺, Ca²⁺, general regulatory mechanisms involving protein phosphorylation, the organization and dynamics of structures playing key roles in the localization and transfer of molecular components within subcellular compartments. In the case of azaspiracids (AZAs) and yessotoxins (YTXs), the molecular target(s) responsible for the effects triggered by subnanomolar concentrations remain(s) undetermined [18], but it is recognized that the inhibition of endocytosis and cell death ensues when cells are exposed to low levels of these toxins [18,23].

The biological relevance of molecules targeted by microalgal toxins fully explains their frequent use as tools to investigate fundamental molecular processes in living systems. For instance, the capacity of okadaic acid (OA) to inhibit ser/thr phosphoprotein phosphatases (PPases) [33] has been exploited to study protein phosphorylation in biological systems so that more than 4700 references could be retrieved from a literature search about the toxin in the PubMed website (<http://www.ncbi.nlm.nih.gov/pubmed>) in November 2010.

The quest for a better characterization of the molecular events participating to toxicity pathways of algal toxins is supported also by compelling reasons. A recognition of key steps in the molecular responses triggered by different toxins, in fact, can be proposed only in some cases and for some effects. A few examples are described to substantiate this statement.

The molecular bases of paralytic shellfish poisoning could provide a first case of well-characterized mechanism. The binding of saxitoxin (STX) to site 1 of the α subunit in the voltage-dependent sodium channel, in fact, blocks sodium conductance of the channel and membrane depolarization,

preventing the transmission of the action potential in excitable cells, and causing the loss of neuromuscular functioning that leads to respiratory paralysis and death [18,22,34]. Similar mechanistic considerations can be put forth when considering the major steps involved in the neurotoxic response found in amnesic shellfish poisoning induced by domoic acid, proceeding through toxin binding to non-NMDA glutamate receptors, Ca^{2+} overload in the cells, and tissue damage in some regions in the brain [29,35–38]. It should be noticed that the two preceding cases highlight key steps of responses, but the molecular details of the full train of events responsible for those effects have not been completely characterized.

Less defined pictures are found, in turn, when approaching the molecular mechanisms responsible for toxic effects of other groups of toxins.

The responses of biological systems to OA can be one such case. It has long been recognized that this toxin is responsible for diarrhetic shellfish poisoning [39], and early investigations led to recognition that type 1 and type 2A ser/thr PPases represent cellular receptors for this toxin [33]. Based on general knowledge regarding the role of protein phosphorylation in the control of their catalytic activity or otherwise regulatory functions, it was originally proposed that the diarrhetic response could be due to altered properties of ion transport systems in intestinal epithelia, due to the maintenance of their phosphorylated states upon inhibition of PPases [40]. This contention was perfectly in line with the knowledge on the role of protein phosphorylation available in the 1980s [41]. Subsequent studies, however, have provided evidence that the water accumulation inside the intestine in animals exposed to OA [42,43] does not result from increased ion secretion, but represents the disruption of the barrier function of intestinal epithelia, leading to increased paracellular permeability [44,45]. Interestingly, this conclusion underscores the property of OA to damage cells and tissues [42,43,45,46], at variance with another effect that has been described in the early investigations onto OA. By the use of two-stage carcinogenesis models, it was concluded that OA represents a tumor promoter [47–49]. Thus, the recognition of type 1 and type 2A ser/thr PPases as receptors of OA is matched by a picture encompassing responses, whose reduction to a single noncontradictory model of the toxin's mode of action, in the lack of further information, seems problematic.

Overall, one should recognize that, in the best cases, our knowledge of the molecular basis of effects triggered by different toxins is patchy, and considerable gaps in our understanding of mechanistic aspects of the toxins' modes of action still remain.

Additional uncertainties exist if we consider the need to account for the molecular basis of toxic responses when biological systems are exposed to mixtures of agents possessing different receptors/targets and mechanisms of action. The relevance of such an issue is not based simply on the general recognition that living systems are continuously exposed to a variety of

biologically active agents, including toxic compounds. Our consideration, in turn, primarily stems from the fact that seafood contamination by microalgal toxins belonging to separate chemical groups and possessing different mechanisms of action is relatively frequent [39,50–52], posing risks whose real dimension remains essentially undetermined. The combined effects exerted by mixtures of toxicants including one or more microalgal toxins, in fact, have been investigated only in a few cases (see, for instance Refs. [53,54]).

It might appear paradoxical, but the recognition of existing deficiencies in our understanding of the molecular mechanisms and modes of action of toxins is a consequence of extensive and careful investigations carried out in the past 20 years by many scientists. Thus, the quest for a better knowledge actually stems from the existing strong scientific background, which is a good basis to achieve further conceptual advancements.

In the case of proteomic studies devoted to microalgal toxins, the investigations reported so far can be broadly divided into the two major lines of intervention found in the area of general and environmental toxicology. These comprise the characterization of the mode of action of toxins in biological systems, and the prediction of toxicity of biological materials in the environment, including the detection of toxins in suspected samples by the effects they induce in biological systems [11,55–57]. Both types of investigations include some search for and the use of biomarkers of response to specific toxins, and their general experimental strategy can be represented by the scheme shown in Figure 2. Two major classes of biological systems are then used in these studies, depending on the line of intervention. When investigations are devoted to molecular bases of effects induced by toxins, model systems are preferred, consisting primarily of established cell lines. Animal species, however, are found as models for analysis of toxic responses at an organismal level. If investigations are more focused onto responses

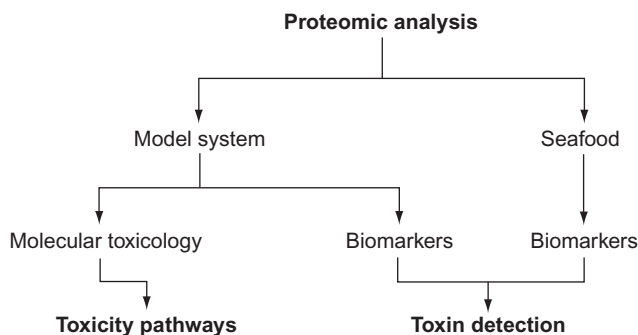


Figure 2 The use of proteomics in the study of molecular mechanisms of toxicity and biomarkers of toxin exposure in the area of microalgal toxins.

detectable in biological systems naturally exposed to toxins, studies have an obvious application to environmental analysis and the detection of animal/food contamination by toxins. In these cases, edible mollusks, such as mussels, appear as the preferred choice, due to their capacity to accumulate toxin. As already mentioned, the identification of biomarkers of toxin action is a relevant output of these investigations, that may be eventually used to develop cell-based assays for the detection and quantification of toxins [58].

Considering the general structure of the studies reported in Figure 2, it can certainly represent ongoing investigations based on *omics* technology in the algal biotoxin area well beyond proteomics. In particular, transcriptomic studies can fit the scheme [59–63], and some of those existing in the literature will be mentioned, when approaching the molecular modes of action of distinct groups of toxins, with regard to possible complementation of data on cell responses based on different systemic approaches.

The distinction between mechanistic as opposed to predictive studies mentioned above does not appear to be very strict when considering existing contributions on differential expression proteomics in the area of algal toxins. In the next two sections, however, we will present the results and major conclusions of those investigations following the broad classification of mechanistic as opposed to predictive studies, to stress the potential of proteomics in the two areas. Focusing on differential expression proteomics in a toxicological context, targeted studies where proteomic tools have been employed to characterize protein components that might interact with toxins under cell-free conditions (see, for instance, Refs. [64,65]) will be considered when their content is directly relevant to mechanistic issues discussed in the following sections. Moreover, we will not present studies when differential expression proteomics has been applied to the characterization of toxic microalgae. In these latter cases, in fact, investigations were essentially aimed at defining protein profiles for either toxic species recognition [66–68] or components associated with toxin production and its regulation [66,69], that are not dealt with in this review.



4. PROTEOMIC STUDIES AIMED AT THE CHARACTERIZATION OF MODES OF ACTION OF ALGAL TOXINS

Differential proteomics has been introduced in the area of microalgal toxins only recently, and reports describing the effects exerted by different toxins are limited to MCs, OA, azaspiracid-1, YTX, Pacific ciguatoxin-1, gambierol (GB), and PITX. These studies will be described below.

4.1. Microcystins

To the best of our knowledge, the first article reporting results from an investigation exploiting a differential expression proteomic approach in the area of microalgal toxins has appeared in 2005 [59] and was devoted to a MC (MC-LR). This group of compounds consists of cyclic heptapeptides [70] produced by some genera of cyanobacteria, including *Microcystis*, *Nostoc*, and others [71]. Severe episodes of human and animal poisoning, primarily due to drinking freshwater contaminated with these toxins, have been recorded worldwide, and MCs are believed to pose relevant risks to humans and animals [21,72]. MCs are taken up by cells expressing specific transport systems, particularly in hepatocytes [21], and liver has been found severely damaged in both animals and humans exposed to these toxins, leading to classification of MCs among hepatotoxins [21,73].

The recognized molecular mechanism of action of MCs is very similar to that of OA and involves toxin binding to ser/thr PPases, particularly type 1 and type 2A isoforms [21,74]. The interaction of MC with a PPase causes the inhibition of its catalytic activity and leads to stabilization of phosphorylated states of proteins [74]. The binding of MCs to their targets is not fully reversible, however, because covalent bonds between the enzyme and the interacting MC slowly ensue, essentially withdrawing the involved PPase molecules from the cellular pool of functional proteins [75].

MCs have been found to possess tumor-promoting activity in experimental systems [49], and are potent inducers of cell death, particularly when cultured cells are exposed to the toxin [76]. The general pattern of responses to MCs then displays the contradictory feature of those found in systems exposed to OA [46], as mentioned above.

The study by Chen *et al.* [59] was carried out in an animal model (BALB/c mouse), focusing the attention on the liver as major target organ of MC-LR, and was aimed at gaining a better understanding of the molecular mechanisms of apoptotic responses triggered by this toxin in mouse liver and finding biomarkers of toxin exposure. Three different doses of MC-LR (50, 60, and 70 $\mu\text{g/kg}$ b.w.) were administered by intraperitoneal injection into the mice, and livers were dissected from animals sacrificed 24 h after toxin injection. The study was developed following an experimental strategy marked by a combination of techniques, as systemic approaches (transcriptomic and proteomic analyses) were complemented by immunological and biochemical tools as well as mathematical modeling [59]. Proteomic analysis was performed using proteins that had been ethanol precipitated from tissue homogenates, following the general scheme of 2D electrophoresis, protein staining, detection of relevant proteins by image analyses, and protein identification in the relevant spots by MS, as outlined in the previous section. Sixty-five proteins were found to be significantly changed in extracts from MC-LR-treated mouse livers, including 35

upregulated and 30 downregulated components. Some components of the Bcl-2 family [59] and other proteins involved in oxidative stress and apoptosis were investigated in more detail. BAX, BID, and Bcl-2, which could not be detected by gel staining, probably due to their low levels in cell extracts, but whose differential expression in livers from toxin-treated mice had been shown by transcriptomic profiles, were analyzed by immunoblotting, and dose-dependent changes in their levels were found [59]. In particular, the three proteins were upregulated at the lower dose (50 $\mu\text{g/kg}$ b.w.), but their behavior differed at higher doses, as BAX upregulation was maintained, whereas the levels of BID and Bcl-2 were decreased. Kinetic analysis confirmed the different behavior of these mitochondrial proteins [59].

Many proteins involved in cellular responses to oxidative stress were also found to be changed in extracts from livers of toxin-treated mice, including peroxiredoxins (isoforms 1, 2, and 6), ferritin, glutathion-S-transferase, and thiosulfate sulfotransferase [59]. Some of these components are mechanistically linked in the reactions removing free radicals in oxidative stress responses [77–79], and their changes in liver of mice exposed to MC-LR indicate that oxidative stress was triggered as part of the tissue response to the toxin. In keeping with the results obtained with proteins of the Bcl-2 family, different patterns of expression were found with different components. For instance, upregulation of ferritin and peroxiredoxin 2 was accompanied by downregulation of peroxiredoxin 1 and 6 [59]. Among proteins whose expression was affected by MC-LR in mouse liver, chaperonin 10, ATP synthase, and nucleoside diphosphate kinase might be of some interest with regard to the toxicity pathways triggered by inhibitors of PPases and the biomarkers of responses shared by these substances (see below and Sections 5 and 6).

Based on the sets of data gathered by a combined strategy, Chen *et al.* have proposed a model of the responses recorded in mouse liver exposed to MC-LR comprising two distinct apoptotic pathways, which would be preferentially triggered by low and high doses of MC-LR, respectively. The two pathways would involve components of the Bcl-2 protein family and reactive oxygen species, respectively [59]. Further, ferritin and peroxiredoxins were proposed as potential biomarkers for hepatotoxicological mechanisms [59].

The molecular mechanisms of MC toxicity have been studied also in cultured cells. An initial study by Fu *et al.* [80] was carried out with a human amnion epithelial cell line in culture, which was exposed to three different concentrations (0.25, 1, and 2 μM) of MC-RR. The cell treatment comprised the removal of the toxin-containing medium at the end of first 2.5 h incubation, and cells were then maintained with fresh medium devoid of toxin for further 12 h, before being processed for the preparation of cell extracts. Control and MC-treated cells were then lysed with a buffer system

containing detergents; the cell lysate was subjected to ultracentrifugation to eliminate cell debris and particulate material, yielding clear cell extracts. These samples were then used for proteomic analyses, following the general scheme of 2D electrophoresis, protein staining, detection of relevant spots by image analyses, and identification of relevant proteins by MS, as outlined in the previous section.

The protein spots recorded in those gels by image analyses were about 1200, and about 100 of them showed significant quantitative differences between control and toxin-treated samples [80]. Among the differentially expressed proteins of toxin-treated samples, 59 components could be identified by MS analyses with high confidence, and the list reported in the paper included 16, 27, and 45 different proteins in extracts from cells exposed to 0.25, 1, and 2 μ M MC-RR, respectively. As these authors noted, only a few proteins showed dose-dependent changes in their expression levels in toxin-treated cells. The dose-dependent increase of p44 ERK and p53 proteins was shown by an immunoblotting procedure, but data reported in the paper regarding other protein components [80] would not allow any further consideration about dose-relatedness of recorded responses.

The differential expression of relevant proteins was discussed in the paper by Fu *et al.* [80], taking into consideration the recorded effects of MCs and the recognized functional roles of individual components. The increased expression of p44 ERK in cells exposed to MC-RR was considered particularly relevant because different isoforms of this type of protein kinase are key players in the regulatory processes of cell proliferation and differentiation, where their activity is induced by dual phosphorylation (in two threonine and tyrosine residues separated by a proline) catalyzed by specific kinases (*mitogen activated/extracellular signal regulated protein kinase*, MEK) in signaling cascades triggered by a variety of extracellular signals [81,82]. The phosphorylation state of ERK proteins is controlled by PPases [83], and the cell exposure to inhibitors of PPases is known to result in hyperphosphorylation of ERK isoforms [46,84,85]. Based on the recording of increased levels of an ERK activating kinase MEK isoform, the upregulation of GRB2 protein in cells exposed to MC-RR, and the recognized role played by these two components in the cascade leading to ERK activation [81,82], it was speculated that MC-RR could modulate the signal transduction pathway involving the Ras-Raf-ERK cascade [80]. No information regarding the phosphorylation state of p44 ERK in amnion cells, however, was provided in the study by Fu *et al.* [80].

The increased expression of the p53 protein in cells exposed to MC-RR was also approached, taking into consideration the recognized roles of p53 as an inducer of apoptosis and tumor suppression (for a recent review, see Ref. [86]). The changes in expression of p53 recorded in amnion cells had been already observed in other systems exposed to inhibitors of PPases

[46,87], and its upregulation by MC-RR could play a key role in the responses induced by the toxin, providing a proper background to propose the increased expression of p53 as a biomarker of system exposure to MC-RR [80].

Other proteins differentially expressed in amnion cells exposed to MC-RR were discussed, including the 14-3-3 proteins, tubulin, and peroxiredoxin 2, whose roles in the cell response to MC-RR were proposed with regard to both cell survival (14-3-3, peroxiredoxin 2) and apoptosis (tubulin) [80], confirming the need for a better clarification of the mode of action of MCs.

In a subsequent study [88], Fu *et al.* extended the investigation on human amnion cells by proteomic analyses and performed time-course studies of responses triggered by MC-RR. The general methodology did not differ from that used in their initial study, and cell treatment comprised an initial toxin treatment (1 μ M MC-RR for 2 h), followed by removal of medium containing MC-RR and further incubation of cells with fresh medium for 3, 12, or 24 h [88].

Several proteins were found differentially expressed in cells exposed to MC-RR (a total of 137), and some of them could be identified with high confidence at the three time points, including the 31, 40, and 42 components listed in the paper. The authors noted that none of the proteins had altered expression levels at the three time points studied, and most of the proteins identified at each time point differed from those found in the other time points [88]. The recorded changes in the levels of a PPase 2A subunit and of hsp 70, chosen as reference proteins, were validated by immunoblotting analysis, and their possible role in the response induced by MC-RR in amnion cells was discussed [88]. In particular, the increased levels of a 65-kDa regulatory subunit of PPase 2A, detected 12 and 24 h after completion of the 2 h toxin treatment, were proposed to play a role in the inhibitory effect exerted by MCs on PPase, by favoring the formation of the inactive holoenzyme complex, including the 36-kDa catalytic subunit in association with the inhibitory 65 kDa subunit, rather than by the interaction of the toxin with the enzyme [88]. This molecular mechanism of action of the toxin on the PPase would be at variance with its recognized action [21,74,75], but could participate in secondary effects, reinforcing the inhibition of the enzyme. In any case, its relevance with regard to the toxicity of MCs remains to be established. The effect of MC-RR on the levels of hsp 70, in turn, was discussed with regard to the role of this stress response protein, and the increased expression in cells exposed to the toxin was proposed to be related to its tumor-promoting action [88].

The differential expression of other proteins in cells exposed to MC-RR was also considered, and particular relevance was given to proteins involved in the ubiquitin-proteasome protein degradation pathways, some of which were found to be decreased by MC-RR in amnion cells [88]. Although the

importance of the ubiquitin–proteasome pathways in the mode of action of MC-RR was pointed out by Fu *et al.*, no indication on the possible consequences of the recorded effects was mentioned, beyond the consideration that the turnover of cellular proteins might be affected in cells exposed to MC-RR [88].

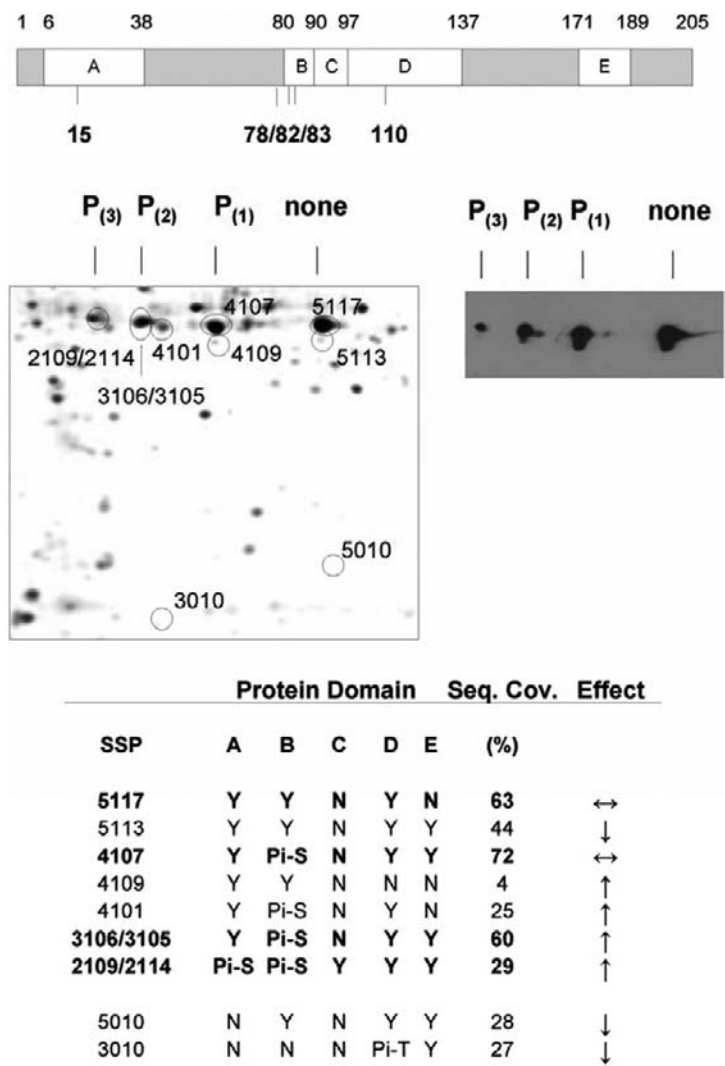
If the data obtained by proteomic analyses in studies involving MC-RR are considered as a whole, they include a number of candidate effector proteins, most of which do not appear to be affected in a dose- and time-dependent manner [80,88]. It is presently undetermined whether this feature of responses might be explained at least in part by the fact that the protocol of cell incubation involved cell harvest after several hours of toxin removal from culture medium [80,88], whereby the newly synthesized toxin-sensitive PPases would be unaffected by prior cell exposure to MC-RR, rescuing the system from an inhibition involving already existing enzyme molecules that had been inactivated by the covalent binding of the toxin during the first phase of cell treatment [75]. Thus, the mechanistic relevance of the dose- and time-independent molecular responses to MC-RR would require further study. More importantly, the precise functional roles of the components differentially expressed by the toxin have not been clarified with regard to the general antinomy tumor promotion/cell death that has been recorded in systems exposed to components of this group of toxins [76]. Thus, further information remains to be gathered to understand the apparently contradictory effects of inhibitors of PPases, including MCs (see below).

4.2. Okadaic acid

This toxin has long been recognized to share the molecular targets of MCs, in that it acts by inhibiting type 1 and type 2A PPases [33,40,49]. The differential expression of proteins in epithelial cells exposed to OA has been studied in the MCF-7 human breast cancer cell line, where OA induces cell death [89]. The proteomic analyses were carried out in an investigation aimed at characterizing combined responses of a cellular system to toxin mixtures [54], whose findings will be considered in a separate part of this section. As far as the response to OA is concerned, MCF-7 cells were treated with 50 nM OA for 24 h, an experimental condition that was chosen to include the early phases of cell death, before extensive cell disposal takes place [89]. The differential expression of proteins induced by OA in this experimental system was studied by proteomic analyses of cytosolic extracts prepared by centrifugation of whole cell lysates, and was performed by 2D electrophoresis and image analysis of stained gels, followed by tryptic digestion of relevant proteins and analysis of fragmented peptides by MS [54]. This experimental setting led to detection of several hundred proteins, 30 of which had levels that were changed in MCF-7 cells

exposed to OA in a significant manner [54]. Using the Gene Ontology (GO) database (GOTERM_MF_ALL) on the proteins identified with at least 15% of sequence coverage, components were assigned to different classes, including protein-binding components and enzymes. Interestingly, about 50% of the differentially expressed components (14 of 30) can be reduced to three functional groups. The first group includes eight isoforms of the same protein, the heat shock protein (hsp 27), the second group includes three components of two enzymes involved in ATP metabolism (the α and δ subunits of ATP synthase, and nucleoside diphosphate kinase A), and the third group involves three proteins participating to cellular responses to oxidative stress (superoxide dismutase (SOD), peroxiredoxin-5, thioredoxin) [54].

The hsp 27 isoforms differentially expressed in OA-treated cells included both intact and proteolytic fragments as well as proteins differing according to their phosphorylation state [54]. A preliminary reconstruction of the hsp 27 system in MCF-7 cells under the conditions of our study is outlined in Figure 3. This representation is based on MS data [54] and immunoblotting analyses using antibodies recognizing either total hsp 27 (phosphorylated and nonphosphorylated) or isoforms phosphorylated in Ser₈₂ [90,91] and shows that at least nine components can be detected in MCF-7 cells exposed to OA. The pattern of hsp 27 isoforms we detected after prolonged (24 h) cell treatment with OA is quite similar to that found in fibroblasts after a short (15–30 min) exposure to this toxin [92,93]. Seven isoforms are bona fide intact proteins, can be distinguished by their isoelectric point, and should then differ according to their phosphorylation states (Figure 3). The other two proteins are small MW components and should represent degradation products of hsp 27. Using the codes marking the proteins in our original 2D gels, components 5117 and 4107 represent the most abundant intact hsp 27 isoforms in both control and OA-treated cells (Figure 3). The different pI of these two isoforms shows that 4107 is more acidic than 5117, suggesting that it is phosphorylated. The MS data [54] indicated that the phosphorylated residue should be within a peptide fragment (Figure 3) containing three serine residues (Ser₈₂, Ser₈₃, Ser₈₆), one of which is known to be phosphorylated in human hsp 27 *in vivo* [93,94]. The antibody specific for isoforms phosphorylated in Ser₈₂ used in immunoblotting analyses, however, did not bind to 4107 under those conditions (Refs. [90,91], see also Figure 8 in this review), indicating that 4107 should be a monophosphorylated isoform of hsp 27 whose phosphorylated residue is not Ser₈₂ (Figure 3). The antibody specific for isoforms phosphorylated in Ser₈₂, in turn, detected components 3105 and 2109 [90,91], which should then represent isoforms containing two and three phosphorylated residues, respectively, including Ser₈₂ (Refs. [90,91], see also Figure 8 in this review). The detailed phosphorylation state of isoforms detected in MCF-7 cells is presently under investigation in our group, and further data are needed to



fully clarify the molecular isoforms whose levels are increased in cells exposed to OA. Based on original MS [54] and immunological data [90,91], many phosphorylation patterns can be hypothesized, according to the number of phosphorylated residues, as depicted in Figure 3. In the first instance, results obtained by 2D gels, including immunoblotting analyses, are compatible with comigration of multiple isoforms, differing by the combinations of phosphorylated amino acids but not their number in the proteins of the same spot. Further, the patterns of phosphorylated sites might differ depending on either cellular conditions or experimental treatments, and it may not be excluded that amino acids other than Ser₁₅, Ser₇₈, and Ser₈₂, which have been shown to be phosphorylated *in vivo* [93,94], might be involved in phosphorylations stabilized by OA. Data obtained by MS analysis, for instance, indicated Thr₁₁₀ in peptide D as a phosphorylated amino acid in spot 3010 (Figure 3 and Ref. [54]).

Based on already published data, however, some preliminary conclusions can be put forth. The cellular levels of major isoforms of hsp 27 (the bona fide nonphosphorylated 5117 protein and the monophosphorylated isoform 4107) do not greatly change as a consequence of prolonged (24 h) OA treatment (Refs. [54,91] and Figure 3). The toxin, in turn, causes a net increase in the levels of the bis- and tris-phosphorylated isoforms (Refs. [54,91] and Figure 3). Further, the antibody specific for isoforms phosphorylated in Ser₈₂ could detect two components more acidic than 2109 in extracts obtained from OA-treated MCF-7 cells (Refs. [54,91] see also Figure 8 in this review), indicating that the toxin causes an increase in multiphosphorylated hsp 27 isoforms in MCF-7 cells.

The second group of proteins whose expression is changed in MCF-7 cells treated with OA includes components of two enzymes involved in ATP metabolism. These enzymes are ATP synthase, which catalyzes the synthesis of ATP [95], and nucleoside diphosphate kinase, which is responsible for the interconversion of nucleoside diphosphates into triphosphates, most often at the expense of cellular ATP [96]. The cellular levels of α and δ subunits of ATP synthase have been found to be altered by OA, resulting in upregulation of the δ subunit and the downregulation of the α subunit of the enzyme [54]. The catalytically active synthase is composed of the two

obtained by immunoblotting of proteins in the higher portion of a gel, as shown on the left, using antibodies recognizing total hsp 27 and the procedure described in Ref. [90]. The most likely number of phosphorylated residues in the isoforms is indicated on the top of the images. Bottom: tabular representation of the peptides of hsp 27, as detected by MS analysis of indicated isoforms. The detection of the peptide (Y, yes; N, no) and its phosphorylation state (Pi-S, detection of a P-Ser; Pi-T, detection of a P-Thr) is indicated. The effect of OA on individual isoforms is shown in the first column on the right. Portions of this figure have been reproduced from Refs. [54,90] with slight modifications.

major portions F_0/F_1 , each of which contains multiple subunits in a well-defined stoichiometric composition [95]. Thus, the significance of the opposite changes that OA causes on two subunits of this enzyme is unclear. One possibility is that these contradictory effects testify the derangement of cellular regulatory mechanisms, during the onset of the death response induced by the toxin. The downregulation of nucleoside diphosphate kinase under the same conditions [54], which could alter the maintenance of proper cellular pools of nucleoside triphosphates, and might then impair several fundamental cellular processes, such as nucleic acid and protein synthesis, could be in line with this interpretation.

A third group of proteins differentially expressed in MCF-7 cells exposed to OA comprises three components involved in cellular responses to oxidative stress, all of which are downregulated by toxin treatment. These components are mechanistically linked because SOD 1 destroys radicals (such as $\cdot O_2^-$) which are normally produced within the cells and are toxic to biological systems, converting them to hydrogen peroxide. This oxidant is then converted to water by peroxiredoxins (such as peroxiredoxin-5), using reducing equivalents donated by reduced glutathione and/or thioredoxin [77–79]. The disulfide bridge between two molecules of oxidized glutathione can be reduced in various redox reactions, one of which may involve the active center dithiol of thioredoxin that is converted to a disulfide. Thus, the downregulation of these three proteins in OA-treated cells indicates that the mechanisms of cell protection from oxidative stress are disrupted by the toxin in MCF-7 cells, in line with observations obtained with other systems [97,98].

Overall, the changes induced by OA in the proteome of MCF-7 cells is marked by an increase in phosphorylated hsp 27 protein, determining an extensive alteration of relative proportions of isoforms in this model system, which is accompanied by the downregulation of most of differentially expressed proteins [54]. The general features of molecular responses induced by OA, as detected by proteomic analysis, are then in line with investigations targeted to specific cellular components [46,76,84,85,89,92,93,97,98], supporting the notion that this toxin is primarily inducing cell death in biological systems [46]. This conclusion matches the cytotoxic action of MCs, although the proteins found differentially expressed in cells exposed to the two toxins in existing studies are not identical (see the next section).

4.3. Azaspiracids

The specific mechanism of action of azaspiracids remains undetermined at the moment [18], and gathering information regarding the molecular responses induced by these toxins in sensitive systems is extremely relevant. The cellular mechanisms of azaspiracid toxicity have been investigated by

proteomic analyses using a neuronal cell line in culture [99]. The methodological setting of this study differs from those described above because the differential expression of proteins was not detected by comparison of images obtained by staining of proteins in 2D gels. The quantitative analysis of proteins expressed in the extracts, in fact, was performed by exploiting a procedure termed stable-isotope labeling with amino acids in culture (SILAC) [99], whose features allow a very accurate matching of samples from control and toxin-treated cells. In this methodological setting (for a presentation of its characteristic features, see Ref. [14]), the two cell populations, to be matched for the identification of differentially expressed proteins, are incubated with culture media differing with respect to the physical properties of one or more amino acids. One cell population receives “heavy” amino acids (lysine and arginine), containing either ^{13}C - or ^{15}N -labeled compounds, whereas “light”, unlabeled amino acids (^{12}C - or ^{14}N -containing compounds) are included in the culture medium of the other cell population. The incorporation of amino acids into proteins leads to metabolic labeling of molecules in one cell population, but not in its counterpart, and the tryptic digestion of proteins in cell extracts leads to peptides terminating with a labeled amino acid in samples from cells incubated with heavy amino acids, whereas an unlabeled amino acid is present in the same peptides when extracts from the other cell population are subjected to the same enzymatic treatment. If extracts containing the tryptic peptides from the two cell populations are mixed, and subjected to analysis by MS, each peptide in the mix is detected as a pair, differing by a defined mass, depending on the isotope used in the metabolic labeling. Thus, the peptides from the different cell populations can be discriminated even if they are present in the same mixture, and the relative proportion of peptides from the two cell populations depends on two major factors. Peptides from proteins whose expression levels do not differ in the two cell populations show a fractional value that is constant, and represents the ratio of total protein chosen when mixing the two original extracts. The peptides from proteins differentially expressed in the two cell populations, in turn, show a fractional value departing from that reference figure. An advantage of this methodological setting, therefore, is the possibility to overcome possible errors when protein quantification is carried out by comparison of different samples analyzed by separate procedures (for instance, matching of images from different 2D gels).

Kellmann *et al.* used the SILAC procedure with the neuroblastoma SH-SY5Y cell line and analyzed the changes that an incubation with 15 nM AZA-1 for 12 h could induce in the protein expression profiles [99]. The peptides corresponding to about 1000 different proteins were quantified, and a linear regression of fractional values (quantitation ratios) obtained for those proteins led to identification of the upregulated (a total of 59) and downregulated (a total of 47) components. The classification of those

proteins according to gene ontologies showed that most of differentially expressed components could be grouped into few categories. Interestingly, upregulated and downregulated proteins could be distinguished in separate categories [99]. The upregulated components included proteins involved in energy metabolism, most of which are located in mitochondria, and proteins involved in cytoskeletal organization. Most of the downregulated proteins, in turn, comprised components involved in mRNA splicing, the control of gene transcription, protein synthesis and maturation, nucleotide metabolism as well as vesicle and protein transport [99]. The findings of that study were validated by immunoblotting of AHNAK and calpain, whose levels were found to be increased by AZA-1 treatment of SH-SY5Y cells, confirming the results obtained by SILAC procedure.

The use of different techniques allowed Kellmann *et al.* to probe some molecular and cytological features related to the findings obtained by proteomic analysis. For instance, the findings that several enzymes involved in energy metabolism were upregulated by AZA-1 led to the measurement of the effect of the toxin on mitochondrial membrane potential, the cellular concentrations of ATP and ADP, and the levels of lactate in the culture medium. Thus, it was found that AZA-1 did not significantly alter the mitochondrial membrane potential (at least within the first h of cell treatment), caused a transient, but severe depletion of cellular ATP and ADP, indicating that mitochondria were intact and the oxidative phosphorylation was not uncoupled in cells exposed to AZA-1. Interestingly, AZA-1 was not found to alter the levels of lactate in culture medium, indicating that the toxin did not increase the rate of anaerobic glycolysis under those experimental conditions. Thus, a significant alteration of cellular metabolism would be part of the response induced by AZA-1 in SH-SY5Y cells [99], confirming the conclusions obtained by the analysis of transcription profiles in lymphocytes [61].

The changes AZA-1 induced in the expression of proteins involved in cytoskeletal structure/functioning [99] were expected, considering that AZAs have been found to alter actin-based cytoskeleton in several cell lines [100–103]. The mechanistic implications of changes recorded by Kellmann *et al.*, however, were not readily apparent, considering the diverse biological functions of those proteins [99].

The downregulation of components involved in mRNA splicing, the control of gene transcription, protein synthesis and maturation as well as nucleotide metabolism would indicate extensive impairment of macromolecular synthesis, primarily RNA and proteins. This is consistent with the inhibition of cell growth exerted by AZA-1 [99], a response recorded in several experimental systems [100–106].

The downregulation of proteins involved in vesicle and protein transport [99] could contribute to the mechanisms of cell toxicity induced by AZA-1 by a disruption of regulated movements of components among

relevant subcellular structures. Thus, the reduction in the number of early endosomes [99] would be part of this functional alteration induced by AZA-1 in SH-SY5Y cells and could represent a general aspect of the responses induced by AZAs in sensitive systems [18]. The capacity of AZA-1 to inhibit endocytosis of plasma membrane proteins has been shown in epithelial cells [103] and could play a key role in the perturbation of cellular functions induced by AZA-1, leading to cell death [18].

4.4. Yessotoxins

This group of sulfated polyether toxins has an as yet unknown molecular mechanism of action [18]. The health risk posed by these toxins is highly debated, because they have been found to cause animal death by *i.p.* injection, but severe adverse effects have not been recorded after oral administration of YTX, the parent compound of the group, and no human intoxication has been linked to this group of natural substances so far [18]. The detected low oral toxicity of YTX is probably due to low absorption of the compound in the gastrointestinal tract, as low concentrations (about 3 nM) have been found in the blood of mice that received 1 mg YTX/kg b.w. daily, for seven consecutive days, by gavage [107].

Many groups have studied the mechanism of action and molecular responses induced by YTX in cellular systems [18,23]. In several instances, however, experimental systems have been exposed to high YTX concentrations (10^{-7} – 10^{-6} M), that may not be compatible with those expected to occur in humans ingesting naturally contaminated shellfish [108]. Thus, the toxicological relevance of findings obtained by exposing experimental systems to YTX concentrations higher than 10^{-8} M, in the lack of dose–response analyses showing that recorded effects can be induced also at lower YTX doses (around 10^{-9} M), remains uncertain [18].

The lack of knowledge regarding the mechanism of action of YTX and the variety of effects recorded in cellular systems exposed to this toxin has been at the basis of a study carried out in HepG2 cells, where the differential expression of proteins after exposure of the system to YTX was analyzed, following the classical methodological setting of protein fractionation by 2D gels, image analysis, and identification of differentially expressed proteins by MS analyses of their tryptic peptides [109]. In this study, cells were exposed to 1.4 μ M YTX and cells were harvested 3–24 h after toxin addition, for the preparation and analysis of soluble extracts from cell lysates. Fifty-two proteins, whose levels were statistically different in YTX-treated cells, as compared to controls, were identified by MS analyses and found to include components differing with regard to their functional roles and subcellular location [109]. In particular, proteins could be grouped among components of heterogeneous nuclear ribonucleoprotein particles (hnRNP), the cytoskeleton, lysosomal proteases, and heat shock proteins.

The hnRNPs differentially expressed in cells exposed to YTX included members of the groups A/B, E, H, K, L, which are involved in distinct steps of RNA processing, such as hnRNA splicing (A/B, E, H, K, L), mRNA trafficking (A/B), stability (A/B, E, H, K, L), and translational regulation (A/B, E, K, L) as well as chromatin remodeling (E, K) [110]. No unique pattern of response for those proteins could be identified, as both up- and downregulation of hnRNPs were detected, and differentially affected components could consist of degradation products [109]. Lamins A/C and B1, which participate to the intermediate filaments underneath the inner side of the nuclear membrane, were affected by YTX in an opposite fashion, as lamins A/C were upregulated and lamin B1 was downregulated [109]. The expression of cathepsins (B and D) changed in a biphasic fashion in cells treated with YTX, as increased levels were detected 3 h after toxin addition, but were downregulated thereafter [109]. The cellular levels of several heat shock proteins were found to be affected by YTX, which mostly caused a downregulation of components (hsp 70, hsp 90). These changes were accompanied by the upregulation of hsp gp96 and of disulfide isomerase precursors, indicating that stress response proteins were involved in the processes triggered by YTX [109]. Overall, the changes in the levels of hnRNPs, the upregulation of lamin A/C, and stress response proteins (hsp gp96 and of disulfide isomerase precursors), as well as the decreased levels of cathepsin D, supported the conclusions that YTX altered protein degradation processes and induced apoptosis in HepG2 cells. These conclusions are in keeping with literature data regarding the capacity of YTX to alter protein degradation by inhibition of endocytosis and phagocytosis [111,112], to perturb lysosomal activity [113], as well as to the induction of apoptosis in several cell lines [18,113–118]. Taking into consideration that the study by Young *et al.* has been carried out by cell exposure to 1.4 μM YTX [109], a concentration that is about three orders of magnitude higher than those that are expected in animals exposed to the toxin by the oral route [107], further analyses by differential proteomics in cellular systems exposed to nM YTX seem important for probing the toxicological relevance of the effects found in HepG2 cells.

Within this constraint, it should be stressed that the pathway analysis reported in this study is a very important contribution [109], whereby the potential functional relationships of proteins differentially expressed in YTX-treated cells are considered with regard to their participation to biological networks. To the best of our knowledge, this represents the first published attempt to identify the biological networks [7] that could embody the pathways of molecular responses triggered/affected by a microalgal toxin, as defined by differential expression proteomics. Considering the data obtained at the first time point (3 h), the best ranking pathways included components involved in posttranslational modifications, protein folding, and cell cycle, whereas those of the three subsequent time points

(12.5, 18, and 24 h), included posttranslational modifications, protein folding, and cell death, supporting the conclusion that extensive cell damage and cell death represent major features of molecular responses induced by YTX in cellular systems [18,113–118].

Considering the uncertainties regarding the mechanism of action of YTX, the findings reported in a recent paper, obtained by a targeted proteomic approach, might be of particular interest [65]. In this study, lysates were prepared from human blood cell membranes and were incubated with beads containing immobilized desulfated YTX (dsYTX), aiming at separating proteins selectively bound to the ligand by a pull-down procedure. The tryptic peptides obtained from the affinity purified material were subjected to MS analysis, and the proteins that had the best matches with the detected peptide sequences included several members of the superfamily of Ras proteins, including Rap 1A, Rap 1B, Rho A, Rho C, Rac 1, Rac 2, and K-Ras [65].

These findings might be particularly relevant with regard to ongoing efforts to clarify the molecular mechanism of action of YTX. Members of the Ras superfamily proteins, in fact, have been shown to play key roles in the regulation of cell proliferation [119], the regulation of cell adhesion [120,121], as well as vesicle trafficking [122]. YTX, in turn, has been shown to alter the ultra-structure of the E-cadherin–catenin system and to block E-cadherin endocytosis *in vitro* [111,123,124], as well as to perturb the turnover of E-cadherin in the colon of mice orally administered with YTX [125]. Taking into consideration that the E-cadherin system plays a key role in cell–cell adhesion of epithelia [126], it is tempting to speculate that Ujihara *et al.* might have obtained the first indications regarding the molecular target of YTX [65].

4.5. Ciguatoxins

The toxins of this group are recognized to cause ciguatera in animals, including humans, as a consequence of eating fish contaminated with compounds produced by the toxic alga *Gambierdiscus toxicus* (for reviews, see Refs. 18,25,127). Ciguatera has highly variable symptoms, affecting primarily the gastrointestinal tract and the nervous system, which are recorded within hours from the ingestion of contaminated food, and may last for long periods [25,128,129]. The complexity of the symptoms of this poisoning, including the case of chronic ciguatera, remains only partially understood, and could be due to the fact that the microalga *G. toxicus* produces several toxins, in addition to multiple ciguatoxin congeners, including maitotoxin and GB. Different molecular mechanisms of action, in fact, have been recognized for these compounds [18]. More specifically, ciguatoxins bind to site 5 of voltage-gated sodium channels, causing uncontrolled entrance of Na⁺ ions into the cells [25,130]. Maitotoxin, in turn,

affects calcium channels, leading to increased intracellular calcium levels [26,32], whereas low concentrations of GB inhibit voltage-dependent potassium channels [131,132].

The study by Ryan *et al.* [60] took into consideration the complexity of ciguatera symptoms, and the possibility that recorded effects might involve nonexcitable cells. Thus, the investigation was aimed at probing whether alterations of the immune system might be caused by ciguatoxins in an animal system. Mice were used in this study, were exposed to 264 ng of P-CTX-1/kg by *i.p.* injection, and blood was collected 1, 4, and 24 h after the administration of the toxin, to obtain peripheral leukocytes and serum. Leukocytes were used for an analysis of transcription profiles, by the use of oligonucleotide microarrays, whereas serum was used for the measurement of proteins participating to immune responses (mostly cytokines), through a selective immunoassay [60]. The proteomic approach in this investigation was then applied to a targeted subproteome of blood serum. Further, the complementing of transcriptomic and proteomic methodologies represented an interesting feature of this study.

Four serum proteins were found significantly changed in samples from mice exposed to P-CTX-1 for 4 h, comprising chemokine ligand 2 (Ccl2), and Ccl12, CD40, and macrophage colony stimulating factor (M-CSF). A matching of results with transcription profiles of leukocytes did not provide significant agreement between the two sets of results, which could be due to the fact that serum proteins could originate from cells of organs other than blood leukocytes themselves, as the authors pointed out [60]. Within this limitation, however, the observation that decreased levels of Ccl2 protein in mouse serum were matched by a reduced transcription of the gene coding for *Ccr2*, the receptor of Ccl2, in leukocytes, 4 h after P-CTX-1 administration, represented an interesting finding, considering that the expression of *Ccr2* gene has been found to affect the levels of Ccl2 in the mouse [133].

Other data in the study by Ryan *et al.* [60] indicated that the transcription of several components of immune response in leukocytes were affected by P-CTX-1 administration to mice, and the finding that the transcription of the gene coding for histidine decarboxylase was upregulated was found to be of particular interest with regard to some recorded symptoms of ciguatera in patients. This enzyme, in fact, catalyzes the conversion of histidine into histamine, and it was speculated that increased histamine production could contribute to the breathing difficulties found in animals and humans in response to CTX exposure [60,128,129].

Overall, the data obtained in that study, including the finding that P-CTX-1 causes changes in the serum levels of several cytokines, support the conclusion that this toxin affects the levels of a number of components involved in immune response [60], providing further indications on the complexity of molecular bases of ciguatera poisoning, and the need to expand studies at a system level [60,62].

4.6. Gambierol

Differential proteomics has been used to study cellular responses to the ciguatera toxin GB. The investigation was not aimed, however, at a better characterization of the molecular mechanism of action of this toxin, as it was devoted to probe major features of molecular responses to toxin mixtures at a system level, using OA and GB [54]. The rationale and experimental strategy of that study, as well as its major findings and implications, will be described below. In any case, the differential expression of proteins induced by GB alone was analyzed in that study, providing a preliminary picture of components affected by this toxin. The investigation was carried out in MCF-7 cells, which were treated with 50 nM GB for 24 h. The differential expression of proteins was studied in soluble extracts prepared by centrifugation of whole cell lysates and was performed by 2D electrophoresis and image analysis of stained gels, followed by tryptic digestion of relevant proteins and analysis of fragmented peptides by MS [54]. The cellular levels of nine components were found to be significantly changed by GB treatment. Four hsp 27 isoforms were upregulated by GB and included both intact and proteolytic fragments of the protein. The levels of three enzymes were found changed in extracts from cells exposed to GB, including the upregulation of the subunit δ of ATP synthase [54]. On the basis of the increased levels of the stress response protein hsp 27 and of the reported increase in cellular levels of ATP synthase subunit δ in stress responses in different experimental systems [134–137], it was concluded that GB induced a stress condition in MCF-7 cells [54]. A matching of results obtained in the same system after exposure to a different toxin (OA) and to the mixture OA + GB, however, had wider implications with regard to the patterns of response to toxin mixtures, that will be considered below.

4.7. Palytoxin

This compound is one of the largest microalgal toxins isolated so far (reviewed in Ref. [137]). It was originally found in zoantids [138], and it has been shown to be produced by benthic dinoflagellatae of the genus *Ostreopsis* [138]. In the past, this microalga has been mostly recorded in tropical areas [139], but its distribution has changed in recent years, and widespread occurrence in the Mediterranean Sea has been recognized [18]. Recently, blooms of *Ostreopsis* species have been suspected to be the cause of human intoxications [140,141], extending existing records of toxic episodes linked to PITX and related compounds [142]. Indeed, the toxicity of PITX is being debated with regard to the possible routes of exposure, the time frames of responses, and the molecular bases of recorded effects [143,144]. Thus, a unified model combining acute lethal effects involving excitable tissues, prolonged nonlethal effects, and responses involving nonexcitable cells, as well as tumor-promoting activity

[142–144] of PITX is not available, in spite of the significant existing knowledge on its mechanism of action [30,31]. After about 40 years of investigations, the early recognition that PITX binds to Na^+, K^+ -ATPase and converts the pump into a nonselective cation channel [145,146] is fully accepted. In keeping with this notion, it is recognized that the disruption of ion homeostasis is the basis of effects exerted on excitable tissues (reviewed in Ref. [31]). A less clear picture, in turn, exists with regard to effects recorded in nonexcitable cells, where different sets of proteins and signaling pathways can be affected by the toxin, stressing the complexity of the mode of action of PITX [30,147–149]. For instance, PITX can induce activation of protein kinases involved in the control of cell proliferation [147], and these responses might play a role in the tumor-promoting activity of this toxin [49,150]. However, PITX has been also shown to possess a potent cytotoxic activity [149], as found with toxins inhibiting type 1 and type 2A PPases, such as OA and MCs (see above).

The potent ($\text{EC}_{50} \approx 10^{-11} \text{ M}$) and rapid (2–12 h, depending on experimental conditions) cytolytic activity of PITX in the MCF-7 cell line [151] has stimulated a study at a system level, aimed at the characterization of proteins participating to the cell death response induced by the toxin in nonexcitable cells [90]. To this end, the experimental system was treated for 8 h with 0.03 nM PITX, representing the toxin's EC_{50} under those conditions, resulting in cell cultures undergoing a death response, without detection of extensive cell disruption [90]. The differential expression of proteins was studied by the procedures used in other proteomics studies using the same system [54,90], and it was found that PITX induced changes in the levels of four proteins, comprising three isoforms of hsp 27 and one isoform of the DJ-1/PARK7 protein. The results obtained by image analysis of stained gels were fully validated by immunoblotting procedures after protein separation by both one- and 2D gel electrophoresis [90]. The three upregulated hsp 27 isoforms comprised the putative mono-, bis-, and tris-phosphorylated proteins, including isoforms containing a phosphorylated Ser_{82} (Ref. [90], see also Figures 3 and 8 in this review). The DJ-1 protein in MCF-7 cell extracts was found to include two major isoforms, differing according to their isoelectric point, and PITX was found to increase the more acidic protein, while leaving the levels of the other isoform unchanged [90]. The acidic shift in the pI of DJ-1 was undistinguishable from that reported in the literature for the protein isoforms containing an oxidized cysteine [152–154], and it was concluded that PITX induced an increase in oxidized DJ-1 [90]. Based on the literature data showing that increased cellular levels of oxidized DJ-1 are associated with stress conditions [152–155], as well as the recognized role of hsp 27 in cell stress responses [156–161], it was concluded that the toxicity pathway of PITX in MCF-7 cells involves increased posttranslational modifications of stress response proteins, leading to higher cellular levels of phosphorylated hsp 27 and oxidized DJ-1 [90]. Although the death response induced by PITX had

been shown to be inhibited by ouabain in MCF-7 cells [151], indicating that a perturbed functioning of Na^+, K^+ -ATPase was triggering the recorded effects, no specific information regarding the chain of events in the toxicity pathway of PITX was obtained in that study [90].

4.8. Toxin mixtures

Biological systems can be exposed to mixtures of toxic compounds in ordinary living conditions, and it is known that seafood can be contaminated by multiple components belonging to different groups of toxins at the same time [39,50–52]. Thus, investigations aimed at characterizing responses of a biological system to mixtures of toxins is justified by both general and factual considerations, as the consumers might become exposed to multiple toxins by ingestion of contaminated seafood. Further, possible interactions and synergistic effects of different groups of microalgal toxins are essentially undetermined, posing additional reasons of concern.

Differential expression proteomics has been used to investigate onto the pattern of responses induced in a model system, aiming at identifying sets of components and possible interactions between toxicity pathways, as inferred by the proteins involved in the responses induced by two different toxins. This study was carried out by treating MCF-7 cells with OA, GB, as well as a mixture of the two compounds [54]. The data obtained when the system was exposed to each of the two toxins, separately, have been described above. The choice to carry out the study using a mixture of OA and GB was not based on recorded co-occurrence of the two components in contaminated materials, but it was actually due to considerations regarding the general strategy to use in that study [54]. In particular, the level of complexity of results expected from proteomic analyses, and the hypothesis that possible interactions between toxicity pathways might be responsible for some of the effects eventually found in the model system, were considered. Thus, MCF-7 cells were exposed to toxins that are considered to possess completely distinct molecular mechanisms of action, aiming at reducing possible interactions between separate mechanisms at the cellular level, and, possibly, simplifying the interpretations.

The expected complexity of results was confirmed in the initial part of that investigation, when image analysis of stained gels revealed that multiple patterns of response were detected, depending on individual protein spots. Thus, independent, synergistic, similar, and antagonistic responses were detected, based on recorded intensity of protein spots in 2D gels [54]. This kind of result was unexpected, and findings were analyzed by hierarchical matching of data. Results were primarily analyzed to define the significance ($p < 0.05$) of changes found in combined treatments, as opposed to controls (set 1). A second level of analysis, in turn, included the components whose changes were significant in cells treated with one

Primary set	Mix vs Controls	Secondary set	Mix vs OA	Mix vs GB	Action
1	Y	A	Y	Y	Synergism
		B		N	
		C	N	Y	Independent
		D		N	
2	N	A	Y	Y	Antagonistic
		B		N	
		C	N	Y	
		D		N	

Figure 4 Patterns of responses in MCF-7 cells after a combined treatment with okadaic acid and gambierol. The figure has been reproduced from Ref. [54] with slight modifications.

toxin, individually, but not when the combined treatment was carried out [54]. The whole set of results was then distributed into a matrix, where the patterns of response were found to relate to specific subsets of data, based on their significance (Figure 4).

When the components were identified, some evaluation of possible modes of action of the toxins was attempted, but the limited number of proteins found to be differentially affected in a significant manner by OA and GB, both individually and in combination under the conditions of this study, allowed only some preliminary consideration [54]. The hsp 27 system, comprising both intact and fragmented proteins in their distinct phosphorylated states, appeared particularly affected by OA and GB, both individually and in combination. In particular, OA favored increases in the levels of phosphorylated hsp 27 isoforms, whereas GB treatment increased the levels of less phosphorylated counterparts, in an independent manner, whereas the combination of the two toxins increased the cellular levels of degradation products of hsp 27 synergistically. These findings were considered within the frame of toxicity pathways [54]. Based on the view that life versus death responses could be related to the opposition between phosphorylated and nonphosphorylated pools of cellular hsp 27 [54], the effects induced by OA and GB on this cellular stress response protein were interpreted in terms of an OA-induced death response associated with increased cellular phosphorylated hsp 27, and with a survival response to GB supported by increased cellular levels of non(less)-phosphorylated hsp 27 in MCF-7 cells [54]. The synergistic increase in cellular levels of fragmented hsp 27 in cells exposed to the mixture of toxins, in turn, was proposed to

result from a combination of the increased proteolysis of hsp 27 in cells that are being destroyed in the course of the death response (OA effect), and the normal degradation process of the cellular pool of the non(less)-phosphorylated isoforms when a higher content of hsp 27 protein exists, as a response to a cellular stress (GB effect) [54].

The need of more detailed quantitative analyses of responses, to fully evaluate proposed interpretations, was indicated in that study and should be stressed here. In any case, the finding that multiple patterns of response to toxin mixtures can be detected in a cellular system, depending on individual proteins, indicates that interactions between toxins with distinct mechanisms of action are component-related [54], and a mechanistic explanation of complex responses would then require targeted analysis of effector molecules, as well as careful consideration of cross-talks between toxicity pathways. In our opinion, further studies on molecular responses of cells to toxin mixtures are needed, to probe the potential of differential expression proteomics in this kind of investigations [54,162].



5. PROTEOMIC ANALYSES FOR PREDICTIVE TOXICOLOGY AND THE DETECTION OF ALGAL TOXIN CONTAMINATIONS

The potential of proteomics in predictive toxicology has been highlighted in recent reviews [11,13,55] as a relevant approach for the identification of sets of biomarkers exploitable for ecotoxicological evaluations, including the assessment of food safety with regard to possible toxin contamination [56,57]. Within this frame, the identification of sets of biomarkers for defined environmental stress/contaminations in sentinel species (mussels, clams, etc.) is attracting increasing interests from investigators [11,55,57,163].

Two general areas of intervention are then defined by studies exploiting proteomic tools in predictive toxicology, including the characterization of toxicological responses and the identification of contaminations. In both cases, the identification of biomarkers in biological materials is a primary goal, and the two areas of intervention are actually intertwined, as will be apparent in the studies we will describe below, which might be distinguished mostly by the general strategy used in investigations. When toxicological responses are investigated by proteomics, the experimental setting involves exposure of a model system to a defined toxin under controlled conditions (see, for instance, Refs. [136,164–167]). Materials naturally contaminated by toxins, in turn, represent the preferred source of extracts when a direct relationship between some contaminant and protein biomarkers is investigated (see, for instance, Refs. [168,169]). Indeed, the first type of study is quite similar to those developed for the characterization of the

molecular modes of action of toxins described in the preceding section, although emphasis in the studies described in this section is on the identification of biomarkers for monitoring levels of exposures to toxins, rather than the characterization of mechanisms whereby recorded effects are induced in the model system.

Investigations onto MC-LR, OA-group compounds, and AZAs are presented below.

5.1. Microcystins

The search for biomarkers of toxin exposure to MCs has been developed in different animal systems, including fishes (*Oryzias latipes* and *Danio rerio*) and a freshwater clam (*Corbicula fluminea*), under controlled laboratory conditions [136,164–167]. Different kinds of exposure were chosen, including waters containing controlled levels of either MC-LR [164,167] or one of MC algal producers, *Microcystis aeruginosa* [166], as well as direct toxin administration by gavage [136,165]. In these studies, proteomic analyses followed the basal setting of 2D gels and MS identification of relevant proteins in extracts obtained from animal tissues, which were prepared by distinct protocols, contributing to some differences among separate studies.

In the first study by Mezhoud *et al.* [164], medaka fishes (*O. latipes*) were exposed to 1 mg MC-LR/L in the water of aquaria for 30 and 60 min at 25 °C, livers were excised and the cytosolic fraction of cellular extracts was obtained by a commercial kit. Fluorescent staining of proteins was then used to distinguish between total and phosphorylated proteins, thereby distinguishing a subproteome of phosphorylated components that accounted for about 10% of the total proteome [164]. A total of 15 proteins differentially expressed in livers of fishes exposed to MC-LR were identified by MS in the cytosolic fraction, including five phosphoproteins, all of them being upregulated by MC-LR, and 10 putatively nonphosphorylated components [164]. Relevant proteins were involved in oxidative stress, apoptosis, and cellular ultrastructures. In particular, increased levels of phosphorylated keratin 18 were found, and were considered to be related to the disruption of cytoskeleton [164], which is a recognized tissue response to MC [170–173]. Oxidative stress and apoptosis are cellular responses to MC (reviewed in Ref. [76]), and the findings that proteins with antioxidant action, such as DJ-1 and the NKEF peroxiredoxin, are downregulated as a consequence of fish exposure to MC-LR [164] are in line with that notion. Interestingly, the 14-3-3 protein was found affected by MC-LR in medaka fish liver [164], confirming that this component could be a biomarker of system exposure to MC [80]. Interestingly, downregulation of 14-3-3 was detected in the liver extracts from fish exposed to MC-LR [164], whereas upregulation was induced by MC-RR in FL cells [80].

The study on medaka fishes was further developed by examining the effects of MC-LR exposure through a different route, and the administration of the toxin by gavage (5 μ g MC-LR/g b.w. of fish) allowed a better control over the levels of toxin actually introduced in experimental animals [165]. Two hours after gavage, animals were killed and livers were used for the preparation of cytosolic extracts, which were subjected to proteomic analyses [165]. The use of fluorescent probes to distinguish between proteome and phosphorylated subproteome was applied also to this study, and 17 proteins were identified with high confidence among those differentially expressed in extracts from livers of fishes exposed to MC-LR. Cytoskeletal proteins (α - and β -tubulin) and components involved in cellular responses to oxidative stress (ferritin H and peroxiredoxin) were found to be affected by MC-LR, and these findings were related to the apoptotic and oxidative stress responses induced by MC, as mentioned above. Although the overlapping between the components found to be affected by MC-LR in the two studies by the same group was only about 30% [164,165], some findings could be of particular interest. For instance, β -tubulin was downregulated by MC-LR in medaka fish liver [165], in keeping with the data obtained with FL cells [80]. Similar considerations can be put forth regarding the upregulation of ferritin, and a peroxiredoxin isoform [165], confirming that increased levels of these proteins can be found in systems exposed to MC [59,80] and lending support to the notion that they could represent biomarkers of system exposure to MC (see Section 6).

In another study on medaka fish, the proteomic analysis was extended to include proteins from cellular fractions other than cytosol, and the samples obtained by homogenization of livers were fractionated to yield extracts containing proteins from membrane and organelles, using a commercial kit [136]. In this latter investigation, the toxin exposure protocol and the methodology used for differential detection of proteins and phosphoproteins were identical to those employed when analysis of cytosolic fractions had been carried out [165]. Thus, the results of the two studies might then provide an integrated picture of the effects of medaka fish exposure to MC-LR on different subproteomes of liver cells. A total of 79 protein spots were found to significantly differ in the extracts from livers of fishes exposed to MC-LR, as opposed to controls, including 21 phosphoproteins and 58 proteins, respectively [136]. Seventeen proteins were identified, among which some components appear of interest with regard to data obtained in other studies on effects induced by inhibitors of PPases, including both MC and OA. The downregulation of β -tubulin as well as of β and δ subunits of ATP synthase [136], in particular, might be relevant with regard to identification of specific biomarkers (see Section 6).

The proteomic analysis of extracts from gills and digestive tract of the freshwater clam *C. fluminea*, which were prepared from animals after a 24 h feeding with an MC-producing strain of toxic *M. aeruginosa*, essentially

confirmed that cytoskeletal proteins are sensitive to MC in short-term studies [166]. In particular, upregulation of actin isoforms and downregulation of β -tubulin were recorded. Overall, the results obtained with medaka fish and *C. fluminea* indicate that acute effects triggered by MC-LR exposures through different routes involve stress response and cytoskeletal proteins [166].

A different picture, however, has been obtained when proteomics has been used to identify biomarkers of chronic toxicity induced by this toxin in zebrafish (*D. rerio*) liver. In the study by Wang *et al.* [167], zebrafishes were kept in water tanks and were exposed to low doses of MC-LR (2 or 20 $\mu\text{g/L}$ of water) for 30 days when livers were dissected from fishes. Liver extracts were obtained by homogenizing tissues with a solution containing trichloroacetic acid/acetone, leading to precipitation of macromolecules, and protein samples were then obtained by centrifugation yielding materials which were dissolved in an appropriate buffer and used for 2D gel analysis [167]. Twenty-two protein spots were found to significantly change in extracts from animals exposed to MC-LR, and their identification was achieved by MS analysis. The differentially expressed proteins identified in this study include enzymes involved in digestion of macromolecules and in cellular metabolism (14 components), 2 cytoskeletal proteins, and 6 proteins with either unknown or apparently unrelated functions. The enzymes found to be differentially expressed by both MC-LR doses used in this study included activities involved in fatty acid metabolism (2-hydroxyacyl-CoA-lyase 1) and glucose oxidation (pyruvate kinase, 6-gluconolactonase), as well as hydrolytic enzymes acting on starch (amylase α 2A) or proteins (elastase 3), all of which were downregulated by MC-LR [167]. Downregulation was observed also in the case of the two cytoskeletal components α 4 actinin and profilin 2-like protein [167]. In turn, a threefold increase in SOD was detected. Thus, the results of this study indicate that chronic exposure to MC-LR would result in changes of liver functioning characterized by a state of response to oxidative stress, and altered carbohydrate and lipid metabolism. Taking into consideration, the pervasive role that protein phosphorylation plays in the control of carbohydrate and lipid metabolism in liver [174–177], the conclusion that chronic exposure to a toxin inhibiting PPases leads to altered levels of metabolic enzymes in this organ [167] is relevant, although the phosphorylation states of individual components (such as pyruvate kinase) remain to be established.

5.2. Okadaic acid

To the best of our knowledge, the first study exploiting a differential proteomic approach using samples directly harvested in their natural environment, and leading to identification of protein biomarkers of toxin contamination in seafood appeared in 2008 [168]. The general structure of this study involved the instrumental measurement of different microalgal

toxins and the proteomic analysis of the same samples, aiming at identifying protein biomarkers for individual toxin groups. The toxins quantified by LC-MS included OA-group compounds (OA, DTX-1, DTX-2), YTX, homoYTX, pectenotoxin-2, and 13-desmethyl-spirolide-C [167]. Thus, the study was not targeted to any specific toxin, although a significant correlation was eventually found only with OA-group compounds [167].

Owing to the general question at the basis of this investigation, and the use of the digestive gland (DG) of a filter-feeding mollusk (*Mytilus galloprovincialis*) as the source of extracts, the experimental strategy was defined taking into consideration major sources of variability and possible confounding factors [167]. In particular, the possibility that protein profiles of extracts from DG might be affected by prevailing algal populations existing in the sampling site and in different periods of sampling, as well as individual factors were considered. Mussels were then harvested in four different sites of the Northern Adriatic Sea (Italy) in an area of about 400 km, to compensate for possible geographic variability, during an 18-month period, to compensate for seasonal variations [167]. The possible effects of interindividual variability on protein profiles, in turn, were eliminated by pooling DG dissected from at least 50 different individuals in each sample. Further, the possible unwanted degradation of proteins in crude extracts of DG by endogenous proteases under uncontrolled cell-free conditions was approached by resuspending tissue samples in acetone, thereby causing protein denaturation [167]. The proteins that remained soluble in acetone extracts were then subjected to proteomic analysis by 2D gels and identification of relevant components was achieved by MS analysis. The levels of two protein components in the extracts from mussel DG were found to increase as a function of their content in OA-group compounds [167]. Database search of peptides identified by MS indicated that the two relevant proteins showed homologies with domains in a component of photosystem II and subunit 5 of NADH dehydrogenase from *Mytilus*, respectively [167].

The increased levels of putative subunit 5 of NADH dehydrogenase in extracts from the DG of mussels naturally contaminated with OA-group toxins were discussed with reference to apoptotic responses induced by these toxins [46], in line with the notion that this protein could represent a biomarker of OA contamination in environmental samples [167]. The detection of a protein that shows homology with a component expressed in photosynthetic organisms, in turn, might not be considered an endogenous component, and the possibility that its detection was due to materials from algae present in the DG of a filter-feeding organism was evaluated. On the basis of the recognition that OA-group toxins are produced by photosynthetic algae of the genera *Dinophysis* and *Prorocentrum* [17], a BLAST search was carried out to evaluate possible homologies of the photosystem II protein from different species, using a peptide in the detected protein. By this search, it could be concluded that the relevant peptide is part of

the photosystem II protein in several species of *Dinophysis* but not in *Prorocentrum* [167], and this finding was in line with the recognition that OA contaminations in mussels from the Northern Adriatic Sea are due to *Dinophysis* blooms [178,179].

Overall, the data in the study by Ronzitti *et al.* showed that toxin contamination in natural samples can be detected by a differential expression proteomic approach through both endogenous and exogenous protein biomarkers [167]. The two kinds of components, however, should be considered with reference to different biological processes, that is, endogenous biomarkers represent molecular effects induced by toxins in the host, whereas exogenous biomarkers would consist of cocontaminants [167].

5.3. Azaspiracids

A targeted proteomic approach was aimed at identifying proteins that might be physically associated with AZAs in DGs of contaminated mussels [180]. In this study, extracts from mussel DG were subjected to preparative isoelectric focusing, and the fractions containing AZAs were pooled and subjected to size exclusion chromatography and SDS-PAGE. Paired analyses of relevant fractionated materials showed that fractions in extracts from DG of AZA-contaminated mussels contained five bands whose intensity was much higher than those found in extracts from control mussels [180]. The five bands had electrophoretic mobilities corresponding to components of 21.8–45.3 kDa, two of which were proposed to represent biomarkers of AZA contamination in mussels [180]. The identification of those components was accomplished in a subsequent study, by MS analyses of materials in four major bands separated by SDS-PAGE in extracts from the DG of AZA-contaminated mussels [169]. The proteins identified in three bands showing an electrophoretic mobility corresponding to components in the 20–50 kDa MW range, included cathepsin D, p53 family proteins, SOD, glutathione-S-transferase, and multidrug resistance-associated protein [169]. The higher levels of those proteins were discussed with reference to apoptotic effects (cathepsin D, p53 family proteins) and stress responses (SOD, glutathione-S-transferase, multidrug resistance-associated protein), which would be in line with the known toxic effects of AZAs *in vitro* and *in vivo* [18,28,99–106].

The fourth band, in turn, contained a protein showing homology with a flagellar P-ring protein precursor of bacterial origin (*Methylobacterium populi*), and the ubiquitous characteristic of bacteria from the *Methylobacterium* genus was considered to explain the detection of the protein in mussels as a result of bacterial infection [169].

The detection of a bacterial protein in extracts from mussel DG is in keeping with the detection of a photosynthetic component showing homology with *Dinophysis* species in the DG of OA-contaminated mussels [168], suggesting that proteins from organisms introduced by feeding

habit, or else associated with mollusks, might ordinarily co-occur in samples from tissues of filter-feeding animals.

6. PRELIMINARY CONSIDERATIONS ON STRENGTHS AND WEAKNESSES OF PROTEOMIC APPROACHES IN INVESTIGATIONS ONTO TOXICITY PATHWAYS

Less than 20 reports on the molecular basis and modes of action of microalgal toxins, as studied by differential expression proteomics, can be found in the literature and have been discussed with some detail in the previous sections. Different model systems were used in those studies, including tissues from intact animals, as well as cultured cell lines, to investigate onto six distinct chemical groups of toxins. Overall, the background knowledge available for an evaluation of progress made in the area is very limited. Nonetheless, we will discuss major indications stemming from those studies, because they can be useful for both sketching the core items of toxicity pathways emerging from data on different toxins, as well as the identification of major bottlenecks and limitations appearing from ongoing investigations. It is our opinion that the variety of distinct systems and existing differences in experimental designs are actually providing significant information by consideration of their strengths and limitations, supporting refinements of research activities on modes of action of microalgal toxins using differential expression proteomics.

6.1. Quantitative issues in differential expression proteomics

A summary of major quantitative differential expression proteomics data retrieved from the literature on biological responses to microalgal toxins is reported in Table 2. In most cases, less than 100 proteins were found to be differentially expressed as a consequence of toxin treatment. This low number of components, as compared to estimated values of 10^5 or more different proteins expressed in eukaryotic cells [9,181,182], confirms that the potential to detect changes in protein profiles by available proteomic techniques is still limited. The use of protein staining after their separation by 2D gels is the most likely explanation, as it is recognized that the concentrations of proteins *in vivo* can differ by several orders of magnitude [9,10,183], whereas the dynamic range of staining procedures in most cases is limited to one to two orders of magnitude [184]. While this implies that only the most abundant cellular proteins are detected by methodologies involving protein staining [9,10], this condition should not nullify the significance of existing proteomics data (see below).

Protein staining and image analysis are often used to detect proteins in most of the existing studies on microalgal toxins. This methodological

Table 2 Summary of differential expression proteomics data from studies on modes of action of microalgal toxins

Toxin	Biological system ^a	Proteins ^b	Validated proteins ^c	Reference
Microcystins	Mouse liver	65	BAX ^d BID ^d Bcl-2X ^d	[59]
	FL cells	110	ERK 1 p53	[80]
	Medaka fish liver	15	None	[164]
	Medaka fish liver	46	None	[165]
	FL cells	42 ^e	PP2A (A subunit) hsp 70	[88]
	Medaka fish liver	58	None	[136]
	Clam gills	16	None	[166]
	Clam digestive tract	13	None	[166]
	Zebrafish liver	22	None	[167]
Okadaic acid	MCF-7 cells	30	None ^f	[54]
Azaspiracid-1	SH-SY5Y cells	106	AHNAK calpain	[99]
	Mussel digestive gland	9 ^g	None	[169]
Yessotoxin	HepG2 cells	55	hnRNP H1 (spot 29)	[109]
Gambierol	MCF-7 cells	9	None ^f	[54]
Palytoxin	MCF-7 cells	4	“Acidic” hsp 27 ^h Two isoforms of hsp 27 phosphorylated in Ser ₈₂ Acidic isoform of DJ-1	[90]

^a When tissues are used, the contribution of different cell populations is undetermined.

^b The indicated figure is the total number of proteins whose expression was significantly affected by toxin treatment, as indicated by authors in the paper.

^c Data refer to proteins whose levels were quantified in the published paper by immunoblotting procedures.

^d The differential expression of proteins was validated on the basis of results obtained by transcriptomic analysis because the indicated proteins were not detected by protein staining of 2D gels.

^e Data have been taken from Table 2 of the paper, referring to the materials harvested 12 h after toxin removal from culture medium, representing the experimental condition that best matches those of Ref. [80].

^f Data on 2 isoforms of hsp 27 protein have been validated in Ref. [91] (see also Figure 8 in this review).

^g Data have been taken from Table 2 of Ref. [169].

^h Acidic hsp 27 is spot 4107 in the center panel of Figure 3 in this review, and most likely represents an hsp 27 isoform phosphorylated in a residue other than Ser₈₂ [90].

choice may be a source of error in the detection and quantification of differentially expressed components [9,14,55], and alternatives include either the use of more accurate methodologies to detect relevant proteins or the confirmation of detected changes by immunoblotting of proteins using specific antibodies, after their fractionation by one-dimensional (1D) SDS-PAGE. The use of the SILAC procedure is considered an efficient way to obtain more accurate quantitative estimates of differentially expressed proteins [14,55], and it has been used to study the effect of AZA-1 [99]. This methodology, however, has not been widely used in studying microalgal toxins, so far. Likewise, the validation of results obtained by image analysis of stained gels using immunoblotting procedures has not been extensively carried out, as indicated by the data of Table 2. Thus, a more frequent use of immunoblotting analysis to confirm results obtained by proteomics would be appropriate. In some cases, for instance, data obtained by image analysis of stained gels do not show clear dose-response or time-response relationships. This can be eventually clarified by immunoblotting procedures [80,88]. In other cases, immunological tools can strengthen proteomic studies, by characterizing molecular features of relevant components. The many isoforms of hsp 27 and their different phosphorylation states can provide a first example. The single band detectable by immunoblotting analysis of an extract by 1D electrophoresis (Figure 5) may not resolve

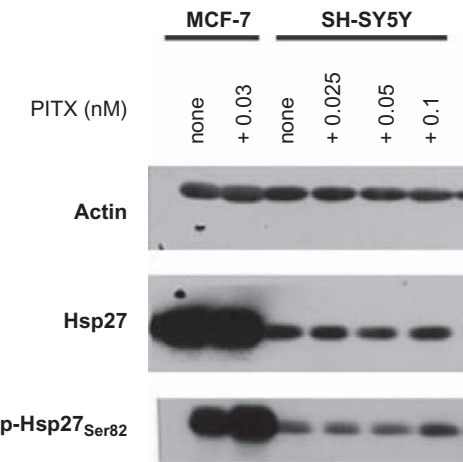


Figure 5 Effect of palytoxin on the phosphorylation state of hsp 27 in MCF-7 and SH-SY5Y cells. Cells received the indicated concentrations of PITX, and were incubated for 8 h at 37 °C, before being processed for the preparation and immunoblotting analysis of cytosoluble extracts, using the procedures described in Ref. [90]. The figure shows the results obtained when immunoblotting analysis was carried out using antibodies specific for actin, total (both phosphorylated and nonphosphorylated isoforms) hsp 27, and hsp 27 isoforms phosphorylated in Ser₈₂, as indicated.

isoforms of similar mass but different isoelectric points. Thus, no relevant changes are detected in the total levels of hsp 27 between control and PITX-treated cells in the two experimental systems, which clearly differ with regard to their respective endogenous concentration of hsp 27, based on their actin content, being higher in the epithelial MCF-7 cells than in the neuronal SH-SY5Y cell line. In turn, an increase in the isoforms phosphorylated in Ser₈₂ is visualized by immunoblotting with a specific antibody in the extracts from cells exposed to PITX (Figure 5). Additional information can be obtained if better resolution of components is achieved by coupling 2D electrophoresis and immunoblotting (Refs. [90,91], and Figures 3 and 8 in this review). Likewise, immunoblotting analyses of proteins resolved by 2D gels have shown that both OA and PITX induce increases in cellular levels of an acidic DJ-1 isoform [64,90]. Interestingly, other differences among DJ-1 isoforms are apparent when considering these studies [64], further supporting the conclusion that the use of distinct methodologies to complement proteomic analyses can become particularly informative when approaching molecular bases of biological functions.

6.2. Characterization of toxicity pathways

The capacity of proteomics to tackle the complexity of sets of components in living organisms is a key element of its potential in defining molecular steps of toxicity pathways. The data gathered by differential expression proteomics, as applied to the study of the modes of action of microalgal toxins, then provide the material for preliminary analysis of major elements that could bring about their cellular responses. In our discussion on the characterization of toxicity pathways, the results reported in the papers discussed in previous sections will be the primary source of information, in keeping with our focus on proteomics studies, but additional data obtained by more classical “reductionistic” approaches will complement our considerations, whenever they appear to relate to the issues being analyzed. MCs have been studied more extensively than other groups of microalgal toxins and provide the widest set of toxicoproteomic data at the moment. Taking into consideration that type 1 and type 2A ser/thr PPases are targeted by both MCs and OA, the data regarding this latter toxin can contribute to evaluations regarding the modes of action of these toxins. Thus, our preliminary considerations on the contribution of differential expression proteomics to the characterization of toxicity pathways will be mostly confined to these toxins. A summary of data is presented in Table 3, which is limited to the proteins whose functional roles and significance have been stressed in respective studies.

If we consider data on MCs, listed components can be primarily classified among proteins involved in apoptosis, oxidative stress, and cytoskeleton, as already noted (Sections 4 and 5). A limited matching of components,

Table 3 Major proteins found affected in biological systems exposed to toxins acting by inhibiting type 1 and type 2A ser/thr phosphoprotein phosphatases, as established by differential expression proteomics

Toxin	Microcystin-LR					Microcystin-RR			Okadaic acid	
Biological system ^a	Mouse liver		Medaka fish liver		Clam gills and digestive tract	Zebrafish liver	FL cells		MCF-7 cells	Tentative matching ^b
Major proteins ^c	BAX <i>BID</i> <i>Bcl-2</i> Ferritin <i>Peroxiredoxin 1</i> Peroxiredoxin 2 <i>Peroxiredoxin 6</i>	Phospho-keratin 18 <i>DJ-1</i> <i>Peroxiredoxin</i> (<i>NKEF</i>) <i>14-3-3</i>	<i>β-Tubulin</i> Ferritin Peroxiredoxin (NKEF)	<i>β-Tubulin ATP synthase (β and δ subunits)</i>		<i>Pyruvate kinase</i> 6-Glucono lactonase <i>2-Hydroxyacyl-CoA-lyase 1</i> <i>Amylase α 2A</i> <i>Elastase 3</i> <i>α4 actinin</i> <i>Profilin 2-ike protein</i> Superoxide dismutase (Cu-Zn)	ERK 1 p53 14-3-3 <i>β Tubulin</i> Peroxiredoxin 2	PP2A (A subunit) hsp 70 <i>Proteasome β subunits 2, 4, 6, 9</i> Ubiquitin fusion degradation 1-like	Phospho-hsp 27 <i>ATP synthase (α subunit and δ subunit)</i> <i>Nucleoside diphospho kinase A</i> <i>Superoxide dismutase (Cu-Zn)</i> <i>Peroxiredoxin 5</i> <i>Thioredoxin</i>	<i>Peroxiredoxins</i> <i>Thioredoxin</i> <i>Ferritin</i> <i>Superoxide dismutase (Cu-Zn)</i> <i>BAX</i> <i>BID</i> <i>Bcl-2</i> <i>hsp 27</i> <i>ATP synthase</i> <i>DJ-1</i> <i>β-Tubulin</i>
Reference	[59]	[164]	[165]	[136]	[166]	[167]	[80]	[88]	[54]	

^a When tissues are used, the contribution of different cell populations is undetermined.

^b The indicated proteins have been selected on the basis of results shown in the quoted studies and their relationship to additional data existing in literature, as described in the text. Isoforms/subunits remain to be defined.

^c The listed components represent the proteins whose expression levels were altered by the toxin and whose functional roles and significance have been discussed with reference to the studied system in the indicated reference. Upregulated proteins are in bold, whereas downregulated components are in italics.

however, can be found among different biological systems and/or studies (Table 3). Although cellular abundance of indicated proteins, as well as the difficulties in data analysis and quantification most likely contribute to recorded differences (see Section 6.1), the use of distinct experimental systems and conditions could be the primary source of variability in these studies (for instance, acute vs. chronic toxicity studies). Within these limitations, apparent matching might highlight components sharing important roles in the signaling pathway and/or molecular response to the toxin in different model systems and experimental conditions. The differential expression of peroxiredoxins (different isoforms), ferritin, and β -tubulin is mentioned in at least two different reports and would represent the most likely candidates for a tentative list of relevant components of toxicity pathways of MCs. If this analysis is extended to include proteins differentially affected by OA, other components can be added to the list, including proteins involved in oxidative stress, such as SOD (Cu-Zn) and the donor of reducing equivalents thioredoxin, hsp 27, some subunits of ATP synthase, as well as proteins of the Bcl-2 family and DJ-1 (Table 3).

The inclusion of these additional components to the list of tentative matchings stems from several considerations. On the first instance, some of these components are differentially expressed by both MCs and OA, as apparent either from the entries of the table or from inspection of tables in original studies, as is the case of hsp 27 (see Table 2 in Ref. [80]). A different situation, in turn, applies to components of the Bcl-2 family and DJ-1. As far as the components of the Bcl-2 family are concerned, their involvement in the apoptotic responses induced by MCs and by OA has long been recognized (see Ref. [46] and references therein as well as Refs. 59,87,89,98,185,186). With regard to DJ-1, its involvement in responses to OA has been documented by a recent paper, where the toxin was shown to affect the cellular pool of several DJ-1 isoforms, differing according to their size and isoelectric point in a dynamic fashion, and this response was accompanied by changes in the direct interactions of DJ-1 with other cellular proteins [64]. Interestingly, if total DJ-1 was analyzed by immunoblotting of proteins separated by 1D SDS-PAGE, changes in the cellular levels were transient and were not detected upon prolonged cell exposure to OA [64]. Thus, subtle changes in the cellular pool of DJ-1 isoforms are caused by OA, but their detection requires analytical procedures capable of distinguishing them, for instance by immunoblotting of proteins separated by 2D gels [64], in keeping with results obtained on hsp 27 [90].

The similar patterns of response of hsp 27 and DJ-1 molecular systems to OA and PITX [54,64,90] are interesting, although they can be framed by distinct molecular mechanisms sharing only some components. The phosphorylation of hsp 27, in fact, is catalyzed by protein kinases whose activity is under the control of phosphorylations by upstream activating kinases (reviewed in Ref. [161]). Thus, the inhibition of PPases by OA, and a

mechanism activating relevant kinases, as documented in the case of PITX [187,188], could converge toward similar patterns of hsp 27 phosphorylation. Analogous considerations can be put forward for the molecular mechanisms responsible for the accumulation of acidic DJ-1 [64]. Thus, it seems likely that MCs, OA, and PITX might share some steps in their respective mechanisms leading to cytotoxic effects.

On the basis of available data and the above considerations, a working model of processes that could be shared by the toxicity pathways of MCs, OA, and PITX is shown in Figure 6. In this model, the inhibition of PPases by MCs and OAs would trigger a toxic response converging toward the induction of oxidative stress in exposed cells. The response would involve oxygen radicals and the production of H_2O_2 by SODs, but the peroxides would be reduced by peroxiredoxins, using reducing equivalents transferred through thioredoxin. MCs and OA would affect the cellular levels and functioning of components of this process (SODs, peroxiredoxins, thioredoxin). Other components might contribute to this oxidative stress response, such as ferritin [59,165] and ATP synthase [54,136,189]. The role we hypothesized for ATP synthase in this model is inferred from the recorded proteomic data [54,136], as differential expression of some subunits of this multimeric enzymatic system might indicate an impairment of its activity, and based on the finding that MC-LR could covalently bind to the β subunit of ATP synthase [189], an effect that could alter the catalytic function of the enzyme. Thus, if ATP synthase is malfunctioning in cells exposed to MCs and OA, some impairment of oxidative phosphorylation and the electron transport process should be considered as a possible effect, and this alteration might contribute to increased production of oxygen radicals, as indicated in the model (Figure 6). The oxidative stress would then cause increased cellular levels of oxidized proteins, such as DJ-1, and the phosphorylation of stress proteins, such as hsp 27 and proapoptotic components, such as BAX. Cell death by apoptosis would then result in systems exposed to MCs and OA under those conditions [46,76].

The toxicity pathway of PITX could share some of the processes outlined in Figure 6, including increased cellular levels of oxidized proteins (DJ-1) and the phosphorylation of stress proteins (hsp 27). The cell death response, however, would have toxin-specific features, linked to the ion imbalance induced by PITX in affected cells through the conversion of Na^+, K^+ -ATPase into a cation channel [30,31,145,146]. In fact, no clear sign of apoptosis has been reported in cells exposed to PITX, where cell death has been shown to involve apparently different mechanisms [145,149,151,190–193].

The model depicted in Figure 6 includes also some events that could be part of a survival pathway triggered by GB. On the basis of the finding that this toxin induces increases in hsp 27 isoforms in a low phosphorylation state [54] and of some isoform of DJ-1 (Gian Luca Sala *et al.*, unpublished

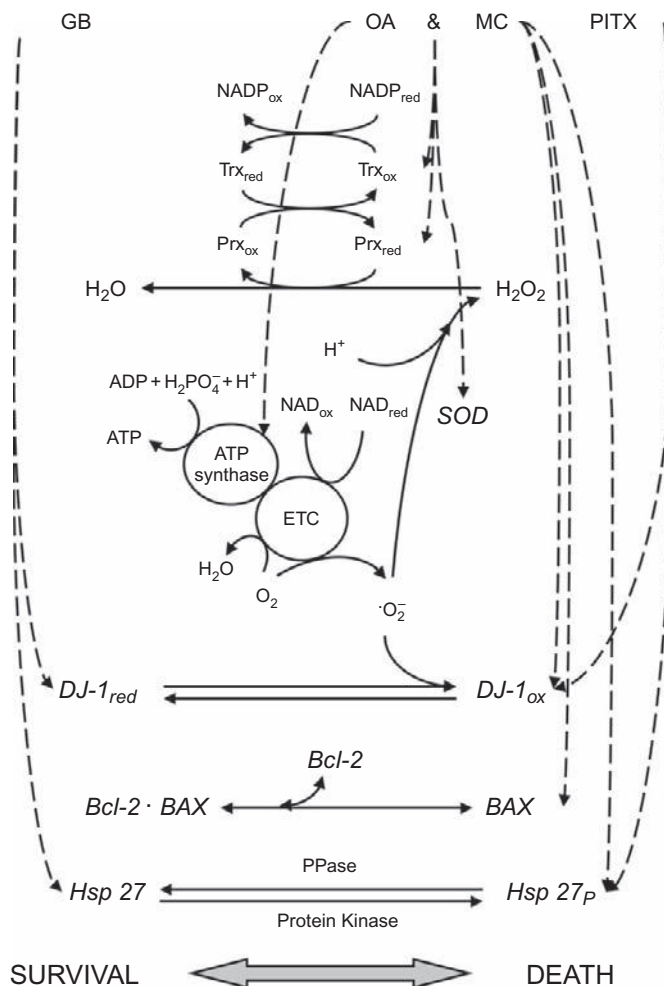


Figure 6 Working model incorporating some processes participating to toxicity pathways of microcystins, okadaic acid, and palytoxin. See text for explanation. GB, gambierol; OA, okadaic acid; MC, microcystin; PITX, palytoxin; Trx, thioredoxin; Prx, peroxiredoxin; SOD, superoxide dismutase; ETC, mitochondrial electron transport chain.

observations), it is speculated that GB would induce a stress response in MCF-7 cells, but not cell death, by favoring increased levels of stress proteins. The isoforms whose cellular levels are increased by GB might then represent those that are downregulated in cytotoxic responses, and would have a protective role in the cells.

We wish to stress that the working model of Figure 6 is speculative, and this feature is the basis for other hypotheses for model refinement. The unbiased sets of observational data resulting from proteomic investigations, in fact, provide the starting point for both top-down and bottom-up developments of working models, and we will use the existing proteomic data on MCs and OA, to illustrate this contention.

Top-down developments are apparent when considering the model of Figure 6 as a whole, which may not account for the full responses of cells exposed to individual toxins, but it rather rationalizes data regarding some of its (bona fide) constitutive events. To illustrate this point and some of its implications with regard to the characterization of toxicity pathways, we wish to use the scheme presented in Figure 7. In this scheme, full responses to toxins include an initial phase brought about by toxin interaction with its molecular target, an execution phase that proceeds through the chains of reactions triggered by the initial molecular alteration at the toxin's receptor

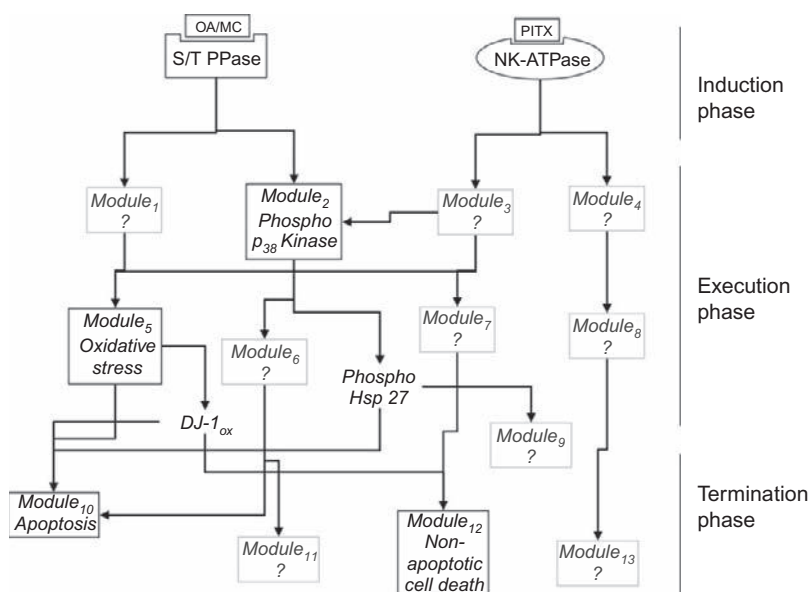


Figure 7 Schematic representation of modules composing the toxicity pathways of microcystins, okadaic acid, and palytoxin. This speculative scheme includes the full chain of events bringing about the responses to the toxins, from the interaction with respective receptorial components to the conclusion of cellular effects, organized within modules of reactions. The molecular processes participating to responses already described in the literature are indicated in black, whereas hypothetical modules that might complete toxicity pathways are indicated in gray. See text for a full explanation of the scheme. OA, okadaic acid; MC, microcystin; PITX, palytoxin; S/T PPase, ser/thr phosphoprotein phosphatase; NK-ATPase, N^+ , K^+ -ATPase.

level, and it is terminated by a set of events that are determined by the preceding molecular processes. The full response is then made of separate modules [194,195] of interacting processes, within a normal signaling network [195–198] which is perturbed by a toxin. The representation of interacting modules participating to the responses to different toxins (i.e., OA/MC vs. PlTX) is instrumental to stressing that the real cellular conditions include signaling networks, rather than distinct toxicity pathways. Thus, the elements outlined in Figure 6 would catch only features of some modules of the execution phase of cellular responses to toxins, without accounting for other molecular events preceding, accompanying, and following those outlined in that model, a concept presented by including additional undefined modules in the scheme of a complete response in Figure 7. For instance, the model in Figure 6 does not include any information regarding molecular mechanism by which the inhibition of PPases induces an oxidative stress response, and the specific features of the apoptotic response that would follow.

The bottom-up approaches to model refinement, in turn, would aim at characterizing the single molecular steps within modules, and the reactions/processes connecting individual modules. Three examples might illustrate this point, stemming from the differential expression of SOD, peroxiredoxins, and 6-gluconolactonase in systems exposed to MCs/OA (Table 3). The importance of SOD in the toxic response has been stressed with reference to oxygen radicals produced in connection with the activity of the electron transfer chain and oxidative phosphorylation (Figure 6), which is located at the level of the inner mitochondrial membrane. The SOD differentially expressed in response to MC-LR and OA, in turn, represents the isoform containing Cu–Zn, which is located outside mitochondria [78], posing issues regarding the mechanisms involved in the process. Similarly, multiple peroxiredoxin isoforms have been found to be differentially expressed in response to MC-LR and OA (Table 3), including mitochondrial (isoforms 3, 5) and cytoplasmic (isoforms 1, 2, 6) enzymes [199], but the model would account for only some of them and does not specify the organization of reactions with reference to their subcellular location (Figure 6). Further, the proposed stimulation of reactions contributing to oxidative stress in cells exposed to MCs and OA would be in line with the finding that increased levels of 6-gluconolactonase are found in toxin-treated systems, as reduced NADP, the electron donor for the reduction of thioredoxin [77–79], is produced in the reactions preceding and following that catalyzed by 6-gluconolactonase [79,177]. This condition, however, would require further characterization because pyruvate kinase is downregulated under the experimental conditions used in the model system [167], posing issues regarding the actual state of metabolic pathways responsible for glucose oxidation in cells exposed to MC. Further, the metabolism of carbohydrates is tightly regulated by a number of coordinated phosphorylation reactions of enzymes

participating in the metabolic pathways [174–177], whose phosphorylation states are affected by system exposure to inhibitors of PPases [200]. The phosphorylation state of relevant enzymes, including pyruvate kinase, however, remains undetermined under the conditions of those studies.

Thus, the identification of portions of toxicity pathways through unbiased proteomics can provide relevant information with regard to more advanced targeted investigations onto protein components and cell metabolites participating to toxic responses. Indeed, most of the working hypotheses mentioned above, stemming from open issues raised by top-down and bottom-up approaches, can be subjected to experimental testing and exemplify the tremendous potential of proteomics in supporting the characterization of molecular mechanisms of toxic responses at a system level. In any case, a mechanistic account of toxic responses demands the characterization of its modules and intermodular cross-talks. Further, a precise knowledge of covalent modifications, subcellular distribution, and protein isoforms participating to individual modules is needed for the characterization of toxicity pathways.

6.3. Distinguishing artifacts from biomarkers of toxicity

The characterization of toxicity pathways is a key achievement for the understanding of molecular mechanisms of action of toxicants and the possibility to make predictions regarding the adverse effects they would cause to humans, as well as other biological systems and the environment [3]. Within this perspective, the description of sequences of events describing some response in a particular experimental system may not suffice. In turn, robust characterization of molecular processes accounting for modes of action in living systems is needed. On a general ground, the robustness of models should be fully matched by corroboration of experimental findings in multiple biological systems. Taking into consideration the limited dynamic range of existing proteomic tools and the recognition that a limited set of proteins are amenable to analysis with existing methodology [9,10], the argument that only proteins expressed at high levels in the cells are actually being evaluated by current investigations using differential expression proteomics is serious and deserves consideration.

The inspection of Table 3 reveals that 5 of the 11 proteins included as tentative matching for key players in toxicity pathways of indicated toxins are among the most frequently detected proteins identified by differential expression proteomics, as determined by meta-analysis of published data [201,202]. Peroxiredoxins, SOD (Cu–Zn), hsp 27, ATP synthase, and β -tubulin are the five components, and we wish to discuss them with reference to the antinomy “artifacts versus universal sensors” [201].

A general consideration approaching this issue is that the abundance of a cellular protein may not by itself exclude a relevant functional role for the

protein in question. In fact, any conclusion regarding the mechanistic relevance of a component in a process is strictly related to the role played by the component in that process, as recognized either by already established knowledge or by evidence obtained through a methodology that, in this particular case, should be independent of those used in differential expression proteomics. With regard to the five components considered above, we think that the significance of at least three of them in the toxicity pathways of those toxins can be supported.

The first protein to be considered is hsp 27, which represents the most frequently found protein in differential expression proteomics using human material, being detected in about one-third of the studies [201]. What is indicated by the term hsp 27 actually consists of several different proteins. At least nine components can be distinguished in the MCF-7 cell system (Figure 3), which have been considered with reference to the molecular response induced by OA [54,91]. Further, simple chemical considerations indicate that the four acidic isoforms of hsp 27 with distinct isoelectric points most likely include multiple components differing for their pattern, but not their total number of phosphorylated amino acids (see Section 4). Indeed, if immunoblotting analysis is carried out using antibodies recognizing either total hsp 27 (nonphosphorylated and phosphorylated isoforms) or the hsp 27 isoform phosphorylated in Ser₈₂, after protein separation is achieved by 2D gels, a minimum of six spots differing according to their isoelectric point are resolved (Figure 8). The three less acidic isoforms are detected in control cells, whereas the remaining three are detected in cells exposed to OA, where their phosphorylation states are stabilized (Figure 8). The immunoblotting analysis carried out with the antibody recognizing the hsp 27 isoform phosphorylated in Ser₈₂ provides another relevant piece of information, as it shows that the differential expression of isoforms follows distinct patterns, according to the toxin that has been used in the incubation of the model system. Thus, relevant changes of the bona fide mono- and bis-phosphorylated isoforms (see Figure 3 and Section 4) shown in Figure 8 would not occur in cells exposed to either YTX or AZA-1, whereas changes in multiphosphorylated forms could be detected after cell exposure to either OA or PITX, as compared to controls [54,90,91]. Moreover, in the case of cell treatment with OA and PITX, the pattern of upregulated phosphorylated isoforms would be toxin-specific (Refs. [54,90,91] and Figure 8). Interestingly, the effect of PITX on hsp 27 phosphorylation can be found in cells with different abundance of this protein (Figure 5). In the case of hsp 27, therefore, the results obtained by differential expression proteomics in cells exposed to different toxins are confirmed by immunoblotting analyses and are better explained by mechanism-related arguments, rather than by the abundance of hsp 27 in some experimental model, such as the MCF-7 cell line.

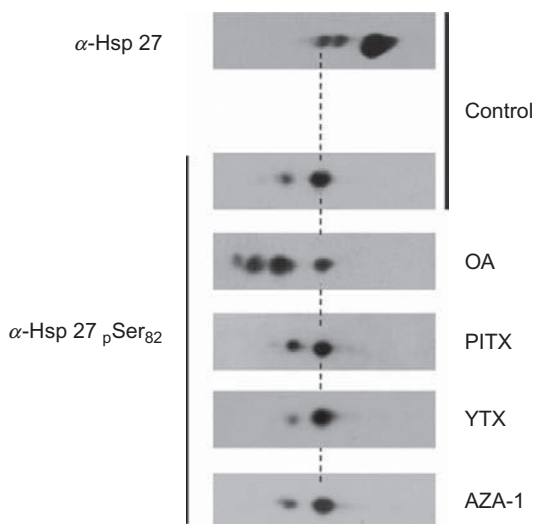


Figure 8 Effect of different toxins on the phosphorylation pattern of hsp 27 in MCF-7 cells. Cells were incubated for either 24 h with 50 nM OA, 1 nM YTX, 1 nM AZA-1, or 8 h with 0.03 nM PITX, or were left untreated, as indicated. At the end of the incubations, cells were used for the preparation of extracts which were subjected to 2D electrophoresis and immunoblotting, using the methods described in Ref. [90]. A 7 cm strip was used for the separation of cell proteins in the first dimension. Immunoblotting analyses were carried out using antibodies specific for total (both phosphorylated and nonphosphorylated isoforms) hsp 27, and hsp 27 isoforms phosphorylated in Ser₈₂, as indicated. The dashed line is introduced for alignment of components with reference to isoform marked 3105 in Figure 3 of this review. Portions of this figure have been reproduced from Ref. [90] with slight modifications.

The emphasis put onto the differences among phosphorylation states of hsp 27 stems from the recognition that this kind of covalent modification of proteins is a major mechanism controlling their activities and functional roles. Moreover, the concept that phosphorylation of a single amino acid can represent an on/off switch should be considered an oversimplification, because complex patterns of protein phosphorylation, including site-specific and/or hierarchical phosphorylations [203,204] are frequently found in regulatory mechanisms of biological activities [175,176,205,206]. In a functional perspective, therefore, protein molecules with identical amino acid sequence and displaying different phosphorylation states should be regarded as distinct components possessing different activities.

The considerations presented with reference to hsp 27 can be applied to results obtained with the DJ-1 protein [64,90], and their implication is that oxidative stress is actually induced in cells exposed to OA and PITX [64,90], confirming literature data [97,98], and lending support to the notion that

differential expression of peroxiredoxins and SOD (Cu–Zn) is in line with those findings and might not need to be explained only by the cellular abundance of proteins detected by differential expression proteomics.

Overall, the identification of components detected by differential expression proteomics as either biomarkers of toxicity or relevant components of toxicity pathways should be made with caution, with a careful consideration of their artifactual detection in relevant samples. In our opinion, collecting additional data on relevant proteins by methodologies independent of proteomic tools can be an effective way to approach specificity issues.

6.4. Experimental systems and variables which may affect mechanistic interpretations

The biological frame of differential expression proteomics includes the recognition that proteomes are inherently dynamic sets of components, whose characteristics, at both molecular and system levels, change continuously over time, representing the actual phenotype of the living entity under the specific conditions of individual studies. A direct consequence of this basic consideration is the huge combinations of experimental systems and conditions amenable of investigations by differential expression proteomics, even confining the approach to molecular toxicology. We have stressed the advantages inherent into the availability of data regarding a single toxin group and obtained in many different systems with regard to the robustness of conclusions drawn on toxicity pathways. The discussion of possible shortcomings, however, has also highlighted the need for in-depth evaluations of experimental findings, aimed at better characterizing molecular entities and processes which can help to build hypotheses amenable of further experimental testing, in a process of model development and refinement. Thus, considering the available data obtained by differential expression proteomics and the preliminary conclusions derived from those findings with regard to the characterization of molecular mechanisms of toxicity and toxicity pathways, a strong indication for both extensive and intensive approaches in future studies is emerging.

The complexity of the issues under study, however, should be considered with regard to choices on approaches and model systems. The clarification of toxicity pathways, with its technical and theoretical difficulties, should be part of a wider effort, as the whole system actually combines pathways in networks which would result from the cross-talks between interconnected modules. A toxicity network would then emerge when some of its pathways/modules are altered beyond a point susceptible of recovery within the homeostatic mechanisms of cell functions, in keeping with the concept of toxicity pathway [3,6]. Although the need to derive robust models of toxicity pathways is a strong argument favoring the

exploitation of differential expression proteomics in a number of distinct models, the complexity of the general issue should indicate the need for the identification of one or a few model systems for in-depth integrated studies. The complexity of the issues posed by obtaining quantitative, predictive models of signaling networks has been at the basis of the choice made by the Alliance for Cellular Signaling to study pathways intensively in two cell lines, the mouse B lymphocytes and cardiac myocytes [207]. Likewise, the need to develop suites of predictive assays based on the use of human cell lines [3] should be a powerful drive for the identification of few model systems for the characterization of toxicity pathways and toxicity networks. The opportunity of finding some consensus regarding the use of a few cell lines to identify molecular biomarkers of responses to marine biotoxins has already been mentioned, with particular reference to the use of *omics* approaches in the area [58].

Finding a consensus among investigators, to approach the characterization of toxicity pathways and toxicity networks, seems unavoidable, aiming at more effective action for the achievement of the goal as well as saving time and economical resources needed to tackle such a complex topic. Although the two cell lines chosen by the Alliance for Cellular Signaling might be relevant options, in keeping with the concept that toxicity pathways/networks are severely perturbed versions of normal processes, other cell lines of human origin could be considered. In the area of microalgal toxins, some cell lines appear recurrent in investigations onto the molecular mechanisms of action of toxins developed by both reductionistic and systemic approaches. The cell lines used in these studies include SH-SY5Y (neuronal), MCF-7 and Caco-2 (epithelial), and HepG2 (derived from a liver cancer), which could be considered among possible reference model systems.

In our opinion, finding a consensus and making methodological choices about model systems is urgent and should be also considered with regard to ecotoxicological issues, including choices on sentinel species. The concept that procedures for the preparation of cell/tissue extracts essentially determine the subproteome that will be eventually analyzed should also receive proper consideration, when approaching methodological choices.

6.5. Bioinformatic tools and databases in differential expression proteomics

The bioinformatic tools used in proteomics are another relevant point to be considered while discussing methodological issues. In fact, these tools play a key role in the development of the investigation as well as the interpretation of experimental data (Section 2), and, therefore, may have a considerable impact on the robustness of conclusions. The absolute need for computational tools designed for application in system biology was early recognized

(see for instance Ref. 208), and bioinformatics has been a field of intense development (see for instance Refs. [6,55,197,209,210]). Two major topics appear critical in the area of differential expression proteomics, including the interpretation of MS data coupled to the identification of proteins, and the analysis of functional significance of the identified set(s) of proteins.

MS techniques have been fundamental for the identification of components in proteomics, and the increasing number of molecular components whose analysis is pursued within a single experiment [14,181–183] has contributed to the development of advanced bioinformatic tools, including softwares to manage the large sets of data gathered in the course of the studies, and their matching with existing information in databases. Several initiatives have been developed to collect and classify existing data for the identification of proteins, and databases are easily accessible through the web [211–214]. The harmonization and standardization of procedures have lagged behind, however, and data analysis is not brought about by a reference data repository. In turn, multiple systems for archival and annotation purposes have been developed, differing with regard to the methodology used for the database, their taxonomic completeness, as well as the possible redundancy among the terms they contain. Thus, the multiple opportunities regarding bioinformatic tools are accompanied by some difficulties when analysis of bibliographic data demands the matching of components identified by the use of different databases. The need that items in any database must be unequivocally identified by a specific code, in fact, is accompanied by the existence of different codes in distinct databases for the same component. Similarly, inconsistencies may be found when proteins are identified only by the use of their name [215]. Further, a single entry in a database may find multiple matchings in a distinct database, introducing additional uncertainties and determining the need of manual validation of the identification by the operator. The general difficulties in interpretation of MS data and protein identification outlined above become of particular relevance when analysis refers to proteins obtained by species whose genome has not been sequenced, as genomic data represent the basis of existing databases and bioinformatic tools [55–57,168,216].

With regard to analysis of functional significance of the sets of proteins identified by differential expression proteomics, an analysis of annotations regarding proteins in databases and their matching becomes particularly important, and it often involves evaluation of possible similarities (molecular function, biological process, subcellular location) existing among identified components, that is, their ontological classification. GO is the most commonly used system for analysis of semantic similarities (see section 4). GO classifies gene products on the basis of three primary categories (molecular function, biological process, and cellular component) each of which includes subclassifications [214,217]. Within a classification, one gene product can play roles in more than one biological process, be part of different

cellular compartments, and participate in multiple functions. Ontologies may then display inhomogeneities among single entries, which are related to the multiplicity of biological issues they are involved in, as well as the depth of existing information about them. Thus, similarities may be inconclusive when approaching the functional significance of experimental data, and the efficacy in the use of ontological classifications as well as semantic similarities calls into question the knowledge of the operator.



7. CONCLUSIONS AND PERSPECTIVES

*What's in a name? That which we call a rose
By any other word would smell as sweet*

(William Shakespeare; Romeo and Juliet; Act II, Scene II)

Differential expression proteomics has been a very powerful non-biased approach to identify cellular components of potential relevance in biological processes, building bases for molecular analyses of phenotypes and their dynamics at a system level. The nominalistic drift that has been characterizing the first 10 years of differential expression proteomics, however, has been providing lists of components whose actual roles in biological processes has been questioned [201,202]. Countermeasures are under development, and targeted proteomic approaches are being used to overcome existing difficulties and obtain robust models. The major lines of intervention appear to involve methodologies for more accurate quantification of components and their changes upon system exposure to perturbing events, including toxins [14,55,99]. With specific reference to the area of microalgal toxins, major efforts are focused onto the effects these components might induce on protein–protein interactions and postransductional covalent modifications of relevant proteins [64,90,91,99,164,165]. These developments are in line with the recognition that biological processes involve defined sets of proteins, whose actual functioning depends on the activity inherent into their specific structures and the interactions involving individual components under defined conditions. The identification of proteins that might be participating in toxicity pathways by differential expression proteomics, therefore, would represent preliminary information to approach their chemical characterization, a concept which is being taken more and more into consideration in proteomic studies beyond the area of toxicants [14].

Obtaining the characterization of changing structures for individual protein components, the definition of dynamic patterns of interactions, as well as an accurate quantification of relevant proteins at a system level will

require considerable efforts. A critical evaluation of findings presented in this review shows that most robust data have been frequently contributed by investigations involving reductionistic approaches. Indeed, our preliminary, tentative representation of models, as well as the discussion on major issues which should be approached to obtain a better understanding of toxicity pathways, has been based on information obtained by complementary experimental strategies. We expect that the integration of systemic and reductionistic approaches will be essential to obtain quantitative, robust models of toxicity pathways and toxicity networks. Within this frame, computational tools will be needed as much as the intervention of scientists.

ACKNOWLEDGMENTS

The investigations on molecular mechanisms of action of biotoxins carried out by our group have been supported by the Italian Ministero dell'Istruzione, dell'Università e della Ricerca, and the Italian Ministero della Salute (Grants IZSAM PR10.2 and IZSAM 09/06 RC).

REFERENCES

- [1] R. Ulrich, S.H. Friend, Toxicogenomics and drug discovery: Will new technologies help us produce better drugs? *Nat. Rev. Drug. Discov.* 1 (2002) 84–88.
- [2] D.R. Boverhof, T.R. Zacharewski, Toxicogenomics in risk assessment: Applications and needs, *Toxicol. Sci.* 89 (2006) 352–360.
- [3] NRC, Toxicity Testing in the 21st Century: A Vision and a Strategy. National Academies Press, Washington, DC, 2007.
- [4] F.S. Collins, G.M. Gray, J.R. Bucher, Transforming environmental health protection, *Science* 319 (2008) 906–907.
- [5] T. Hartung, Lessons learned from alternative methods and their validation for a new toxicology in the 21st century, *J. Toxicol. Environ. Health* 13 (2010) 277–290.
- [6] M.E. Andersen, J.E. Dennison, R.S. Thomas, R.B. Conolly, New directions in incidence-dose modeling, *Trends Biotechnol.* 23 (2005) 122–127.
- [7] M. Buchanan, G. Caldarelli, P. De Los Rios, F. Rao, M. Vendruscolo (Eds.), *Networks in Cell Biology*, Cambridge University Press, Cambridge, 2010.
- [8] A. Abbott, And now for the proteome. . ., *Nature* 409 (2001) 747.
- [9] A. Pandey, M. Mann, Proteomics to study genes and genomes, *Nature* 405 (2000) 837–846.
- [10] L.H. Huber, Is proteomics heading in the wrong direction? *Nat. Rev. Mol. Cell Biol.* 4 (2003) 74–80.
- [11] S. Kennedy, The role of proteomics in toxicology: Identification of biomarkers of toxicity by protein expression analysis, *Biomarkers* 7 (2002) 269–290.
- [12] S. Bodovitz, T. Joos, The proteomic bottleneck: Strategies for preliminary validation of potential biomarkers and drug targets, *Trends Biotechnol.* 22 (2004) 4–7.
- [13] V.A. Dowling, D. Sheehan, Proteomics as a route to identification of toxicity targets in environmental toxicology, *Proteomics* 6 (2006) 5597–5604.
- [14] C. Choudhary, M. Mann, Decoding signalling networks by mass spectrometry-based proteomics, *Nat. Rev. Mol. Cell Biol.* 11 (2010) 427–439.

- [15] N.G. Anderson, N.L. Anderson, Twenty years of two-dimensional electrophoresis: Past, present and future, *Electrophoresis* 27 (1996) 443–453.
- [16] M.A. Moseley, Current trends in differential expression proteomics: Isotopically coded tags, *Trends Biotechnol.* 19 (2001) S10–S16.
- [17] G.M. Hallegraeff, Harmful algal blooms: A global overview, in: G.M. Hallegraeff, D.M. Anderson, A.D. Cembella (Eds.), *Manual on Harmful Marine Microalgae*, UNESCO, Paris, 2004, pp. 25–49.
- [18] G.P. Rossini, P. Hess, Phycotoxins: Chemistry, mechanisms of action, and shellfish poisoning, in: A. Luch (Ed.), *Molecular, Clinical and Environmental Toxicology*, vol. 2, Birkhäuser-Verlag AG, Basel, 2010, pp. 65–122.
- [19] G.M. Hallegraeff, D.M. Anderson, A.D. Cembella (Eds.), *Manual on Harmful Marine Microalgae*, UNESCO, Paris, 2004.
- [20] L.M. Botana (Ed.), *Seafood and Freshwater Toxins*, CRC Press, Taylor & Francis Group, Boca Raton, FL, 2008.
- [21] M. Craig, C.F.B. Holmes, Freshwater hepatotoxins: Microcystin and nodularin, mechanisms of toxicity and effects on health, in: L.M. Botana (Ed.), *Seafood and Freshwater Toxins*, Marcel Dekker, New York, 2000, pp. 643–671.
- [22] L.E. Llewellyn, Saxitoxin, a toxic marine natural product that targets a multitude of receptors, *Nat. Prod. Rep.* 23 (2006) 200–222.
- [23] G.P. Rossini, G. Ronzitti, F. Callegari, The modes of action of yessotoxin and the toxic responses of cellular systems, in: F. Goudey-Perrière, E. Benoit, M. Goyffon, P. Marchot (Eds.), *Toxines et Cancer*, Lavoisier, Paris, 2006, pp. 67–76.
- [24] J.S. Ramsdell, The molecular and integrative basis to brevetoxin toxicity, in: L.M. Botana (Ed.), *Seafood and Freshwater Toxins*, CRC Press, Taylor & Francis Group, Boca Raton, FL, 2008, pp. 519–550.
- [25] R.J. Lewis, J. Molgó, D.J. Adams, Ciguatera toxins: Pharmacology of toxins involved in ciguatera and related fish poisonings, in: L.M. Botana (Ed.), *Seafood and Freshwater Toxins*, Marcel Dekker, New York, 2000, pp. 419–447.
- [26] C.L. Trevino, L. Escobar, L. Vaca, V. Morales-Tlalpan, A.Y. Ocampo, A. Darszon, Maitotoxin: A unique pharmacological tool for elucidating Ca^{2+} -dependent mechanisms, in: L.M. Botana (Ed.), *Seafood and Freshwater Toxins*, CRC Press, Taylor & Francis Group, Boca Raton, FL, 2008, pp. 503–516.
- [27] N. Vilariño, B. Espiña, Pharmacology of pectenotoxins, in: L.M. Botana (Ed.), *Seafood and Freshwater Toxins*, CRC Press, Taylor & Francis Group, Boca Raton, FL, 2008, pp. 361–369.
- [28] M.J. Twiner, N. Rehmann, P. Hess, G.J. Doucette, Azaspiracid shellfish poisoning: A review on the chemistry, ecology and toxicology with an emphasis on human health impacts, *Mar. Drugs* 6 (2008) 39–72.
- [29] O.M. Pulido, Domoic acid toxicologic pathology: A review, *Mar. Drugs* 6 (2008) 180–219.
- [30] G.P. Rossini, A. Bigiani, Palytoxin action on the Na^+ , K^+ -ATPase and the disruption of ion equilibria in biological systems, *Toxicon* 57 (2011) 429–439.
- [31] E. Habermann, Palytoxin acts through Na^+ , K^+ -ATPase, *Toxicon* 27 (1989) 1171–1187.
- [32] F. Gusovsky, J.L. Daly, Maitotoxin: A unique pharmacological tool for research on calcium-dependent mechanisms, *Biochem. Pharmacol.* 39 (1990) 1633–1639.
- [33] C. Bialojan, A. Takai, Inhibitory effect of a marine sponge toxin, okadaic acid, on protein phosphatases, *Biochem. J.* 256 (1988) 283–290.
- [34] R.P. Hartshorne, W.A. Catterall, The sodium channel from rat brain. Purification and subunit composition, *J. Biol. Chem.* 259 (1984) 1667–1675.

- [35] J.S. Teitelbaum, R.J. Zatorre, S. Carpenter, D. Gendron, A.C. Evans, A. Gjedde, N.R. Cashman, Neurologic sequelae of domoic acid intoxication due to the ingestion of contaminated mussels, *N. Engl. J. Med.* 322 (1990) 1781–1787.
- [36] A. Novelli, J. Kispert, M.T. Fernández-Sánchez, A. Torreblanca, V. Zitko, Domoic acid-containing toxic mussels produce neurotoxicity in neuronal cultures through a synergism between excitatory amino acids, *Brain Res.* 577 (1992) 41–48.
- [37] B. Jakobsen, A. Tasker, J. Zimmer, Domoic acid neurotoxicity in hippocampal slice cultures, *Amino Acids* 23 (2002) 37–44.
- [38] D.A. Doucette, R.A. Tasker, Domoic acid: Detection methods, pharmacology, and toxicology, in: L.M. Botana (Ed.), *Seafood and Freshwater Toxins*, CRC Press, Taylor & Francis Group, Boca Raton, FL, 2008, pp. 397–429.
- [39] T. Yasumoto, M. Murata, Y. Oshima, M. Sano, G.K. Matsumoto, J. Clardy, Diarrhetic shellfish toxins, *Toxicon* 41 (1985) 1019–1025.
- [40] P. Cohen, C.F.B. Holmes, Y. Tsukitani, Okadaic acid: A new probe for the study of cellular regulation, *Trends Biochem. Sci.* 15 (1990) 98–102.
- [41] E.G. Krebs, The phosphorylation of proteins: A major mechanism for biological regulation, *Biochem. Soc. Trans.* 13 (1985) 813–820.
- [42] Y. Hamano, Y. Kinoshita, T. Yasumoto, Enteropathogenicity of diarrhetic shellfish toxins in intestinal models, *J. Food Hyg. Soc. Jpn.* 27 (1986) 375–379.
- [43] L. Edebo, S. Lange, X.P. Li, S. Allenmark, Toxic mussels and okadaic acid induce rapid hypersecretion in the rat small intestine, *APMIS* 96 (1988) 1029–1035.
- [44] J. Tripuraneni, A. Koutsoris, L. Pestic, P. De Lanerolle, G. Hect, The toxin of diarrhetic shellfish poisoning, okadaic acid, increases intestinal epithelial paracellular permeability, *Gastroenterology* 112 (1997) 100–108.
- [45] M. Hosokawa, H. Tsukada, T. Saitou, M. Kodama, M. Onomura, H. Nakamura, K. Fukuda, Y. Seino, Effects of okadaic acid on rat colon, *Dig. Dis. Sci.* 43 (1998) 2526–2535.
- [46] G.P. Rossini, Neoplastic activity of DSP toxins - The effects of okadaic acid and related compounds on cell proliferation: Tumor promotion or induction of apoptosis? in: L.M. Botana (Ed.), *Seafood and Freshwater Toxins*, Marcel Dekker, New York, 2000, pp. 257–288.
- [47] M. Suganuma, H. Fujiki, H. Suguri, S. Yoshizawa, M. Hirota, M. Nakayasu, M. Ojika, K. Wakamatsu, K. Yamada, T. Sugimura, Okadaic acid: An additional non-phorbol-12-tetradecanoate-13-acetate-type tumor promoter, *Proc. Natl. Acad. Sci. USA* 85 (1988) 1768–1771.
- [48] M. Suganuma, M. Tatematsu, J. Yatsunami, S. Yoshizawa, S. Okabe, D. Uemura, H. Fujiki, An alternative theory of tissue specificity by tumor promotion of okadaic acid in glandular stomach of SD rats, *Carcinogenesis* 13 (1992) 1841–1845.
- [49] H. Fujiki, M. Suganuma, Carcinogenic aspects of protein phosphatase 1 and 2A inhibitors, in: N. Fusetani, W. Kem (Eds.), *Marine Toxins as Research Tools*, Springer-Verlag, Berlin, 2009, pp. 221–254.
- [50] H. Goto, T. Igarashi, M. Yamamoto, M. Yasuda, R. Sekiguchi, M. Watai, K. Tanno, T. Yasumoto, Quantitative determination of marine toxins associated with diarrhetic shellfish poisoning by liquid chromatography coupled with mass spectrometry, *J. Chromatogr. A* 907 (2001) 181–189.
- [51] L. MacKenzie, P. Holland, P. McNabb, V. Beuzenberg, A. Selwood, T. Suzuki, Complex toxin profiles in phytoplankton and Greenshell mussels (*Perna canaliculus*), revealed by LC-MS/MS analysis, *Toxicon* 40 (2002) 1321–1330.
- [52] P. Ciminiello, C. Dell'Aversano, E. Fattorusso, M. Forino, L. Tartaglione, L. Boschetti, S. Rubini, M. Cangini, S. Pigozzi, R. Poletti, Complex toxin profile of *Mytilus galloprovincialis* from the Adriatic Sea revealed by LC-MS, *Toxicon* 55 (2010) 280–288.

- [53] G. Souid-Mensi, S. Moukha, K. Maaroufi, E.E. Creppy, Combined cytotoxicity and genotoxicity of a marine toxin and seafood contaminant metal ions (chromium and cadmium), *Environ. Toxicol.* 23 (2008) 1–8.
- [54] G.L. Sala, G. Ronzitti, M. Sasaki, H. Fuwa, T. Yasumoto, A. Bigiani, G.P. Rossini, Proteomic analysis reveals multiple patterns of response in cells exposed to a toxin mixture, *Chem. Res. Toxicol.* 22 (2009) 1077–1085.
- [55] V.J. Nesatyy, M.J.-F. Suter, Analysis of environmental stress response on the proteome level, *Mass Spectrom. Rev.* 27 (2008) 556–574.
- [56] H. Davies, A role for “omics” technologies in food safety assessment, *Food Control* 21 (2010) 1601–1610.
- [57] C. Piñeiro, B. Cañas, M. Carrera, The role of proteomics in the study of the influence of climate change on seafood products, *Food Res. Int.* 43 (2010) 1792–1802.
- [58] G.P. Rossini, Functional assays in marine biotoxin detection, *Toxicology* 208 (2005) 451–462.
- [59] T. Chen, Q. Wang, J. Cui, W. Yang, Q. Shi, Z. Hua, J. Ji, P. Shen, Induction of apoptosis in mouse liver by microcystin-LR, *Mol. Cell. Proteomics* 4 (2005) 958–974.
- [60] J.C. Ryan, M.-Y. Bottein Dechraoui, J.S. Morey, A. Rezvani, E.D. Levin, C.J. Gordon, J. S. Ramsdell, F.M. Van Dolah, Transcriptional profiling of whole blood and serum protein analysis of mice exposed to the neurotoxin Pacific Ciguatoxin-1, *Neurotoxicology* 28 (2007) 1099–1109.
- [61] M.J. Twiner, J.C. Ryan, J.S. Morey, F.M. Van Dolah, P. Hess, T. McMahon, G.J. Doucette, Transcriptional profiling and inhibition of cholesterol biosynthesis in human T lymphocyte cells by the marine toxin azaspiracid, *Genomics* 91 (2008) 289–300.
- [62] J.S. Morey, J.C. Ryan, M.-Y. Bottein Dechraoui, A.H. Rezvani, E.D. Levin, C.J. Gordon, J.S. Ramsdell, F.M. Van Dolah, Liver genomic responses to ciguatoxin: Evidence for activation of phase I and phase II detoxification pathways following an acute hypothermic response in mice, *Toxicol. Sci.* 103 (2008) 298–310.
- [63] K.A. Lefebvre, S.C. Tilton, T.K. Bammler, R.P. Beyer, S. Srinouanprachan, P.L. Stapleton, F.M. Farin, E.P. Gallagher, Gene expression profiles in zebrafish brain after acute exposure to domoic acid at symptomatic and asymptomatic doses, *Toxicol. Sci.* 107 (2009) 65–77.
- [64] J.A. Opsahl, L.V. Hjørnevik, V.H. Bull, L. Fismen, A.K. Frøyset, D. Gromyko, T. Solstad, K.E. Fladmark, Increased interaction between DJ-1 and the Mi-2/nucleosome remodelling and deacetylase complex during cellular stress, *Proteomics* 10 (2010) 1494–1504.
- [65] S. Ujihara, T. Oishi, R. Mouri, R. Tamate, K. Konoki, N. Matsumori, M. Murata, Y. Oshima, N. Sugiyama, M. Tomita, Y. Ishihama, Detection of Rap1A as a yessotoxin binding protein from blood cell membranes, *Bioorg. Med. Chem. Lett.* 20 (2010) 6443–6446.
- [66] L.L. Chan, I.J. Hodgkiss, P.K.-S. Lam, J.M.-F. Wan, H.-N. Chou, J.H.-K. Lum, M.G.-Y. Lo, A.S.-C. Mak, W.-H. Sit, S.C.-L. Lo, Use of two-dimensional gel electrophoresis to differentiate morphospecies of *Alexandrium minutum*, a paralytic shellfish poisoning toxin-producing dinoflagellate of harmful algal blooms, *Proteomics* 5 (2005) 1580–1593.
- [67] L.L. Chan, W.-H. Sit, P.K.-S. Lam, D.P.H. Hsieh, I.J. Hodgkiss, J.M.-F. Wan, A.Y.-T. Ho, N.M.-C. Choi, D.-Z. Wang, D. Dudgeon, Identification and characterization of a “biomarker of toxicity” from the proteome of the paralytic shellfish toxin-producing dinoflagellate *Alexandrium tamarense* (Dinophyceae), *Proteomics* 6 (2006) 654–666.

- [68] F. Pomati, R. Kellmann, R. Cavalieri, B.P. Burns, B.A. Neilan, Comparative gene expression of PSP-toxin producing and non-toxic *Anabaena circinalis* strains, *Environ. Int.* 32 (2006) 743–748.
- [69] L.L. Chan, I.J. Hodgkiss, J.M.-F. Wan, J.H.-K. Lum, A.S.-C. Mak, W.-H. Sit, S.C.-L. Lo, Proteomic study of a model causative agent of harmful algal blooms. *Prorocentrum triestinum* II: The use of differentially expressed protein profiles under different growth phases and growth conditions for bloom prediction, *Proteomics* 4 (2004) 3214–3226.
- [70] F.S. Chu, Freshwater hepatotoxins: Chemistry and detection, in: L.M. Botana (Ed.), *Seafood and Freshwater Toxins*, Marcel Dekker, New York, 2000, pp. 613–642.
- [71] G. Cronberg, E.J. Carpenter, W.W. Carmichael, Taxonomy of harmful cyanobacteria, in: G.M. Hallegraeff, D.M. Anderson, A.D. Cembella (Eds.), *Manual on Harmful Marine Microalgae*, UNESCO, Paris, 2004, pp. 523–562.
- [72] Y. Ueno, S. Nagata, T. Tsutsumi, A. Hasegawa, M.F. Watanabe, H.D. Park, G.C. Chen, S.H. Yu, Detection of microcystins, a blue-green algal hepatotoxin in drinking water sampled in Haimen and Fusui, endemic areas of primary liver cancer in China, by highly sensitive immunoassays, *Carcinogenesis* 17 (1996) 1317–1321.
- [73] R.E. Guzman, P.F. Solter, Characterization of sublethal microcystin-LR exposure in mice, *Vet. Pathol.* 39 (2002) 17–26.
- [74] S. Yoshizawa, R. Matsushima, M.F. Watanabe, K. Harada, A. Ichihara, W.W. Carmichael, H. Fujiki, Inhibition of protein phosphatases by microcystins and nodularin associated with hepatotoxicity, *J. Cancer Res. Clin. Oncol.* 116 (1990) 609–614.
- [75] M. Craig, H.A. Luu, T.L. McCready, D. Williams, R.J. Andersen, C.F.B. Holmes, Molecular mechanism underlying the interaction of motupurin and microcystins with type-1 and type-2A protein phosphatases, *Biochem. Cell Biol.* 74 (1996) 569–578.
- [76] M.M. Gehringer, Microcystin-LR and okadaic acid-induced cellular effects: A dualistic response, *FEBS Lett.* 557 (2004) 1–8.
- [77] M. Koháryová, M. Kollárová, Oxidative stress and thioredoxin system, *Gen. Physiol. Biophys.* 27 (2008) 71–84.
- [78] M.K. Ahsan, I. Lekli, D. Ray, J. Yodoi, D.K. Das, Redox regulation of cell survival by the thioredoxin superfamily: An implication of redox gene therapy in the heart, *Antioxid. Redox Signal.* 11 (2009) 2741–2758.
- [79] M.L. Circu, T.Y. Aw, Reactive oxygen species, cellular redox systems, and apoptosis, *Free Radic. Biol. Med.* 48 (2010) 749–762.
- [80] W. Fu, L. Xu, Y. Yu, Proteomic analysis of cellular response to microcystin in human amnion FL cells, *J. Proteome Res.* 4 (2005) 2207–2215.
- [81] W. Kolch, Coordinating ERK/MAPK signalling through scaffolds and inhibitors, *Nat. Rev. Mol. Cell Biol.* 6 (2005) 827–837.
- [82] M. Katz, I. Amniz, Y. Yarden, Regulation of MAPKs by growth factors and receptor tyrosine kinases, *Biochim. Biophys. Acta* 1773 (2007) 1161–1176.
- [83] M.R. Junttila, S.-P. Li, J. Westermarck, Phosphatase-mediated crosstalk between MAPK signaling pathways in the regulation of cell survival, *FASEB J.* 22 (2008) 954–965.
- [84] Y. Sonoda, T. Kasahara, Y. Yamaguchi, K. Kuno, K. Matsushima, N. Mukaida, Stimulation of interleukin-8 production by okadaic acid and vanadate in a human promyelocyte cell line, an HL-60 subline: Possible role of mitogen-activated protein kinase on the okadaic acid-induced NF- κ B activation, *J. Biol. Chem.* 272 (1997) 15366–15372.
- [85] G.P. Rossini, C. Pinna, C. Malaguti, Different sensitivities of p42 mitogen activated protein kinase to phorbol ester and okadaic acid tumor promoters among cell types, *Biochem. Pharmacol.* 58 (1999) 279–284.

- [86] V. Zuckerman, K. Wolyniec, R.V. Sionov, S. Haupt, Y. Haupt, Tumor suppression by p53: The importance of apoptosis and cellular senescence, *J. Pathol.* 219 (2009) 3–15.
- [87] W. Fu, J. Chen, X. Wang, L. Xu, Altered expression of p53, Bcl-2 and BAX induced by microcystin-LR *in vivo* and *in vitro*, *Toxicol.* 46 (2005) 171–177.
- [88] W. Fu, Y. Yu, L. Xu, Identification of temporal differentially expressed protein responses to microcystin in human amniotic epithelial cells, *Chem. Res. Toxicol.* 22 (2009) 41–51.
- [89] C. Malaguti, G.P. Rossini, Recovery of cellular E-cadherin precedes replenishment of estrogen receptor and estrogen-dependent proliferation of breast cancer cells rescued from a death stimulus, *J. Cell. Physiol.* 192 (2002) 171–181.
- [90] G.L. Sala, M. Bellocchi, G.P. Rossini, The cytotoxicity pathway triggered by palytoxin involves a change in the cellular pool of stress response proteins, *Chem. Res. Toxicol.* 22 (2009) 2009–2016.
- [91] G.L. Sala, G. Ronzitti, M. Bellocchi, M. Sasaki, H. Fuwa, T. Yasumoto, A. Bigiani, G.P. Rossini, Proteomic analyses for the characterization of toxicity pathways and their interactions in human cells: Learning from marine biotoxins, in: E. Benoit, F. Goudey-Perrière, P. Marchot, D. Servent (Eds.), *Toxines et Signalisation*, Lavoisier, Paris, 2009, pp. 57–61.
- [92] G.R. Guy, X. Cao, S.P. Chua, Y.H. Tan, Okadaic acid mimics multiple changes in early protein phosphorylation and gene expression induced by tumor necrosis factor or interleukin-1, *J. Biol. Chem.* 267 (1992) 1846–1852.
- [93] J. Cairns, S. Qin, R. Philp, Y.H. Tan, G.R. Guy, Dephosphorylation of the small heat shock protein Hsp 27 *in vivo* by protein phosphatase 2A, *J. Biol. Chem.* 269 (1994) 9176–9183.
- [94] J. Landry, H. Lambert, M. Zhou, J.N. Lavoie, E. Hickey, L.A. Weber, C.W. Anderson, Human HSP27 is phosphorylated at serines 78 and 82 by heat shock and mitogen-activated kinases that recognize the same amino acid motif as S6 kinase II, *J. Biol. Chem.* 267 (1992) 794–803.
- [95] C. von Ballmoos, A. Wiedenmann, P. Dimroth, Essentials for ATP synthesis by F1F0 ATP synthases, *Annu. Rev. Biochem.* 78 (2009) 649–672.
- [96] M. Véron, A. Tepper, M. Hildebrandt, I. Lascu, M.L. Lacombe, J. Janin, S. Moréra, J. Cherfils, C. Dumas, M. Chiadmi, Nucleoside diphosphate kinase: An old enzyme with new functions? *Adv. Exp. Med. Biol.* 370 (1994) 607–611.
- [97] A. Ferrero-Gutiérrez, A. Pérez-Gómez, A. Novelli, M.T. Fernández-Sánchez, Inhibition of phosphoprotein phosphatases impairs the ability of astrocytes to detoxify hydrogen peroxide, *Free Radic. Biol. Med.* 44 (2008) 1806–1816.
- [98] R. Antony, W.J. Lukiw, N.G. Bazan, Neuroprotectin D1 induces cell dephosphorylation of bcl-xL in a PP2A-dependent manner during oxidative stress and promotes retinal pigment epithelial cell survival, *J. Biol. Chem.* 285 (2010) 18301–18308.
- [99] R. Kellman, C.A.M. Schaffner, T.A. Grønset, M. Satake, M. Ziegler, K.E. Fladmark, Proteomic response of human neuroblastoma cells to azaspiracid-1, *J. Proteomics* 72 (2009) 695–707.
- [100] M.J. Twiner, P. Hess, M.-Y. Bottein Dechraoui, T. McMahon, M.S. Samons, M. Satake, T. Yasumoto, J.S. Ramsdell, G.J. Doucette, Cytotoxic and cytoskeletal effects of azaspiracid-1 on mammalian cell lines, *Toxicol.* 45 (2005) 891–900.
- [101] N. Vilarinho, K.C. Nicolaou, M.O. Frederick, E. Cagide, I.R. Ares, M.C. Louzao, M.R. Vieytes, L.M. Botana, Cell growth inhibition and actin cytoskeleton disorganization induced by azaspiracid-1 structure-activity studies, *Chem. Res. Toxicol.* 19 (2006) 1459–1466.
- [102] G. Ronzitti, P. Hess, N. Rehmann, G.P. Rossini, Azaspiracid-1 alters the E-cadherin pool in epithelial cells, *Toxicol. Sci.* 95 (2007) 427–435.

- [103] M. Bellocchi, G.L. Sala, F. Callegari, G.P. Rossini, Azaspiracid-1 inhibits endocytosis of plasma membrane proteins in epithelial cells, *Toxicol. Sci.* 117 (2010) 109–121.
- [104] C. Vale, K.C. Nicolaou, M.O. Frederick, B. Gómez-Limia, A. Alfonso, M.R. Vieytes, L.M. Botana, Effects of azaspiracid-1, a potent cytotoxic agent, on primary neuronal cultures. A structure–activity relationship study, *J. Med. Chem.* 50 (2007) 356–363.
- [105] C. Vale, K.C. Nicolaou, M.O. Frederick, M.R. Vieytes, L.M. Botana, Cell volume decrease as a link between azaspiracid-induced cytotoxicity and c-Jun-N-terminal kinase activation in cultured neurons, *Toxicol. Sci.* 113 (2010) 158–168.
- [106] Z. Cao, K.T. Lepage, M.O. Frederick, K.C. Nicolaou, T.F. Murray, Involvement of caspase activation in azaspiracid-induced neurotoxicity in neocortical neurons, *Toxicol. Sci.* 114 (2010) 323–334.
- [107] A. Tubaro, A. Giangaspero, M. Ardizzone, M.R. Soranzo, F. Vita, T. Yasumoto, J.M. Maucher, J.S. Ramsdell, S. Sosa, Ultrastructural damage to heart tissue from repeated oral exposure to yessotoxin resolves in 3 months, *Toxicol.* 51 (2008) 1225–1235.
- [108] EFSA, Marine biotoxins in shellfish—Yessotoxin group, Scientific Opinion of the Panel on Contaminants in the Food chain. *EFSA J.* 907 (2008) 1–62.
- [109] C. Young, P. Truman, M. Boucher, R.A. Keyzers, P. Northcote, T.W. Jordan, The algal metabolite yessotoxin affects heterogeneous nuclear ribonucleoproteins in HepG2 cells, *Proteomics* 9 (2009) 2529–2542.
- [110] S.P. Han, Y.H. Tang, R. Smith, Functional diversity of the hnRNPs: Past, present and perspectives, *Biochem. J.* 430 (2010) 379–392.
- [111] F. Callegari, G.P. Rossini, Yessotoxin inhibits the complete degradation of E-cadherin, *Toxicology* 244 (2008) 133–144.
- [112] C.F. Orsi, B. Colombari, F. Callegari, A.M. Todaro, A. Ardizzone, G.P. Rossini, E. Blasi, S. Peppoloni, Yessotoxin inhibits phagocytic activity of macrophages, *Toxicol.* 55 (2010) 265–273.
- [113] D. Malagoli, E. Marchesini, E. Ottaviani, Lysosomal as target of yessotoxin in invertebrate and vertebrate cells, *Toxicol. Lett.* 167 (2006) 75–83.
- [114] F. Leira, C. Alvarez, J.M. Vieites, M.R. Vieytes, L.M. Botana, Characterization of distinct apoptotic changes induced by okadaic acid and yessotoxin in the BE(2)-M17 neuroblastoma cell line, *Toxicol. In Vitro* 16 (2002) 23–31.
- [115] C. Malaguti, P. Ciminiello, E. Fattorusso, G.P. Rossini, Caspase activation and death induced by yessotoxin in HeLa cells, *Toxicol. In Vitro* 16 (2002) 357–363.
- [116] A. Pérez-Gomez, A. Ferrero-Gutiérrez, A. Novelli, J.-M. Franco, B. Paz, M.T. Fernández-Sánchez, Potent neurotoxic action of the shellfish biotoxin yessotoxin on cultured cerebellar neurons, *Toxicol. Sci.* 90 (2006) 168–177.
- [117] M. Suárez Korsnes, D.L. Hetland, A. Espenes, M.A. Tranulis, T. Aune, Apoptotic events induced by yessotoxin in myoblast cell lines from rat and mouse, *Toxicol. In Vitro* 20 (2006) 1077–1087.
- [118] V. Dell’Ovo, E. Bandi, T. Coslovich, C. Florio, M. Sciancalepore, G. Decorti, S. Sosa, P. Lorenzon, T. Yasumoto, A. Tubaro, In vitro effects of yessotoxin on a primary culture of rat cardiomyocytes, *Toxicol. Sci.* 106 (2008) 392–399.
- [119] J.F. Hancock, Ras proteins: Different signals from different locations, *Nat. Rev. Mol. Cell Biol.* 4 (2003) 373–384.
- [120] A. Ben-Baruch, Site-specific metastasis formation: Chemokines as regulators of tumor cell adhesion, motility and invasion, *Cell Adh. Migr.* 3 (2009) 328–333.
- [121] E.W. Frschie, F.J. Zwartkruis, Rap1, a mercenary among the Ras-like GTPases, *Dev. Biol.* 340 (2010) 1–9.
- [122] H. Stenmark, Rab GTPases as coordinators of vesicle traffic, *Nat. Rev. Mol. Cell Biol.* 10 (2009) 513–525.

- [123] G. Ronzitti, F. Callegari, C. Malaguti, G.P. Rossini, Selective disruption of the E-cadherin-catenin system by an algal toxin, *Br. J. Cancer* 90 (2004) 1100–1107.
- [124] G. Ronzitti, G.P. Rossini, Yessotoxin induces the accumulation of altered E-cadherin dimers that are not part of adhesive structures in intact cells, *Toxicology* 244 (2008) 145–156.
- [125] F. Callegari, S. Sosa, S. Ferrari, M.R. Soranzo, S. Pierotti, T. Yasumoto, A. Tubaro, G.P. Rossini, Oral administration of yessotoxin stabilizes E-cadherin in mouse colon, *Toxicology* 227 (2006) 145–155.
- [126] F. Nollet, P. Kools, F. van Roy, Phylogenetic analysis of the cadherin superfamily allows identification of six major subfamilies besides several solitary members, *J. Mol. Biol.* 299 (2000) 551–572.
- [127] T. Yasumoto, M. Murata, Marine toxins, *Chem. Rev.* 93 (1993) 1897–1909.
- [128] J.E. Randall, A review of ciguatera, tropical fish poisoning, with a tentative explanation of its cause, *Bull. Mar. Sci. Gulf Carib.* 8 (1958) 236–267.
- [129] R.J. Lewis, The changing face of ciguatera, *Toxicon* 39 (2001) 97–106.
- [130] A. Lombert, J.N. Bidard, M. Lazdunski, Ciguatoxins and brevetoxins share a common receptor site on the neuronal voltage-dependent Na⁺ channel, *FEBS Lett.* 219 (1987) 355–357.
- [131] V. Ghiaroni, M. Sasaki, H. Fuwa, G.P. Rossini, G. Scalera, T. Yasumoto, P. Pietra, A. Bigiani, Inhibition of voltage-gated potassium currents by gambierol in mouse taste cells, *Toxicol. Sci.* 85 (2005) 657–665.
- [132] E. Cuypers, Y. Abdel-Mottaleb, I. Kopljär, J.D. Rainier, A.L. Raes, D.J. Snyders, J. Tytgat, Gambierol, a toxin produced by the dinoflagellate *Gambierdiscus toxicus*, is a potent blocker of voltage-gated potassium channels, *Toxicon* 51 (2008) 974–983.
- [133] L.A. Tylaska, L. Boring, W. Weng, R. Aiello, I.F. Charo, B.J. Rolling, R.P. Gladue, CCR2 regulates the level of MCP-1/CCL2 in vitro and at inflammatory sites and controls T-cell activation in response to alloantigen, *Cytokine* 18 (2002) 184–190.
- [134] J.H. Yu, S.Y. Yun, J.W. Lim, H. Kim, K.H. Kim, Proteome analysis of rat pancreatic acinar cells: Implication for cerulein-induced acute pancreatitis, *Proteomics* 3 (2003) 2446–2453.
- [135] M. Basso, S. Giraudo, D. Corpillo, B. Bergamasco, L. Lopiano, M. Fasano, Proteome analysis of human substantia nigra in Parkinson's disease, *Proteomics* 4 (2004) 3943–3952.
- [136] M. Malécot, K. Mezhoud, A. Marie, D. Praseuth, S. Puisieux-Dao, M. Edery, Proteomics study of the effects of microcystin-LR on organelle and membrane proteins in medaka fish liver, *Aquatic Toxicol.* 94 (2009) 153–161.
- [137] P. Ciminiello, C. Dell'Aversano, E. Fattorusso, M. Forino, L. Grauso, L. Tartaglione, A 4-decade-long (and still ongoing) hunt for palytoxins chemical architecture, *Toxicon* 57 (2011) 362–367.
- [138] R.E. Moore, P.J. Scheuer, Palytoxin: A new marine toxin from a coelenterate, *Science* 172 (1971) 495–498.
- [139] L. Rhodes, World-wide occurrence of the toxic dinoflagellate genus *Ostreopsis* Schmidt, *Toxicon* 57 (2011) 400–407.
- [140] M. Gallitelli, N. Ungaro, L.M. Addante, N. Gentiloni, C. Sabbà, Respiratory illness as a reaction to tropical algal blooms occurring in a temperate climate, *JAMA* 293 (2005) 2599–2600.
- [141] P. Ciminiello, C. Dell'Aversano, E. Fattorusso, M. Forino, S. Magno, L. Tartaglione, C. Grillo, N. Melchiorre, The Genoa outbreak. Determination of putative palytoxin in Mediterranean *Ostreopsis ovata* by a new liquid chromatography tandem mass spectrometry method, *Anal. Chem.* 78 (2006) (2005) 6153–6159.
- [142] J.R. Deeds, M.D. Schwartz, Human risk associated with palytoxin exposure, *Toxicon* 56 (2010) 150–162.

- [143] EFSA, Scientific Opinion on marine biotoxins in shellfish – palytoxin group, Scientific Opinion of the Panel on Contaminants in the Food chain., EFSA J. 1393 (2009) 1–38.
- [144] R. Munday, Palytoxin toxicology: Animal studies, *Toxicon* 57 (2011) 470–477.
- [145] E. Habermann, G.S. Chhatwal, Ouabain inhibits the increase due to palytoxin of cation permeability of erythrocytes, *Naunyn-Schmiedeberg Arch. Pharmacol.* 319 (1982) 101–107.
- [146] N.A. Castle, G.R. Strichartz, Palytoxin induces a relatively non-selective cation permeability in frog sciatic nerve which can be inhibited by cardiac glycosides, *Toxicon* 26 (1988) 941–951.
- [147] E. Wattenberg, Modulation of protein kinase signaling cascades by palytoxin, *Toxicon* 57 (2011) 440–448.
- [148] M.C. Louzao, I.R. Ares, E. Cagide, B. Espiña, N. Vilariño, A. Alfonso, M.R. Vieytes, L.M. Botana, Palytoxins and cytoskeleton: An overview, *Toxicon* 57 (2011) 460–469.
- [149] M. Bellocci, G.L. Sala, S. Prandi, The cytolytic and cytotoxic activities of palytoxin, *Toxicon* 57 (2011) 449–459.
- [150] H. Fujiki, M. Suganuma, M. Nakayasu, H. Hakii, T. Horiuchi, S. Takayama, T. Sugimura, Palytoxin is a non-12-O-tetradecanoylphorbol-13-acetate type tumor promoter in two-stage mouse skin carcinogenesis, *Carcinogenesis* 7 (1986) 707–710.
- [151] M. Bellocci, G. Ronzitti, A. Milandri, N. Melchiorre, C. Grillo, R. Poletti, T. Yasumoto, G.P. Rossini, A cytolytic assay for the measurement of palytoxin based on a cultured monolayer cell line, *Anal. Biochem.* 374 (2008) 48–55 An Addendum has appeared in *Anal. Biochem.* 380 (2008) 178.
- [152] R.M. Canet-Avilés, M.A. Wilson, D.W. Miller, R. Ahmad, C. McLendon, S. Bandyopadhyay, M.J. Baptista, D. Ringe, G.A. Petsko, M.R. Cookson, The Parkinson's disease protein DJ-1 is neuroprotective due to cysteine-sulfenic acid-driven mitochondrial localization, *Proc. Natl. Acad. Sci. USA* 101 (2004) 9103–9108.
- [153] J. Choi, M.C. Sullards, J.A. Olzmann, H.D. Rees, S.T. Weintraub, D.E. Bostwick, M. Gearing, A.I. Levey, L.-S. Chin, L. Li, Oxidative damage of DJ-1 is linked to sporadic Parkinson and Alzheimer diseases, *J. Biol. Chem.* 281 (2006) 10816–10824.
- [154] T. Kinumi, J. Kimata, T. Taira, H. Ariga, E. Niki, Cysteine-106 of DJ-1 is the most sensitive residue to hydrogen peroxide-mediated oxidation in vivo in human umbilical vein endothelial cells, *Biochem. Biophys. Res. Commun.* 317 (2004) 722–728.
- [155] A. Mitsumoto, Y. Nakagawa, A. Takeuchi, K. Okawa, A. Iwamatsu, Y. Takanezawa, Oxidized forms of peroxiredoxins and DJ-1 on two-dimensional gels increased in response to sublethal levels of paraquat, *Free Radic. Res.* 35 (2001) 301–310.
- [156] K. Kato, K. Hasegawa, S. Goto, Y. Inaguma, Dissociation as a result of phosphorylation of an aggregated form of the small stress protein, hsp27, *J. Biol. Chem.* 269 (1994) 11274–11278.
- [157] T. Rogalla, M. Ehrmsperger, X. Preville, A. Kotlyarov, G. Lutsch, C. Ducasse, C. Paul, M. Wieske, A.-P. Arrigo, J. Buchner, M. Gaestel, Regulation of hsp27 oligomerization, chaperone function, and protective activity against oxidative stress/tumor necrosis factor α by phosphorylation, *J. Biol. Chem.* 274 (1999) 18947–18956.
- [158] C. Garrido, Size matters: Of the small HSP27 and its large oligomers, *Cell Death Differ.* 9 (2002) 483–485.
- [159] H.M. Beere, “The stress of dying”: The role of heat shock proteins in the regulation of apoptosis, *J. Cell Sci.* 117 (2004) 2641–2651.
- [160] D. Lanneau, M. Brunet, E. Frisan, E. Solary, M. Fontenay, C. Garrido, Heat shock proteins: Essential proteins for apoptosis regulation, *J. Cell. Mol. Med.* 12 (2008) 743–761.
- [161] S. Kostenko, U. Moens, Heat shock protein 27 phosphorylation: Kinases, phosphatases, functions and pathology, *Cell. Mol. Life Sci.* 66 (2009) 3289–3307.

- [162] Anonymous, Proteomics of a toxin mix., *Chem. Res. Toxicol.* 22 (2009) 966.
- [163] A.D. Benninghoff, Toxicoproteomics—The next step in the evolution of environmental biomarkers? *Toxicol. Sci.* 95 (2007) 1–4.
- [164] K. Mezhoud, D. Praseuth, S. Puisieux-Dao, J.-C. François, C. Bernard, M. Edery, Global quantitative analysis of protein expression and phosphorylation status in the liver of the medaka fish (*Oryzias latipes*) exposed to microcystin-LR. I. Balneation study, *Aquatic Toxicol.* 86 (2008) 166–175.
- [165] K. Mezhoud, A.L. Bauchet, S. Château-Joubert, D. Praseuth, A. Marie, J.-C. François, J.J. Fontaine, J.P. Jaeg, J.P. Cravedi, S. Puisieux-Dao, M. Edery, Proteomic and phosphoproteomic analysis of cellular responses in medaka fish (*Oryzias latipes*) following oral gavage with microcystin-LR, *Toxicon* 51 (2008) 1431–1439.
- [166] J.C. Martins, P.N. Leão, V. Vasconcelos, Differential protein expression in *Corbicula fluminea* upon exposure to a *Microcystis aeruginosa* toxic strain, *Toxicon* 53 (2009) 409–416.
- [167] M. Wang, L.L. Chan, M. Si, H. Hong, D. Wang, Proteomic analysis of hepatic tissue of zebrafish (*Danio rerio*) experimentally exposed to chronic microcystin-LR, *Toxicol. Sci.* 113 (2010) 60–69.
- [168] G. Ronzitti, A. Milandri, G. Scortichini, R. Poletti, G.P. Rossini, Protein markers of algal toxin contamination in shellfish, *Toxicon* 52 (2008) 705–713.
- [169] K.J. Nzoughe, J.T.G. Hamilton, C.H. Botting, A. Douglas, L. Devine, J. Nelson, C.T. Elliott, Proteomics identification of azaspiracid toxin biomarkers in blue mussels, *Mytilus edulis*, *Mol. Cell. Proteomics* 8 (2009) 1811–1822.
- [170] J.E. Eriksson, D. Toivola, J.A. Meriluoto, H. Karaki, Y.G. Han, D. Hartshorne, Hepatocyte deformation induced by cyanobacterial toxins reflects inhibition of protein phosphatases, *Biochem. Biophys. Res. Commun.* 173 (1990) 1347–1353.
- [171] T. Ohta, R. Nishiwaki, J. Yatsunami, A. Komori, M. Suganuma, H. Fujiki, Hyperphosphorylation of cytokeratins 8 and 18 by microcystin-LR, a new liver tumor promoter, in primary cultured rat hepatocytes, *Carcinogenesis* 13 (1992) 2443–2447.
- [172] S. Ghosh, S.A. Khan, M. Wickstrom, V. Beasley, Effects of microcystin-LR on actin and the actin-associated proteins alpha-actinin and talin in hepatocytes, *Nat. Toxins* 3 (1995) 405–414.
- [173] D.M. Toivola, R.D. Goldman, D.R. Garrod, J.E. Eriksson, Protein phosphatases maintain the organization and structural interactions of hepatic keratin intermediate filaments, *J. Cell Sci.* 110 (1997) 23–33.
- [174] M.C. Sugden, R.M. Howard, M.R. Munday, M.J. Holness, Mechanisms involved in the coordinate regulation of strategic enzymes of glucose metabolism, *Adv. Enzyme Regul.* 33 (1993) 71–95.
- [175] T. Hunter, Protein kinases and phosphatases: The yin and yang of protein phosphorylation and signaling, *Cell* 80 (1995) 225–236.
- [176] A.R. Saltiel, C.R. Khan, Insulin signalling and the regulation of glucose and lipid metabolism, *Nature* 414 (2001) 799–806.
- [177] T.M. Devlin, *Textbook of Biochemistry with Clinical Correlations*, seventh ed., Wiley-Liss, New York, 2010.
- [178] E. Fattorusso, P. Ciminiello, V. Costantino, S. Magno, A. Mangoni, A. Milandri, R. Poletti, M. Pompei, R. Viviani, Okadaic acid in mussels of the Adriatic Sea, *Marine Pol. Bull.* 24 (1992) 234–237.
- [179] L. Sidari, P. Nichetto, S. Cok, S. Sosa, A. Tubaro, G. Honsell, R. Della Loggia, Phytoplankton detection and DSP toxicity: Methodological considerations, *J. Appl. Phycol.* 7 (1995) 163–166.

- [180] K.J. Nzougheh, J.T.G. Hamilton, S.D. Floyd, A. Douglas, J. Nelson, L. Devine, C.T. Elliott, Azaspiracid: First evidence of protein binding in shellfish, *Toxicon* 51 (2008) 1255–1263.
- [181] R.D. Smith, G.A. Anderson, M.S. Lipton, L. Pasa-Tolic, Y. Shen, T.P. Conrads, T.D. Veenstra, H.R. Udseth, An accurate mass tag strategy for quantitative and high-throughput proteome measurements, *Proteomics* 2 (2002) 513–523.
- [182] M.S. Lipton, L. Paša-Tolić, G.A. Anderson, D.J. Anderson, D.L. Auberry, J.R. Battista, M.J. Daly, J. Fredrickson, K.K. Hixson, H. Kostandarites, C. Masselon, L.M. Markillie, *et al.*, Global analysis of the *Deinococcus radiodurans* proteome by using accurate mass tags, *Proc. Natl. Acad. Sci. USA* 99 (2002) 11049–11054.
- [183] M. Washburn, D. Wolters, J.R. Yates 3rd, Large-scale analysis of the yeast proteome by multidimensional protein identification technology, *Nat. Biotechnol.* 19 (2001) 242–247.
- [184] I. Miller, J. Crawford, E. Giannazza, Protein stains for proteomic applications: Which, when, why? *Proteomics* 6 (2006) 5385–5408.
- [185] M. Xin, X. Deng, Protein phosphatase 2A enhances the proapoptotic function of Bax through dephosphorylation, *J. Biol. Chem.* 281 (2006) 18859–18867.
- [186] M.L. Xing, X.F. Wang, X. Xhu, X.D. Zhou, L.H. Xu, Morphological and biochemical changes associated with apoptosis induced by okadaic acid in human amniotic FL cells, *Environ. Toxicol.* 24 (2009) 437–445.
- [187] S. Li, E.V. Wattenberg, Differential activation of mitogen-activated protein kinases by palytoxin and ouabain, two ligands for the Na⁺, K⁺-ATPase, *Toxicol. Appl. Pharmacol.* 151 (1998) 377–384.
- [188] S. Li, E.V. Wattenberg, Cell-type-specific activation of p38 protein kinase cascades by the novel tumor promoter palytoxin, *Toxicol. Appl. Pharmacol.* 160 (1999) 109–119.
- [189] A. Mikhailov, A.-S. Härmälä-Braskén, J. Hellman, J. Meriluoto, J.E. Eriksson, Identification of ATP-synthase as a novel intracellular target for microcystin-LR, *Chem. Biol. Interact.* 142 (2003) 223–237.
- [190] E. Habermann, G. Ahnert-Hilger, G.S. Chhatwal, L. Beress, Delayed haemolytic action of palytoxin general characteristics, *Biochim. Biophys. Acta* 649 (1981) 481–486.
- [191] W.P. Schilling, D. Snyder, W.G. Sinkins, M. Estacion, Palytoxin-induced cell death cascade in bovine aortic endothelial cells, *Am. J. Physiol. Cell Physiol.* 291 (2006) C657–C667.
- [192] C. Vale, A. Alfonso, C. Suñol, M.R. Vieytes, L.M. Botana, Modulation of calcium entry and glutamate release in cultured cerebellar granule cells by palytoxin, *J. Neurosci. Res.* 83 (2006) 1393–1406.
- [193] A. Pérez-Gómez, A. Novelli, M.T. Fernández-Sánchez, Na⁺/K⁺-ATPase inhibitor palytoxin enhances vulnerability of cultured cerebellar neurons to domoic acid via sodium-dependent mechanisms, *J. Neurochem.* 114 (2010) 28–38.
- [194] L.H. Hartwell, J.J. Hopfield, S. Leibler, A.W. Murray, From molecular to modular cell biology, *Nature* 402 (Suppl.) (1999) c47–c52.
- [195] J.A. Papin, T. Hunter, B.O. Palsson, S. Subramaniam, Reconstruction of cellular signalling networks and analysis of their properties, *Nat. Rev. Mol. Cell Biol.* 6 (2005) 99–111.
- [196] A.-L. Barabasi, Z.N. Oltvai, Network biology: Understanding the cell's functional organization, *Nat. Rev. Genet.* 5 (2004) 101–113.
- [197] A.R. Joyce, B.Ø. Palsson, The model organism as a system: Integrating “omics” data sets, *Nat. Rev. Mol. Cell Biol.* 7 (2006) 198–210.

- [198] G.P. Rossini, Signalling networks, in: M. Buchanan, G. Caldarelli, P. De Los Rios, F. Rao, M. Vendruscolo (Eds.), *Networks in Cell Biology*, Cambridge University Press, Cambridge, 2010, pp. 135–169.
- [199] A.G. Cox, C.C. Winterbourn, M.B. Hampton, Mitochondrial peroxiredoxin involvement in antioxidant defence and redox signalling, *Biochem. J.* 425 (2010) 313–325.
- [200] T.A.J. Haystead, A.T.R. Sim, D. Carling, R.C. Honnor, Y. Tsukitani, P. Cohen, D.G. Hardie, Effects of the tumor promoter okadaic acid on intracellular protein phosphorylation and metabolism, *Nature* 337 (1989) 78–81.
- [201] J. Petrak, R. Ivanek, O. Toman, R. Cmejla, J. Cmejlova, D. Vyoral, J. Zivny, C.D. Vulpe, *Déjà vu* in proteomics. A hit parade of repeatedly identified differentially expressed proteins, *Proteomics* 8 (2008) 1744–1749.
- [202] P. Wang, F.G. Bouwman, E.C.M. Mariman, Generally detected proteins in comparative proteomics—A matter of cellular stress response? *Proteomics* 9 (2009) 2955–2966.
- [203] P.J. Roach, Multisite and hierarchical protein phosphorylation, *J. Biol. Chem.* 266 (1991) 14139–14142.
- [204] L.A. Pinna, M. Ruzzene, How do protein kinases recognize their substrates? *Biochim. Biophys. Acta* 1314 (1996) 191–225.
- [205] B.N. Kholodenko, Cell-signalling dynamics in time and space, *Nat. Rev. Mol. Cell Biol.* 7 (2006) 165–176.
- [206] M. Thomson, J. Gunawardena, Unlimited multistability in multisite phosphorylation systems, *Nature* 460 (2009) 274–277.
- [207] Participating investigators and scientists of the Alliance for Cellular Signaling, Overview of the Alliance for Cellular Signaling., *Nature* 420 (2002) 703–706.
- [208] J. Quackenbush, Computational analysis of microarray data, *Nat. Rev. Genet.* 2 (2001) 418–427.
- [209] K.A. Janes, D.A. Lauffenberger, A biological approach to computational models of proteomic networks, *Curr. Opin. Chem. Biol.* 10 (2006) 73–80.
- [210] C.J. Miller, T.K. Attwood, Bioinformatics goes back to the future, *Nat. Rev. Mol. Cell Biol.* 4 (2003) 157–162.
- [211] The UniProt Consortium, The Universal Protein Resource (UniProt). *Nucleic Acids Res.* 37 (Suppl. 1) (2009) D169–D174.
- [212] T.J. Hubbard, B.L. Aken, S. Ayling, B. Ballester, K. Beal, E. Bragin, S. Brent, Y. Chen, P. Clapham, L. Clarke, G. Coates, S. Fairley, *et al.*, Ensembl 2009, *Nucleic Acids Res.* 37 (Suppl. 1) (2009) D690–D697.
- [213] P.J. Kersey, J. Duarte, A. Williams, Y. Karavidopoulou, E. Birney, R. Apweiler, The International Protein Index: An integrated database for proteomics experiments, *Proteomics* 4 (2004) 1985–1988.
- [214] M. Ashburner, C.A. Ball, J.A. Blake, D. Botstein, H. Butler, J.M. Cherry, A.P. Davis, K. Dolinski, S.S. Dwight, J.T. Eppig, M.A. Harris, D.P. Hill, *et al.*, Gene ontology: Tool for the unification of biology. The Gene Ontology Consortium, *Nat. Genet.* 25 (2000) 25–29.
- [215] R. Malik, K. Dulla, E.A. Nigg, R. Körner, From proteome lists to biological impact—Tools and strategies for the analysis of large MS data sets, *Proteomics* 10 (2010) 1270–1283.
- [216] J. López-Barea, J.L. Gómez-Ariza, Environmental proteomics and metallomics, *Proteomics* 6 (Suppl.) (2006) S51–S62.
- [217] Gene Ontology Consortium, The Gene Ontology (GO) database and informatics resource., *Nucleic Acids Res.* 32 (Suppl. 1) (2004) D258–D261.

This page intentionally left blank

THE MOLECULAR TOXICOLOGY OF CHEMICAL WARFARE NERVE AGENTS

Kimberly D. Spradling¹ and James F. Dillman III*

Contents

1. Introduction	112
2. Nerve Agent Toxicity	114
2.1. Route of exposure	114
2.2. Acute toxicity of OP nerve agents	114
3. Current Medical Countermeasures to Nerve Agent Toxicity	116
4. Global Molecular Screening Approaches Enable the Identification of Molecular Mechanisms of Toxicant Exposure	117
4.1. Genomics	117
4.2. Proteomics	118
4.3. Metabolomics	120
4.4. Bioinformatic tools	120
5. Global Molecular Techniques Support the Three-Phase Model of Nerve Agent Toxicity	121
6. Global Molecular Techniques Provide Evidence for Non-AChE Mechanisms of OP Nerve Agent Toxicity and Reveal Secondary Effects of Exposure	123
6.1. Oxidative stress	124
6.2. Mitochondrial dysfunction	125
6.3. Apoptosis	126
6.4. Inflammation	128
6.5. BBB dysfunction	130
6.6. Repair and recovery	132
7. Future Directions in the Molecular Toxicology of Nerve Agents	134
8. Conclusions	135
Acknowledgments	138
References	138

Cell and Molecular Biology Branch, US Army Medical Research Institute of Chemical Defense, Aberdeen Proving Ground, Maryland, USA

*Corresponding author. Tel.: +1 410-436-1723; Fax: +1 410-436-1960

E-mail address: james.dillman@us.army.mil

¹ Current address: Department of Genetics, Texas Biomedical Research Institute, San Antonio, Texas, USA.

Abstract

Chemical warfare nerve agents continue to be a threat to both military personnel and civilian populations. Organophosphorus nerve agents irreversibly inhibit the enzyme acetylcholinesterase, resulting in accumulation of high levels of the neurotransmitter acetylcholine (ACh) at muscarinic and nicotinic receptors. This accumulation of ACh induces clinical symptoms including myosis, difficulty in breathing, convulsions, seizures, and can result in death. Current medical countermeasures for treating nerve agent intoxication increase survival if administered rapidly after exposure but may not fully prevent brain injury. The downstream neurological damage induced by nerve agent exposure is not well characterized. Researchers are now utilizing molecular approaches to understand the molecular pathways involved in nerve agent-induced brain injury, with the goal of developing treatment strategies that are effective when administered after the onset of seizures and secondary responses that lead to nerve agent-induced brain injury.

1. INTRODUCTION

Chemical weapons have been used for centuries to incapacitate or kill the enemy in times of war. Arrows dipped in scorpion and serpent venoms were used in the late Stone Age and are among the earliest documented chemical weapons [1]. Since then, chemical weapons have evolved and have been successfully used on the battlefield and in terrorist attacks [1–5]. The most toxic chemical warfare agents known to date are organophosphorus (OP) nerve agents, which were first developed in the 1930s by German scientists who were originally tasked with synthesizing more potent pesticides using organic phosphoric acid esters [3,6] (Figure 1).

Chemist Dr. Gerhard Schrader synthesized the first German nerve agent (or G-agent) in 1936. It was the cyanide-containing compound ethyl dimethylamidocyanophosphate, which was later named tabun (GA) [3]. After the realization that tabun was extremely toxic to humans and therefore unsuitable for use as a plant protectant, the German army immediately began producing it as an agent of chemical warfare. Further studies of this toxic compound led Schrader and his colleagues to synthesize the fluorine-containing nerve agent sarin (GB; isopropyl methanefluorophosphonate) in 1938, which was determined to be more than 10 times as toxic as tabun. The most toxic G-agent, soman (GD; *o*-pinacolyl methylphosphonofluoridate), was then synthesized by Dr. Richard Kuhn in 1944. Cyclosarin (GF; cyclohexyl methylphosphonofluoridate) was later synthesized by Schrader and colleagues in 1949 [3]. Although the German army produced large quantities of these nerve agents, there is no evidence indicating that they used them as chemical weapons.

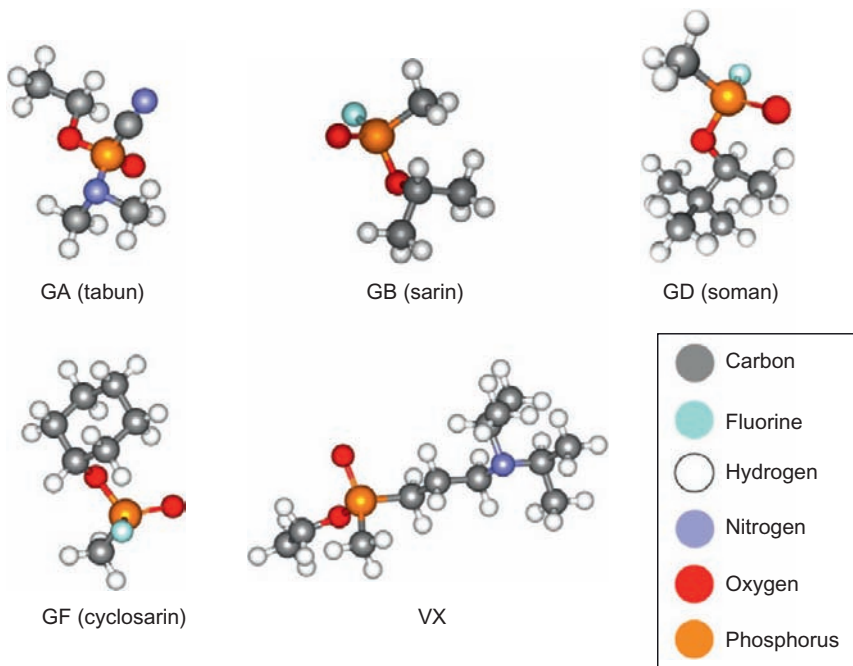


Figure 1 Structures of G-series and V-series organophosphorus nerve agents.

Following the discovery of the G-series agents, Drs. Ranajit Ghosh and J. F. Newman first discovered the V-agents in 1952 at the Plant Protection Laboratories of Britain's Imperial Chemical Industries while studying a class of organophosphate compounds. As with tabun, scientists soon realized that these agents were too toxic to be used as plant protectants. These agents were further evaluated at the British Armed Forces research facility at Porton Down in the United Kingdom, where the most studied compound in this family of nerve agents, VX (*o*-ethyl-*s*-[2(diisopropylamino)ethyl] methylphosponothioate), was synthesized in 1954. Unlike the G-series agents, all of the V-agents are persistent, meaning that they can remain on skin and other surfaces for long periods of time. The V-series agents are ~10 times more toxic than the G-agent sarin and are the most highly toxic chemical warfare nerve agents synthesized to date [3,7].

Despite the development and military proliferation of chemical weapons in the first half of the twentieth century, the worldview on these weapons has changed in recent history. In 1991, UN Resolution 687 established the term "weapon of mass destruction" and called for the immediate destruction of chemical weapons in Iraq and the eventual destruction of all chemical weapons globally. Further, the Chemical Weapons Convention

of 1993 banned the production, stockpiling, and use of chemical warfare agents. Despite these extensive efforts to prevent their use, OP nerve agents still remain a threat to soldiers in time of war as well as to the civilian population in the event of a terrorist attack, such as the terrorist sarin attack on the Tokyo subway in 1995 by members of the Japanese cult Aum Shinrikyo. The attack resulted in 12 deaths and injuries to more than 5500 civilians [2,4]. OP nerve agents are likely to be a weapon of choice for many other terrorist organizations as well because they are relatively accessible or simple to produce, easy to transport, and can be delivered in mass quantities [5,6].



2. NERVE AGENT TOXICITY

2.1. Route of exposure

The various OP nerve agents differ in their water solubility and volatility, which influences an agent's route of exposure and potential as a chemical warfare agent. Most nerve agents exist as liquids and are readily absorbed through the skin and eyes; however, the G-agents (especially sarin) are highly volatile. Therefore, inhalation exposure also poses a threat. Unlike the G-agents, the V-agents have an oil-like consistency; therefore, the route of exposure for V-agents is considered to be primarily dermal. However, it should be noted that VX, which is the least volatile nerve agent, can vaporize in high temperatures or explosive conditions. In military use, V-agents would most likely be aerosolized into tiny droplets or vaporized for dispersion, thereby easily entering the body through the skin and mucous membranes or through inhalation [7,8]. Although ingestion of nerve agents is expected to be relatively rare compared to inhalation exposure or skin contact, they are readily absorbed from the GI tract and are highly toxic.

2.2. Acute toxicity of OP nerve agents

Neurotransmitters, such as acetylcholine (ACh), are endogenous chemicals that transmit signals from a neuron to a target cell across the chemical synapse, which allows the nervous system to connect to and control other systems of the body. The binding of ACh to its receptor sites on the postsynaptic membrane stimulates actions in the body such as breathing, digestion, and muscular contraction. The enzyme acetylcholinesterase (AChE) then inactivates ACh to terminate this synaptic transmission and allow the muscle, gland, or organ to relax.

It is well established that the acute toxicity of OP nerve agents results from the irreversible inhibition of AChE through the formation of a

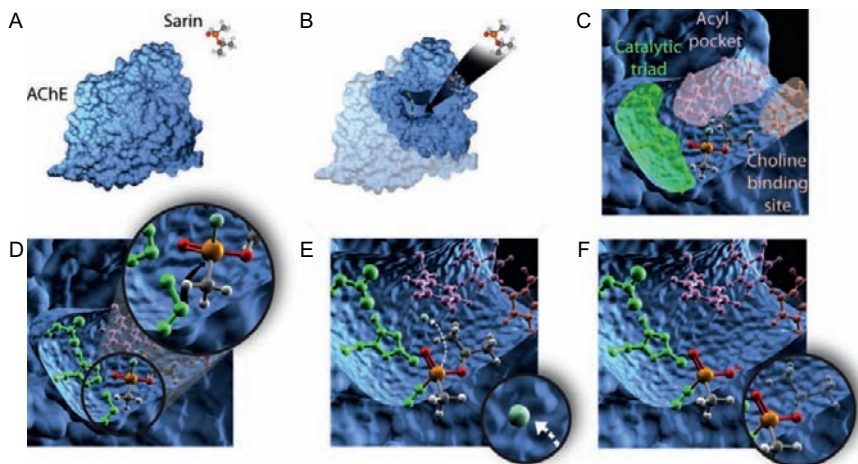


Figure 2 Interaction of sarin with acetylcholinesterase (AChE). (A) Structures of sarin and AChE. (B) Entry of sarin into the active site gorge of AChE. (C) Orientation of sarin in the active site of AChE relative to the catalytic triad. The catalytic center of AChE is a triad comprising serine-200, histidine-440, and glutamate-327. (D) Sarin binding to the catalytic serine, which prevents binding of ACh. (E) Following attachment to AChE, the fluoride ion of sarin (the leaving group) is cleaved from the bound molecule. (F) The active site serine is covalently adducted. The sarin bound to AChE can then undergo dealkylation in a process referred to as “aging,” which results in irreversible enzyme inhibition. Illustration by Alexandre Katos.

covalent bond between the nerve agent and the site on the enzyme where ACh normally undergoes hydrolysis (Figure 2). The catalytic center of AChE is a triad comprising serine-200, histidine-440, and glutamate-327. Nerve agents bind to the catalytic serine, thereby preventing ACh binding and inhibiting cholinesterase (ChE) activity. The inhibited enzyme can be reactivated by a strong nucleophile, such as an oxime, which removes the neurotoxicant from the AChE molecule. However, the efficacy of AChE reactivation is dependent on the nerve agent with which the ChE was inhibited and the therapeutic oxime used. Following attachment to AChE, a portion of the nerve agent, called the leaving group, is cleaved from the bound molecule. OPs bound to AChE can then undergo dealkylation in a process referred to as “aging.” This aged complex results in irreversible enzyme inhibition. Oximes have no effect and cannot reactivate the aged OP–enzyme conjugate [9]. The aging half-time for OP nerve agents is variable; it can be as short as 2 min for soman or as long as 48 h for VX [10]. This AChE inhibition causes a toxic accumulation of ACh at cholinergic synapses and results in the overstimulation of muscarinic and nicotinic ACh receptors (nAChRs) in the central and peripheral nervous system, including the neuromuscular junction [6,11,12].

Acute exposure to an OP nerve agent initially results in symptoms such as myosis, tightening of the chest, difficulty breathing, and a general loss of bodily functions. As symptoms progress, the victim suffers from convulsive spasms and seizures, which can lead to death if left untreated [6,11–15]. In animals surviving an experimental convulsive dose of nerve agent, spiking activity appears in the electroencephalogram (EEG) in less than 10 min, and it rapidly progresses into status epilepticus that lasts for hours [16,17]. Although the intensity of seizures decreases over time, the EEG is still abnormal days after the intoxication [18].



3. CURRENT MEDICAL COUNTERMEASURES TO NERVE AGENT TOXICITY

OP nerve agents can be fatal at low concentrations, but even a nonlethal dose can cause permanent neurological damage if the person does not receive proper medical attention immediately. Based on the previous scientific findings discussed in the section above, current medical countermeasures to nerve agent intoxication include an anticholinergic (e.g., atropine) that blocks excess ACh at muscarinic receptors to alleviate parasympathetic overstimulation, an oxime (e.g., 2-pyridine aldoxime methylchloride [2-PAM] or 1-2-hydroxylminomethyl-1-pyridino-3-(4-carbamoyl-1-pyridino-2-oxapropane dichloride) [HI-6]) to reactivate inhibited AChE molecules, and an anticonvulsant such as diazepam [11–13,19]. These therapeutics increase survival if administered within a short period of time following exposure, but they may not fully prevent neurological damage or functional impairment [2,6,11,15,20–22]. This is of great concern because although these countermeasures are readily available to soldiers in a combat setting, they are not accessible to the general public in case of a terrorist attack. Rapidly terminating nerve agent-induced seizures is critical because their duration and intensity have been directly linked to brain damage following exposure [19,23–25]. Studies have shown signs of neuropathology present within 20 min of seizure onset and have demonstrated the increased difficulty in terminating seizures that have lasted beyond 40 min [15,23]. These findings are important considering that the anticipated response time to treat civilian casualties exposed to nerve agent is estimated to be at least 30 min [15], and many will have already initiated seizures by the time medical personnel arrive.

Survivors of nerve agent poisoning can experience long-term neurological and behavioral outcomes months or years following exposure [2]. Previous findings by Scremin *et al.* [26] revealed that sarin-exposed rats showed behavioral abnormalities up to 16 weeks post-exposure. To date, most of our understanding on this issue in humans comes from studies performed on

survivors of the Tokyo subway attack. More recently, Loh and colleagues [5] reported on the long-term cognitive sequelae of a soldier exposed to sarin by means of an improvised explosive device (IED) while he was deployed to Iraq in 2004. Testing performed 10 months following exposure revealed that the victim suffered from reduced information processing speed, poor focused attention, and difficulty in motor coordination. Despite these studies, the long-term neurologic sequelae of nerve agent exposure are still unclear. Therefore, the molecular effects and biological pathways involved in nerve agent-induced neurodegeneration need to be examined to determine drug treatments that would be effective when administered after the onset of seizures and secondary responses that lead to brain injury.



4. GLOBAL MOLECULAR SCREENING APPROACHES ENABLE THE IDENTIFICATION OF MOLECULAR MECHANISMS OF TOXICANT EXPOSURE

To date, most scientific investigations of nerve agent toxicity have involved classical toxicology where physical symptoms of exposure, tissue histopathology, and AChE activity are used to indicate adverse effects of exposure. While these measurements are useful indicators of acute OP exposure, they are not as effective in studying the molecular mechanisms of toxicity or providing insight into the long-term effects of OP exposure. To help determine the molecular mechanisms of nerve agent toxicity, scientists have recently begun using “omics” technologies to assess the toxicological effects and physiological mechanisms of OP nerve agents, expanding beyond AChE inhibition. In the life sciences, the suffix *omics* refers to the study of large sets of biological molecules [27]. This field of molecular biology includes genomics (focused on the genome sequence or genomic expression, also referred to as “transcriptomics” or “gene expression profiling”), proteomics (focused on large sets of proteins, the proteome), and metabolomics (focused on large sets of small molecules, the metabolome). These multiplex technologies offer a global screening approach for OP nerve agent toxicity, and subsequent bioinformatic analyses enable the identification of biological pathways and molecular functions significantly affected by nerve agent exposure.

4.1. Genomics

Before genomics, molecular biology techniques (e.g., Northern blot or real-time polymerase chain reaction [PCR]) were used to detect and quantify the expression level of individual genes, making it difficult to see the “big picture” of gene function in a cell. Technological developments, such as the introduction of chip-based assays (e.g., DNA microarrays), have had a

major impact on the resolution and throughput of omic-based studies. Since their development in the 1990s, DNA microarrays have had an important influence on the fields of molecular biology and toxicology. These arrays are commonly used to simultaneously measure the mRNA (mRNA) levels of thousands of genes in a cell and are capable of detecting even subtle changes in gene expression. DNA arrays monitor the expression of a gene by measuring its level of hybridization to a target sequence localized to a specific region on an array. In brief, RNA is extracted from a biological sample of interest and used as a template to synthesize labeled nucleic acid probe. Labeled probe is then hybridized to the array that contains thousands of gene targets and binds to complementary target sequences on the array. Quantitative imaging coupled with clone database information allows measurement of the amount of labeled probe that hybridized to each target sequence, resulting in the identification and relative quantification of the genes expressed in the biological sample [28,29]. Given that this technique provides a quantitative overview of the mRNA transcripts present in a biological sample by detecting the genes that are up- or down-regulated at any given time and in any physiological situation, it can be used to determine which genes are differentially expressed as a result of nerve agent exposure and aid in identifying mechanisms of toxicity. Using a global approach to analyze thousands of genes in a single experiment, it is easier to assay the overall molecular response of a cell, tissue, or organ and then identify specific genes and/or groups of genes altered following a chemical exposure. Moreover, these global molecular techniques are capable of identifying differentially expressed molecules between samples without any prior knowledge of their functions. Thus, scientists can detect potentially interesting genes and molecular mechanisms that were not previously suspected to be important for biological processes and can generate new biological hypotheses [30].

4.2. Proteomics

Although gene expression profiling provides many advantages for studying the molecular mechanisms of nerve agent toxicity, such as being able to use one biological sample to measure the expression of thousands of genes simultaneously, DNA microarrays can only monitor cellular responses at the mRNA level and provide little information regarding the functional state of the proteins they encode. Even though all proteins are based on mRNA precursors, post-translational modifications and environmental interactions make it impossible to predict abundance of specific proteins based on gene expression analysis alone. Previous studies have shown that mRNA is not always translated into protein, and the amount of protein produced depends on the physiological state of the cell. Further, a single gene can give rise to a number of functionally different proteins through various

molecular processes such as alternative splicing of pre-mRNAs, attachment of carbohydrate residues to form glycoproteins, or addition of phosphate groups to serine, threonine, or tyrosine amino acids in the protein. Thus, genomic data need to be complemented with protein expression data to truly determine the molecular mechanisms of toxicity of nerve agents.

Many proteomic technologies are currently available to quantify protein abundance and some aspects of the activation state. Proteomic studies usually involve the physical separation of proteins by techniques such as sodium dodecyl sulfate polyacrylamide gel electrophoresis (SDS-PAGE), two-dimensional SDS-PAGE (2D-PAGE), or column chromatography (e.g., ion-exchange chromatography, gel filtration chromatography, affinity chromatography, or high-pressure liquid chromatography [HPLC]). Once separated, proteins of interest can then be detected. The traditional methods of detection used in protein chemistry, such as Western blot analysis, have the capacity to detect only one protein at a time. Although this approach remains valuable for a detailed understanding of a protein of interest, it does not provide information on the interactions between numerous proteins in a system, unless a large number of consecutive experiments are performed. Combining a protein separation method with mass spectrometry (MS) has the potential to overcome the limitations encountered in traditional protein analysis techniques. The rapid evolution in MS has led to significant improvements in protein identification. Combining liquid chromatography (LC) with MS-based analyses of complex mixtures overcomes many of the drawbacks to gel-based methods, such as limited dynamic range and sensitivity, as well as low throughput with respect to protein identification [31]. Further, the addition of stable isotopes to the proteome allows simultaneous protein identification. A shotgun proteomic technique, such as iTRAQ (isobaric tags for relative and absolute quantitation), involves isotopic labeling of peptides for the simultaneous identification and quantification of proteins in two or more samples in a single experiment [32]. With this method, isobaric tags of varying mass are used to label the primary amines of peptides from different biological samples. The labeled peptides from each sample are then mixed, separated by two-dimensional LC, and analyzed using tandem mass spectrometry (MS/MS) to identify global changes in the proteome. This approach has been successfully used to study global protein expression in neuronal systems [33]. Phosphorylation enrichment schemes, such as immobilized metal affinity chromatography (IMAC) [34], can also be used prior to MS analysis to enrich for signaling phosphoproteins, which are usually of low abundance and/or are phosphorylated at low stoichiometry. Identifying changes in the global phosphorylation status of the proteome upon nerve agent exposure using iTRAQ and IMAC techniques can be used to characterize proteome-wide signaling pathways by probing many signaling phosphoproteins simultaneously. This approach would permit the identification of molecular pathways perturbed by nerve agent exposure and elucidate mechanisms of toxicity.

The newest approach to analyzing the proteome involves the use of protein microarrays, which are based on the same concept as DNA microarrays discussed above. The most common protein microarrays are antibody arrays used to profile a complex mixture of proteins and measure protein expression levels in the mixture [35]. Although simple in principle, protein microarrays are more difficult to work with than DNA microarrays because proteins vary in their chemistry (e.g., hydrophobic vs. hydrophilic), and they bind to each other by several types of noncovalent interactions. Fragments of DNA, however, vary only in their nucleotide sequence and bind to their partners by simple Watson–Crick base pairing. Despite these challenges, this field of proteomic analysis is expected to make rapid progress and to move toward standardized protocols as with transcriptomics.

4.3. Metabolomics

The newest field of global molecular profiling is metabolomics. Metabolic phenotypes are the by-products that result from the interaction between genetic, environmental, and other factors [27]. In contrast to the genome and proteome, the metabolome consists of small molecules that are also known as metabolites. As their name suggests, metabolites are involved in the energy transmission, or metabolism, in cells. Metabolic profiling is performed on easily collected biological samples such as urine, saliva, or plasma. The metabolome consists of a wide range of chemical structures, and like the genome and proteome, it is highly variable and time-dependent following toxicant exposure. The techniques currently used in metabolomics give researchers the ability to make an unbiased assessment of biochemical status at the cellular, tissue, or organism level. MS and nuclear magnetic resonance (NMR) are the primary technologies used for metabolomic studies [36]. Both technologies have made recent advances in sensitivity and data manipulation and storage. MS is the most common technique due to its high accuracy and sensitivity. The main advantage of NMR is that it does not require any upfront chromatographic separation, and it does not destroy the samples during analysis. NMR has the ability to measure molecular compartmentalization and dynamic biochemical changes in real time. An important challenge of metabolomics is to acquire qualitative and quantitative information concerning the metabolites that occur under normal circumstances and detect perturbations in the complement of metabolites as a result of changes in environmental factors [27].

4.4. Bioinformatic tools

Although these global molecular techniques are powerful tools to explore the expression levels of thousands of genes, proteins, or metabolites after toxicant exposure, a major challenge lies in the interpretation of the massive

amounts of data collected in each scientific study. The rapid advancement of microarray technology increased the need for integration of higher-order statistical analyses and data management (e.g., [37]), and these same analysis tools are being applied in the field of proteomics and metabolomics.

In the past few years, there has been rapid advanced development of software programs for comprehensive pathway analysis and literature mining. These bioinformatic tools have enabled the interpretation of large, complex datasets and have allowed scientists to better identify biological pathways and molecular mechanisms involved in toxicant exposure, such as those seen during nerve agent poisoning. However, with the continuing advancement of molecular techniques, it is likely that the methods used for collecting data will again surpass our capacity to adequately analyze the results. Therefore, scientists must continually develop more advanced bioinformatic tools and methods to interpret these large datasets.



5. GLOBAL MOLECULAR TECHNIQUES SUPPORT THE THREE-PHASE MODEL OF NERVE AGENT TOXICITY

The neuropathology resulting from OP nerve agent exposure is typically thought to result from sustained seizure activity. Seizure-related brain damage occurs in numerous sensitive areas in the brain such as the amygdala, hippocampus, piriform cortex, septum, and thalamus [6,15,23,25,38–40]. In a three-phase model proposed by McDonough and Shih [11], seizure initiation is a cholinergic phenomenon that lasts from the time of exposure to ~5 min after seizure onset. It has been reported that a convulsant dose of soman immediately inhibits brain ChE with maximum inhibition within 10 min and a large increase in ACh concentration at the time of seizure initiation [41,42]. If seizures are not stopped immediately, a transition phase occurs 5–40 min post-exposure in which other neurotransmitter systems are perturbed. During this phase, the level of excitatory amino acids (EAAs), such as glutamate, increases and potentiates seizure activity [11,43]. Shortly after the onset of soman-induced seizures, choline (Ch) levels increase [41], likely due to increased hydrolysis of phospholipids [44]. This leads to the last phase of the model, which is predominantly a non-cholinergic phenomenon, starting ~40 min after seizure onset. It is postulated that the seizure activity is maintained from this point on by excessive glutamate stimulation, and that the glutamatergic hyperactivity causes an opening of *N*-methyl-D-aspartate (NMDA) calcium channels, leading to subsequent increases in intracellular calcium [11,13,45], which in turn initiates signaling cascades that cause neuronal death. It is proposed that this excess influx of calcium is the ultimate cause of neuropathology following nerve agent exposure as it can hyperactivate enzymes such as lipases, proteases, endonucleases, kinases,

or phosphatases that can cause damage to cell membranes and the cytoskeleton, as well as to organelle structure and function [18,45].

A large amount of data obtained from scientific studies utilizing global molecular techniques support the temporal model proposed by McDonough and Shih [11] that links nerve agent-induced seizures to resulting neuropathology. Studies using microarray analysis have shown that many genes and signaling pathways are altered within the first 15 min after acute sarin exposure [39,40,46]. Among these significantly altered genes are those involved in cholinergic signaling, catecholaminergic signaling (which modulates seizure susceptibility in animal models of epilepsy [47]), γ -aminobutyric acid (GABA)ergic signaling, glutamate and aspartate signaling, calcium channels and binding proteins, neurotransmission and neurotransmitter transporters, neuropeptides, and ligand-gated ion channels that open and close in response to the binding of a neurotransmitter (e.g., nAChR, GABA receptor, and NMDA receptor [46]). At 2-h post-exposure, Damodaran and colleagues [48] continued to observe sarin-induced alterations in the mRNA expression of neurotransmitter transporters (such as synaptobrevin 1, syntaxin 6, and SV2), signaling receptors (such as the GABA-A receptor ρ -2 subunit and AMPA2), and ligand-gated ion channels. The transcriptional response at these early time points following acute sarin exposure clearly relates to the three phases of nerve agent toxicity and supports the model proposed by McDonough and Shih [11].

Spradling and colleagues also used oligonucleotide microarrays to study the changes in gene expression profiles after a $1 \times \text{LD}_{50}$ sarin exposure in a rat model over a 24-h time period [39,40]. Consistent with the findings of Damodaran *et al.* [46,48], the findings of Spradling *et al.* at 15 min after seizure onset support the transition phase of the model. For example, D-glutamine and D-glutamate metabolism and glutamate receptor signaling were two of the canonical pathways significantly altered immediately after seizure onset. Previous studies have shown an increase in choline, a precursor for ACh, 15–30 min after nerve agent exposure [41] due to increased hydrolysis of phospholipids [44], which supports the presence of phospholipid degradation among the significant pathways at this early time point in the work by Spradling *et al.* The most significantly altered pathway at 15 min was inositol metabolism. Inositol works closely with Ch as a primary component of cell membranes. It is necessary for normal nerve and brain function as it is required for proper action of several neurotransmitters, such as ACh and serotonin. Studies have shown that membrane phosphoinositide (PI) is hydrolyzed following the activation of neurotransmitter receptors, such as NMDA, to yield inositol 1,4,5-triphosphate (IP_3), a second messenger that transmits signals from the receptor into the cell by releasing calcium from non-mitochondrial intracellular stores [11,13,45].

In addition to these earlier time points, Damodaran and colleagues [46] also examined the transcriptional response at 3 months following sarin

exposure. The authors noted persistent alteration of calcium/calmodulin-dependent kinase II (CamKII) from 2 h to 3 months (along with other calcium transporter molecules), which indicates that calcium-induced changes persist for a long time and likely play an important role in sarin-induced pathology [46]. Day and Greenfield [49] suggested that CamKII, which is integrally involved with glutamate receptors in the processes of learning and memory, is activated by calcium influx through NMDA receptors, resulting in mitochondrial dysfunction and free radical formation, followed by caspase activation and apoptotic cell death of sensitive brain regions [46]. Uncovering the roles of calcium during nerve agent poisoning is complicated due to the role calcium plays in both neuronal survival and programmed cell death [50].



6. GLOBAL MOLECULAR TECHNIQUES PROVIDE EVIDENCE FOR NON-AChE MECHANISMS OF OP NERVE AGENT TOXICITY AND REVEAL SECONDARY EFFECTS OF EXPOSURE

Since the development of the three-phase model by McDonough and Shih [11], studies using global molecular techniques have also indicated the presence of non-cholinergic and non-glutamatergic systems during the late phase response to nerve agents, providing critical insight into the secondary effects leading to nerve agent-induced neuropathology. Blanton *et al.* [51] conducted one of the first high-density gene expression profiling analyses to identify genes altered by nerve agent exposure. In this study, the authors employed microarray analysis to analyze gene responses following a 2-week low-level (0.1, 0.2, and 0.4 LD₅₀) exposure to VX. Their results revealed altered expression profiles of non-AChE targets in the mouse hippocampus and cortex following exposure, which returned to normal levels by 2 weeks after the final exposure. In this early genomic study of nerve agent exposure, Blanton and colleagues used self-organizing maps (SOMs) to identify clusters of genes that were similarly affected by VX poisoning. They identified neuronal genes encoding receptors, vesicle-related proteins, and molecular motors as well as genes associated with neurogenesis/maintenance as being upregulated in the hippocampus following exposure. They also identified similar functional categories of genes being altered in the cortex. Although the authors identified numerous genes with altered expression patterns following VX exposure, they were unable to identify a complete alternate pathway from the dataset.

Since the study by Blanton *et al.* [51], scientists have continued using global molecular techniques to understand in greater detail the molecular responses of sensitive brain regions to nerve agent exposure. The correlation

between neuronal activity and the expression of specific genes has led to an increase of scientific data related to the long-lasting functional changes that underlie nerve agent toxicity [48]. Gene expression profiling has been successfully used to investigate the mechanisms of toxicity and resulting effects of sarin [39,40,46,48,52] and soman [53]. In 2006, Damodaran and colleagues published two papers detailing sarin-induced gene expression changes in male Sprague–Dawley rat brains following a $0.5 \times \text{LD}_{50}$ exposure at 15 min [46] and 2 h [48] and a $1 \times \text{LD}_{50}$ exposure at a later time point of 3 months. In their studies, the animals were challenged with the appropriate dose of sarin (im, diluted in saline), and the animals were anesthetized with 100 $\mu\text{g}/\text{kg}$ ketamine/xylazine prior to brain dissection. In the study by Dillman *et al.* [53], male Sprague–Dawley rats were pretreated with 125 mg/kg of the oxime HI-6 (ip) 30 min prior to exposure of 180 $\mu\text{g}/\text{kg}$ soman (sc, diluted with 0.9% sodium chloride). One minute after soman challenge, the animals were treated with atropine methyl nitrate (2 mg/kg, im). The hippocampi were immediately collected after deep anesthesia using sodium pentobarbital (65 mg/kg, ip) at 1, 3, 6, 12, 24, 48, 72, 96, and 168 h after the onset of convulsions. The microarray studies by Spradling and colleagues in 2010 [39,40] also involved the use of male Sprague–Dawley rats. The animals were challenged with $1 \times \text{LD}_{50}$ sarin (sc, diluted in saline). One minute after seizure onset, the animals were treated with atropine sulfate (2 mg/kg) and the oxime 2-PAM (25 mg/kg), both administered in a single injection (im). Thirty minutes later, the animals were given the anticonvulsant diazepam (10 mg/kg, sc). The amygdala, hippocampus, piriform cortex, septum, and thalamus were immediately collected at 15 min, 1, 3, 6, and 24 h after seizure onset following decapitation. These studies helped uncover the secondary molecular effects of intracellular calcium overload that are expected to produce important cerebral biochemical and metabolic disruption [18].

6.1. Oxidative stress

Previous data have shown that the hyperactivation of enzymes resulting from intracellular calcium overload during nerve agent poisoning promotes oxidative stress [54]. Results have implicated exposure to OP nerve agents in the generation of free radicals (e.g., hydrogen peroxide [H_2O_2], superoxide [O_2^-], nitric oxide [NO], and peroxynitrite [ONOO^-]) and the alteration of the antioxidative scavenging system. The accumulation of reactive oxygen species during an oxidative stress response induces various defense mechanisms or programmed cell death. Damodaran and colleagues [46] noted an induction of nitric oxide synthase (NOS)-2 mRNA expression following sarin exposure, which supported their previous finding of nitrotyrosine production in sarin-exposed rats [55]. Further, Damodaran *et al.* [46] saw a reduction in mRNA expression level for glutathione

S-transferase A2 (GSTA2), which serves as an important protective mechanism for minimizing oxidative damage in the cell. The authors speculate that this reduction in GSTA2 may potentiate damage to dopamine and GABA populations due to an alteration in the mRNA expression of dopamine receptor type 4 and GABA receptor, respectively.

The occurrence of oxidative stress during nerve agent poisoning can be linked to numerous downstream molecular effects. The macromolecular targets of oxidative damage include lipids, proteins, and both nuclear and mitochondrial DNA. Oxidative stress affects numerous genes, including those involved in modulating the production of free radicals, repairing target macromolecules, and specifying the orderly replacement of effector cells [46]. One of the consequences of oxidative stress is lipid peroxidation, which has previously been shown in the CNS of sarin-exposed rats [56] and was further supported by the observed alteration in lipophilin gene expression [46]. One mechanism in which the cells suppress oxidative-induced toxicity is through the activation of heat shock proteins (HSPs) [57,58]. The production of HSPs has been observed following nerve agent exposure [39,40,48,59]. These proteins are thought to provide cellular protection during nerve agent poisoning through their roles in protein trafficking, protein folding, and regulation of cell death pathways.

6.2. Mitochondrial dysfunction

Mitochondria are responsible for producing energy through the coupling of oxidative phosphorylation to respiration in order to provide ATP for most cellular processes that require energy. There is a large amount of evidence suggesting that mitochondrial dysfunction in the CNS is linked to epileptic seizures [60]; therefore, it may play a role in seizure-related brain damage following nerve agent exposure.

Previous studies have shown that neuronal mitochondria are important for intracellular calcium sequestration, so a major form of damage likely results from mitochondrial swelling as the mitochondria take up and scavenge the excess calcium produced during nerve agent poisoning. Therefore, mitochondria may be subjected to stress and even collapse if calcium levels exceed a physiological threshold [50].

Another important trigger for mitochondrial stress is the production of reactive oxygen species, which have been suggested to activate mitochondrial permeability transition pores and release mitochondrial cytochrome *c*. These oxygen radicals are generated when the mitochondrial respiratory chain is inhibited [61,62]. When excess amounts of these reactive oxygen species are produced, they can overload the endogenous protective enzymes (e.g., glutathione peroxidase, superoxide dismutase, and catalase) and result in the oxidative damage of proteins, phospholipids, and DNA [60]. Alternatively, oxygen radicals themselves can inhibit the mitochondrial

respiratory chain [63] to create a very toxic and vicious cycle. This cyclic mechanism is thought to cause the progressive respiratory chain impairment in the CA1 and CA3 hippocampal subfields of pilocarpine-treated chronic epileptic rats [60,64].

In addition to the alteration of neuronal calcium homeostasis, mitochondrial dysfunction likely results in decreased intracellular ATP levels, which could increase neuronal excitability. This is supported by previous genomic studies indicating the significant alteration of cyclic nucleotide signaling and purinergic signaling within 15 min of sarin exposure [39,40,46]. Damodaran and colleagues [48] also noted the significant alteration of four ATPases and four ATP-based transporters at 2 h after sarin exposure. The data obtained in these studies support earlier findings showing a large increase in blood glucose concentration in the first hours of soman-induced seizures [65] and increased glucose utilization in nerve agent-damaged brain areas [66].

Status epilepticus-induced neuronal injury by the anticholinesterase diisopropylfluorophosphate (DFP) or the carbamate carbofuran has been linked to excitotoxicity, energy impairment, and oxidative stress [67]. The authors found an inverse relationship between an NO increase and a decrease in high-energy phosphates in the CNS of rats exposed to these AChE inhibitors. They attributed this finding to NO-induced impairment of mitochondrial respiration leading to depletion of energy metabolites. This was supported later by the findings of Damodaran *et al.* [46], who noted alterations in the transcription levels of brain Acyl-CoA synthetase and leptin along with a decrease in the mRNA levels of key mitochondria-associated proteins such as B-cell lymphoma (BCL)-2-associated X protein (i.e., BAX) and BCL-2-related ovarian killer protein (BOK). The authors suggest that OP chemicals may alter cytochrome P-450 and generate oxidants in their metabolic process that would subsequently oxidize a wide range of endogenous chemicals.

6.3. Apoptosis

In addition to supplying ATP for cellular functions, mitochondria also regulate apoptosis by controlling the release of mitochondrial proteins such as cytochrome *c* and other apoptotic factors. Members of the BCL-2 family are involved in the regulation of apoptosis. Some of the BCL-2 family members (including BCL-2, BCL-extra large [BCL-XL], and BCL-2-like protein 2 [BCL-W]) are considered to be anti-apoptotic, whereas other members (including BCL-2-associated death promoter [BAD], BAX, and BCL-2 homologous antagonist/killer [BAK]) induce apoptosis.

Although the neurotoxic mechanism of nerve agent poisoning has yet to be clearly defined, much of the scientific data suggest that it involves

apoptotic neuronal cell death similar to that proposed following exposure to a micromolar concentration of L-glutamate [46]. Scientific support for an apoptotic mechanism of AChE-induced cell death was provided by Day and Greenfield [49]. They used a peptide derived from the C-terminus of AChE, which was homologous to β -amyloid, along with inhibitors of various cellular processes to trace the cell death pathway in organotypic hippocampal cultures and found that pathophysiological activity was produced via an apoptotic pathway. Their results indicated that the AChE peptide activated $\alpha 7$ nicotinic ACh receptor ($\alpha 7$ nAChR) and resulted in the activation of NMDA receptors, calcium release, mitochondrial dysfunction, and production of free radicals, leading to apoptotic cell death. They demonstrated that the activation of the caspase family is likely the key step in the apoptotic execution process, as they were able to block apoptotic cell death with caspase inhibitors. Day and Greenfield [49] state that similar conclusions have been drawn for β -amyloid toxicity and suggest that the induction of apoptotic cell death may be a common feature shared by neurotoxic β -sheet peptides.

Further, multiple genomic studies [39,40,46,48,52] have shown significant dysregulation of mitochondrial-associated genes, including several *Bcl-2*-related genes. For example, the study by Damodaran *et al.* [48] revealed overexpression of both anti-apoptotic (*Bcl-X*) and proapoptotic (*Bcl211* and *caspase 6*) genes at 2 h following sarin exposure, indicating complex cell death/protection-related mechanisms soon after exposure.

The approach used by Pachappan and colleagues [52] to investigate the mechanisms of nerve agent toxicity differed from the other transcription profiling studies of nerve agent exposure because they examined gene expression responses in human neuronal cells (SH-SY5Y cells), rather than in brain tissues, following exposure. In their study, they identified 224 genes whose expression was significantly altered by at least threefold following sarin exposure. Similar to the other genomic studies, they identified transcriptional changes related to dose and time of exposure. But unlike the other genomic studies, the authors identified a mitochondrial death pathway regulated by the transcription factor ETS2 as the main neurodegenerative signaling pathway activated in response to sarin. This unique finding is likely due to the use of a single cell type versus whole brain tissue where multiple cell types are represented.

In addition to the scientific data supporting an apoptotic mechanism of neuronal death, Baille *et al.* [25] also provide evidence for a necrotic mechanism of nerve agent-induced cell death within the first 24 h following a convulsant dose of soman and show very few apoptotic cells following the 24-h time period. They attribute the lack of apoptotic cells to a number of factors, including the rapid occurrence of apoptosis (suggesting that they would not see the apoptotic cells due to their elimination within a few hours). Another possibility for the lack of apoptotic cells is that apoptosis is

an energy-dependent process, and since cellular energy is limited during nerve agent-induced excitotoxicity, cells may not have enough energy for apoptosis. The presence of an inflammatory response during nerve agent poisoning (discussed below) also supports a necrotic mechanism of nerve agent-induced cell death because inflammation is considered to be a key contributing factor to necrosis [68]. Therefore, nerve agent toxicity likely involves a form of programmed cell death with both apoptotic and necrotic characteristics.

6.4. Inflammation

Since the development of the model proposed by McDonough and Shih [11], many studies have shown that there is also an increase in proinflammatory cytokine mRNA and protein expression following nerve agent exposure that lasts hours to days later [38–40,46,48,53,69–74]. Further, there has been increasing evidence over the past several years implicating inflammatory reactions in the pathogenesis of several neurodegenerative disorders, such as Alzheimer's disease, Parkinson's disease, multiple sclerosis, and epilepsy [75,76]. Studies using various seizure models have shown an increase in cytokine mRNA and protein expression levels within 30 min following seizure induction in brain regions involved in seizure onset and spread [77–81]. Therefore, it is likely that the late phase of the model involves neuroinflammatory processes that lead to neuropathology following nerve agent exposure.

Spradling and colleagues recently analyzed sarin-induced gene expression changes in the rat amygdala, hippocampus, piriform cortex, septum, and thalamus [39,40], which are areas of the rat brain known to be affected by nerve agent-induced seizure [6,15,23,38]. A multitude of biological functions and canonical pathways were identified as being significantly altered following sarin-induced seizure. Many of the canonical pathways identified as being most significantly affected across all of the brain regions were indicative of an inflammatory response and included many proinflammatory cytokines such as interleukin (IL)-1 β , IL-6, and tumor necrosis factor (TNF)- α . These significantly altered pathways included ataxia telangiectasia-mutated protein (ATM) signaling, CD40 signaling, IL-10 signaling, IL-6 signaling, macrophage migration inhibitory factor (MIF) regulation of innate immunity, role of double-stranded RNA-activated protein kinase (PKR) in interferon induction and antiviral response, toll-like receptor signaling, and triggering receptor expressed on myeloid cells 1 (TREM1) signaling. Further, proinflammatory cytokines were among the top *de novo* networks identified as most significantly affected in all five brain regions from sarin-exposed seizing animals. Two of the top six networks were associated with an inflammatory response. One network of genes was centered on TNF- α as a central node and the other on IL-6 as a central node.

A significant increase in proinflammatory gene expression was seen as early as 15 min following sarin-induced seizure onset, and this inflammatory response was still present at the latest observed time point of 24 h [39,40]. In support of this finding, Damodaran *et al.* [46,48] and Chapman *et al.* [72] also observed an increase in cytokine expression following sarin-induced seizure activity. Damodaran *et al.* [46,48] reported numerous changes in gene expression profiles immediately following sarin exposure with cytokines being among the significantly altered signal transduction pathways. Chapman and colleagues [72] monitored protein expression levels of IL-1 β , IL-6, TNF- α , and prostaglandin E2 (PGE2) in the hippocampus and cortex at 2, 4, 6, 8, 24, 48, and 144 h, as well as 30 days, following sarin-induced seizure. They observed a significant increase in cytokine expression starting at their earliest time point of 2 h and peaking at 2–24 h following sarin.

Further support of a neuroinflammatory response following nerve agent exposure is provided by studies of soman intoxication. Svensson *et al.* [69,71] previously showed increases in IL-1 β mRNA and protein levels following soman exposure. In addition, Dhote *et al.* [73] and Williams *et al.* [70] used quantitative RT-PCR to analyze the neuroinflammatory gene response following a convulsant dose of soman ($1.6 \times \text{LD}_{50}$). Dhote *et al.* [73] showed an increase of IL-1 β , TNF- α , IL-6, intercellular adhesion molecule-1 (ICAM-1), and suppressor of cytokine signaling (SOCS) 3 mRNA in the whole cortex at 0.50, 1, 2, 6, 24, 48, and 168 h following soman exposure, which confirmed the earlier findings of Williams *et al.* [70] where they saw an initial upregulation of TNF- α mRNA at 2 h post-exposure followed by an increase in IL-1 β and IL-6 mRNAs 6 h later. Johnson and Kan [74] have recently quantified the protein levels of these cytokines in vulnerable brain regions following soman-induced seizure onset. They saw a significant increase in IL-1 β , IL-6, and TNF- α protein levels between 10 and 18 h after the peak mRNA expression levels. Dillman *et al.* [53] used oligonucleotide arrays to analyze gene expression profiles of rat hippocampi at 1, 3, 6, 12, 24, 48, 72, 96, and 168 h following exposure to a convulsant dose of soman. In agreement with the transcriptional response to sarin [39,40], they saw an increasing alteration in gene expression profiles over the first 24 h following soman exposure. Within this time frame, they identified a strong inflammatory response with the presence of immunological and inflammatory disease among the top biological processes altered, and the top canonical signaling pathways including p38 MAPK, toll-like receptor, IL-6, and IL-10. Angoa-Pérez and colleagues [19] recently studied the effects of soman on the expression of cyclooxygenase-2 (COX-2), which is the initial enzyme in the biosynthetic pathway of proinflammatory prostaglandins (PGEs) and a factor that has been implicated in seizure initiation and propagation. They found that the induction of COX-2 expression and subsequent production of PGEs correlated with seizure intensity in the rat brain from 4 h to 7 days, suggesting that these molecules could play a

role in neuronal degeneration well after the cholinergic and glutamatergic response. Angoa-Pérez and colleagues hypothesize that seizures occurring in response to a PGE overload would likely not respond to the standard treatment of anticholinergics and benzodiazepines, indicating that other therapeutics, such as COX-2 inhibitors, should be added to prevent or minimize neuropathology that occurs in the later phase of the McDonough and Shih model [11].

Proinflammatory cytokines are known to mediate cellular communication and play a significant role in the pathological processes involved in various brain diseases, such as status epilepticus [75,76,78,81,82]. Although picomolar or low nanomolar ranges of cytokines enhance neuronal survival, higher concentrations have deleterious effects on neuronal viability [83]. Based on the findings of Spradling *et al.* and the findings of other investigators, inflammatory signaling pathways appear to be an important component of nerve agent-induced brain injury; however, the molecular mechanisms by which nerve agent-induced seizures produce acute neuroinflammation or how this phenomenon contributes to the ensuing neuropathology following exposure is still unclear. *In vitro* studies have shown that proinflammatory cytokines play a role in glutamate toxicity since they inhibit glial cells from taking up excess extracellular glutamate [84]. Cytokines are thought to further enhance this glutamatergic hyperactivity by increasing NMDA receptor activity [85], which promotes excitotoxic neuronal cell death [86,87].

6.5. BBB dysfunction

The blood–brain barrier (BBB) maintains the homeostasis of the CNS environment to ensure proper function [88]. Previous studies have shown that sarin [89] and soman [90–93] can cause breakdown of the BBB in sensitive areas such as the thalamus. Therefore, this disruption likely plays an important role in nerve agent-induced cell death in the sensitive brain regions. Further support of these findings was provided by Damodaran and colleagues [46,48], who identified numerous BBB-related genes that were altered at 15 min, 2 h, and 3 months following 0.5 and 1.0 \times LD₅₀ sarin exposure. Their data identified multiple cell adhesion and cytoskeleton-related molecules altered at 15 min following sarin exposure, some of which were related to BBB function (neurexin 1- α ; neurexin 1- β , PSD-95/SAP90-associated protein 4). Alteration in lipophilin mRNA levels at 15 min and 2 h indicated active degradation of CNS myelin. Lipophilin and myelin basic protein have been implicated for efficient axonal signal propagation and provide extrinsic trophic signals that affect the development and long-term survival of axons. The authors also noted the persistence of neurexin 1- β at 3 months, possibly indicating a continued dysfunctional BBB [46].

The mechanism by which nerve agents break down the BBB is still unknown. An increase in BBB permeability typically involves vesicular

transport and/or opening of tight junctions [94]. The findings of Grange-Messent *et al.* [92] indicate that soman-induced seizure increases the number of endothelial vesicles, but their data did not show any structural changes in the endothelial tight junctions, suggesting that tight-junction opening is not an essential mechanism for BBB dysfunction in soman poisoning. However, it should be noted that the authors point out that vascular leakage could occur through very few damaged tight junctions and may not be included in the small tissue sample selected for study. In the microarray study by Damodaran *et al.* [46], the authors attribute nerve agent-induced BBB permeability to the early (15 min) alteration of CAMKII and MAP kinase cascades followed by tyrosine phosphorylation, which was supported by the upregulation of tyrosine kinase receptor EHK-3 at 2 h post-exposure [48]. They speculated that this phosphorylation event might increase tight-junction permeability, which was supported by their observation that sodium-dependent neurotransmitter transporters and ATP-based transporters were also altered. Further, they point to the role of NO, which is a primary mediator of injury-induced BBB disruption. Induction of NOS-2 along with the changes in EDN3 (preproendothelin) expression indicates such a scenario. They speculate that agents involved in regulating vasoactive processes, such as vasoactive intestinal receptor-1 (VIPR1) and 2 (VIPR2), may be involved in the biochemical opening of the BBB, as shown for other vasoactive genes like bradykinin and angiotensin [46].

This scenario opens the door to another possible mechanism in which proinflammatory cytokines could contribute to nerve agent toxicity. The brain is normally isolated from the peripheral immune system via the BBB; however, a neurotoxic insult, such as a convulsant dose of sarin, can induce both a local and peripherally recruited inflammatory response. BBB damage has been seen in many neurodegenerative diseases and animal models of seizure [95], and studies have shown that proinflammatory cytokines including TNF- α , IL-1 β , IL-6, and interferon- λ are implicated in the regulation of BBB permeability [96–98]. For example, IL-1 β can affect the permeability of the BBB via disruption of the tight-junction organization or production of NO and matrix metalloproteinases in endothelial cells [98]. The observed gene response following sarin exposure [39,40] indicates that there could be a breakdown of the BBB as well. This was indicated by the upregulation of ICAM1 and E-selectin in the amygdala, hippocampus, piriform cortex, septum, and thalamus. These molecules are thought to be linked to signal transduction cascades leading to junctional reorganization as they can interact with the actin cytoskeleton, which in turn is an indicator of infiltration of peripheral leukocytes into damaged brain regions through the BBB [96]. There was also a decrease in occludin expression levels, which is one of the main components of tight junctions, indicating a possible loss of tight-junction integrity. The mechanism by which nerve agents cause seizure-related opening of the BBB is still unclear and requires further investigation.

6.6. Repair and recovery

Victims of nerve agent poisoning often suffer long-term neurological deficits accompanied by brain neuronal cell death. Some survivors of the sarin Tokyo subway attack developed long-term chronic neurotoxicity characterized by CNS deficits and neurobehavioral impairments. Animal studies have also demonstrated that exposure to sarin caused brain neuronal cell death [89]. In the longer-term genomic studies of nerve agent exposure by Dillman *et al.* [53] and Damodaran *et al.* [46], it is apparent that nerve agent-induced transcriptional changes are still present weeks to months following exposure.

The data presented by Dillman and colleagues [53] provide insight into the temporal gene response of rat hippocampi following soman exposure. As discussed above, the significant biological processes and canonical pathways appeared to represent an inflammatory response during the first 24 h of the time course, which was also seen in the 24 h time course of sarin toxicity [39,40]. In the middle to late portions of the time course (24–96 h), Dillman and colleagues identified acute phase response pathway, complement system, and coagulation system as being significantly impacted by soman exposure 48–96 h post-exposure. The authors state that these findings are consistent with previous studies reporting the formation of gliotic scarring following soman exposure [99]. Collombet *et al.* [99] identified increases in GFAP and VEGF by immunohistochemistry in the hippocampi of soman-exposed mice during the time period of gliotic scar formation, which corresponded to the observed significant increases in GFAP and VEGF mRNA levels after soman exposure in the microarray study by Dillman *et al.* [53]. At the latest point of the time course (168 h), the significant biological processes and pathways appeared to follow the course of a recovery response, as suggested by biological processes such as RNA damage and repair, connective tissue development and function, and cell-to-cell signaling and interaction, and pathways such as glutamate metabolism, alanine and aspartate metabolism, D-glutamate metabolism, and D-glutamine metabolism. The authors used principal component analysis (PCA) to identify sources of relative variability among the hippocampal gene expression profiles (Figure 3). From their analysis, they identified exposure conditions (i.e., naive, vehicle-exposed, or soman-exposed) and post-exposure time point as the primary sources of variability in the dataset. The PCA in Figure 3 shows that sample groups for the 1, 3, 6, and 12-h time points partition progressively further away from the control sample group, while the 24, 72, 96, and 168-h sample groups partition progressively closer to the controls. Although these data suggest that gene expression profiles are returning to control levels, the three-dimensional plot indicates that none of the late time point groups partition with the control sample group, indicating altered gene expression at 168 h after soman exposure. Due to the similarities during the first 24 h of sarin [39,40] and soman [53] intoxication, we would anticipate a similar shift

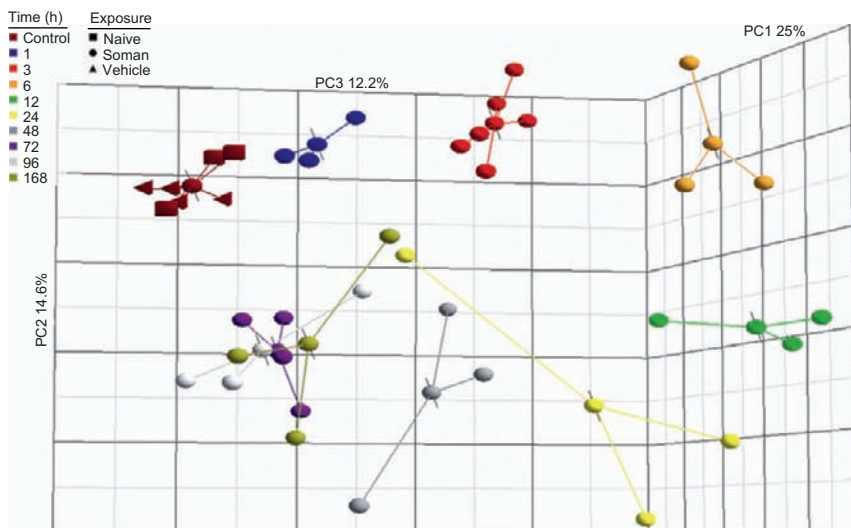


Figure 3 Principal component analysis (PCA) of hippocampal gene expression profiles from soman-exposed rats identifies exposure conditions and post-exposure time point as primary sources of relative variability in the dataset. Hippocampal tissues were isolated at the indicated time points following soman exposure and processed for oligonucleotide microarray analysis. The raw signal intensities were normalized using robust multiarray averaging (RMA) algorithm and visualized using PCA to identify major sources of variability in the data. Each point on the three-dimensional graph represents the gene expression profile of an individual biological sample. The distance between any two points is a function of the relative similarity between the two samples. Sample points that are near each other on the plot have a relatively similar gene expression profile, while sample points that are far apart are relatively different in a large number of variables. Point shape corresponds to exposure condition, and point color corresponds to the post-exposure time point. The centroid of each time point group is shown as a sphere with an angled black line through its center. Each centroid is connected by vectors to each of the sample points in its corresponding time point group. Naive controls were unexposed, and vehicle controls received all treatments except soman. The principal components in the three-dimensional graph represent the variability in gene expression levels seen within the dataset. The PCA plot rendered 51.8% of the total information content. Principal component 1 (PC1, *x*-axis) accounts for 25% of the variability in the data; PC2 (*y*-axis) represents 14.6% of the variability; and PC3 (*z*-axis) represents 12.2% of the variability in gene expression levels seen within the dataset. Reprinted from Ref. 53. Published 2009 American Chemical Society [53].

in gene expression involving molecular processes and pathways involved in an injury and recovery phase following sarin exposure. However, further studies analyzing gene expression profiles over a 168-h time period are needed to confirm this same mechanism of action following sarin-induced seizure.

The study by Damodaran *et al.* [46] detailed multiple gene alterations present at 3 months following sarin exposure. They noted the presence of

ACCN1, SCN9A, ATPases, and ATP-based transporters, indicating that sarin-induced electrophysiological changes initiated early were minimized but did not completely return to normal. Genes classified as cytoskeletal and cell adhesion molecules were among the most significantly altered genes at 3 months after sarin exposure. β -Arrestin and neurexin1- β both maintained their altered state at 3 months. The authors state that the continued down-regulation of neurexin clearly supports the idea that BBB-related perturbations still persist at 3 months posttreatment, while persistent upregulation of β -arrestin confirms the continued aberrant signaling pathways mediated by G-protein-coupled receptors, which was evidenced by the continued over-expression of several classes of G-protein-coupled receptors (CAMKI and II, M2-AChR, GALR1, and CRLR). The authors speculate that the persistence of sarin-induced hyperphosphorylation causes defects in the tissue repair process. Therefore, long-term changes in certain molecules indicate that they likely play important roles in preserving, amplifying, and transmitting altered gene expression until a later time point, which could be either degenerative or regenerative in nature.



7. FUTURE DIRECTIONS IN THE MOLECULAR TOXICOLOGY OF NERVE AGENTS

The biological pathways and molecular mechanisms underlying nerve agent toxicity are still poorly understood. To help determine the molecular mechanisms of nerve agent toxicity, scientists have recently begun using “omics” technologies to assess the toxicological effects and physiological mechanisms of OP nerve agents. In a recent review [31], Everley and Dillman discuss how genomic and proteomic technologies have been used in over 50,000 research studies since the 1990s to help determine various biological processes, but there have been very few systems biology-related studies focusing on chemical warfare agents, especially OP nerve agents. In fact, there have been no large-scale proteomic studies of OP nerve agents. Previous, smaller-scale studies have shown that OP nerve agent exposure leads to the activation of many downstream proteins involved in numerous cellular signaling pathways regulated by protein phosphorylation [74,100]; however, additional studies need to be performed to investigate large-scale protein changes after nerve agent exposure. Also, in the study by Fauvelle *et al.* [18], the largest metabolomic study of nerve agent exposure to date, proton high-resolution magic angle spinning nuclear magnetic resonance spectroscopy (^1H HRMAS NMR) was used to describe the complex metabolic changes occurring in the piriform cortex and cerebellum of soman-exposed mice over a 7-day period. Using this global approach, the authors analyzed individual variation in the concentration of 13 metabolites.

As this technology matures, there should be a growing number of metabolic studies involving nerve agents. These studies will provide valuable information regarding the molecular mechanisms of nerve agent toxicity leading to cell/tissue damage and long-term neurobehavioral deficits.

The typical methodology for studying nerve agents involves the use of animal models. This approach requires specialized facilities and support staff and can be expensive and time-consuming for large studies. Another approach would involve the use of an *in vitro* model system coupled with global molecular techniques to establish a high-throughput screening method to rapidly assess the molecular targets and toxicological mechanisms of any nerve agent. Although this approach was recently used by Pachiappan *et al.* [52], it should be noted that their study was performed using a neuroblastoma cell line (SH-SY5Y), which may not truly represent *in vivo* mechanisms. Dissociated primary nerve cell cultures, however, may more closely resemble *in vivo* biology than immortalized neuronal cells. This model system is well established in the field of neuroscience [101–104] and has previously been used to evaluate neurotoxicant effects [103]. A major concern of using an *in vitro* system involves the lack of important functional features, such as the BBB, heterogeneous cell–cell interactions, and seizure propagation that faithfully mimics what is observed *in vivo*. However, *in vitro* systems may offer some advantages for neurotoxicity assessment over *in vivo* models, including the ability to study the molecular effects of toxicants in pure populations of specific cell types. This capability not only highlights the vulnerability of a particular cell type (e.g., neurons or glial cells) but also prevents significant changes in one cell type from being “diluted out” or masked by the changes seen in a complex mixture of cells, such as in whole tissue. Moreover, the use of an *in vitro* model system would easily allow the application of other molecular technologies that are not currently feasible in *in vivo* systems. For example, RNA interference (RNAi), a method of posttranscriptional gene silencing, has rapidly become the high-throughput system of choice in the biotechnology industry for mechanistically assessing gene function on a global scale [104]. This technique paired with microarray analysis for genome-wide expression profiling has proved to be effective in identifying and validating molecular mechanisms [105].

8. CONCLUSIONS

The development of global molecular technologies has enabled scientists to look at the complete complement, expression, and regulation of genes, proteins, and metabolites involved in the response to various toxicants [27]. These techniques coupled with pathway modeling provide a powerful approach in the development of neuroprotectants against nerve

agent exposure since they identify potential biomarkers of exposure and targets for therapeutic intervention. Because current countermeasures may not fully prevent neurological damage, particularly in scenarios where treatment is delayed (e.g., civilian terrorist attack), this type of in-depth analysis is critical to examine the molecular effects following nerve agent exposure and to identify therapeutics that can reduce or block the cascade of secondary events that lead to neuropathology and associated functional impairments.

A large amount of data obtained from scientific studies utilizing global molecular techniques support the temporal model proposed by McDonough and Shih [11] as well as provide further evidence for the presence of non-cholinergic and non-glutamatergic systems during the late phase response to nerve agent poisoning (Figure 4), which was first suggested from studies using AChE knockout mice [106]. These studies showed that acute nerve agent exposure alters the expression of multiple genes and pathways at an early time point (0.25–2 h) following exposure, suggesting concurrent activation of protective mechanisms as well as neurodegenerative changes [39,40,46,48,53]. These data also suggest that the persistence and magnitude of early gene expression changes predict long-term pathological developments [46].

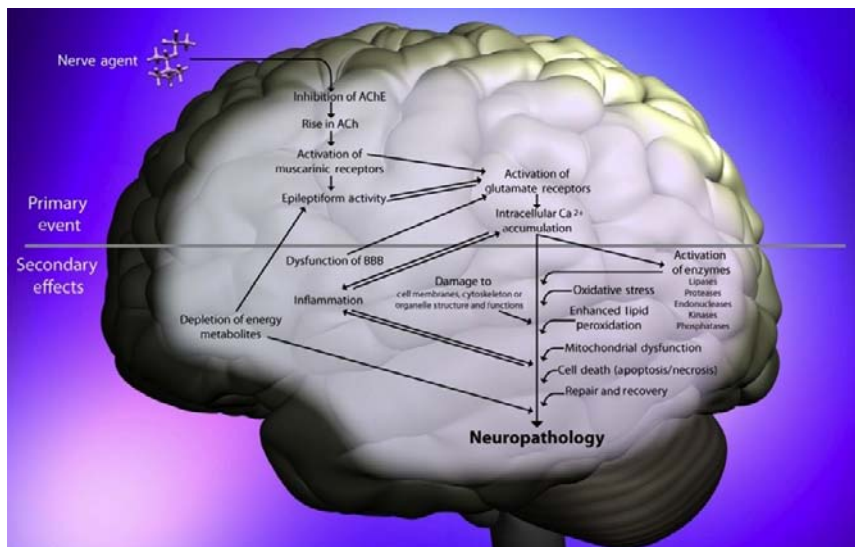


Figure 4 Overview of the neurotransmitter and nonneurotransmitter systems that are impacted by nerve agent intoxication. Data from a variety of sources, as described in the text, suggest cholinergic and non-cholinergic mechanisms involved in downstream sequelae after nerve agent exposure, leading to neuropathology. Illustration by Alexandre Katos.

Mitochondria are proposed to play a significant role in seizure generation in certain forms of epilepsy, and multiple genomic studies [39,40,46,48,52] have shown significant dysregulation of mitochondrial-associated genes, including several BCL-2-related genes, following nerve agent exposure. Therefore, these mitochondrial genes should be considered as promising targets for future therapeutic strategies to treat nerve agent poisoning. Also, the rapid and persistent alteration of proinflammatory cytokines seen in these studies strongly suggests that they may play a causal role in long-term pathological changes following exposure to OP nerve agents. Therefore, antagonism of proinflammatory molecules, as well as their receptors and signaling pathways, may represent a novel approach for the development of drug therapies that would reduce neurological damage when given after the onset of seizures and secondary responses that lead to brain injury.

Data obtained from these global molecular assays have increased our understanding of the molecular response to nerve agent exposure during the acute toxic response as well as during the neurodegenerative and recovery processes [53]. The findings of Dillman *et al.* [53] show a gradual but incomplete return to control gene expression profiles at 168 h following soman exposure, but the extent of recovery at the molecular level over a longer time-frame (weeks or months) is uncertain. Even though the gene expression levels appear to be returning to normal after exposure, cell death and/or neuronal rewiring that occurred during upregulation may be irreversible [46,53].

Gene expression profiling has provided insight into the mechanisms of nerve agent-induced brain injury by identifying the initial molecular responses as well as secondary responses to nerve agent poisoning. However, determining the exact sequence of events is difficult due to the temporal overlap of many of the identified processes and pathways. The use of global profiling techniques will further accelerate our understanding of nerve agent toxicity and help determine the mechanisms of toxicity. Large-scale proteomic and metabolomic studies using nerve agents have been lacking. Just as microarrays have been used to map signaling networks for sarin and soman, these techniques could also complement and expand on that work to identify additional signaling pathways impacting nerve agent toxicity [31]. Further, these “omic” techniques could be applied to other nerve agents (such as tabun and VX) to determine if these agents have molecular effects similar to those of sarin and soman. The use of global molecular profiling techniques, such as genomics, proteomics, and metabolomics, will further accelerate our understanding of the molecular mechanisms involved in nerve agent-induced toxicity and identify therapeutics that can reduce or block the cascade of secondary events that lead to neuropathology and associated functional impairments.

ACKNOWLEDGMENTS

We thank Mr. Alexandre Katos for assistance with Figure 1 and graphic design of Figures 2 and 4; and Drs. Albert Ruff, John McDonough, and Tsung-ming Shih for critical reading of the chapter. Dr. Spradling was supported by the CounterACT Program, National Institutes of Health Office of the Director and the National Institute of Allergy and Infectious Diseases (OD# Y1-OD-9613-01; Dr. Tsung-Ming Shih, PI). Dr. Dillman was supported by the CounterACT Program, National Institutes of Health Office of the Director and the National Institute of Allergy and Infectious Diseases (OD# Y1-OD-9613-01; Dr. Tsung-Ming Shih, PI) and the Defense Threat Reduction Agency-Joint Science and Technology Office, Medical S&T Division.

Disclaimer: The opinions or assertions contained herein are the private views of the authors and are not to be construed as official or as reflecting the views of the Department of the Army or the Department of Defense.

REFERENCES

- [1] H. Salem, A.L. Ternay Jr., J.K. Smart, Brief history and use of chemical warfare agents in warfare and terrorism, in: J.A. Romano Jr., B.J. Lukey, H. Salem (Eds.), *Chemical Warfare Agents: Chemistry, Pharmacology, Toxicology, and Therapeutics*, CRC Press-Taylor & Francis Group, LLC, Boca Raton, FL, 2008, pp. 1–20.
- [2] M.A. Brown, K.A. Brix, Review of health consequences from high-, intermediate and low-level exposure to organophosphorus nerve agents, *J. Appl. Toxicol.* 18 (1998) 393–408.
- [3] F. Schmaltz, Neurosciences and research on chemical weapons of mass destruction in Nazi Germany, *J. Hist. Neurosci.* 15 (2006) 186–209.
- [4] A. Hoffman, A. Eisenkraft, A. Finkelstein, O. Schein, E. Rotman, T. Dushnitsky, A decade after the Tokyo sarin attack: A review of neurological follow-up of the victims, *Mil. Med.* 172 (2007) 607–610.
- [5] Y. Loh, M.M. Swanberg, M.V. Ingram, J. Newmark, Case report: long-term cognitive sequelae of sarin exposure, *Neurotoxicology* 31 (2010) 244–246.
- [6] V. Aroniadou-Anderjaska, T.H. Figueiredo, J.P. Aplan, F. Qashu, M.F.M. Braga, Primary brain targets of nerve agents: The role of the amygdala in comparison to the hippocampus, *Neurotoxicology* 30 (2009) 772–776.
- [7] N.B. Munro, K.R. Ambrose, A.P. Watson, Toxicity of the organophosphate chemical warfare agents GA, GB, and VX: Implications for public protection, *Environ. Health Perspect.* 102 (1994) 18–38.
- [8] T. Martin, S. Lobert, Chemical warfare: Toxicity of nerve agents, *Crit. Care Nurse* 23 (2003) 15–20.
- [9] F. Worek, L. Szinicz, P. Eyer, H. Thiermann, Evaluation of oxime efficacy in nerve agent poisoning: Development of a kinetic-based dynamic model, *Toxicol. Appl. Pharmacol.* 209 (2005) 193–202.
- [10] M.A. Dunn, B.E. Hackley, F.R. Sidell, Pretreatment for nerve agent exposure, in: F.R. Sidell, E.T. Takafuji, D.R. Franz (Eds.), *Textbook of Military Medicine: Medical Aspects of Chemical and Biological Warfare*, Borden Institute, Walter Reed Army Medical Center, Washington, DC, 1997, pp. 181–196.
- [11] J.H. McDonough Jr., T.M. Shih, Neuropharmacological mechanisms of nerve agent-induced seizure and neuropathology, *Neurosci. Biobehav. Rev.* 21 (1997) 559–579.
- [12] J. Bajgar, Complex view on poisoning with nerve agents and organophosphates, *Acta Med. (Hradec Králové)* 48 (2005) 3–21.

- [13] M. Filbert, E. Levine, G. Ballough, Neuroprotection for nerve agent-induced brain damage by blocking delayed calcium overload: A review, *J. Med. Chem. Biol. Radiol. Def.* 3 (2005) 1–21.
- [14] T. Myhrer, S. Enger, P. Aas, Efficacy of immediate and subsequent therapies against soman-induced seizures and lethality in rats, *Basic Clin. Pharmacol.* 98 (2006) 184–191.
- [15] T. Myhrer, Neuronal structures involved in the induction and propagation of seizures caused by nerve agents: Implications for medical treatment, *Toxicology* 239 (2007) 1–14.
- [16] J.H. McDonough Jr., T.M. Shih, Pharmacological modulation of soman-induced seizures, *Neurosci. Biobehav. Rev.* 17 (1993) 203–215.
- [17] P. Carpentier, A. Foquin Tarricone, N. Bodjarian, G. Rondouin, M. Lerner Natoli, J.M. Kamenka, G. Blanchet, M. Denoyer, G. Lallement, Anticonvulsant and antilethal effects of the phencyclidine derivative TCP in soman poisoning, *Neurotoxicology* 15 (1994) 837–852.
- [18] F. Fauvelle, F. Dorandeu, P. Carpentier, A. Foquin, H. Rabeson, D. Graveron-Demilly, P. Arvers, G. Testylier, Changes in mouse brain metabolism following a convulsive dose of soman: A proton HRMAS NMR study, *Toxicology* 267 (2010) 99–111.
- [19] M. Angoa-Pérez, C.W. Kreipke, D.M. Thomas, K.E. Van Shura, M. Lyman, J.H. McDonough, D.M. Kuhn, Soman increases neuronal COX-2 levels: Possible link between seizures and protracted neuronal damage, *Neurotoxicology* 31 (2010) 738–746.
- [20] J. Bajgar, L. Ševelová, G. Krejčová, J. Fusek, J. Vachek, J. Kassa, J. Herink, Biochemical and behavioral effects of soman vapors in low concentrations, *Inhal. Toxicol.* 16 (2004) 497–507.
- [21] T. Myhrer, S. Enger, P. Aas, Anticonvulsant effects of damage to structures involved in seizure induction in rats exposed to soman, *Neurotoxicology* 28 (2007) 819–828.
- [22] M.J.A. Joosen, E. Jousma, T.M. van den Boom, W.C. Kuijpers, A.B. Smit, P.J. Lucassen, H.P.M. van Helden, Long-term cognitive deficits accompanied by reduced neurogenesis after soman poisoning, *Neurotoxicology* 30 (2009) 72–80.
- [23] J.H. McDonough Jr., L.W. Dochterman, C.D. Smith, T.M. Shih, Protection against nerve agent induced neuropathology, but not cardiac pathology, is associated with the anti-convulsant action of drug treatment, *Neurotoxicology* 15 (1995) 123–132.
- [24] T.M. Shih, S.M. Duniho, J.H. McDonough Jr., Control of nerve agent-induced seizures is critical for neuroprotection and survival, *Toxicol. Appl. Pharmacol.* 188 (2003) 69–80.
- [25] V. Baille, P.G.H. Clarke, G. Brochier, F. Dorandeu, J.M. Verna, E. Four, G. Lallement, P. Carpentier, Soman-induced convulsions: The neuropathology revisited, *Toxicology* 15 (2005) 1–24.
- [26] O.U. Scremin, T.M. Shih, L. Huynh, M. Roch, R. Booth, D.J. Jenden, Delayed neurologic and behavioral effects of subtoxic doses of cholinesterase inhibitors, *J. Pharmacol. Exp. Ther.* 304 (2003) 1111–1119.
- [27] J. Vlaanderen, L.E. Moore, M.T. Smith, Q. Lan, L. Zhang, C.F. Skibola, N. Rothman, R. Vermeulen, Application of omics technologies in occupational and environmental health research; current status and projection, *Occup. Environ. Med.* 67 (2010) 136–143.
- [28] M. Schena, D. Shalon, R.W. Davis, P.O. Brown, Quantitative monitoring of gene expression patterns with complementary DNA microarray, *Science* 270 (1995) 467–470.
- [29] C.A. Afshari, Perspective: Microarray technology, seeing more than spots, *Endocrinology* 143 (2002) 1983–1989.

- [30] J.F. Hocquette, I. Cassar-Malek, A. Scalbert, F. Guillou, Contribution of genomics to the understanding of physiological functions, *J. Physiol. Pharmacol.* 60 (Suppl. 3) (2009) 5–16.
- [31] P.A. Everley, J.F. Dillman III, Genomics and proteomics in chemical warfare agent research: Recent studies and future applications, *Toxicol. Lett.* 198 (2010) 297–303.
- [32] K. Aggarwal, L.H. Choe, K.H. Lee, Shotgun proteomics using the iTRAQ isobaric tags, *Brief. Funct. Genomic Proteomic* 5 (2006) 112–120.
- [33] T. Liu, J. Hu, H. Li, iTRAQ-based shotgun neuroproteomics, *Methods Mol. Biol.* 566 (2009) 201–216.
- [34] J.V. Olsen, B. Blagoev, F. Gnäd, B. Macek, C. Kumar, P. Mortensen, M. Mann, Global, in vivo, and site-specific phosphorylation dynamics in signaling networks, *Cell* 127 (2006) 635–648.
- [35] D.A. Hall, J. Ptacek, M. Snyder, Protein microarray technology, *Mech. Ageing Dev.* 128 (2007) 161–167.
- [36] J.C. Lindon, E. Holmes, J.K. Nicholson, Metabonomics techniques and applications to pharmaceutical research and development, *Pharm. Res.* 23 (2006) 1075–1088.
- [37] J.F. Dillman III, A.I. Hege, C.S. Phillips, L.D. Orzolek, A.J. Sylvester, C. Bossone, C. Henemyre-Harris, R.C. Kiser, Y.W. Choi, J.J. Schlager, C.L. Sabourin, Microarray analysis of mouse ear tissue exposed to bis-(2-chloroethyl) sulfide: Gene expression profiles correlate with treatment efficacy and an established clinical endpoint, *J. Pharmacol. Exp. Ther.* 317 (2006) 76–87.
- [38] L.A. Zimmer, M. Ennis, M.T. Shipley, Soman-induced seizures rapidly activate astrocytes and microglia in discrete brain regions, *J. Comp. Neurol.* 378 (1997) 482–492.
- [39] K.D. Spradling, L.A. Lumley, C.L. Robison, J.L. Meyerhoff, J.F. Dillman, III, Genomic analysis of piriform cortex following exposure to the organophosphonate anticholinesterase sarin reveals gene expression profile differences correlated with seizure induction, submitted for publication (copy on file with author).
- [40] K.D. Spradling, L.A. Lumley, C.L. Robison, J.L. Meyerhoff, J.F. Dillman, III, Transcriptional response of the nerve agent-sensitive regions amygdala, hippocampus, piriform cortex, septum, and thalamus to the anticholinesterase sarin, submitted for publication (copy on file with author).
- [41] T.M. Shih, Time course effects of soman on acetylcholine and choline levels in six discrete areas of the rat brain, *Psychopharmacology (Berlin)* 78 (1982) 170–175.
- [42] G. Lallement, P. Carpentier, A. Collet, D. Baubichon, I. Pernot Marino, G. Blanchet, Extracellular acetylcholine changes in rat limbic structures during soman-induced seizure, *Neurotoxicology* 13 (1992) 557–568.
- [43] G. Lallement, P. Carpentier, A. Collet, I. Pernot Marino, D. Baubichon, G. Blanchet, Effects of soman-induced seizures on different extracellular amino acid levels and on glutamate uptake in rat hippocampus, *Brain Res.* 563 (1991) 234–240.
- [44] C.J. Flynn, L. Wecker, Elevated choline levels in brain: A non-cholinergic component of organophosphate toxicity, *Biochem. Pharmacol.* 35 (1986) 3115–3121.
- [45] M.J. Berridge, Unlocking the secrets of cell signaling, *Annu. Rev. Physiol.* 67 (2005) 1–21.
- [46] T.V. Damodaran, A.G. Patel, S.T. Greenfield, H.K. Dressman, S.M. Lin, M.B. Abou-Donia, Gene expression profiles of the rat brain both immediately and 3 months following acute sarin exposure, *Biochem. Pharmacol.* 71 (2006) 497–520.
- [47] D. Weinshenker, P. Szot, The role of catecholamines in seizure susceptibility: New results using genetically engineered mice, *Pharmacol. Therapeut.* 94 (2002) 213–233.
- [48] T.V. Damodaran, S.T. Greenfield, A.G. Patel, H.K. Dressman, S.K. Lin, M. B. Abou-Donia, Toxicogenomic studies of the rat brain at an early time point following acute sarin exposure, *Neurochem. Res.* 31 (2006) 367–381.

- [49] T. Day, S.A. Greenfield, A peptide derived from acetylcholinesterase induces neuronal cell death: Characterisation of possible mechanisms, *Exp. Brain Res.* 153 (2003) 334–342.
- [50] C. Cerella, M. Diederich, L. Ghibelli, The dual role of calcium as messenger and stressor in cell damage, death, and survival, *Int. J. Cell Biol.* 2010 (2010) 1–14.
- [51] J.L. Blanton, J.A. D'Ambrozio, J.E. Sistrunk, E.G. Midboe, Global changes in the expression patterns of RNA isolated from the hippocampus and cortex of VX exposed mice, *J. Biochem. Mol. Toxicol.* 18 (2004) 115–123.
- [52] A. Pachiappan, M.M. Thwin, L. Weng Keong, F.K. Lee, J. Manikandan, V. Sivakumar, P. Gopalakrishnakone, ETS2 regulating neurodegenerative signaling pathway of human neuronal (SH-SY5Y) cells exposed to single and repeated low-dose sarin (GB), *Chem. Res. Toxicol.* 22 (2009) 990–996.
- [53] J.F. Dillman III, C.S. Phillips, D.M. Kniffin, C.P. Tompkins, T.A. Hamilton, R.K. Kan, Gene expression profiling of rat hippocampus following exposure to the acetylcholinesterase inhibitor soman, *Chem. Res. Toxicol.* 22 (2009) 633–638.
- [54] T.L. Pazdernik, M.R. Emerson, R. Cross, S.R. Nelson, F.E. Samson, Soman-induced seizures: Limbic activity, oxidative stress and neuroprotective proteins, *J. Appl. Toxicol.* 21 (2001) S87–S94.
- [55] A.W. Abu-Qare, M.B. Abou-Donia, Combined exposure to sarin and pyridostigmine bromide increased levels of rat urinary 3-nitrotyrosine and 8-hydroxy-2'-deoxyguanosine, biomarkers of oxidative stress, *Toxicol. Lett.* 123 (2001) 51–58.
- [56] M.B. Abou-Donia, A.M. Dechkovskaia, L.B. Goldstein, S.L. Bullman, W.A. Khan, Sensorimotor deficit and cholinergic changes following coexposure with pyridostigmine bromide and sarin in rats, *Toxicol. Sci.* 66 (2002) 148–158.
- [57] M.J. Barrett, V. Alones, K.X. Wang, L. Phan, R.H. Swerdlow, Mitochondria-derived oxidative stress induces a heat shock protein response, *J. Neurosci. Res.* 78 (2004) 420–429.
- [58] B. Kalmar, L. Greensmith, Induction of heat shock proteins for protection against oxidative stress, *Adv. Drug Deliv. Rev.* 61 (2009) 310–318.
- [59] V. Baille-Le Crom, J.M. Collombet, M.F. Burckhart, A. Foquin, I. Pernot-Marino, G. Rondouin, G. Lallement, Time course and regional expression of C-FOS and HSP70 in hippocampus and piriform cortex following soman-induced seizures, *J. Neurosci. Res.* 45 (1996) 513–524.
- [60] G. Zsurka, W.S. Kunz, Mitochondrial dysfunction in neurological disorders with epileptic phenotypes, *J. Bioenerg. Biomembr.* 42(6) (2010) 443–448.
- [61] A.P. Kudin, D. Malinska, W.S. Kunz, Sites of generation of reactive oxygen species in homogenates of brain tissue determined with the use of respiratory substrates and inhibitors, *Biochim. Biophys. Acta* 1777 (2008) 689–695.
- [62] D. Malinska, B. Kulawiak, A.P. Kudin, R. Kovacs, C. Huchzermeyer, O. Kann, A. Szewczyk, W.S. Kunz, Complex III-dependent superoxide production of brain mitochondria contributes to seizure-related ROS formation, *Biochim. Biophys. Acta* 1797 (2010) 1163–1170.
- [63] A.P. Kudin, N.Y.B. Bimpong-Buta, S. Vielhaber, C.E. Elger, W.S. Kunz, Characterization of superoxide-producing sites in isolated brain mitochondria, *J. Biol. Chem.* 279 (2004) 4127–4135.
- [64] A.P. Kudin, T.A. Kudina, J. Seyfried, S. Vielhaber, H. Beck, C.E. Elger, W.S. Kunz, Seizure-dependent modulation of mitochondrial oxidative phosphorylation in rat hippocampus, *Eur. J. Neurosci.* 15 (2002) 1105–1114.
- [65] R.C. Jovic, Correlation between signs of toxicity and some biochemical changes in rats poisoned by soman, *Eur. J. Pharmacol.* 25 (1974) 159–164.
- [66] T.L. Pazdernik, R.S. Cross, M. Giesler, F.E. Samson, S.R. Nelson, Changes in local cerebral glucose utilization induced by convulsants, *Neuroscience* 14 (1985) 823–835.

- [67] R.C. Gupta, D. Milatovic, W.D. Dettbarn, Depletion of energy metabolites following acetylcholinesterase inhibitor-induced status epilepticus: Protection by antioxidants, *Neurotoxicology* 22 (2001) 271–282.
- [68] P.G.H. Clarke, Apoptosis versus necrosis—how valid a dichotomy for neurons? in: V.E. Koliatsos, R.R. Ratan (Eds.), *Cell Death and Diseases of the Nervous System*, Humana Press, Inc., Totowa, NJ, 1999, pp. 3–28.
- [69] I. Svensson, L. Waara, L. Johansson, A. Bucht, G. Cassel, Soman-induced interleukin-1 β mRNA and protein in rat brain, *Neurotoxicology* 22 (2001) 355–362.
- [70] A.J. Williams, R. Berti, C. Yao, R.A. Price, L.C. Velarde, I. Koplovitz, S.M. Schultz, F.C. Tortella, J.R. Dave, Central neuro-inflammatory gene response following soman exposure in the rat, *Neurosci. Lett.* 349 (2003) 147–150.
- [71] I. Svensson, L. Waara, G. Cassel, Effects of HI 6, diazepam and atropine on soman-induced IL-1 β protein in rat brain, *Neurotoxicology* 26 (2005) 173–181.
- [72] S. Chapman, T. Kadar, E. Gilat, Seizure duration following sarin exposure affects neuro-inflammatory markers in the rat brain, *Neurotoxicology* 27 (2006) 277–283.
- [73] F. Dhote, A. Peinnequin, P. Carpentier, V. Baille, C. Delacour, A. Foquin, G. Lallement, F. Dorandeu, Prolonged inflammatory gene response following soman-induced seizures in mice, *Toxicology* 238 (2007) 166–176.
- [74] E.A. Johnson, R.K. Kan, The acute phase response and soman-induced status epilepticus: Temporal and regional changes in rat brain cytokine concentrations, *J. Neuroinflamm.* 7 (2010) 1–9.
- [75] A. Vezzani, Inflammation and epilepsy, *Epilepsy Curr.* 5 (2005) 1–6.
- [76] J. Choi, S. Koh, Role of brain inflammation in epileptogenesis, *Yonsei Med. J.* 49 (2008) 1–18.
- [77] M. Minami, Y. Kuraishi, M. Satoh, Effects of kainic acid on messenger RNA levels of IL-1 beta, IL-6, TNF alpha and LIF in the rat brain, *Biochem. Biophys. Res. Commun.* 176 (1991) 593–598.
- [78] M.G. De Simoni, C. Perego, T. Ravizza, D. Moneta, M. Conti, F. Marchesi, A. De Luigi, S. Garattini, A. Vezzani, Inflammatory cytokines and related genes are induced in the rat hippocampus by limbic status epilepticus, *Eur. J. Neurosci.* 12 (2000) 2623–2633.
- [79] K.A. Lehtimäki, J. Peltola, E. Koskikallio, T. Keränen, J. Honkaniemi, Expression of cytokines and cytokine receptors in the rat brain after kainic acid-induced seizures, *Mol. Brain Res.* 110 (2003) 253–260.
- [80] M. Oprica, C. Riksson, M. Schultzberg, Inflammatory mechanisms associated with brain damage induced by kainic acid with special reference to the interleukin-1 system, *J. Cell. Mol. Med.* 7 (2003) 127–140.
- [81] B. Voutsinos-Porche, E. Koning, H. Kaplan, A. Ferrandon, M. Guenounou, A. Nehlig, J. Motte, Temporal patterns of the cerebral inflammatory response in the rat lithium-pilocarpine model of temporal lobe epilepsy, *Neurobiol. Dis.* 17 (2004) 385–402.
- [82] B. Viviani, S. Bartsaghi, E. Corsini, C.L. Galli, M. Marinovich, Cytokines role in neurodegenerative events, *Toxicol. Lett.* 149 (2004) 85–89.
- [83] M.C. Morganti-Kossmann, T. Kossmann, S.M. Wahl, Cytokines and neuropathology, *Trends Pharmacol. Sci.* 13 (1992) 286–291.
- [84] Z.C. Ye, H. Sontheimer, Cytokine modulation of glial glutamate uptake: A possible involvement of nitric oxide, *Neuroreport* 7 (1996) 2181–2185.
- [85] B. Viviani, S. Bartsaghi, F. Gardoni, A. Vezzani, M.M. Behrens, T. Bartfai, M. Binaglia, E. Corsini, M. Di Luca, C.L. Galli, M. Marinovich, Interleukin-1 β enhances NMDA receptor-mediated intracellular calcium increase through activation of the Src family of kinases, *J. Neurosci.* 23 (2003) 8692–8700.

- [86] T. Ravizza, S.M. Lucas, S. Balosso, L. Bernardino, G. Ku, F. Noé, J. Malva, J.C.R. Randle, S. Allan, A. Vezzani, Inactivation of caspase-1 in rodent brain: A novel anticonvulsive strategy, *Epilepsia* 47 (2006) 1160–1168.
- [87] T. Ravizza, B. Gagliardi, F. Noé, K. Boer, E. Aronica, A. Vezzani, Innate and adaptive immunity during epileptogenesis and spontaneous seizures: Evidence from experimental models and human temporal lobe epilepsy, *Neurobiol. Dis.* 29 (2008) 142–160.
- [88] F. Joo, Endothelial cells of the brain and other organ systems: Some similarities and differences, *Prog. Neurobiol.* 48 (1996) 255–273.
- [89] A. Abdel-Rahman, A.K. Shetty, M.B. Abou-Donia, Acute exposure to sarin increases blood brain barrier permeability and induces neuropathological changes in the rat brain: Dose-response relationships, *Neuroscience* 113 (2002) 721–741.
- [90] Y. Ashani, G.N. Catravas, Seizure-induced changes in the permeability of the blood-brain barrier following administration of anticholinesterase drugs to rat, *Biochem. Pharmacol.* 30 (1981) 2593–2601.
- [91] P. Carpentier, I.S. Delamanche, M. Le Bert, G. Blanchet, C. Bouchaud, Seizure-related opening of the blood-brain barrier induced by soman: Possible correlation with the acute neuropathology observed in poisoned rats, *Neurotoxicology* 541 (1990) 293–299.
- [92] V. Grange-Messent, C. Bouchaud, M. Jamme, G. Lallement, A. Foquin, P. Carpentier, Seizure-related opening of the blood-brain barrier produced by the anticholinesterase compound, soman: New ultrastructural observations, *Cell. Mol. Biol.* 45 (1999) 1–14.
- [93] J.P. Petrali, D.M. Maxwell, D.E. Lenz, K.R. Mills, A study of the effects of soman on rat blood-brain barrier, *Anat. Rec.* 211 (1991) 351–352.
- [94] G.E. Palade, Blood capillaries of the heart and other organs, *Circulation* 24 (1961) 368–384.
- [95] P.M. Carvey, B. Hendey, A.J. Monahan, The blood-brain barrier in neurodegenerative disease: A rhetorical perspective, *J. Neurochem.* 111 (2009) 291–314.
- [96] S.J. Bolton, D.C. Anthony, V.H. Perry, Loss of the tight junction proteins occludin and zonula occludens-1 from cerebral vascular endothelium during neutrophil-induced blood-brain barrier breakdown in vivo, *Neuroscience* 86 (1998) 1245–1257.
- [97] W.G. Mayhan, Cellular mechanisms by which tumor necrosis factor- α produces disruption of the blood-brain barrier, *Brain Res.* 927 (2002) 144–152.
- [98] S.M. Allan, P.J. Tyrrell, N.J. Rothwell, Interleukin-1 and neuronal injury, *Nat. Rev.* 5 (2005) 629–640.
- [99] J.M. Collombet, E. Four, W. Fauquette, M.F. Burckhart, C. Masqueliez, D. Bernabé, D. Baubichon, G. Lallement, Soman poisoning induces delayed astroglial scar and angiogenesis in damaged mouse brain areas, *Neurotoxicology* 28 (2007) 38–48.
- [100] L.N. Bottalico, G.D. Minsavage, J.F. Dillman, III, Proteomic analysis of rat hippocampus following soman exposure. Society of Toxicology Annual Meeting, March 16–20, 2008, Seattle, WA, Abst 153.
- [101] P.G. Nelson, Neuronal cell cultures as toxicologic test systems, *Environ. Health Perspect.* 26 (1978) 125–133.
- [102] C.A. Tyson, N.H. Stacey, In vitro technology, trends, and issues, in: J.M. Frazier (Ed.), *In Vitro Toxicity Testing: Applications to Safety Evaluation*, Marcel Dekker, Inc., New York, 1992, pp. 13–43.
- [103] R.F.M. Silva, A.S. Falcão, A. Fernandes, A.C. Gordo, M.A. Brito, D. Brites, Dissociate primary nerve cell cultures as models for assessment of neurotoxicity, *Toxicol. Lett.* 163 (2006) 1–9.

- [104] V. Mittal, Improving the efficiency of RNA interference in mammals, *Nat. Rev. Genet.* 5 (2004) 355–365.
- [105] P. Stålberg, M. Santesson, S. Ekeblad, M.H. Lejonklou, B. Skogseid, Recognizing genes differentially regulated in vitro by the multiple endocrine neoplasia type I (MEN1) gene, using RNA interference and oligonucleotide microarrays, *Surgery* 140 (2006) 921–931.
- [106] E.G. Duysen, B. Li, W. Xie, L.M. Schopfer, R.S. Anderson, C.A. Broomfield, O. Lockridge, Evidence for nonacetylcholinesterase targets of organophosphorus nerve agent: Supersensitivity of acetylcholinesterase knockout mouse to VX lethality, *J. Pharmacol. Exp. Ther.* 299 (2001) 528–535.

TOXICITY OF METAL OXIDES NANOPARTICLES

Masanori Horie^{1,*} and Katsuhide Fujita²

Contents

1. Introduction	146
2. Oxidative Stress	147
2.1. Introduction	147
2.2. Inducement of intracellular oxidative stress by metal oxide nanoparticles	149
2.3. Biological effects due to CeO ₂	151
3. Apoptosis	152
4. Inflammation Response	153
5. Long-Term Effects	154
6. Biological Effect Factors Due to Metal Oxide Nanoparticles	155
6.1. Particle size: Primary particle, aggregate, and agglomerate	155
6.2. Surface area and surface activity	157
6.3. Solubility	159
6.4. Adsorption	160
6.5. Zeta potential	160
6.6. Other factors	161
7. Methods of Evaluating Biological Effects of Metal Oxide Nanoparticles	162
8. Gene Expression Profiling for Evaluating the Biologic Effects of Manufactured Nanomaterials	165
8.1. Application of DNA microarray-based gene expression profiling analysis to the toxicological responses in the pulmonary system	165
8.2. <i>In vivo</i> studies of manufactured nanomaterials	166
8.3. <i>In vivo</i> DNA microarray analysis of manufactured nanomaterials	167

¹ Health Research Institute, National Institute of Advanced Industrial Science and Technology (AIST), Ikeda, Osaka, Japan

² Research Institute of Science for Safety and Sustainability, AIST, Tsukuba, Ibaraki, Japan

*Corresponding author. Tel.: +81 72 751 9693; Fax: +81 72 751 9964

E-mail address: masa-horie@aist.go.jp

8.4. Conclusions	169
9. Summary	169
References	171

Abstract

Metal oxide nanoparticle is one of the important industrial materials. Compared with fine particles, nanoparticles have higher chemical and physical activity, such as ion release, adsorption ability, and reactive oxygen species production. These properties are important for industry use. However, these properties of nanoparticles also induce biological influences including toxic activity.

Recently, many investigations about toxicology of nanoparticles have been reported. *In vitro* studies showed that the some nanoparticles induce oxidative stress, apoptosis, production of cytokines, and cell death. Characterization of chemical and physical properties about individual nanoparticles is essential for evaluation of their biological effect.

In this chapter, we outline recent studies of evaluation of biological influences induced by metal oxide nanoparticles. Moreover, we also introduce current studies about influence factors.

1. INTRODUCTION

“Nano-objects” are defined as substances which are one or more external dimensions in the nanoscale (1–100 nm) (ISO/TS 27687: 2008, Nanotechnologies—Terminology and definitions for nano-objects—nanoparticle, nanofibre, and nanoplate). Among such objects, particle-shaped substances with a diameter of 100 nm or less are known as “nanoparticles.” Surface area per unit weight increases with nanoparticles, and thus there is a dramatic increase over fine particles in physical and chemical activity, such as absorption of light of specific wavelengths and catalytic activity. These properties of nanoparticles are important industrially, and progress is being made in research and application development for this new functional material. Metal oxide nanoparticles are produced industrially in large volumes and are the most frequently used. In addition to industrial uses, such as catalysts, these are also used in products familiar to ordinary consumers such as sunscreens, cosmetics, pharmaceutical products, and fuel additives. On the other hand, the increase in physical and chemical activity suggests the potential for increased bioactivity, that is, an increase in biological effects including toxic activity. In recent years, there has been active research on nanoparticles in the field of toxicology, and there have been many reports that nanoparticles are harmful to the body. In the twentieth century, people were shocked to find that asbestos—previously regarded as harmless to the human body and widely used in buildings, etc.—causes severe oxidative stress and

mesothelioma. Since nanoparticles have only been used in commercial applications for a short time, epidemiological findings have not been collected as in the case of asbestos' effects on humans. Even though metal oxide nanoparticles such as TiO_2 are already at the stage of practical use, their biological effects have not been adequately studied, and many points have yet to be elucidated. However, due to energetic research by many researchers in recent years, we are acquiring a certain degree of knowledge regarding the biological effects of metal oxide nanoparticles.

Metal oxide nanoparticles are a promising and important material not only in industry but also in the fields of ecology and medicine. However, to ensure proper use, it is essential to develop an accurate understanding of the biological effects of nanoparticles based on an appropriate evaluation system. When using nanoparticles, they will not be accepted by customers without a risk evaluation. There is, so to speak, no market without data of risk assessment. Since nanoparticles exhibit different characteristics from conventional materials, it is important to understand what factors are involved in their biological effects. However, it is questionable whether conventional techniques for evaluating toxicity are appropriate with metal oxide nanoparticles having physical and chemical characteristics like those described above [1]. Evaluating nanoparticles with an evaluation system that is inappropriate and inadequate may result in underestimation or overestimation of the biological effects of nanoparticles and throw off findings relating to the biological effects of nanoparticles. In risk assessment of metal oxide nanoparticles, physical and chemical characterization, *in vitro* examinations (with cells and without cells), and *in vivo* examinations are individually significant, but it is necessary to consider the results from these examinations comprehensively [2]. For these reasons, research has also been reported in recent years on systems for evaluating biological effects of nanoparticles, particularly in *in vitro* experiments.

This section reviews previously obtained findings regarding the biological effects of metal oxides. It focuses, in particular, on oxidative stress and apoptosis, where many studies have suggested an involvement of nanoparticles in biological effects. Evaluation systems are also described.



2. OXIDATIVE STRESS

2.1. Introduction

A widely accepted definition of oxidative stress is “a disturbance in the pro-oxidant/antioxidant system in favor of the former” [3]. Oxidative stress is involved in a variety of biochemical reactions *in vivo*. *In vivo*, homeostasis is maintained through various chemical reactions. The individual substances that make up the body are constantly and fluidly synthesized and broken

down, thus maintaining stability of the organism as a whole. The organism is exposed to various types of stress from the outside world, but it has acquired various compensating systems to maintain homeostasis. Among stresses on organisms, oxidative stress is the most important factor. The molecules, proteins, fats, and nucleic acids that make up the body are easily oxidized, and oxidation of these molecules not only results in loss of the original function of molecules making up the body but also disturbs maintenance of homeostasis due to dysfunction of enzyme proteins, etc. When the organism is exposed to oxidative stress, the antioxidation system functions and acts to reduce oxidative stress. At the cellular level, glutathione is a typical component of the body's antioxidation system. Glutathione has a thiol group in the molecule and is itself easily oxidized, and in that way, it prevents oxidation of biomolecules. As glutathione is consumed, glutathione synthesis enzymes such as GST are synthesized. Also, heme oxygenase is an enzyme which catalyzes the reaction that breaks down hemes and produces iron, and biliverdin and carbon monoxide are produced at that time. Biliverdin is reduced by biliverdin reductase to bilirubin. Both bilirubin and nitrogen monoxide have antioxidant activity, and thus increased expression of heme oxygenase acts to mitigate oxidative stress [4]. Expression of the isozyme HO-1 of heme oxygenase increases due to oxidative stress, heavy metals, and cytokines, and it acts to reduce these stresses [5]. Water and lipid-soluble antioxidants—such as ascorbic acid and tocopherol—function *in vivo* and alleviate oxidative stress. Oxidative stress occurs in the first place due to respiration by mitochondria in normal cells, and reactive oxygen species (ROS) are also produced when digesting organic materials and bacteria phagocytized by immune cells such as macrophages and neutrophils. Oxidative stress constantly occurs *in vivo* in order to maintain homeostasis, and a mild state of oxidative stress is regarded as “eustress” because it activates the aforementioned antioxidation system and immune system [6]. On the other hand, if excessive “distress” occurs due to exposures to nanoparticles, it cannot be suppressed with the antioxidation system, and biomolecule oxides accumulate. Among biomolecules, lipids and unsaturated fatty acids, in particular, are molecules susceptible to oxidation, and oxidized lipid peroxides themselves act as oxidants. The relationship has been pointed out between the accumulation of such lipid peroxides and various illnesses. Further, oxidation of nucleic acids has the potential to disturb genetic information.

Therefore, *in vivo* oxidative stress markers can be classified into three types: (1) ROS, metals, and other substances which cause oxidation–reduction reactions; (2) markers related to the antioxidation system such as glutathione and its synthesis enzymes (GST), redox-related enzymes which act to remove ROS (e.g., CAT, SOD), ascorbic acid, and tocopherol; and (3) oxides of biomolecules which arise as a result of oxidation reactions such as lipid peroxides, 8-OHdG and other oxides of nucleic

acids, and proteins. Many studies have measured these markers, and the results suggest that nanoparticles of metal oxides induce oxidative stress *in vivo*. A rise in the oxidative stress level is thought to be involved in the biological effect of metal oxide nanoparticles. The following describes changes in oxidative stress markers due to metal oxide nanoparticles.

2.2. Inducement of intracellular oxidative stress by metal oxide nanoparticles

Many studies have measured the intracellular ROS level in cells to which metal oxide nanoparticles have been administered using the DCFH method, and confirmed a rise in the intracellular ROS level due to nanoparticle administration. It has been reported that, in many cases, oxides of biomolecules are produced and the antioxidation system is activated when the intracellular ROS level rises due to administration of metal oxide nanoparticles.

Karlsson *et al.* [7] investigated the cellular effects of many types of metal oxide nanoparticles. When CuO, TiO₂, ZnO, CuZnFe₂O₄, Fe₃O₄, and Fe₂O₃ were administered to A549 cells derived from human lung carcinomas, a rise in intracellular ROS level was seen only with CuO, and oxidative DNA damage was evident with Fe₃O₄, CuZnFe₂O₄, ZnO, and CuO. CuO nanoparticles were found to have strong cellular effects on cultured cells (decrease of cell viability, decrease of mitochondria activity, and oxidative DNA damage), and these effects were stronger with nanoparticles than with fine particles. (With nanoparticles, there was a significant increase in oxidative DNA damage in particular, but no significant increase was found with fine particles.) [8]

Other studies have also reported that CuO and ZnO produce oxidative stress on cells. CuO causes a rise in intracellular ROS and lipoperoxidation level, and reduces the intracellular GSH level and cell viability, but the reduction in lipoperoxidation and cell viability is suppressed by the simultaneous presence of CuO nanoparticles and the antioxidant resveratrol. In addition, although administration of CuO increases GPx activity, it inhibits the activity of GR and catalase [9]. Inhibition of catalase activity has also been observed due to administration of Fe₂O₃ nanoparticles.

In a report comparing the cellular effects of SiO₂ and ZnO nanoparticles, 24 h after administration both particles caused an increase in the intracellular ROS level, drop in the GSH and SOD level, and an increase in the lipoperoxidation level dependent on the concentration. The oxidative stress load on cells due to ZnO nanoparticles was markedly greater than that due to SiO₂. In other words, ZnO nanoparticles caused a marked increase in intracellular ROS level, reduction in GSH and SOD level, and increase in lipid peroxides in primary mouse embryo fibroblasts, resulting in cell death [10]. There is a report where oxidative stress induced by ZnO

particles was similar between nanoparticles and fine particles [11]. Lin *et al.* concluded that free Zn^{2+} was not correlated with induction of oxidative stress because Zn^{2+} was not released in the medium. However, cellular uptake and intracellular Zn^{2+} release of ZnO were unclear.

On the other hand, TiO_2 nanoparticles have been found to significantly increase oxidative stress, although the effect is weaker than with CuO and ZnO. The authors have reported that anatase TiO_2 nanoparticles cause an increase in intracellular ROS level in cultured cells [12]. In this case, the rise in intracellular ROS in cells to which 30 mg/mL of TiO_2 nanoparticles were administered for 24 h was roughly 1.5–2 times that in cells to which no nanoparticles were administered.

Gurr *et al.* [13] compared the reactivity of TiO_2 nanoparticles and fine particles in BEAS-2B cells. They reported that anatase with primary particle diameters of 10 and 20 nm causes a rise in intracellular ROS, oxidative damage to DNA, and peroxidation of lipids, but those reactions do not occur with 200 nm anatase. However, TiO_2 nanoparticles formed large aggregates at this time, and it is not clear what sort of factors are involved in the cellular response.

No drop in the viability of BEAS-2B cells was evident with TiO_2 , but when ZnO nanoparticles were administered, there was a drop in viability over time, dependent on the concentration [14].

A rise in the intracellular ROS level and calcium concentration was also evident at this time. Damage to cells due to ZnO nanoparticles is suppressed by adding NAC which has antioxidant action (after being incorporated into cells, it returns to glutathione), and this suggests that oxidative stress and cytotoxicity are closely related.

In a report on immune cells, it was found that, at the initial stage of administration to RAW264.7 cells, TiO_2 caused a temporary rise in ROS level, but later it dropped back to the control level. On the other hand, ZnO caused a sustained rise to a high ROS level immediately after administration [15].

Cases have also been reported where administration of ZnO does not affect the intracellular ROS level [7]. In this case, there was little DNA damage, and administration of 80 $\mu\text{g}/\text{mL}$ for 18 h resulted in a cell viability of 60%.

In the experiments described above, concentration of the metallic oxide administered to the cell was in the range of 5–500 $\mu\text{g}/\text{mL}$, in which a lot of examinations were performed at concentrations of 10–100 $\mu\text{g}/\text{mL}$.

In *in vivo* research using animals, there are reports that metal oxide nanoparticles induce oxidative stress, and those effects match reports based on *in vitro* experiments. When a single dose of iron oxide was administered to mice intratracheally, there was a drop in the intracellular GSH content of bronchoalveolar lavage fluid (BALF) [16].

As indicated above, induction of oxidative stress is important in biological reactions due to metal oxide nanoparticles. When cells or tissues were damaged, either *in vitro* or *in vivo*, a rise in oxidative stress was evident

at all stages. On the other hand, weak oxidative stress is associated with activation of the antioxidation system, and as a result, there are cases where resistance to oxidative stress is greater than with untreated cells. Elution of metal ions, as described below, is thought to be an important influencing factor in induction of oxidative stress due to metal oxide nanoparticles. That is, in many cases, there is a tendency for strong oxidative stress to be induced by metal oxides which dissolve. The degree of the oxidative stress induced at this time depends on the type of metal ion. Strong oxidative stress is induced with Zn, Cu, Ni, etc.

2.3. Biological effects due to CeO₂

CeO₂ also has applications in cosmetics, but it is mainly used as a catalyst. In Europe, CeO₂ is used as a fuel additive. There are reports that CeO₂ nanoparticles produce oxidative stress on cultured cells, and conflicting reports that CeO₂ nanoparticles themselves have antioxidant action, and act to alleviate oxidative stress on cells.

Park *et al.* have shown that in BEAS-2B cells derived from human bronchial tubes, administration of CeO₂ nanoparticles results in a rise in intracellular ROS level and a drop in GSH, and that there is an increase in expression of redox-related enzymes such as HO-1, GST, catalase, and thioredoxin reductase. In this case, there is a decrease over time in the cell viability [17]. On the other hand, no decrease in cell viability is evident with H9C2 cells or T98G cells. The rise in intracellular ROS level in BEAS-2B is about 1.5 times that of nonadministered cells, and the reduction in cell viability is about 80% after 24 h, which is roughly the same as TiO₂. In BEAS-2B, nuclear translocation of Nrf2 has been confirmed due to administration of CeO₂ nanoparticles, and there are reports that expression of HO-1 also rises. On the other hand, activation of NF-κB does not occur [18]. Another report also found that CeO₂ nanoparticles cause a rise in intracellular ROS levels in BEAS-2B cells and A549 cells and reduce cell viability [18,19]. In these studies, CeO₂ nanoparticles produced a drop in cell viability through oxidative stress on cultured cells at a concentration of 3.5–40 mg/mL.

On the other hand, CeO₂ and Y₂O₃ nanoparticles protect nerve cells from cell death caused by oxidative stress due to glutamic acid. Glutamic acid induces oxidative stress on nerve cells, but the rise in ROS and cell death are suppressed by treating the cells with CeO₂ and Y₂O₃ nanoparticles [20]. There are also reports that CeO₂ suppresses apoptosis due to diesel exhaust particles (DEPs) [15]. It has been reported that CeO₂ nanoparticles have the ability to scavenge radicals and suppress inflammation [21]. When CeO₂ nanoparticles were administered to human aortic endothelial cells (HAECs), there was only modest expression of inflammation markers such as IL-8 and monocyte chemoattractant protein (MCP-1), even at a high

concentration of 50 mg/mL [22]. Biological effects due to CeO_2 included in fuel additive have not been reported [23,24]. Moreover, CeO_2 nanoparticles did not induce DNA damage [25].

As indicated above, there are conflicting assessments of the biological effects due to CeO_2 nanoparticles. In any case, CeO_2 nanoparticles have smaller effects on cells and the body than ZnO and CuO nanoparticles. When nanoparticles are administered to a cell, the particles are taken up into the cell by phagocytosis and subsequently, oxidative stress is induced. Internalized nanoparticles induce activation of NF- κ B via MARK activation and nuclear transit of Nrf2 [26]. Nrf2 regulates various antioxidative-related enzymes, and these antioxidant systems are activated by nuclear transit of Nrf2 [27,28]. Therefore, cellular effects of metal oxide nanoparticles, particularly low physicochemical activity nanoparticles such as CeO_2 , arise as a result of oxidative and antioxidative strength balance. Even assuming that CeO_2 nanoparticles produce oxidative stress, they induce activity of the antioxidation system, and there is also a possibility that apparent resistance to oxidative stress is acquired. Further study will be needed to elucidate that mechanism of biological effects due to CeO_2 .

3. APOPTOSIS

It has been reported that metal oxide nanoparticles induce apoptosis together with oxidative stress. Apoptosis is also called programmed cell death, and it is the active death of cells strictly controlled by the signal transmission of apoptosis. Cells that have undergone apoptosis are phagocytized and digested by macrophages. Normally, in cell death due to apoptosis, there is no leakage of the cytoplasm and expression of cytokines, and thus inflammation does not occur. In general, apoptosis occurs in order to actively remove damaged cells, and thereby keep the individual in better condition.

In terms of induction of apoptosis by metal oxide nanoparticles, it has been reported that TiO_2 nanoparticles induce apoptosis in cultured cells. However, apoptosis was confirmed at the same time with TiO_2 fine particles, and there does not appear to be any size dependence [29]. On the other hand, Gurr *et al.* [13] have shown that TiO_2 nanoparticles with primary particle diameters of 10 and 20 nm cause micronucleation in BEAS-2B cells, but this does not occur with 200 nm fine particles. However, in this case, the TiO_2 nanoparticles form large aggregates, and the size of the secondary particles is greater than the nonaggregated fine particles, and thus the authors state that “it is impossible to make a size dependence comparison.” Rahman *et al.* [30] observed micronuclei, DNA fragmentation, and formation of apoptotic bodies in golden hamster fetal fibroblast (Syrian Hamster Embryo: SHE) cells to which TiO_2 nanoparticles were

administered. Shi *et al.* [31] have reported that TiO₂ nanoparticles induce apoptosis in BEAS-2B cells. Activation of caspase-9 and caspase-3 has been found in induction of apoptosis by TiO₂, but there is no activation of caspase-8. Horie *et al.* [12] have also reported a moderate rise in intracellular ROS and activation of caspase-3 in HaCaT cells to which TiO₂ nanoparticles were administered. This result suggests that apoptosis due to TiO₂ nanoparticles is induced via mitochondria. There are many reports of apoptosis induction due to administration of nanoparticles, but their significance is not clear. Oxidative stress is also involved in induction of apoptosis. Apoptosis is induced under weak oxidative stress, and necrosis is induced under strong oxidative stress [32]. As discussed in the previous section, since metal oxide nanoparticles induce oxidative stress, it is likely that oxidative stress is involved in induction of apoptosis by metal oxide nanoparticles.

4. INFLAMMATION RESPONSE

In terms of biomarkers for inflammation response, there is a rise in expression of inflammatory cytokines such as IL-1, IL-6, and TNF- α . During inflammation, these cytokines are secreted from epithelial cells and immune cells, thereby promoting concentration of macrophages and neutrophils, and producing inflammation. There are reports that many metal oxide nanoparticles induce an inflammation response.

ZnO induces production of TNF- α in immune cells (RAW264.7) and production of IL-8 in epithelial cells (BEAS-2B), but such production is not induced by TiO₂ and CeO₂ [15]. Veranth *et al.* [33] have examined effects on interleukin production by BEAS-2B cells using nanoscale and microscale Al₂O₃, CeO₂, Fe₂O₃, NiO, SiO₂, and TiO₂.

Y₂O₃ and ZnO induce expression of inflammation markers in aortic endothelial cells but there is no evidence of expression of these markers with CeO₂ [22].

When iron oxide nanoparticles were instilled into the trachea of mice, there was found to be a rise in proinflammatory cytokines, IL-1, IL-6, and TNF- α in BALF and serum 1 day after instillation. In addition to IL-1, IL-6, and TNF- α , there was also found to be a rise in IL-2 (Th0 cytokine), IL-12 (Th1 type cytokine), IL-4, IL-5 (Th2 type cytokines), TGF- β , and IgE, even 28 days later. Further, there was an increase in the distribution of B cell and CD8+ T cells in blood lymphocytes, a rise in inflammation involving MMP and heat shock proteins, and an increase in the expression of proteins related to tissue damage [16]. Since a reduction in GSH was found, Park *et al.* [16] state that the inflammation response due to iron oxide is mediated by oxidative stress.

In experiments where NiO nanoparticles having a 26 nm secondary particle diameter were administered (0.1 or 0.2 mg) intratracheally in rats, there was a rise in two types of chemokines (cytokine-induced neutrophil chemoattractant-1 (CINC-1) and CINC-2alpha) in BALF from 3 days to 3 months after instillation [34]. In rats where NiO nanoparticles (26 nm, 0.2 mg) were instilled intratracheally, infiltration of alveolar macrophages was observed, and there was a rise in IL-1a and IL-1b in lung tissue, and a rise in monocyte chemotactic protein-1 in BALF [35].

In an experiment where mice inhaled nanoscale TiO₂, SiO₂, and silica-coated TiO₂, there was a significant inflammation response with TiO₂ (anatase and rutile) and SiO₂, but, on the other hand, in examining silica-coated TiO₂ *in vitro*, it induced TNF- α and neutrophil-attracting chemokines when administered to human macrophages [36].

Solubility of metal oxide particle is an important factor in lung inflammation. The difference in solubility of *in vitro* and *in vivo* systems is important for understanding of biological influences of metal oxides. For example, in cadmium compounds, although both cadmium oxide and cadmium sulfide particles are insoluble in water, cadmium oxide easily dissolves in the lung [37]. On the other hand, cadmium sulfide particles are removed from lung by macrophage. Additionally, NiO nanoparticles release more amounts of Ni²⁺ in biological fluid such as serum and culture medium than that in water [38]. Inhalation of TiO₂ and SiO₂ nanoparticles did not induce inflammation in mice lung; however, silica-coated TiO₂ induced pulmonary neutrophilia and secretion of cytokines such as TNF- α by macrophages [36]. These observations suggest that surface area theory cannot explain the inflammatory reaction caused by the metal oxide nanoparticle. In fact, surface reactivity such as radical formation capability and solubility are important factors of the inflammatory reaction by metal oxide nanoparticles.

5. LONG-TERM EFFECTS

TiO₂ and NiO are covered in reports examining the long-term effects of metal oxide nanoparticles. The main end points of long-term effects are fibrosis and then carcinogenesis.

When there is exposure to metal oxide nanoparticles due to inhalation, clearance from the lungs is an important factor influencing long-term effects. There are known to be species differences in reactions such as inflammation, fibrosis, and carcinogenesis in the lungs [39]. When rats, mice, and hamsters are exposed to high-concentration carbon black (CB), diesel particles, and TiO₂, a strong effect is found in rats, but the effects are comparatively mild in mice and hamsters. Clearance of particles from the lungs is slower in rats than that in hamsters. Progression of lung lesions in

rats is faster than that in mice and hamsters [40]. When exposed continuously to TiO_2 nanoparticles at a maximum concentration of 20 mg/m^3 for 6 h a day, 5 days a week for 3 weeks, an inflammation response occurred at 2 mg/m^3 for rats, and 10 mg/m^3 for mice. There is a possibility that effects such as carcinogenesis in rats under high-concentration exposure conditions are a reaction specific to rats. The possibility has been suggested that with poorly soluble particles, clearance is slow due to high-concentration administration, thus causing sustained strong inflammation, and eventually resulting in carcinogenesis [41]. Even if a particle has poor solubility and low toxicity (PSLT), clearance in alveoli is inhibited if the dosage is excessive, and an overload state occurs. Here, the question arises whether there is difference in clearance between nanoparticles and fine particles. Oberdörster *et al.* [42] exposed rats to TiO_2 nanoparticles with a particle diameter of 20 nm and fine particles with a particle diameter of 250 nm at almost the same concentration and observed their lungs afterward. As a result, it was shown that the inflammation response and problems seen at the initial exposure disappeared after 1 year.

In carcinogenesis in the lungs, clearance of inhaled particles is slow, and chronic inflammation develops. As a result, primary and secondary oxidative stresses occur, and that results in tissue damage and dysfunction of biomolecules. When this state persists further, it may result in fibrosis and the development of cancer. It has been reported that the dose which induces carcinogenesis with PSLT is about 10 times the dose which causes inflammation [43].

After inhalation, TiO_2 nanoparticles were observed in the luminal side of airways and alveoli, in all major lung tissue compartments and cells, and within capillaries of the rat [44]. According to an *in vitro* study, Geiser *et al.* indicated that cellular uptake of nanoparticles occurred by diffusion or adhesive interactions, not endocytosis.

To understand the long-term effects of metal oxide nanoparticles, it will be necessary to conduct *in vitro* experiments of oxidative stress and inflammation, understand reactions in the acute phase, and also examine clearance by conducting animal experiments.



6. BIOLOGICAL EFFECT FACTORS DUE TO METAL OXIDE NANOPARTICLES

6.1. Particle size: Primary particle, aggregate, and agglomerate

Discussions of particle diameter focus on primary particle diameter or secondary particle diameter. Many previous studies have discussed primary particle diameter. On the other hand, nanoparticles have a strong tendency

to aggregate, and it is unusual for them to exist as independent primary particles without special processing. Secondary particles come in two types: aggregates where the primary particles are strongly bonded, and agglomerates which are looser groupings. Aggregates are groupings of primary particles which are solidly bonded through covalent bonds, and they do not easily decrease in size due to ultrasound or bead mill treatment. On the other hand, agglomerates are formed by loose bonding due to van der Waals' forces and single physical entanglement between aggregated particles. They can be easily reduced in size by ultrasonic treatment or agitation.

In ISO (ISO/TS 27687: 2008), it is defined that the external specific surface area of an aggregate is smaller than the total surface area of primary particles constituting the aggregate because primary particles are strongly bonded or fused to each other. It is also defined that in agglomerates, the external specific surface area is similar to the total surface area of its constituents (particles or aggregates) because they are weakly or loosely bonded. However, the term secondary particle is described as "Aggregates are also termed secondary particles and the original source particles are termed primary particles" or "Agglomerates are also termed secondary particles and the original source particles are termed primary particles." As seen above and in many other cases not cited here, the definition of term secondary particle is unclear, noting that both aggregates and agglomerates are included in the term.

In biological fluids such as pulmonary surfactant and culture medium, particles or aggregates will adsorb proteins and salts [45]. It can be expected that under *in vivo* and *in vitro* conditions, "secondary particles" might be a complex of aggregates of primary particles and biomolecules such as proteins.

In terms of primary particles, many reports have found that nanoparticles have greater cytotoxicity and biological effects than fine particles [8,38,46]. However, there are also cases such as ZnO where there is no relationship between particle diameter and toxicity [47]. In examining the biological effects of nanoparticles, comparisons of primary particle diameters are frequently seen, but in reality, nanoparticles have a strong tendency to aggregate, and it is unusual for them to exist as primary particles. In explaining cosmetics using nanoparticles, it is sometimes said that "the nanoparticles penetrate to the dermis and exhibit their effects," but experimentally speaking, transit to the subcutaneous of metal oxide nanoparticles coated on the skin has not been confirmed [48].

In a study using TiO₂, Gurr *et al.* [13] found that nanoparticles (10 and 20 nm) have stronger cellular effects than fine particles (200 nm). In that study, the nanoparticles aggregated, and the largest secondary particles reached a diameter of 1000 nm. Fine particles, on the other hand, did not aggregate, and thus their size was smaller at the secondary particle level.

There are reports on the aggregate size, secondary particle size, and biological effects of TiO₂. When anatase TiO₂ nanoparticles with different

primary particle diameters, but the same secondary particle diameters, were administered to cultured cells, differences were not seen in biological effects (intracellular oxidative stress, cell viability) between the two types of particles [12].

Further, even in experiments where TiO_2 nanoparticles from the same manufacturer were administered intratracheally to rats, no particular differences in effects on the lungs were seen between the case where primary particle diameter is the same but secondary particle diameter is different, and the case where primary particle size is different and secondary particle size is different [49]. It is likely that the size of the secondary particle diameter affects phagocytosis by macrophages. The alveolar macrophage works on clearance of particles in the lung [50]. However, the *in vivo* phagocytosis mechanism of metal oxide nanoparticles by macrophage is unclear. Phagocytosis of particles by macrophages is involved in clearance inside the body, and is an important biodefense mechanism. If nanoparticles are not recognized by macrophages and other immune cells, clearance is slow, and the particles are likely to remain for a long time in the lungs and other organs. Epithelial cells ordinarily conduct endocytosis to take in nutrients, and in observations with TiO_2 and NiO , both nanoparticles and fine particles were phagocytized into cells [12,38]. The secondary particle diameter is thought to be important for this incorporation of particles into immune cells and epithelial cells via endocytosis but the details are unclear, including the range of secondary particle diameters which can be taken in. This will need to be examined in future research.

6.2. Surface area and surface activity

The increase in specific surface area per unit weight is frequently mentioned as the reason why nanoparticles have greater biological effects than fine particles. An increase in surface area leads to an increase in physical and chemical activity. An increase in physical and chemical activity is related to bioactivity, and thus surface area is likely to be important for the biological effects of nanoparticles.

The reaction most frequently mentioned in connection with surface activity is the production of ROS at the particle surface. In particular, anatase TiO_2 nanoparticles have greater photocatalytic activity than the rutile type, and ROS production due to irradiation with light has an effect on cells [51]. With anatase TiO_2 , ROS such as H_2O_2 and hydroxyl radical are produced at the particle surface due to photoexcitation. This reaction is stronger with nanoparticles, which have a large surface area per unit weight. When anatase TiO_2 nanoparticles are administered to HeLa cells, there are effects on cell survival without light irradiation, but with UV irradiation, cell death occurs in proportion to the irradiation time [52]. This cell death is suppressed by the simultaneous presence of catalase which removes H_2O_2

and tryptophan which removes hydroxyl radical, and this suggests that cell death is caused by ROS produced at the particle surface by UV irradiation. On the other hand, there is no possibility that TiO₂ incorporated into the body through routes such as inhalation exposure will be exposed to exciting light. No evidence has been found that TiO₂ anatase nanoparticles directly produce ROS without exciting light [53]. The applications of TiO₂ nanoparticles where exposure to exciting light is most likely are sunscreen and cosmetics, but most of the TiO₂ used in these products is the rutile type with low photocatalytic activity. In actual use, the photocatalytic activity of TiO₂ is likely to have small effects except in special cases.

The biological activity of metal oxide nanoparticles is affected by modification of particle surface such as addition of functional groups and coatings. After exposure to TiO₂ nanoparticles modified with -OH and -NH₂, cell viabilities were decreased compared with unmodified TiO₂ nanoparticles. Compared with unexposed cells, the cell viabilities of unmodified, -NH₂, and -OH modified TiO₂ were 80%, 75%, and 65%, respectively. On the other hand, -COOH modified TiO₂ nanoparticles did not affect the cell viability [54]. Thevenot *et al.* [54] considered that the surface charge is related with differences in cellular influences. Cellular influence of negative charged particles such as -COOH modified TiO₂ is small because the particles are taken up into cells easily without membrane binding, and subsequently, the particles are submitted to processing inside intracellular compartments.

These results suggest that biological activities of metal oxide nanoparticles are affected by physicochemical properties of particle surface. Also, physicochemical properties are affected by modification of particle surface and adsorption of environmental materials. Oberdörster *et al.* [42] reported that the biological influences of nanoparticles depend more on surface area than on particle mass. In their report, TiO₂ particles (particle sizes: 20 and 250 nm) exposed to rats lungs by intratracheal instillation revealed lung injury dependency to particle surface area. On the other hand, Warheit *et al.* reported that there was no relationship with particle surface area and lung toxicity; significant differences in lung injury and inflammation were not observed in rats exposed to 300 nm rutile- and 10 nm anatase-type TiO₂ nanoparticles [55,56]. Further, Warheit *et al.* injected α -quartz of various sizes and surface areas to rat lung to compare particle surface area and lung injury influence [57]. As a result, differences of lung inflammation and cytotoxicity were not observed between the nanoparticle (primary particle size of 12 nm and specific surface area of 90.5 m²/g) group and fine particle (524 nm, 5.1 m²/g) group. Other examination using TiO₂ also showed that the influence on lungs depended on the surface property [58]. According to these examinations, Warheit *et al.* conclude that pulmonary toxicity of α -quartz and TiO₂ depends on its surface property and that particle size and surface area are not related with pulmonary toxicity.

Because the amount of the functional group and the adsorbed materials correlate to the surface area, the influence of the surface area cannot be disregarded. Nevertheless, it might be difficult to explain the biological influences of the metal oxide nanoparticles only by the surface area theory.

6.3. Solubility

In recent years, *in vitro* research—particularly that using cultured cells—has revealed the finding that elution of metal ions from particles is an important part of the cytotoxicity of metal oxide nanoparticles. In research comparing the toxicity of ZnO, CuO, and TiO₂ nanoparticles and fine particles on *Saccharomyces cerevisiae*, ZnO exhibited the same toxicity in both nanoparticle and microparticle form [59]. Further, the toxicity of these forms of ZnO was the same as soluble ZnSO₄·7H₂O. With CuO, nanoparticles exhibited great effects than fine particles, but their effects were similar to soluble CuSO₄ and the authors explained the difference in toxicity between nanoparticles and fine particles as due to the difference in elutability of Cu ions from the particles. TiO₂ exhibited no effects on *S. cerevisiae*. Studer *et al.* revealed that a strong cytotoxicity of CuO nanoparticles was induced by cellular uptake of CuO nanoparticles and subsequently intracellular Cu²⁺ release [60].

NiO nanoparticles exhibit greater influences than NiO fine particles on cultured cells. Whereas NiO fine particles eluted almost no Ni²⁺ in the culture medium, NiO nanoparticles did elute Ni²⁺ [38]. The cellular effects of NiO nanoparticles resemble soluble NiCl₂, but cytotoxicity is greater than the same concentration of NiCl₂. CuO nanoparticles also exhibit greater cytotoxicity than the same amount of CuCl₂ on cultured cells [7]. It has been observed that NiO nanoparticles are taken into epithelial cells. Various types of cellular effects due to metal oxide nanoparticles are conceivable. In addition to effects due to extracellular elution of metal ions in the culture medium or biological fluids, other possibilities are intake of particles into cells and elution of metal ions inside cells. Metal oxide nanoparticles taken into cells likely act as a source supplying metal ions, and continually elute metal ions into the cytoplasm. With some ions such as Ni²⁺, the influx of extracellular ions into the cell is controlled by ion channels [61,62]. Cu²⁺ and Zn²⁺ are essential for some of the enzymes crucial for maintaining cellular homeostasis such as SOD [63], and an increase in the intracellular concentration of these metal ions can disturb the cell's metabolic system, or produce ROS due to a Fenton-like reaction [64].

The results of *in vitro* studies suggest that elution of metal ions is an important factor in the cellular effects of metal oxide nanoparticles, but there are many points which are unclear, such as the relationship between soluble kinetics and organelles inside the cell. There is a possibility that the same reaction will occur *in vivo*, but there is still no data, and further studies are necessary.

It has been pointed out that NiO and CuO have effects due to elution of metal ions, but both are ordinarily insoluble in water. The material safety data sheet (MSDS) included when purchasing these particles from a manufacturer states: "Solubility in water: insoluble." Actually, although green NiO fine particles are almost completely insoluble in water, green NiO nanoparticles exhibit marked solubility [38]. Further, the solubility of NiO nanoparticles is greater in biological fluids such as culture medium than in water. Elution of metals contained as impurities should also be considered. An increase in solubility is one distinguishing feature of metal oxide nanoparticles, and measuring the elution of metal ions in biological fluids is essential for evaluating the risk of metal oxide nanoparticles.

6.4. Adsorption

Some metal oxide nanoparticles exhibit strong adsorption. In research by the authors [45], nanoparticles adsorbed to proteins derived from serum in a cell culture medium when metal oxide nanoparticles were dispersed in the medium. TiO₂, CeO₂, and ZnO, in particular, exhibited high protein-adsorption capacity. TiO₂ and CeO₂ adsorbed salts in the culture medium, particularly calcium. The surface potential of particles likely contributes to adsorption of these culture medium components, and the details are described in the following section. The fact that many nanoparticles adsorb salts and biomolecules such as proteins suggests the possibility that bioactivity of the particles themselves varies depending on the adsorbed substances. In culturing cells, 10% serum is frequently added to the culture medium. Therefore, in the culture medium, metal oxide nanoparticles form "secondary particles" in the form of complexes with proteins or salts. It has been reported that, in an *in vitro* system, proteins adsorbed to nanoparticles do not affect interaction between cells and particles [65]. On the other hand, in the *in vivo* case, metal oxide nanoparticles which are inhaled or make contact with the skin first make contact with saliva, mucous membranes, alveoli surfactants, and moisture retention components of the skin. These biogenic substances include many biomolecules such as proteins and lipids, and thus metal oxide nanoparticles are likely to adsorb these substances in actual exposure as well. These adsorbed substances are thought to influence biological effects, but there is no data on adsorption *in vivo*, and this is a topic for the future.

6.5. Zeta potential

Zeta potential is related to interactions between particles and biomolecules and is thought to be an important factor for formation of aggregates. When metal oxide nanoparticles are dispersed in water, the zeta potential depends on the molecular species and the surface condition. In *in vitro* experiments, on the other hand, the zeta potential when dispersed in culture medium for

cell culture is about -15 to -20 mV regardless of the type of substance [66]. This is thought to be because, ordinarily, about 10% serum is added to the culture medium when culturing most of the cells used in toxicity assessment experiments, and thus the value reflects the zeta potential due to proteins such as albumin adsorbed to the particle surface. Actually, the charge of bovine serum albumin is negative at neutral pH, and this almost matches the zeta potential of metal oxide nanoparticles in culture medium dispersion fluid. Positively charged particles directly adsorb albumin, and particles with a negative charge such as TiO_2 are thought to adsorb albumin via calcium ions, etc. For example, TiO_2 and CeO_2 exhibit high calcium-adsorption capacity [45]. On the other hand, albumin itself is a typical calcium-binding protein, and thus calcium is thought to play a crucial role in these interactions. However, Patil *et al.* [67] described that protein adsorption is not only due to electrostatic interactions but also due to van der Waals' forces, hydrophobic, hydrophilic, structural, and steric interactions between the protein and the adsorbed material. It is difficult to measure *in vivo* the zeta potential of metal oxide nanoparticles inhaled by humans or animals, but saliva and alveoli surfactants contain many proteins and calcium components. On the epidermis too, there are proteins as well as lipids and salts, and it is likely that metal oxide nanoparticles quickly adsorb these molecules. Therefore, in toxicity assessment, it is probably not appropriate to discuss the correlation with *in vivo* conditions based on the value of the zeta potential measured in aqueous dispersion.

6.6. Other factors

In addition to various biological influence factors noted above (primary/secondary particle size, aggregation/agglomeration state, surface property, solubility (ion release ability), adsorption ability, and surface charge), particle shape and crystalline phase are also suggested as important biological influence factors. Comparison of macrophage phagocytic capacity in Al_2O_3 nanoparticles and oxides-coating Al nanoparticles (thickness of oxide layer was 2–3 nm) showed that phagocytic capacity was more affected by kinds of material than particle size. Al nanoparticles showed stronger cytotoxicity than Al_2O_3 nanoparticles, and phagocytic capacity of macrophage was decreased [68]. Intratracheal instillation of two kinds of TiO_2 nanoparticles which had the same composition and different shape (particle and rod) did not show differences in pulmonary influences [55]. Refer to the review by Oberdörster [69] for details of the difference of biological activities of the fibril and the particulate materials.

In characterization of nanoparticles for toxicity evaluation, understanding the actual state of nanoparticles *in vivo* is very important as well as *in vitro* characterization [70,71]. However, the characterization technique of *in vivo* physicochemical properties is still in progress. The *in vivo* characterization is the next task.

7. METHODS OF EVALUATING BIOLOGICAL EFFECTS OF METAL OXIDE NANOPARTICLES

Nanoparticles exhibit greater physical/chemical activity and bioactivity than fine particles. Nanoparticles have different properties than fine particles, even with the same chemical composition. Therefore, many industrial applications have been attempted, but the question arises: Can substances like this which have new properties be handled with conventional methods of evaluating biological effects? What is important when evaluating the biological effects of nanoparticles is to characterize the various effect factors indicated above together with *in vivo* testing. Typical markers for the evaluation of biological influences are listed in Table 1.

Adsorption often has an effect on *in vitro* testing. Culture medium components are adsorbed to nanoparticles, depending on the test system, and cells become starved [45]. This leads to toxicity being estimated as greater than it really is. Caution regarding depletion of culture medium components due to nanoparticles is necessary in *in vitro* test systems particularly when the particle concentration is high. Further, the MTT (3-(4,5-dimethyl-2-thiazolyl)-2,5-diphenyltetrazolium bromide) method that uses mitochondrial activity as an indicator is one of the most widely used methods of measuring the cell viability. However, MTT assay is not suitable for evaluation of cytotoxic activity of some nano-objects. When MTT assay was conducted to cytotoxic examination of carbon nanotube (CNT), the MTT formazan was adsorbed to CNT and the apparent viability decreased [72]. The effects of metal oxides on the MTT method are unclear, but Veranth *et al.* have reported that when nanoparticles were administered, the interleukin released by cells was adsorbed to nanoparticles, and it was impossible to correctly measure with ELISA [33]. Prior to experiments, it is necessary to ascertain the adsorption of metal oxide nanoparticles.

The solubility of metals from metal oxide nanoparticles is one of the factors which most affect the body. There are some cases where a substance is insoluble as a conventional fine particle and the MSDS states that it is “insoluble,” but it dissolves when in nanoparticle form. Prior to experiments, it is necessary to ascertain solubility. However, there are sometimes differences in solubility of metal oxide nanoparticles in water and biological fluids such as culture medium [38].

It is essential to develop an understanding of the above physical and chemical properties in noncellular system (*in vitro* systems in the narrow sense). On the other hand, the body has various systems to maintain dynamic equilibrium (homeostasis). The next step is to check whether the results from noncellular systems are reflected in *in vitro* systems using cells (*in vitro* in the broad sense).

In vitro experiments using cultured cells are simpler than *in vivo* experiments, and they are essential for understanding the mechanisms of biological effects. They are also less expensive and faster than *in vivo* experiments, and

Table 1 Typical markers for the evaluation of biological influences

	End point	Marker		Measurement method
<i>In vitro</i>	Oxidative stress	ROS production	Intracellular ROS level	DCFH
		Activation of antioxidative potential	GSH level	DTNB
			Antioxidant related enzymes (HO-1, SOD, GST, etc.)	ELISA, Western blot, gene expression
	Apoptosis	Oxidized biomolecule	Lipid peroxide	MDA (TBARS), DPPP
			Protein carbonyls	Western blot
		Activation of caspase pathway		Caspase activity
	Cell viability	Phosphatidylserine on the extracellular surface		Annexin V staining
		Morphology		Microscopic observation
		Mitochondrial activity	Mitochondrial reductase	MTT assay, WST-1 assay
	Cell proliferation	Cell membrane damage	LDH leaking	LDH activity
			PI staining	
		Colony formation	Clonogenic assay	
<i>In vivo</i>	Oxidative stress			Comet assay
				TEM observation
	Inflammation	Activation of antioxidative potential	Antioxidant related enzymes (HO-1, SOD, GST, etc.)	ELISA, Western blot, gene expression
		Oxidized biomolecule	Lipid peroxide	
		Leukocyte	Macrophage, neutrophil	Microscopic observation
	Injury	Cytokine	Interleukin, TNF- α	ELISA, gene expression
			LDH leaking	LDH activity
		Pathological change	Histology finding	Histopathological staining

DCFH, 2',7'-dichlorofluorescein; DTNB, 5,5'-dithiobis-(2-nitrobenzoic acid); DPPP, diphenyl-1-pyrenylphosphine; LDH, lactate dehydrogenase; MTT, 3-(4,5-dimethyl-2-thiazolyl)-2,5-diphenyltetrazolium bromide; MDA, malondialdehyde; TBARS, thiobarbituric acid-reactive substances; WST, water soluble tetrazolium salts.

thus they are also useful for first-stage screening of toxic substances. What is important in evaluating the biological effects of nanoparticles in *in vitro* systems is the homogeneity and stability of the metal nanoparticle dispersion. Culture medium contains salts and proteins, and thus aggregation occurs immediately when nanoparticles are added to culture medium. If secondary particles of various sizes are present in the dispersion, large secondary particles will reach cells due to gravitational sedimentation, while nanoscale secondary particles reach cells through diffusion [73]. Teeguarden *et al.* [73] have reported in detail on this mechanism. If large aggregates/agglomerates are formed, gravity sedimentation led large aggregates to reach the cells faster than small aggregates. Therefore, the dispersion concentration differs from the cell exposure concentration. On the other hand, if dispersion includes only nanoscale aggregates/agglomerates (with size less than 100 nm), the aggregates reach the cells only by diffusion. In this case, the dispersion concentration reflects the cell exposure concentration. Kato *et al.* [74,75] have shown that the dynamic light scattering (DLS) method is effective for evaluating secondary particle size and stability in many dispersions of metal oxide nanoparticles and culture media. Conducting DLS measurement simultaneously with cellular examinations makes it possible to understand the state of the dispersion being administered to cells.

The living organism is more complex than an *in vitro* system using cultured cells. Reports comparing biological effects *in vitro* and *in vivo* are limited in scope, but they do suggest that it is possible to predict *in vivo* results based on *in vitro* tests. In a comparison of *in vitro* and *in vivo* experiments on ZnO nanoparticles and fine particles, an increase in oxidative stress markers and activation of the antioxidation system were observed in both tests [76]. These results suggest that *in vivo* effects due to nanoparticles—such as oxidative stress in the acute stage, inflammation response, and damage due to these reactions—can be screened based on *in vitro* tests. In other words, when cellular damage markers such as lactate dehydrogenase, oxidative stress markers such as intracellular ROS level and lipid peroxidation, and inflammation markers such as interleukin are at a high level in the *in vitro* system, it is highly probable that the substance will have strong effects *in vivo*, and cause oxidative stress and inflammation. However, the doses that cause these reactions are different *in vitro* and *in vivo*, and the times for the reactions to occur are not the same. Adequate caution must be exercised when applying the results of *in vitro* tests to *in vivo* systems. Further, it is impossible at the current stage to predict or screen for long-term effects such as carcinogenesis based on *in vitro* tests. *In vivo* tests are essential for predicting long-term effects [77].

In recent years, there have been reports of effects on the fetus due to exposure of the mother to nanoparticles. When 100 μg of TiO_2 nanoparticles were subcutaneously injected to pregnant mice, the development of fetuses' brain was affected [78]. The particle size of TiO_2 “nanopowder” used in this study was described as 2570 nm (surface area was 2025 m^2/g);

however, the actual particle size in the administration solution is unclear. In another report, abdominal cavity injection of TiO_2 nanoparticles at dose of 5, 10, 50, 100, and 150 mg/kg BW induced oxidative stress in brain of mice [79]. Further, in an experiment with subcutaneous injection of 100 μg of TiO_2 nanoparticles to maternal mouse, TiO_2 nanoparticles were detected in Leydig cells, Sertoli cells, and testicular spermatids of newborns [80]. Sperm morphology did not differ but number of sperm per testis significantly decreased when the mother had been subcutaneously injected with TiO_2 . On the other hand, *in vitro* study showed similar results. When TiO_2 nanoparticles, DEP and CB, were exposed to mouse Leydig TM3 cells, TiO_2 nanoparticle showed cytotoxicity at lower dose than DEP and CB. Toxic influences of TiO_2 on cell viability and proliferation were observed at concentrations of 10 and 100 $\mu\text{g}/\text{mL}$, respectively [81]. These investigations give us meaningful results of disposition of metal oxide nanoparticles.

However, in these reports, the dosage is such that it could not happen under ordinary conditions, and the method of administration is intraperitoneal or subcutaneous implantation. Thus the effects are being examined with a method different from ordinary exposure. Further studies of reproductive toxicity will be necessary in the future, including the validity of experimental methods.

Findings obtained under “impossible” conditions and dosages which normally do not occur, even in *in vivo* experiments, can be used as basic data which suggests the latent effects of the substance, but the results should not be interpreted by extrapolating. The results of tests involving subcutaneous or intraperitoneal implantation of excessively large amounts should be very carefully interpreted, without overestimating or underestimating. In the end, these results are reference data, and it is essential to determine the no observable adverse effect level (NOAEL) by conducting separate additional experiments under conditions which can actually occur.

To ensure accurate and appropriate evaluation of the risk of metal oxide nanoparticles, it is important to ascertain and evaluate information obtained from the results of both *in vitro* and *in vivo* tests conducted using the proper methods.



8. GENE EXPRESSION PROFILING FOR EVALUATING THE BIOLOGIC EFFECTS OF MANUFACTURED NANOMATERIALS

8.1. Application of DNA microarray-based gene expression profiling analysis to the toxicological responses in the pulmonary system

Assessing cellular responses at molecular level upon exposure to intentionally and unintentionally created chemical substances could provide new insights into their toxicological behavior. In the recent decade, DNA

microarray technology has been developed and widely used in the fields of genomic study, disease prevention, drug discovery, and diagnostic microbiology [82]. Among them, the DNA microarray-based approach is beginning to be available to elucidate toxicological responses in the pulmonary system.

cDNA microarrays have been performed to identify clusters of genes involved in the progression of pulmonary fibrosis after bleomycin, a cytotoxic drug, administration [83], and nickel-induced acute lung injury in an experimental animal model [84]. Zuo *et al.* have analyzed samples from patients with histologically proven pulmonary fibrosis (usual interstitial pneumonia) by using oligonucleotide microarrays to elucidate the molecular mechanisms that lead to end-stage human pulmonary fibrosis [85]. Comprehensive gene expression profiling of rat lung revealed distinct acute and chronic responses to cigarette smoke inhalation and identified molecular pathways that could be responsible for the damaging consequences of smoking [86]. These microarray data identified that metabolic processes were most significantly increased early in response to cigarette smoke. After a transient acute response, gene sets related to immunity and defense progressively increased and predominated at the later time points in smoke-exposed rats. The significance of these findings is to represent the transition from acute to chronic smoke exposure by microarray data shown from selected time points at the gene expression level.

8.2. *In vivo* studies of manufactured nanomaterials

In recent years, concern over the influence of various manufactured nanomaterials such as nanoparticles (ultrafine particles), nanofibers, and nanotubes on human health and the environment has risen due to advances in the development of nanotechnology. Especially, based on the clinical assessments of dusts, asbestos, or related exposures, there has been more interest in the influences of manufactured nanomaterials on pulmonary inflammation, fibrosis, and cancer, etc. Whereas it is not easy to predict those potential toxicities because of a unique physicochemical quality of manufactured nanomaterials, the toxicity delivered to the lungs of rodents by inhalation has been performed. There are a lot of reports concerning the toxicological effect of a ultrafine titanium dioxide particles on pulmonary systems [49,58,87].

CNTs are unique in having a high aspect ratio. Due to this fiber-like shape, CNTs introduced into the abdominal cavity may show asbestos-like pathogenicity [88]. The number of reports of inhalation toxicity of multi-walled carbon nanotubes (MWCNTs) or single-walled carbon nanotubes (SWCNTs) has been increasing with the progress in the physicochemical analysis [89–92]. These studies focus on the lung toxicity with respect to inflammatory response, oxidative stress, and immune system, etc.

In addition to these approaches, an *in vivo* biodistribution study revealed that inhaled CNTs reach the subpleural tissue in mice [93].

The use of C₆₀ fullerenes is also expected to increase in diverse industrial fields. Despite interest in the potential toxicological impact of C₆₀ fullerenes, little is known about its mechanism of action *in vivo*. It has been reported that suspensions of C₆₀ fullerenes in water had little or no difference in the lung toxicity effects [94]. The assessment of toxicity resulting from inhalation exposure to C₆₀ fullerene nanoparticles and microparticles revealed minimal changes in the toxicological endpoints [95]. However, the precise underlying mechanism of action is still unknown. A global toxicological research might be useful to evaluate the toxicity of manufactured nanomaterials with an unknown end point.

8.3. *In vivo* DNA microarray analysis of manufactured nanomaterials

Gene expression analysis using DNA microarrays has been used to elucidate the toxicological responses of metal oxide ultrafine particles in *in vivo* studies. Chen *et al.* [96] observed that titanium dioxide nanoparticles (nano-TiO₂) induced pulmonary emphysema, macrophage accumulation, extensive disruption of alveolar septa, type II pneumocyte hyperplasia, and epithelial cell apoptosis by morphometric analysis and dUTP nick-end-labeling (TUNEL) staining. Meanwhile, mouse cDNA microarray reveals that nano-TiO₂ induced differential expression of hundreds of genes including activation of pathways involved in cell cycle, apoptosis, chemokines, and complement cascades. Taken together, the authors suggested that nanoTiO₂ can induce severe pulmonary emphysema, which may be caused by activation of placenta growth factor (PlGF) and related inflammatory pathways [96]. Chou *et al.* [97] have demonstrated that intratracheal instillation of 0.5 mg of SWCNTs into male mice induced alveolar macrophage activation, various chronic inflammatory responses, and severe pulmonary granuloma formation. The authors used oligonucleotide microarrays to investigate the molecular effects on the macrophages when exposed to SWCNT, and suggested that innate and adaptive immune responses may explain the chronic pulmonary inflammation and granuloma formation *in vivo* [97].

Gene expression profiles in rat lungs after intratracheal instillation of ultrafine nickel oxide particles have been analyzed [98]. Genome-wide expression analysis revealed that intratracheal instillation of ultrafine nickel particles led to a rapid increase in the expression of chemokines and genes involved in inflammation. These changes were most pronounced at 1 week postinstillation with ultrafine nickel particles. However, expression returned to control levels by 6 months postinstillation, and expression of

various other genes categorized into the detection of chemical stimulus was increased at this time point. The results corresponded well with the results obtained using conventional methods such as immunohistochemical analysis and BALF cell analysis [34], and expression of inflammation-related cytokines [99]. Taken together, the results suggest that residual ultrafine nickel oxide particles in the lungs subacutely initiated distinct cellular events after resolution of the inflammatory response.

The pulmonary effects of the inhalation of C_{60} fullerenes compared with ultrafine nickel oxide particles have been reported [100,101]. The study was conducted to examine pulmonary response at 3 days, 1 month, and 3 months postexposure to C_{60} fullerene exposure of 6 h a day, and 4 weeks (5 days a week) to assess the short-term effects of the inhalation postexposure. C_{60} fullerenes were found in alveolar epithelial cells at 3 days postexposure, and they were engulfed by macrophages at both 3 days and 1 month postexposure. However, conventional methods such as histochemical analysis, neutrophil and BALF cell analysis demonstrated that C_{60} fullerenes might not have adverse effects on the lung under the inhalation exposure condition. The gene expression profiles of the rat lung after whole body inhalation exposure to C_{60} fullerenes have been simultaneously performed to assess the influence of the nanoparticles on molecular events [101]. Oligo DNA microarray revealed that the few genes involved in the inflammatory response, oxidative stress, apoptosis, and metalloendopeptidase activity were upregulated at both 3 days and 1 month postinstillation. Meanwhile, these results were significantly different from those of ultrafine nickel oxide particles, which induced high expression of genes associated with chemokines, oxidative stress, and matrix metalloproteinase 12 (Mmp12). This suggests that ultrafine nickel oxide particles lead to an acute inflammation for the exposure period, and the damaged tissues are repaired in the post-instillation period. The gene expression profiles provide evidence for the pulmonary toxicity differences in each manufactured nanomaterials.

The pulmonary effects after intratracheal instillation to ultrafine C_{60} fullerene particles compared with those of ultrafine nickel oxide particles have been reported [100]. The gene expression profiles in rat lungs after intratracheal instillation of C_{60} fullerene particles have been examined to characterize time-dependent changes in the gene expression profiles at different dosages and to identify the expressed genes as potential candidates of biomarkers [102]. Gene expression profiling suggested that the expression of some genes is correlated with the dose of intratracheally instilled C_{60} fullerenes. The expression levels of 89 and 21 genes were positively correlated with the C_{60} fullerene dose at 1 week and 6 months after the instillation, respectively. Most of them were involved in "inflammatory response," and the *Ccl17*, *Ctsk*, *Cxcl2*, *Cxcl6*, *Lcn6*, *Orm1*, *Rnase9*, *Slc26a4*, *Spp1*, *Mmp7*, and *Mmp12* genes were overlapped. These genes might be useful

for identifying potential biomarkers in acute phase or persistent responses to C₆₀ fullerenes in the lung tissue.

8.4. Conclusions

We consider that DNA microarray-based gene expression analysis provides useful information about (1) a comprehensive set of the toxicological responses in dose- and time-dependent manner at the molecular level, (2) genes for identifying potential biomarkers in acute phase or persistent responses to nanomaterials, (3) *in vivo* characteristics of manufactured nanomaterials, comparing with the profiling of another kind of manufactured nanomaterials or other chemical materials. Further development of analytical method, accumulation of analytical data, and information-sharing through a public functional genomics data repository are necessary to propel the future study.



9. SUMMARY

At present evaluation of the biological effects of metal oxide nanoparticles is being discussed and researched in many countries.

For industrial applications of metal oxide nanoparticles, it is important to correctly evaluate both risks and benefits, and use the material properly (it is also possible to opt not to use the material). Evaluation using appropriate experimental systems is important for this reason too. It is also crucial to evaluate using appropriate experimental systems when developing an understanding of biological effects due to accidentally or naturally produced nanoparticles (including metal oxides) such as DFP and yellow sand. Further, it is essential to evaluate risks and ascertain latent effects for uses where nanoparticles are actively administered to the body, as with DDS.

Figures 1 and 2 summarize the biological effect factors and evaluation methods for metal oxide nanoparticles. Basically, nanoparticles have greater potential for bioactivity than fine particles. However, it is still unclear whether the fact that they are nanoscale directly affects the body. At present, the greatest effect factor for metal oxide nanoparticles is the increase in solubility. Nanoscale particles have greater solubility due to the increase in surface area per unit weight. Eluted metals have an effect on the body. In terms of biological effects, increased oxidative stress causes apoptosis and inflammation, and in some cases, continuous oxidative stress or inflammation can lead to fibrosis or cancer. "Oxidative stress" is a key word for the biological effects of metal oxide nanoparticles. However, it is not the case that all metal oxide nanoparticles dissolve, and factors such as surface

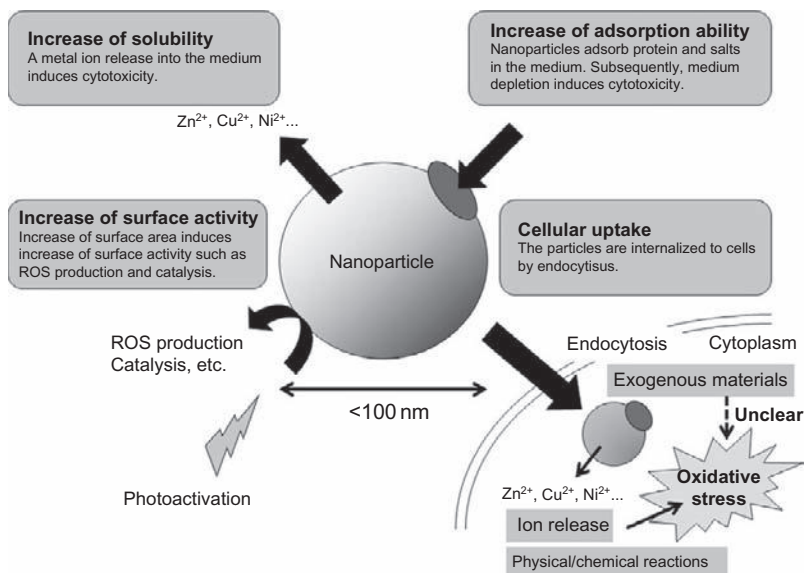


Figure 1 Cellular influence factors induced by metal oxide nanoparticles.

modification also have an effect. Even metal oxide nanoparticles with the same chemical composition (e.g., TiO_2) are likely to have different effects depending on the manufacturer. At the present time, risk evaluation requires characterization of each substance and each product. Recently, some investigations about preparation of nanoparticle dispersion and measurement method for accurate evaluation of biological influences by nanoparticles *in vivo* and *in vitro* have been reported [74,75,103–106]. *In vitro* and *in vivo* tests with no characterization are meaningless, and do nothing but confuse the results. Particle diameter (primary, secondary), specific surface area, dispersion stability, solubility, and adsorption should be ascertained for characterization, and oxidative stress, apoptosis, cytotoxicity (mitochondria activity, colony formation, etc.), and cytokine production should be ascertained for *in vitro* evaluation using cultured cells. For *in vivo* tests, it is valid to adopt acute toxicity (oxidative stress, damage, inflammation, etc.) and long-term toxicity (carcinogenesis) as end points. These items are still being discussed.

Previously, a number of outstanding reviews have been presented regarding the biological effects of nanoparticles [107–111]. Outstanding reviews have also been presented regarding the environmental effects of metal oxides. For matters which could not be adequately explained in this section, such as environmental effects, or for discussion from different perspectives, the reader should refer to these reviews.

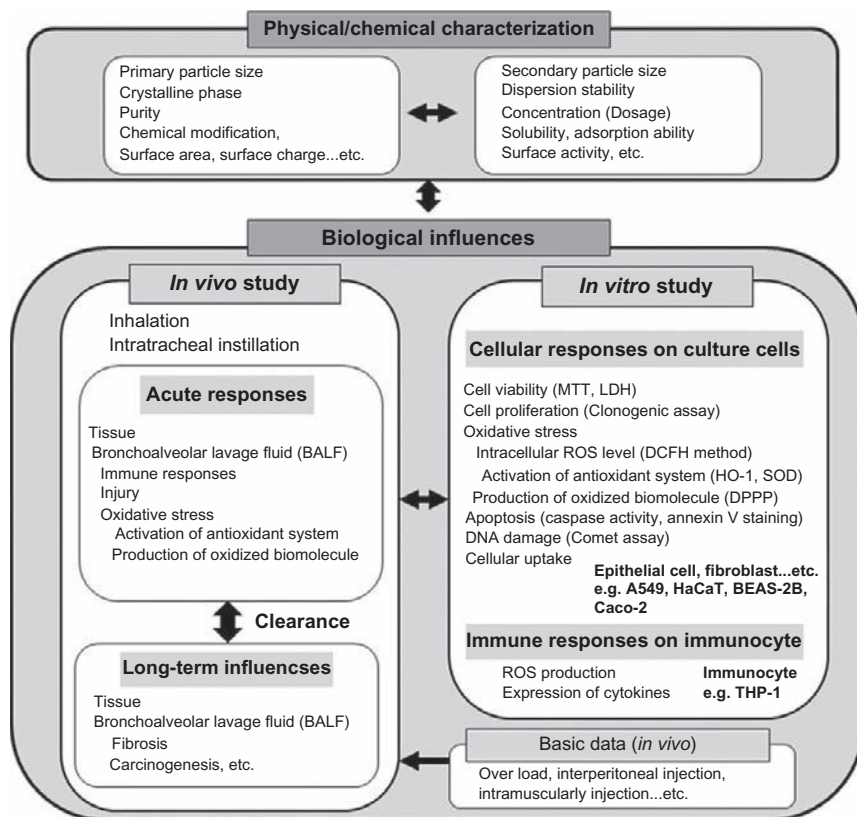


Figure 2 Evaluation of biological influences induced by metal oxide nanoparticles.

REFERENCES

- [1] N.A. Monteiro-Riviere, A.O. Inman, L.W. Zhang, Limitations and relative utility of screening assays to assess engineered nanoparticle toxicity in a human cell line, *Toxicol. Appl. Pharmacol.* 234 (2009) 222–235.
- [2] G. Oberdörster, A. Maynard, K. Donaldson, V. Castranova, J. Fitzpatrick, K. Ausman, J. Carter, B. Karn, W. Kreyling, D. Lai, S. Olin, N. Monteiro-Riviere, *et al.*, ILSI Research Foundation/Risk Science Institute Nanomaterial Toxicity Screening Working Group. Principles for characterizing the potential human health effects from exposure to nanomaterials: Elements of a screening strategy, Part. *Fibre Toxicol.* 2 (2005) 8.
- [3] H. Sies, Oxidative stress: From basic research to clinical application, *Am. J. Med.* 91 (1991) 31S–38S.
- [4] M.D. Maines, Heme oxygenase: Function, multiplicity, regulatory mechanisms, and clinical applications, *FASEB J.* 2 (1988) 2557–2568.
- [5] A.M. Choi, J. Alam, Heme oxygenase-1: Function, regulation, and implication of a novel stress-inducible protein in oxidant-induced lung injury, *Am. J. Respir. Cell Mol. Biol.* 15 (1996) 9–19.

- [6] E. Niki, Eustress and distress, *Nippon Yakurigaku Zasshi* 129 (2007) 76–79.
- [7] H.L. Karlsson, P. Cronholm, J. Gustafsson, L. Möller, Copper oxide nanoparticles are highly toxic: A comparison between metal oxide nanoparticles and carbon nanotubes, *Chem. Res. Toxicol.* 21 (2008) 1726–1732.
- [8] H.L. Karlsson, J. Gustafsson, P. Cronholm, L. Möller, Size-dependent toxicity of metal oxide particles—A comparison between nano- and micrometer size, *Toxicol. Lett.* 188 (2009) 112–118.
- [9] B. Fahmy, S.A. Cormier, Copper oxide nanoparticles induce oxidative stress and cytotoxicity in airway epithelial cells, *Toxicol. In Vitro* 23 (2009) 1365–1371.
- [10] H. Yang, C. Liu, D. Yang, H. Zhang, Z. Xi, Comparative study of cytotoxicity, oxidative stress and genotoxicity induced by four typical nanomaterials: The role of particle size, shape and composition, *J. Appl. Toxicol.* 29 (2009) 69–78.
- [11] W. Lin, Y. Xu, C.C. Huang, Y. Ma, K.B. Shannon, D.R. Chen, Y.W. Huang, Toxicity of nano- and micro-sized ZnO particles in human lung epithelial cells, *J. Nanopart. Res.* 11 (2009) 25–39.
- [12] M. Horie, K. Nishio, K. Fujita, H. Kato, S. Endoh, M. Suzuki, A. Nakamura, A. Miyauchi, S. Kinugasa, K. Yamamoto, H. Iwahashi, H. Murayama, *et al.*, Cellular responses by stable and uniform ultrafine titanium dioxide particles in culture-medium dispersions when secondary particle size was 100 nm or less, *Toxicol. In Vitro* 24 (2010) 1629–1638.
- [13] J.R. Gurr, A.S. Wang, C.H. Chen, K.Y. Jan, Ultrafine titanium dioxide particles in the absence of photoactivation can induce oxidative damage to human bronchial epithelial cells, *Toxicology* 213 (2005) 66–73.
- [14] C.C. Huang, R.S. Aronstam, D.R. Chen, Y.W. Huang, Oxidative stress, calcium homeostasis, and altered gene expression in human lung epithelial cells exposed to ZnO nanoparticles, *Toxicol. In Vitro* 24 (2010) 45–55.
- [15] T. Xia, M. Kovochich, M. Liong, L. Mädler, B. Gilbert, H. Shi, J.I. Yeh, J.I. Zink, A.E. Nel, Comparison of the mechanism of toxicity of zinc oxide and cerium oxide nanoparticles based on dissolution and oxidative stress properties, *ACS Nano* 2 (2008) 2121–2134.
- [16] E.J. Park, H. Kim, Y. Kim, J. Yi, K. Choi, K. Park, Inflammatory responses may be induced by a single intratracheal instillation of iron nanoparticles in mice, *Toxicology* 275 (2010) 65–71.
- [17] E.J. Park, J. Choi, Y.K. Park, K. Park, Oxidative stress induced by cerium oxide nanoparticles in cultured BEAS-2B cells, *Toxicology* 245 (2008) 90–100.
- [18] H.J. Eom, J. Choi, Oxidative stress of CeO₂ nanoparticles via p38-Nrf-2 signaling pathway in human bronchial epithelial cell, Beas-2B, *Toxicol. Lett.* 187 (2009) 77–83.
- [19] W. Lin, Y.W. Huang, X.D. Zhou, Y. Ma, Toxicity of cerium oxide nanoparticles in human lung cancer cells, *Int. J. Toxicol.* 25 (2006) 451–457.
- [20] D. Schubert, R. Dargusch, J. Raitano, S.W. Chan, Cerium and yttrium oxide nanoparticles are neuroprotective, *Biochem. Biophys. Res. Commun.* 342 (2006) 86–91.
- [21] S.M. Hirst, A.S. Karakoti, R.D. Tyler, N. Sriranganathan, S. Seal, C.M. Reilly, Anti-inflammatory properties of cerium oxide nanoparticles, *Small* 5 (2009) 2848–2856.
- [22] A. Gojova, J.T. Lee, H.S. Jung, B. Guo, A.I. Barakat, I.M. Kennedy, Effect of cerium oxide nanoparticles on inflammation in vascular endothelial cells, *Inhal. Toxicol.* 21 (Suppl. 1) (2009) 123–130.
- [23] B. Park, P. Martin, C. Harris, R. Guest, A. Whittingham, P. Jenkinson, J. Handley, Initial in vitro screening approach to investigate the potential health and environmental hazards of Enviroxtrade mark—A nanoparticulate cerium oxide diesel fuel additive, *Part. Fibre Toxicol.* 4 (2007) 12.

- [24] B. Park, K. Donaldson, R. Duffin, L. Tran, F. Kelly, I. Mudway, J.P. Morin, R. Guest, P. Jenkinson, Z. Samaras, M. Giannouli, H. Kouridis, *et al.*, Hazard and risk assessment of a nanoparticulate cerium oxide-based diesel fuel additive—A case study, *Inhal. Toxicol.* 20 (2008) 547–566.
- [25] B.K. Pierscionek, Y. Li, A.A. Yasseen, L.M. Colhoun, R.A. Schachar, W. Chen, Nanoceria have no genotoxic effect on human lens epithelial cells, *Nanotechnology* 21 (2010) 035102.
- [26] F. Marano, S. Hussain, F. Rodrigues-Lima, A. Baeza-Squiban, S. Boland, Nanoparticles: Molecular targets and cell signaling, *Arch. Toxicol.* (2010) May 26. [Epub ahead of print].
- [27] M. Kobayashi, M. Yamamoto, Molecular mechanisms activating the Nrf2-Keap1 pathway of antioxidant gene regulation, *Antioxid. Redox Signal.* 7 (2005) 385–394.
- [28] M. Kobayashi, M. Yamamoto, Nrf2-Keap1 regulation of cellular defense mechanisms against electrophiles and reactive oxygen species, *Adv. Enzyme Regul.* 46 (2006) 113–140.
- [29] J.C. Lai, M.B. Lai, S. Jandhyam, V.V. Dukhande, A. Bhushan, C.K. Daniels, S.W. Leung, Exposure to titanium dioxide and other metallic oxide nanoparticles induces cytotoxicity on human neural cells and fibroblasts, *Int. J. Nanomed.* 3 (2008) 533–545.
- [30] Q. Rahman, M. Lohani, E. Dopp, H. Pemsel, L. Jonas, D.G. Weiss, D. Schiffmann, Evidence that ultrafine titanium dioxide induces micronuclei and apoptosis in Syrian hamster embryo fibroblasts, *Environ. Health Perspect.* 110 (2002) 797–800.
- [31] Y. Shi, F. Wang, J. He, S. Yadav, H. Wang, Titanium dioxide nanoparticles cause apoptosis in BEAS-2B cells through the caspase 8/t-Bid-independent mitochondrial pathway, *Toxicol. Lett.* 196 (2010) 21–27.
- [32] Y. Saito, K. Nishio, Y. Ogawa, J. Kimata, T. Kinumi, Y. Yoshida, N. Noguchi, E. Niki, Turning point in apoptosis/necrosis induced by hydrogen peroxide, *Free Radic. Res.* 40 (2006) 619–630.
- [33] J.M. Veranth, E.G. Kaser, M.M. Veranth, M. Koch, G.S. Yost, Cytokine responses of human lung cells (BEAS-2B) treated with micron-sized and nanoparticles of metal oxides compared to soil dusts, *Part. Fibre Toxicol.* 27 (2007) 2.
- [34] K. Nishi, Y. Morimoto, A. Ogami, M. Murakami, T. Myojo, T. Oyabu, C. Kadoya, M. Yamamoto, M. Todoroki, M. Hirohashi, S. Yamasaki, K. Fujita, *et al.*, Expression of cytokine-induced neutrophil chemoattractant in rat lungs by intratracheal instillation of nickel oxide nanoparticles, *Inhal. Toxicol.* 21 (2009) 1030–1039.
- [35] Y. Morimoto, A. Ogami, M. Todoroki, M. Yamamoto, M. Murakami, M. Hirohashi, T. Oyabu, T. Myojo, K. Nishi, C. Kadoya, S. Yamasaki, H. Nagatomo, *et al.*, Expression of inflammation-related cytokines following intratracheal instillation of nickel oxide nanoparticles, *Nanotoxicology* 4 (2010) 161–176.
- [36] E.M. Rossi, L. Pyllkänen, A.J. Koivisto, M. Vippola, K.A. Jensen, M. Miettinen, K. Sirola, H. Nykäsenoja, P. Karisola, T. Stjernvall, E. Vanhala, M. Kiilunen, *et al.*, Airway exposure to silica-coated TiO₂ nanoparticles induces pulmonary neutrophilia in mice, *Toxicol. Sci.* 113 (2010) 422–433.
- [37] G. Oberdörster, Pulmonary deposition, clearance and effects of inhaled soluble and insoluble cadmium compounds, *IARC Sci. Publ.* 118 (1992) 189–204.
- [38] M. Horie, K. Nishio, K. Fujita, H. Kato, A. Nakamura, S. Kinugasa, S. Endoh, A. Miyauchi, K. Yamamoto, H. Murayama, E. Niki, H. Iwahashi, *et al.*, Ultrafine NiO particles induce cytotoxicity in vitro by cellular uptake and subsequent Ni(II) release, *Chem. Res. Toxicol.* 22 (2009) 1415–1426.
- [39] U. Heinrich, R. Fuhst, S. Rittinghausen, O. Creutzenberg, B. Bellmann, W. Koch, K. Levens, Chronic inhalation exposure of Wistar rats and two different strains of mice to diesel engine exhaust, carbon black, and titanium dioxide, *Inhal. Toxicol.* 7 (1995) 533–556.

- [40] P.M. Hext, J.A. Tomenson, P. Thompson, Titanium dioxide: Inhalation toxicology and epidemiology, *Ann. Occup. Hyg.* 49 (2005) 461–472.
- [41] D.B. Warheit, J.F. Hansen, I.S. Yuen, D.P. Kelly, S.I. Snajdr, M.A. Hartsky, Inhalation of high concentrations of low toxicity dusts in rats results in impaired pulmonary clearance mechanisms and persistent inflammation, *Toxicol. Appl. Pharmacol.* 145 (1997) 10–22.
- [42] G. Oberdörster, J. Ferin, B.E. Lehnert, Correlation between particle size, in vivo particle persistence, and lung injury, *Environ. Health Perspect.* 102 (Suppl. 5) (1994) 173–179.
- [43] P.J. Borm, R.P. Schins, C. Albrecht, Inhaled particles and lung cancer, part B: Paradigms and risk assessment, *Int. J. Cancer* 110 (2004) 3–14.
- [44] M. Geiser, B. Rothen-Rutishauser, N. Kapp, S. Schürch, W. Kreyling, H. Schulz, M. Semmler, V. Im Hof, J. Heyder, P. Gehr, Ultrafine particles cross cellular membranes by nonphagocytic mechanisms in lungs and in cultured cells, *Environ. Health Perspect.* 113 (2005) 1555–1560.
- [45] M. Horie, K. Nishio, K. Fujita, S. Endoh, A. Miyauchi, Y. Saito, H. Iwahashi, K. Yamamoto, H. Murayama, H. Nakano, N. Nanashima, E. Niki, *et al.*, Protein adsorption of ultrafine metal oxide and its influence on cytotoxicity toward cultured cells, *Chem. Res. Toxicol.* 22 (2009) 543–553.
- [46] F. Watari, N. Takashi, A. Yokoyama, M. Uo, T. Akasaka, Y. Sato, S. Abe, Y. Totsuka, K. Tohji, Material nanosizing effect on living organisms: Non-specific, biointeractive, physical size effects, *J. R. Soc. Interface* 6 (Suppl. 3) (2009) S371–S388.
- [47] C.M. Sayes, K.L. Reed, D.B. Warheit, Assessing toxicity of fine and nanoparticles: Comparing in vitro measurements to in vivo pulmonary toxicity profiles, *Toxicol. Sci.* 97 (2007) 163–180.
- [48] K. Adachi, N. Yamada, K. Yamamoto, Y. Yoshida, O. Yamamoto, In vivo effect of industrial titanium dioxide nanoparticles experimentally exposed to hairless rat skin, *Nanotoxicology* 4 (2010) 296–306.
- [49] N. Kobayashi, M. Naya, S. Endoh, J. Maru, K. Yamamoto, J. Nakanishi, Comparative pulmonary toxicity study of nano-TiO₂ particles of different sizes and agglomerations in rats: Different short- and long-term post-instillation results, *Toxicology* 264 (2009) 110–118.
- [50] B.O. Stuart, Deposition and clearance of inhaled particles, *Environ. Health Perspect.* 55 (1984) 369–390.
- [51] C.M. Sayes, R. Wahi, P.A. Kurian, Y. Liu, J.L. West, K.D. Ausman, D.B. Warheit, V.L. Colvin, Correlating nanoscale titania structure with toxicity: A cytotoxicity and inflammatory response study with human dermal fibroblasts and human lung epithelial cells, *Toxicol. Sci.* 92 (2006) 174–185.
- [52] R. Cai, Y. Kubota, T. Shuin, H. Sakai, K. Hashimoto, A. Fujishima, Induction of cytotoxicity by photoexcited TiO₂ particles, *Cancer Res.* 52 (1992) 2346–2348.
- [53] T. Xia, M. Kovochich, J. Brant, M. Hotze, J. Sempf, T. Oberley, C. Sioutas, J.I. Yeh, M.R. Wiesner, A.E. Nel, Comparison of the abilities of ambient and manufactured nanoparticles to induce cellular toxicity according to an oxidative stress paradigm, *Nano Lett.* 6 (2006) 1794–1807.
- [54] P. Thevenot, J. Cho, D. Wavhal, R.B. Timmons, L. Tang, Surface chemistry influences, cancer killing effect of TiO₂ nanoparticles, *Nanomedicine* 4 (2008) 226–236.
- [55] D.B. Warheit, T.R. Webb, C.M. Sayes, V.L. Colvin, K.L. Reed, Pulmonary instillation studies with nanoscale TiO₂ rods and dots in rats: Toxicity is not dependent upon particle size and surface area, *Toxicol. Sci.* 91 (2006) 227–236.
- [56] D.B. Warheit, K.L. Reed, C.M. Sayes, A role for nanoparticle surface reactivity in facilitating pulmonary toxicity and development of a base set of hazard assays as a

- component of nanoparticle risk management, *Inhal. Toxicol.* 21 (Suppl. 1) (2009) 61–67.
- [57] D.B. Warheit, T.R. Webb, V.L. Colvin, K.L. Reed, C.M. Sayes, Pulmonary bioassay studies with nanoscale and fine-quartz particles in rats: Toxicity is not dependent upon particle size but on surface characteristics, *Toxicol. Sci.* 95 (2007) 270–280.
- [58] D.B. Warheit, T.R. Webb, K.L. Reed, S. Frerichs, C.M. Sayes, Pulmonary toxicity study in rats with three forms of ultrafine-TiO₂ particles: Differential responses related to surface properties, *Toxicology* 30 (2007) 90–104.
- [59] K. Kasemets, A. Ivask, H.C. Dubourguier, A. Kahru, Toxicity of nanoparticles of ZnO, CuO and TiO₂ to yeast *Saccharomyces cerevisiae*, *Toxicol. In Vitro* 23 (2009) 1116–1122.
- [60] A.M. Studer, L.K. Limbach, L. Van Duc, F. Krumeich, E.K. Athanassiou, L.C. Gerber, H. Moch, W.J. Stark, Nanoparticle cytotoxicity depends on intracellular solubility: Comparison of stabilized copper metal and degradable copper oxide nanoparticles, *Toxicol. Lett.* 197 (2010) 169–174.
- [61] K. Jones, G.R. Sharpe, Ni²⁺ blocks the Ca²⁺ influx in human keratinocytes following a rise in extracellular Ca²⁺, *Exp. Cell Res.* 212 (1994) 409–413.
- [62] G.G. Fletcher, F.E. Rossetto, J.D. Turnbull, E. Nieboer, Toxicity, uptake, and mutagenicity of particulate and soluble nickel compounds, *Environ. Health Perspect.* 102 (1994) 69–79.
- [63] S.I. Liochev, I. Fridovich, Mechanism of the peroxidase activity of Cu, Zn superoxide dismutase, *Free Radic. Biol. Med.* 48 (2010) 1565–1569.
- [64] N.K. Urbański, A. Beresewicz, Generation of •OH initiated by interaction of Fe²⁺ and Cu⁺ with dioxygen; comparison with the Fenton chemistry, *Acta Biochim. Pol.* 47 (2000) 951–962.
- [65] M.S. Ehrenberg, A.E. Friedman, J.N. Finkelstein, G. Oberdörster, J.L. McGrath, The influence of protein adsorption on nanoparticle association with cultured endothelial cells, *Biomaterials* 30 (2009) 603–610.
- [66] L.K. Limbach, Y. Li, R.N. Grass, T.J. Brunner, M.A. Hintermann, M. Muller, D. Gunther, W.J. Stark, Oxide nanoparticle uptake in human lung fibroblasts: Effects of particle size, agglomeration, and diffusion at low concentrations, *Environ. Sci. Technol.* 39 (2005) 9370–9376.
- [67] S. Patil, A. Sandberg, E. Heckert, W. Self, S. Seal, Protein adsorption and cellular uptake of cerium oxide nanoparticles as a function of zeta potential, *Biomaterials* 28 (2007) 4600–4607.
- [68] A.J. Wagner, C.A. Bleckmann, R.C. Murdock, A.M. Schrand, J.J. Schlager, S.M. Hussain, Cellular interaction of different forms of aluminum nanoparticles in rat alveolar macrophages, *J. Phys. Chem. B* 111 (25) (2007) 7353–7359.
- [69] G. Oberdörster, Toxicokinetics and effects of fibrous and nonfibrous particles, *Inhal. Toxicol.* 14 (2002) 29–56.
- [70] K.W. Powers, S.C. Brown, V.B. Krishna, S.C. Wasdo, B.M. Moudgil, S.M. Roberts, Research strategies for safety evaluation of nanomaterials. Part VI. Characterization of nanoscale particles for toxicological evaluation, *Toxicol. Sci.* 90 (2006) 296–303.
- [71] K.W. Powers, M. Palazuelos, B.M. Moudgil, S.M. Roberts, Characterization of the size, shape, and state of dispersion of nanoparticles for toxicological studies, *Nanotoxicology* 1 (2007) 42–51.
- [72] J.M. Wörle-Knirsch, K. Pulskamp, H.F. Krug, Oops they did it again! Carbon nanotubes hoax scientists in viability assays, *Nano Lett.* 6 (2006) 1261–1268.
- [73] J.G. Teeguarden, P.M. Hinderliter, G. Orr, B.D. Thrall, J.G. Pounds, Particokinetics *in vitro*: Dosimetry considerations for in vitro nanoparticle toxicity assessments, *Toxicol. Sci.* 95 (2007) 300–312.

- [74] H. Kato, M. Suzuki, K. Fujita, M. Horie, S. Endoh, Y. Yoshida, H. Iwahashi, K. Takahashi, A. Nakamura, S. Kinugasa, Reliable size determination of nanoparticles using dynamic light scattering method for in vitro toxicology assessment, *Toxicol. In Vitro* 23 (2009) 927–934.
- [75] H. Kato, K. Fujita, M. Horie, M. Suzuki, A. Nakamura, S. Endoh, Y. Yoshida, H. Iwahashi, K. Takahashi, S. Kinugasa, Dispersion characteristics of various metal oxide secondary nanoparticles in culture medium for in vitro toxicology assessment, *Toxicol. In Vitro* 24 (2010) 1009–1018.
- [76] D.B. Warheit, C.M. Sayes, K.L. Reed, Nanoscale and fine zinc oxide particles: Can in vitro assays accurately forecast lung hazards following inhalation exposures? *Environ. Sci. Technol.* 43 (2009) 7939–7945.
- [77] T.J. Brunner, P. Wick, P. Manser, P. Spohn, R.N. Grass, L.K. Limbach, A. Bruinink, W.J. Stark, *In vitro* cytotoxicity of oxide nanoparticles: Comparison to asbestos, silica, and the effect of particle solubility, *Environ. Sci. Technol.* 40 (2006) 4374–4381.
- [78] M. Shimizu, H. Tainaka, T. Oba, K. Mizuo, M. Umezawa, K. Takeda, Maternal exposure to nanoparticulate titanium dioxide during the prenatal period alters gene expression related to brain development in the mouse, *Part. Fibre Toxicol.* 6 (2009) 20.
- [79] L. Ma, J. Liu, N. Li, J. Wang, Y. Duan, J. Yan, H. Liu, H. Wang, F. Hong, Oxidative stress in the brain of mice caused by translocated nanoparticulate TiO₂ delivered to the abdominal cavity, *Biomaterials* 31 (2010) 99–105.
- [80] K. Takeda, K. Suzuki, A. Ishihara, M. Kubo-Irie, R. Fujimoto, M. Tabata, S. Oshio, Y. Nihei, T. Ihara, M. Sugamata, Nanoparticles transferred from pregnant mice to their offspring can damage the genital and cranial nerve systems, *J. Health Sci.* 55 (2009) 95–102.
- [81] T. Komatsu, M. Tabata, M. Kubo-Irie, T. Shimizu, K. Suzuki, Y. Nihei, K. Takeda, The effects of nanoparticles on mouse testis Leydig cells *in vitro*, *Toxicol. In Vitro* 22 (2008) 1825–1831.
- [82] D.H. Blohm, A. Guiseppi-Elie, New developments in microarray technology, *Curr. Opin. Biotechnol.* 12 (2001) 41–47.
- [83] S. Katsuma, K. Nishi, K. Tanigawara, H. Ikawa, S. Shiojima, K. Takagaki, Y. Kaminishi, Y. Suzuki, A. Hirasawa, T. Ohgi, J. Yano, Y. Murakami, *et al.*, Molecular monitoring of bleomycin-induced pulmonary fibrosis by cDNA microarray-based gene expression profiling, *Biochem. Biophys. Res. Commun.* 288 (2001) 747–751.
- [84] S.A. McDowell, K. Gammon, B. Zingarelli, C.J. Bachurski, B.J. Aronow, D.R. Prows, G.D. Leikauf, Inhibition of nitric oxide restores surfactant gene expression following nickel-induced acute lung injury, *Am. J. Respir. Cell Mol. Biol.* 28 (2003) 188–198.
- [85] F. Zuo, N. Kaminski, E. Eugui, J. Allard, Z. Yakhini, A. Ben-Dor, L. Lollini, D. Morris, Y. Kim, B. DeLustro, D. Sheppard, A. Pardo, *et al.*, Gene expression analysis reveals matrilysin as a key regulator of pulmonary fibrosis in mice and humans, *Proc. Natl. Acad. Sci. USA* 99 (2002) 6292–6297.
- [86] C.S. Stevenson, C. Docx, R. Webster, C. Battram, D. Hynx, J. Giddings, P.R. Cooper, P. Chakravarty, I. Rahman, J.A. Marwick, P.A. Kirkham, C. Charman, *et al.*, Comprehensive gene expression profiling of rat lung reveals distinct acute and chronic responses to cigarette smoke inhalation, *Am. J. Physiol. Lung Cell. Mol. Physiol.* 293 (2007) 1183–1193.
- [87] V.H. Grassian, P.T. O'shaughnessy, A. Adamcukova-Dodd, J.M. Pettibone, P.S. Thorne, Inhalation exposure study of titanium dioxide nanoparticles with a primary particle size of 2 to 5 nm, *Environ. Health Perspect.* 115 (2007) 397–402.

- [88] C.A. Poland, R. Duffin, I. Kinloch, A. Maynard, W.A. Wallace, A. Seaton, V. Stone, S. Brown, W. Macnee, K. Donaldson, Carbon nanotubes introduced into the abdominal cavity of mice show asbestos-like pathogenicity in a pilot study, *Nat. Nanotechnol.* 7 (2008) 423–428.
- [89] D.B. Warheit, B.R. Laurence, K.L. Reed, D.H. Roach, G.A. Reynolds, T.R. Webb, Comparative pulmonary toxicity assessment of single-wall carbon nanotubes in rats, *Toxicol. Sci.* 77 (2004) 117–125.
- [90] L.A. Mitchell, J. Gao, R.V. Wal, A. Gigliotti, S.W. Burchiel, J.D. McDonald, Pulmonary and systemic immune response to inhaled multiwalled carbon nanotubes, *Toxicol. Sci.* 100 (2007) 203–214.
- [91] L. Ma-Hock, S. Treumann, V. Strauss, S. Brill, F. Luizi, M. Mertler, K. Wiench, A.O. Gamer, B. van Ravenzwaay, R. Landsiedel, Inhalation toxicity of multiwall carbon nanotubes in rats exposed for 3 months, *Toxicol. Sci.* 112 (2009) 468–481.
- [92] D.W. Porter, A.F. Hubbs, R.R. Mercer, N. Wu, M.G. Wolfarth, K. Sriram, S. Leonard, L. Battelli, D. Schwegler-Berry, S. Friend, M. Andrew, B.T. Chen, *et al.*, Mouse pulmonary dose- and time course-responses induced by exposure to multi-walled carbon nanotubes, *Toxicology* 269 (2010) 136–147.
- [93] J.P. Ryman-Rasmussen, M.F. Cesta, A.R. Brody, J.K. Shipley-Phillips, J.I. Everitt, E.W. Tewksbury, O.R. Moss, B.A. Wong, D.E. Dodd, M.E. Andersen, J.C. Bonner, Inhaled carbon nanotubes reach the subpleural tissue in mice, *Nat. Nanotechnol.* 11 (2009) 747–751.
- [94] C.M. Sayes, A.A. Marchione, K.L. Reed, D.B. Warheit, Comparative pulmonary toxicity assessments of C₆₀ water suspensions in rats: Few differences in fullerene toxicity in vivo in contrast to in vitro profiles, *Nano Lett.* 7 (2007) 399–406.
- [95] G.L. Baker, A. Gupta, M.L. Clark, B.R. Valenzuela, L.M. Staska, S.J. Harbo, J.T. Pierce, J.A. Dill, Inhalation toxicity and lung toxicokinetics of C60 fullerene nanoparticles and fine-particles, *Toxicol. Sci.* 101 (2008) 122–131.
- [96] H.W. Chen, S.F. Su, C.T. Chien, W.H. Lin, S.L. Yu, C.C. Chou, J.J. Chen, P.C. Yang, Titanium dioxide nanoparticles induce emphysema-like lung injury in mice, *FASEB J.* 20 (2006) 2393–2395.
- [97] C.C. Chou, H.Y. Hsiao, Q.S. Hong, C.H. Chen, Y.W. Peng, H.W. Chen, P.C. Yang, Single-walled carbon nanotubes can induce pulmonary injury in mouse model, *Nano Lett.* 8 (2008) 437–445.
- [98] K. Fujita, Y. Morimoto, A. Ogami, I. Tanaka, S. Endoh, K. Uchida, H. Tao, M. Akasaka, M. Inada, K. Yamamoto, H. Fukui, M. Hayakawa, *et al.*, A gene expression profiling approach to study the influence of ultrafine particles on rat lungs, in: J.Y. Kim, U. Platt, M.B. Gu, H. Iwahashi (Eds.), *Atmospheric and Biological Environmental Monitoring*, Springer-Verlag GmbH, Netherlands, 2009, pp. 221–229.
- [99] Y. Morimoto, A. Ogami, M. Todoroki, M. Yamamoto, M. Murakami, M. Hirohashi, T. Oyabu, T. Myojo, K. Nishi, C. Kadoya, S. Yamasaki, H. Nagatomo, *et al.*, Expression of inflammation related-cytokines following intra-tracheal instillation of nickel oxide nanoparticles, *Nanotoxicology* 4 (2010) 1–16.
- [100] Y. Morimoto, M. Hirohashi, A. Ogami, T. Oyabu, T. Myojo, K. Nishi, C. Kadoya, M. Todoroki, M. Yamamoto, M. Murakami, M. Shimada, W.N. Wang, *et al.*, Inflammogenic effect of well-character sized fullerenes in inhalation and intratracheal instillation studies, Part. *Fibre Toxicol.* 14 (7) (2010) 4.
- [101] K. Fujita, Y. Morimoto, A. Ogami, T. Myojo, I. Tanaka, M. Shimada, W.N. Wang, S. Endoh, K. Uchida, T. Nakazato, K. Yamamoto, H. Fukui, *et al.*, Gene expression profiles in rat lung after inhalation exposure to C₆₀ fullerene particles, *Toxicology* 258 (2009) 47–55.

- [102] K. Fujita, Y. Morimoto, S. Endoh, K. Uchida, H. Fukui, A. Ogami, I. Tanaka, M. Horie, Y. Yoshida, H. Iwahashi, J. Nakanishi, Identification of potential biomarkers from gene expression profiles in rat lungs intratracheally instilled with C(60) fullerenes, *Toxicology* 274 (2010) 34–41.
- [103] J. Jiang, G. Oberdoorster, P. Biswas, Characterization of size, surface charge, and agglomeration state of nanoparticle dispersions for toxicological studies, *J. Nanopart. Res.* 11 (2009) 77–89.
- [104] S.C. Kim, D.R. Chen, C. Qi, R.M. Gelein, J.N. Finkelstein, A. Elder, K. Bentley, G. Oberdörster, D.Y. Pui, A nanoparticle dispersion method for *in vitro* and *in vivo* nanotoxicity study, *Nanotoxicology* 4 (2010) 42–51.
- [105] S. Endoh, J. Maru, K. Uchida, K. Yamamoto, J. Nakanishi, Preparing samples for fullerene C₆₀ hazard tests: Stable dispersion of fullerene crystals in water using a bead mill, *Adv. Powder Technol.* 20 (2009) 567–575.
- [106] M. Shimada, W.N. Wang, K. Okuyama, T. Myojo, T. Oyabu, Y. Morimoto, I. Tanaka, S. Endoh, K. Uchida, K. Ehara, H. Sakurai, K. Yamamoto, *et al.*, Development and evaluation of an aerosol generation and supplying system for inhalation experiments of manufactured nanoparticles, *Environ. Sci. Technol.* 43 (2009) 5529–5534.
- [107] Y. Morimoto, N. Kobayashi, N. Shinohara, T. Myojo, I. Tanaka, J. Nakanishi, Hazard assessments of manufactured nanomaterials, *J. Occup. Health* 52 (2010) 325–334.
- [108] Y.W. Huang, C.H. Wu, R.S. Aronstam, Toxicity of transition metal oxide nanoparticles: Recent insights from *in vitro* studies, *Materials* 3 (2010) 4842–4859.
- [109] H. Tsuda, J. Xu, Y. Sakai, M. Futakuchi, K. Fukamachi, Toxicology of engineered nanomaterials—A review of carcinogenic potential, *Asian Pac. J. Cancer Prev.* 10 (2009) 975–980.
- [110] C.M. Sayes, D.B. Warheit, Characterization of nanomaterials for toxicity assessment, *Wiley Interdiscip. Rev. Nanomed. Nanobiotechnol.* 1 (2009) 660–670.
- [111] M. Valko, C.J. Rhodes, J. Moncol, M. Izakovic, M. Mazur, Free radicals, metals and antioxidants in oxidative stress-induced cancer, *Chem. Biol. Interact.* 160 (2006) 1–40.

TOXICITY OF SILVER NANOMATERIALS IN HIGHER EUKARYOTES

Marcin Kruszewski,^{1,*} Kamil Brzoska,¹ Gunnar Brunborg,²
Nana Asare,² Małgorzata Dobrzyńska,³ Mária Dušinská,^{4,5}
Lise M. Fjellsbø,⁴ Anastasia Georgantzopoulou,⁶
Joanna Gromadzka-Ostrowska,⁷ Arno C. Gutleb,⁶ Anna Lankoff,^{1,8}
Zuzana Magdolenová,⁴ Elise R. Pran,⁴ Alessandra Rinna,⁴
Christine Instanes,² Wiggo J. Sandberg,² Per Schwarze,²
Tomasz Stępkowski,¹ Maria Wojewódzka,¹ and Magne Refsnes²

Contents

1. Introduction	180
2. Cellular Uptake	181
2.1. Kinetics of cellular uptake of AgNPs	181
2.2. Mechanisms of the cellular uptake of AgNPs <i>in vitro</i>	182
2.3. Intracellular distribution of internalized AgNPs	182
3. Toxicity of AgNPs	184
3.1. Toxicity <i>in vitro</i>	184
3.2. <i>In vivo</i> toxicity in mammals	191
3.3. Toxicity in nonmammalian eukaryotes	198
4. Inflammatory Response	205
5. The Role of Oxidative Stress in AgNP-Induced Toxicity and DNA Damage	206
6. Summary	211

¹ Institute of Nuclear Chemistry & Technology, Centre for Radiobiology and Biological Dosimetry
Warsaw, Poland

² Norwegian Institute of Public Health, Department of Air Pollution and Noise, Oslo, Norway

³ National Institute of Public Health-National Institute of Hygiene, Department of Radiation Protection and
Radiobiology Warsaw, Poland

⁴ Norwegian Institute for Air Research, Centre for Ecology and Economics, Health Effects Group, Kjeller,
Norway

⁵ Slovak Medical University, Department of Experimental and Applied Genetics, Bratislava, Slovakia

⁶ Centre de Recherche Public-Gabriel Lippmann, Belvaux, Luxembourg

⁷ Warsaw University of Life Sciences, Faculty of Human Nutrition and Consumer Sciences, Warsaw, Poland

⁸ The Jan Kochanowski University of Humanities and Sciences, Department of Radiobiology and Immunol-
ogy Kielce, Poland

*Corresponding author. Tel.: +48-22-5041118; Fax: +48-22-5041341

E-mail address: m.kruszewski@ichtj.waw.pl

Acknowledgments	212
References	212

Abstract

The rapid expansion of nanotechnology promises to have significant benefits to society, yet there is increasing concern that exposure to nanoparticles (particles typically < 100 nm in size) will have negative impact on both human and environmental health. Due to its well-known bactericide properties, silver nanoparticles (AgNPs) are nowadays among the most commercialized nanomaterials, but surprisingly studies concerning toxicity at the cellular and molecular level are rather limited and the mechanisms that lay behind AgNPs toxicity are far from being understood. This critical review presents a detailed analysis of data on the *in vitro* and *in vivo* uptake, biodistribution, and toxicity of AgNPs. Emphasis is placed on the systematization of data over animal and cell models, organs examined, doses applied, the type of particle administration, and the time of examination.

1. INTRODUCTION

The rapid expansion in the field of nanotechnology is likely to benefit the society, yet there are increasing concerns that human and environmental exposure to nanoparticles (NPs) and nanomaterials may produce adverse effects. NPs and nanomaterials are defined as substances with at least one dimension less than 100 nm in size, such particles can take many different forms, for example, different crystal forms, tubes, rods, wires, spheres or, more elaborate structures, such as core-shell NPs. Due to their small size and high surface area, coupled to other physicochemical properties such as metal contaminants, coating and charged surfaces, and quantum-related effects, introduction of nanomaterials into the human environment may have unexpected consequences, both beneficial and harmful.

Silver is a well-known bactericide, but this review neither considers its antimicrobial effects (for review, see Refs. [1] and [2]) nor includes non-particulate forms of silver, such as silver ions or organic compounds of silver used in many consumer goods; only particulate forms of nanoscale silver are discussed. Silver nanoparticles (AgNPs) are widely used in medicine, physics, material sciences, and chemistry. Many medical products are coated or embedded with nanosilver, for example, contraceptive devices, surgical instruments, bone prostheses, and dental alloys. However, little is known about their *in vivo* behavior, tissue distribution as well as adverse health effects in mammals, including humans. Being present in many consumer goods, AgNPs can easily penetrate the human body through different portals, for example, AgNPs released from different surface coatings can be readily inhaled [3] or AgNPs can be directly absorbed from medical devices, such as catheters or dental and bone implants [4]. AgNPs present in

dressings for burns and bandages and ointments used for wound healing, nanosilver-based textiles, and cosmetics (like antibacterial deodorants) can penetrate into both compromised and intact skin [5,6] and can localize in the stratum corneum and the upper layers of epidermis [7]. These findings raise a concern over the widespread use of AgNPs in consumer products.

AgNPs present in consumer goods are released into the environment, where they could be bioaccumulated or enter the food chain or drinking water supplies [8,9]. The environmental fate of nanosilver will depend upon the nature of the NPs. NPs that aggregate and/or associate with dissolved or particulate natural materials will likely end up deposited in sediments or soils. Some types of AgNPs, however, are engineered to remain dispersed in water. The bioavailability of these materials can be determined by their uptake when in contact with organisms. The potential threat and persistence of these particles, on timescales of environmental relevance (days to years), are not known.

Despite the fact that AgNPs are among the most commercialized nanomaterials, studies concerning toxicity at the cellular and molecular level are rather limited and the mechanisms that lay behind AgNP toxicity are far from being understood. NPs and cellular components share a similar size, and, therefore, it is highly likely that AgNPs could interact with cells and cross barriers, such as cell membranes, potentially resulting in adverse and unpredictable effects.



2. CELLULAR UPTAKE

2.1. Kinetics of cellular uptake of AgNPs

The uptake of AgNPs is relatively fast and time-dependent. Usually after 2 h exposure, the vast majority of cells contains AgNPs. Sometimes, uptake saturation is observed after prolonged incubation [10–13]. Gaiser *et al.* [10] demonstrated that 35 nm AgNPs and bulk silver particles (0.6–1.6 μm) were found in the cytoplasm of C3A human hepatocytes or Caco-2 human intestinal epithelial cells after 2 and 24 h of exposure; however, uptake of the NPs was greater than that of bulk particles. The kinetics of AgNP uptake in relation to shape and form was investigated by Lu *et al.* [11]. The transmission electron microscopy (TEM) showed that both 30 nm silver nanoprisms and 30 nm silver nanospheres penetrated into the human HaCaT keratinocytes and accumulated in the nucleus. Saturation of uptake was reached after 7 h for all the different forms of AgNPs (colloidal and powder spheres, colloidal and powder prisms) with similar dimensions. The uptake kinetics of all forms was nearly the same. In contrast, the surface charge of AgNPs significantly modified their uptake. Internalization of positively or negatively charged Ag dendrimer complexes (3–7 nm) or functionalized 50 nm AgNPs was more effective than that of neutral ones [14,15].

2.2. Mechanisms of the cellular uptake of AgNPs *in vitro*

NPs are taken up by a variety of cell types via different mechanisms, such as macropinocytosis, lipid raft-dependent endocytosis (caveolin-dependent, dynamin-dependent, dynamin-independent), clathrin-dependent endocytosis, and phagocytosis [16–19]. Despite the fact that these mechanisms have been extensively studied to elaborate the uptake of other biologically active molecules, such as viruses, proteins, and DNA, the exact mechanism of AgNP uptake is not completely understood. It is believed that different cell types may have different uptake mechanisms. Further, the mechanism of NP uptake can be influenced by several factors, such as morphology of the NPs, their size, concentration, and surface properties [20]. Attempts to identify the uptake routes of AgNPs led to the conclusion that they are internalized mainly through clathrin-dependent endocytosis and macropinocytosis. AshaRani *et al.* [21] found that the normal human IMR-90 lung fibroblasts and human U251 glioblastoma cells exposed to AgNPs (6–20 nm) at low temperature take up less AgNPs as compared to cells incubated at 37 °C. However, intracellular concentration of AgNPs showed a dose- and time-dependent increase at both temperatures. Inhibition of clathrin pits formation did not result in a complete inhibition of endocytosis. Moreover, TEM micrographs did not show the presence of coated endosomes. Therefore, AgNPs may be internalized by a mechanism different from clathrin-dependent endocytosis. When the cellular uptake through macropinocytosis was abolished, a significant decrease in AgNP uptake followed, suggesting an active involvement of that pathway. Inhibition of the caveolin-mediated endocytosis did not affect AgNP uptake. Similar results were reported by Greulich *et al.* [22] who observed that AgNPs were taken up by clathrin-dependent endocytosis and by macropinocytosis into human mesenchymal stem cells (hMSCs). Cytoplasmic vesicles were also formed in J774 A1 macrophages upon exposure to uncoated and uncharged AgNPs containing clusters of particles suggesting internalization via pinocytosis [23].

Quite often the surface of NPs is modified not only to avoid aggregation but also to prevent the interaction between the particle's surface and the cell. It has been suggested that surface modification can alter AgNPs properties and their subsequent distribution in the organism [24].

2.3. Intracellular distribution of internalized AgNPs

TEM can provide the most detailed information regarding *in vitro* NP uptake and localization by allowing both visualization of NP location within a cell or tissue and, in conjunction with spectroscopic methods, characterization of the composition of the internalized NPs (Figure 1). vanWinkle *et al.* [25] reported that AgNPs (20–40 nm) were found both

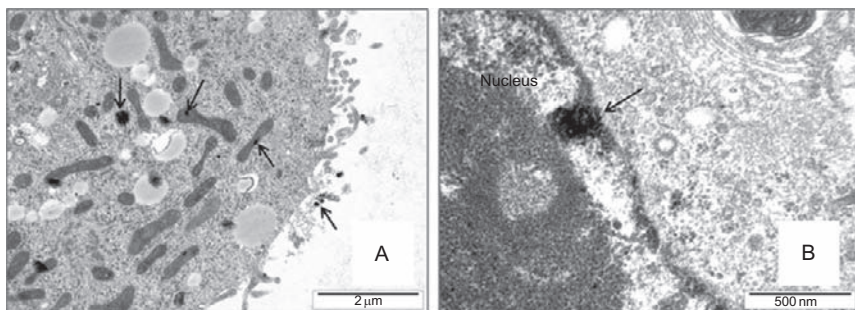


Figure 1 TEM microphotographs showing presence of AgNPs and their agglomerates (indicated by arrows) in cytoplasm and mitochondria (A) and nucleus (B) of HepG2 cells. Cells were treated with 20 nm AgNPs (50 μg/ml) for 2 h.

as agglomerates and as single particles in the cytoplasm, inside the nucleus, in the lysosomal compartment, and in the mitochondrial matrix of rat type I-like alveolar epithelial cell (R3-1). AgNPs lesser than 20 nm were evenly distributed as individual particles inside the R3-1 cells in filipodia, cytosol, cell nucleus, and mitochondria. Moreover, they not only appear not to be restricted to the mitochondrial intermediate space but also were found inside the matrix. The diameter of AgNPs inside the cells was significantly smaller (9–18 nm) than the documented average size (40 nm). This may indicate that only very small AgNPs enter the R3-1 cells and that smaller AgNPs rapidly traverse membranes. Uniform intracellular distribution of AgNPs was also observed by AshaRani *et al.* [21,24] in IMR-90 and U251 cells exposed to 6–20 nm AgNPs. While the peripheral cytoplasm of the treated cells showed numerous endosomes with engulfed NPs, AgNPs were also observed in the nucleus. The authors suggested that the particles may be able to pass through the pores of the nuclear envelope because of their small size. This observation was confirmed by Greulich *et al.* [22] who determined the intracellular distribution of internalized AgNPs in hMSCs after 24 h. They observed that the ingested AgNPs occurred in agglomerates in the perinuclear region. The molecular basis of this intracellular agglomeration of AgNPs is still not known; however, the authors suggested that it is likely that encapsulation in a membrane vesicle might be involved. However, in this study, fluorescent staining of cellular structures showed that AgNPs occurred in endolysosomal structures but not in the cell nucleus, endoplasmic reticulum, or Golgi complex.

The use of fluorescence and laser confocal microscopy in detection of NPs has also allowed researchers to track the paths taken by individual AgNPs within tissues and single living cells. The study performed by Chung *et al.* [26] revealed that spherical AgNPs (3.8 nm) were able to enter platelet cells and 3T3 fibroblasts and reach the cell nucleus within 2 h.

3. TOXICITY OF AgNPs

3.1. Toxicity *in vitro*

Several *in vitro* studies using various cell line-based models for gastrointestinal tract, skin, and lung exposure, etc. suggest that increasing concentrations of AgNPs lead to decreased viability and proliferation and induction of apoptosis (Table 1). Starch-coated AgNPs affected mitochondrial function in IMR-90 and U251 cells. The levels of necrosis and apoptosis were low and together with decreased ATP levels indicate metabolic arrest [24]. Mitochondrial membrane integrity of N2A murine neuroblastoma cells was altered, and actin cytoskeleton was disrupted upon exposure to both uncoated and polysaccharide-coated AgNPs (25 nm). Cell proliferation was decreased, and despite the addition of nerve growth factor, the effect persisted [46]. Induction of G1 arrest was observed in RAW264.7 mouse peritoneal macrophages exposed to uncoated AgNPs [53]. However, when J774 A1 macrophages were exposed to uncoated AgNPs of various sizes (3.1, 5.8, and 24.9 nm), cell proliferation was inhibited only by the smallest-sized NPs [23]. Polyvinylpyrrolidone-coated AgNPs (100 nm) were cytotoxic to hMSCs above 3 $\mu\text{g/ml}$ and caused a decrease of chemotaxis [36].

Polyvinylacetate- and starch-coated AgNPs caused concentration-dependent membrane damage in human erythrocytes and haemagglutination. The cells lost the biconcavity, appeared swollen, and hemolysis was observed. Therefore, it was suggested that wound dressings containing AgNPs could potentially result in hemolysis depending on the concentrations used in the product [27]. Diversion from normal shape and morphology was also apparent in HT-1080 human fibrosarcoma cells and A431 human skin carcinoma cells exposed to uncoated AgNPs. The mitochondrial activity was decreased above 6.25 $\mu\text{g/ml}$, and DNA laddering was observed, indicative of apoptosis [6]. However, cellulose gum-coated AgNPs did not induce cell death after exposure for 24 h up to a concentration of 0.02 ppm and did not enhance the effect of UVB-irradiation on apoptosis [30]. However, the concentrations tested were lower compared to the ones used in other studies, and the average size of the particles was 730.5 nm. Polyethylamine-stabilized AgNPs were toxic to HepG2 human hepatocytes at concentrations above 1 mg/l, whereas at lower concentrations, there was an increase in cell proliferation, suggesting that potential toxic agents could act as stimulants at low concentrations [38]. Viability was restored upon addition of cysteine; however, the morphological aberrations persisted suggesting that there could be a combined effect of both Ag ions and particles [38,39]. A dual effect depending on concentration was also observed in rat coronary endothelial cells exposed to uncoated AgNPs. Cell proliferation was inhibited at low

Table 1 *In vitro* models for AgNP toxicity assessment

Size (nm)	Surface coating	Model	Concentration tested	Exposure duration	Outcome	References
10.88 (PVA) 5.78 (starch)	PVA coated, starch coated	Human erythrocytes	25–400 µg/ml	3 h	Produced more severe effects than uncoated	[27]
30–50	PVP-coated Ag (0.2% PVP)	A549 human lung carcinoma cells	0–20 µg/l	24 h	ROS generation and apoptosis	[28]
18	Uncoated	Baby hamster kidney (BHK21) and human colon adenocarcinoma (HT29) cells	11 µg/ml	12, 24 h	AgNPs induced p53-mediated apoptosis	[29]
730.5	Cellulose gum-coated	Human skin, HaCaT normal human keratinocytes	0.5, 50 ppm (skin), 0.002–0.02 ppm (cells)	24 h	AgNPs did not sensitize keratinocytes to UV-B radiation	[30]
13	Uncoated	Mouse blastocysts	25 and 50 µM	24 h	Embryonic toxicity	[31]
61	Uncoated	MAMCs primary culture murine adrenal medullary chromaffin cells	0.01, 0.1, and 1 nM	24 and 48 h	Cytotoxicity, decreased secretion	[32]
68.9	Uncoated	RAW264.7 mouse peritoneal macrophages	0.2–1.6 ppm	24, 48, 72, and 96 h	Cytotoxicity and oxidative stress	[33]

(Continued)

Table 1 (Continued)

Size (nm)	Surface coating	Model	Concentration tested	Exposure duration	Outcome	References	
20, 50, 80 (uncoated), 25, 35 (coated)	Unwashed, washed, carbon coated	HEKs, human epidermal keratinocytes	0.000544–1.7 µg/ml	24 h	Dose-dependent decrease in cell viability of uncoated nanoparticles while carbon-coated AgNPs were nontoxic	[5]	
30 (spherical)	Uncoated	Japanese medaka (<i>Oryzias latipes</i>) cell line	0.05–5 µg/cm ²	24 h	Toxicity, DNA damage	[34]	
7–20	Uncoated	Mouse fibroblasts and liver cells	10–200 µg/ml	24 h	Reduced cell viability, oxidative stress, and apoptosis	[35]	
35 (0.6–1.6 µm bulk)	Uncoated	C3A human hepatocytes, Caco-2 colon cancer cells	0–1000 µg/ml	24 h	Internalization, cytotoxicity	[10]	
100 (spherical)	PVP coated	Primary trout hepatocytes	hMSCs human mesenchymal stem cells	0.05–50 µg/ml	7 days	Cell proliferation and chemotaxis were decreased, while IL8 release was increased	[36]
50	Uncoated	Bovine retinal endothelial cells	100–500 nM	24 h	Induction of CASP3 activity and DNA ladder formation	[37]	

90	Polyethylenimine stabilized	HepG2 human hepatoma cells	0.1–3 mg/l	24 h	Noncytotoxic doses of AgNPs accelerate DNA damage repair genes and micronuclei induction	[38]
5–10	Uncoated	HepG2 human hepatoma cells	0.1–5 µg/ml	28 h	Cytotoxicity, overexpression of superoxide dismutase, glutathione peroxidase, catalase	[39]
25	PVP coated	Human skin (epidermis and dermis) Franz diffusion cell method	0.46–2.32 ng/cm ²	24 h	AgNPs are able to permeate the damaged skin in an <i>in vitro</i> diffusion cell system	[7]
5–10	Uncoated	HeLa S3 human cervical cancer cells	0–120 µg/ml	24 h	Oxidative stress, apoptosis, <i>HO1</i> and <i>MT2A</i> overexpression	[40]
45	Uncoated	Rat coronary endothelial cells	0.1–100 µg/ml	24 h	At low concentrations, AgNPs act as antiproliferative/ vasoconstrictive factors that impair NO production, at high concentrations the AgNPs stimulate NO-mediated proliferation/ vasorelaxation	[41]

(Continued)

Table 1 (Continued)

Size (nm)	Surface coating	Model	Concentration tested	Exposure duration	Outcome	References
3.08, 5.75, and 24.85	Uncoated	J774 A1 macrophages	1 and 10 ppm	24, 48, and 72 h	Cytotoxicity, production of IL1, IL6, and TNF	[23]
25	Uncoated, polysaccharide coated	Mouse embryonic stem cells (mES), mouse embryonic fibroblasts (MEF)	50 µg/ml	24, 48, and 72 h	Both coated and uncoated AgNPs induced DNA damage and apoptosis.	[42]
7–20	Uncoated	HT-1080 human fibrosarcoma cells derived from dermis, A431 human skin carcinoma cells derived from epidermis	1.56–50 µg/ml	24 h	Reduced cell viability, oxidative stress, DNA fragmentation, and higher CASP3 activity	[6]
6–20	Starch coated	IMR-90 human lung fibroblast, U251 human glioblastoma cells	25–400 µg/ml	24, 48, and 72 h	Oxidative stress, DNA damage, apoptosis, and necrosis	[24]
15, 30, 50	Uncoated	Rat alveolar macrophages	10–75 µg/ml	24 h	ROS generation and oxidative stress mediated toxicity	[43]

1–100	N/A	NIH3T3 mouse fibroblast cells, A10 rat vascular smooth muscle cells, HCT116 human colon cancer cells	0.0005–50 µg/ml	24 h	AgNPs act through ROS and Jnk to induce apoptosis via mitochondrial pathway	[44]
2–5	Uncoated	HeLa S3 human cervical cancer cells	92 µg/ml	3, 4, and 24 h	Cytotoxicity, apoptosis and induction of oxidative stress-related genes	[45]
25	Uncoated, polysaccharide coated	N2A murine neuroblastoma cells	0.5–100 µg/ml	24 h	Oxidative stress, degradation of mitochondrial membrane integrity, disruption of actin cytoskeleton	[46]
100	Uncoated	A549 human alveolar epithelial cells	5–200 µg/ml	24 h	Dose-dependent apoptosis	[47].
3–100	Uncoated	A549 human alveolar epithelial cells	0.01–10 µg/ml	48 h	Oxidative stress, cytokine IL6 and IL8 production	[48]
15	Uncoated	Rat neuroendocrine cells (PC12)	50 µg/ml	24 h	Reduced mitochondrial function and dopamine level	[49]
15	Uncoated	C18-4 mouse spermatogonial stem cells	5–100 µg/l	48 h	Reduced mitochondrial function, increased LDH	[50]

(Continued)

Table 1 (Continued)

Size (nm)	Surface coating	Model	Concentration tested	Exposure duration	Outcome	References
15, 100	Uncoated	BRL 3A rat liver cells	5–50 µg/ml	24 h	Reduced mitochondrial function and GSH level, and increased level of ROS	[51]
25 (uncoated) 20 (coated)	N/A	RAW267.9 mouse alveolar macrophages	0–10 µg/ml	24 h	Citotoxicity	[52]

concentrations (1–10 µg/ml), whereas stimulation was observed at high concentrations (50–100 µg/ml) probably due to size heterogeneity [41].

Studies on embryonic development with the use of mouse blastocysts as a model showed that uncoated AgNPs inhibited cell proliferation and induced apoptosis. The percentage of developed blastocysts from morulas was lower compared to control, and the number of both inner cell mass and trophoctoderm cells was lower. This indicates potential harm of AgNPs on embryonic implantation and development. However, the effect of Ag⁺ ions was stronger [31]. Mouse embryonic stem cells and mouse embryonic fibroblasts demonstrated a decrease in viability and an increase in the expression of annexin upon exposure to both uncoated and polysaccharide (acacia gum)-coated AgNPs. The effect of the coated particles was higher in both cell lines suggesting that surface chemistry does indeed lead to different responses [42]. Mitochondria-dependent apoptosis was also observed in the NIH3T3 but not in the HCT116 cells treated with AgNPs, as suggested by the presence of cytochrome *c* in the cytoplasm and BAX in mitochondria. It was suggested that HCT116 cells are protected by the upregulation of the antiapoptotic BCL2 protein [44]. Although viability is not always compromised, AgNPs can affect other functions of the cell such as exocytosis. Primary culture murine adrenal medullary chromaffin cells exposed to uncoated AgNPs (61 nm) for 24 h exhibited a decrease in epinephrine secretion despite the viability was not decreased [32].

Since the cellular uptake and biological response are dependent on various parameters such as dispersibility, surface properties, aggregation, persistence, or ability to translocate to other organs, etc. [54–56], the same type of particle may exhibit different toxicity varying on the coating agent and functionalization [42,54]. It is crucial to take into account the size, coating, agglomeration in solvents or media to allow comparison across different studies and to obtain reliable, reproducible results [55]. Further, it should be noted that NPs could possibly interfere with some colorimetric assays and mask the effects [5,27]. It has also been shown that the toxicity exhibited in human epidermal keratinocytes exposed to AgNPs was due to contaminants present in the NP solution but not to the NPs themselves [5]. In addition, it has been pointed out that the actual size of the NPs may be different from the size provided by the manufacturer, showing the importance of in house measurements [28,41].

3.2. *In vivo* toxicity in mammals

3.2.1. *In vivo* studies on mammalian animal models

There are relatively few papers describing the effect of AgNPs *in vivo* (Table 2). AgNPs, similar to other NPs, may enter human and animal bodies through different routes of exposure: ingestion [33,63,65], inhalation [57,66,67], dermal contact [5,73], or they can be administered

Table 2 *In vivo* mammalian models for AgNP toxicity assessment

Size (nm)	Surface coating	Model	Concentration tested	Exposure method and duration	Outcome	References
18	None	Sprague–Dawley rats	1.73×10^4 , 1.27×10^5 , 1.32×10^6 particles/cm ³	Inhalation exposure: 6 h/day, 5 days/ week, for 28 days	No significant changes in the hematological and blood biochemical parameters in either male or female rats	[57]
18	None	Sprague–Dawley rats	1.73×10^4 , 1.27×10^5 , 1.32×10^6 particles/cm ³	Inhalation exposure: 6 h/day, 5 days/ week, for 90 days	Decreased tidal volume and alveolar inflammation. Increased bile duct hyperplasia and liver inflammation	[58]
18	None	Sprague–Dawley rats	30, 300, and 1000 mg/kg	Ingestion exposure: Ag NPs mixed with diet for 28 days	Significant dose-dependent changes in alkaline, phosphatase activity, cholesterol level, and slight liver damage	[59]
29	None	C57BL/6N mice	100, 500, and 1000 mg/kg	Intraperitoneally 24 h	Altered gene expression associated with oxidative stress in the caudate, frontal cortex, and hippocampus regions of the brain	[60]
13–15	None	Sprague–Dawley rats	1.73×10^4 , 1.27×10^5 , 1.32×10^6 particles/ cm ³ (61 µg/m ³)	Inhalation exposure: 6 h/day, 5 times/ week, 28 days	Size and number of goblet cells containing neutral mucins increased in lungs	[61]

22	None	C57BL/6 mice	1.91×10^7 particles/ cm^3	Inhalation exposure: 6 h/day, 5 days/ week, 14 days	Expression of several genes in the brain associated with motor neuron disorders, neurodegenerative disease, and immune cell function	[62]
56	None	Fischer F344 rats	30, 125, and 500 mg/kg body weight	Ingestion 90 days	Different adverse effects, including loss of body weight, changes in blood biochemical parameters, bile-duct hyperplasia, fibrosis, and pigmentation. Gender-related differences in accumulation of AgNPs in kidney	[63]
15	None	Fischer F344 rats	Inhalation $133 \mu\text{g}/\text{m}^3$ ($3 \times 10^6 \text{ cm}^3$) Intratracheal 50 μg AgNPs 7 μg AgNO ₃	Inhalation: 6 h Intratracheal: Single administration	Dose-dependent translocation to main organs	[64]
22, 42, 71, and 323	None	Mice	Single dose: 1 mg/kg Repeated doses: 0.25, 0.50, 1.00 mg/kg	Ingestion 14 days Repeated oral toxicity during 28 days (42 nm only)	Single dosage: The largest AgNPs were not found in any of the organs studied. Repeated dosage adversely impacts on liver and kidney in a high dose-treated group (1.00 mg/kg), when determined by blood chemistry and histopathological analysis. Decrease in cytokine levels	[33]

(Continued)

Table 2 (Continued)

Size (nm)	Surface coating	Model	Concentration tested	Exposure method and duration	Outcome	References
60	None	Sprague–Dawley rats	30, 300, 1000 mg/kg	Ingestion 28 days	Translocation to the tissues. Changes in mucus chemistry	[65]
18–19	None	Sprague–Dawley rats	0.6×10^6 , 1.4×10^6 , 3.0×10^6 particles/ cm^3	Inhalation exposure: 6 h/day, 5 days/ week, for 13 weeks	Lung and liver inflammation. Increased bile duct hyperplasia	[66]
	None	Sprague–Dawley rats	0.94×10^6 , 1.64×10^6 , 3.08×10^6 particles/ cm^3	Inhalation exposure: 4 h	No significant changes	[67]
50–100, 2–20 μm	None	Rats	62.8 mg/kg	Subcutaneously	AgNPs traversed the blood–brain barrier (BBB) and move into the brain in the form of particles. Induction of neuronal degeneration and necrosis	[68]
50–100, 2–20 μm	None	Rats	62.8 mg/kg	Subcutaneously	AgNPs translocated to the blood circulation system and distributed throughout the main organs, especially in the kidney, liver, spleen, brain, and lung in the form of particles. Caused neuronal degeneration	[69]

20, 80, 110	None	Rats	23.8, 26.4, 27.6 µg/ml	Intravenously	Size-dependent deposition in all major organs	[70]
50–60	None	Sprague–Dawley rats, mice	Intraperitoneal (50 mg/kg), intravenous (30 mg/kg), intracarotid (2.5 mg/kg)	Single dose, 24 h	Altered the BBB function. Marked decreases in local cerebral blood flow and pronounced brain edema was seen in regional areas associated with BBB leakage. Neuronal cell injuries, glial cell activation, heat shock protein upregulation	[71]
Colloidal silver	None	Piglets	20, 40 mg/kg diet	Ingestion exposure: AgNPs mixed with diet for 5 weeks	No effect was observed, minimal retention of AgNPs in liver	[72]

subcutaneously [68,69], intraperitoneally [60], or intravenously [70,71]. Once entering the body, some AgNPs remain in entry tissues, but generally they can be easily translocated and distributed throughout the body via bloodstream or lymphatic system. Regardless of the routes of exposure, AgNPs are found in all major target organs: lungs, skin, liver, spleen, brain, adrenals, testes, and kidneys [74]. AgNPs easily cross blood vessels walls, and can cross the blood–brain [71], alveoli–capillary vessels [64], blood–testes [74], and skin–blood [5] barriers.

It has been proven that the impact of AgNPs depends not only on their dose [59–61] but also on their size [33,64,70]. Differences between chronic and acute exposure have also been shown [67,70]. In most of the studies, a toxic effect of AgNPs on various organs and tissues has been found, although in one report no effect was found [57], but in this case, only a very small dose was administered.

One of the natural routes by which NPs can penetrate into an organism is the inhalation route. Two weeks of 5 day/week, 6 h/day inhalation exposure of C57BL/6 mice to AgNPs resulted in changes of expression of several genes associated with motor neuron disorders, neurodegenerative disease, and immune cell function in brain, indicating potential neurotoxicity and immunotoxicity associated with AgNP exposure [62]. In a study by Takenaka *et al.* [64], the effect of inhalation of 10 nm AgNPs was compared to that of intratracheal exposure to AgNPs larger than 100 nm. In both cases, the highest levels of AgNPs were found in lungs and blood immediately after the exposure. Inhalation of AgNPs resulted in some silver accumulation in all main organs. After intratracheal administration, massive AgNPs accumulation was found mainly in alveolar walls and alveolar macrophages, suggesting rapid phagocytosis of large silver agglomerates by alveolar macrophages.

A subacute exposure by inhalation to different size AgNPs caused significant change neither in body weight nor in hematological or biochemical blood parameters [57,75]. Although no symptoms have been noticed, AgNPs were found in all investigated organs. The accumulation in lungs, brain, olfactory bulb, and liver was dose related [57]. Similarly, a chronic, repeated oral administration of AgNPs (60 nm) resulted in no significant changes of body and organ weights, despite a dose-dependent deposition of AgNPs in all organs. Two groups [57,61] administered AgNPs to the rats' nasal septum respiratory mucosa during 28 days. Histopathological examination revealed no lesions in nasal cavity and lungs. However, exposure to high AgNP-doses caused significant growth of goblet cells and an increase of neutral mucus production. In another study, AgNPs administrated to rats in an inhalation chamber for 90 days, 6 h/day caused a statistically significant decrease in the tidal volume and minute volume [58]. In a subsequent study, subchronic exposure induced alveolar inflammation and macrophage accumulation in lungs of rats treated with the highest dose used

(3.0×10^6 particle/cm³) [66]. However, acute inhalation (4 h) of the same AgNPs did not show any significant effects on lung function in rats of both sexes [67]. In all studies, dose-dependent AgNPs deposits in main organs have been found. Silver concentration in kidneys of female rats was two- to threefold higher than that in kidneys of male rats. A similar relationship was described for rats exposed by oral route [59,63,75], suggesting gender-specific accumulation of AgNPs to be a common phenomenon, apparently independent of the route of administration.

Kim *et al.* [63] studied the effect of oral administration of AgNPs (56 nm) during 13 weeks to male and female rats, demonstrating dose-dependent liver lesions, manifested as increases in cholesterol and alkaline phosphatase levels in blood, bile-duct hyperplasia as well as necrosis, fibrosis, and/or pigmentation changes in liver tissue. A dose-dependent silver accumulation in all tissues was also observed. Further, Jeong *et al.* [65] found histological changes in the intestinal mucosa and altered properties of mucin after repeated oral administration of AgNPs (60 nm) in rats exposed for 28 days. A dose-dependent increased accumulation of AgNPs was observed in the lamina propria of the small and large intestine. It was also proven that orally administered AgNPs cause secretion of abnormal mucin typical for active ulcerative colitis, small intestine carcinoma, and intoxication.

There are also studies reporting no impact of AgNPs on the gastrointestinal tract. In piglets treated for 5 weeks with low doses of metallic nano-silver in colloidal form, no histopathological changes in ileal mucosa were

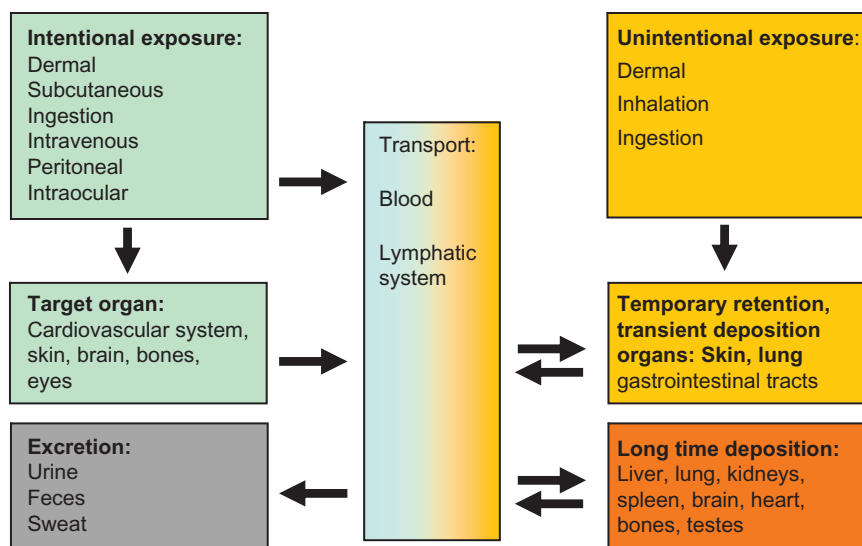


Figure 2 Diagram illustrating the origin and fate of AgNPs in the human body.

found. There was also no AgNPs accumulation in kidneys and skeletal muscles, and only small amounts of AgNPs were found in livers [72]. Notably, even a protective impact of orally administered AgNPs has been demonstrated in a rat model of ulcerative colitis [76] (see Section 4 for more discussion on pro- and anti-inflammatory properties of AgNPs).

To improve our understanding of the impact of AgNPs on the mammalian organism, Tang *et al.* [68] examined the ability of AgNPs and silver microparticles to traverse the blood–brain barrier. Only AgNPs crossed the blood–brain barrier after subcutaneous injection and caused neuronal degeneration/necrosis. All effects were time dependent, reaching a plateau after 12 weeks. The role of the cardiovascular system in AgNPs distribution and discrimination in the body was subsequently examined [69]. A high percentage of AgNPs, but not microparticles, was translocated to the blood circulatory system after their subcutaneous administration and was deposited in all main organs (kidneys, liver, spleen, brain, and lungs). Ultrastructural observations confirmed AgNPs accumulation in renal tubular epithelial cells, hepatocytes, and neurons.

Intraperitoneal or intravenous administration of AgNPs also resulted in silver accumulation in different organs. Lankveld *et al.* [70] described a rapid clearance of AgNPs from blood and deposition after intravenous administration with accumulation of AgNPs depending on particle size, as 20 nm AgNPs were found mainly in liver, kidneys, and spleen, whereas 100 nm AgNPs in spleen, liver, and lungs. In other tissues, the accumulation of AgNPs of different sizes did not vary. Similarly, dose-dependent alteration of expression of genes related to oxidative stress was observed in different parts of brain 24 h after intraperitoneal administration of 25 nm AgNPs to adult male C57BL/6N mice [60].

3.2.2. Humans

Results of the studies of NPs impact on human organism are of particular interest because of the possible uncontrolled contact of humans with AgNPs. Nanosilver is released from consumer products and medical devices and via the bloodstream or lymphatic system is distributed to main organs (Figure 2). A negative impact of AgNPs on humans has been demonstrated in studies on people drinking colloidal silver. The prolonged consumption caused accumulation of silver in their bodies and many adverse effects similar to those observed in model animals (reviewed in Refs. [3,4,77]).

3.3. Toxicity in nonmammalian eukaryotes

Whereas a steady increase in applications using AgNPs in industrial settings and consumer products takes place, still little is known on their potential ecotoxicity. A limited number of nonmammalian test species has been used for toxicity testing of AgNPs (Table 3). Most of these assays are based on

Table 3 *In vivo* nonmammalian models for AgNP toxicity assessment

Size (nm)	Surface coating	Model	Concentration tested	Exposure duration	Outcome	References
81 AgNO ₃ (Ag ⁺)	None	European perch (<i>Perca fluviatilis</i>)	63, 129, 300 ng/ ml AgNPs 39 and 386 µg/l AgNO ₃	24 h	No impact of AgNPs on the Basal Metabolic Rate (BMR), whereas exposure to AgNO ₃ resulted in a significant increase in BMR	[78]
5–20	None	Zebrafish (<i>Danio rerio</i>) adults	30, 60, 120 µg/ ml	24 h	Oxidative stress, induction of DNA damage and proapoptotic markers in liver	[79]
60 and 300	None	Japanese medaka (<i>Oryzias latipes</i>)	N/A	96 h	LC ₅₀ 28 and 67 µg Ag/l for 60 and 300 nm AgNP, respectively. No toxicity if Ag ⁺ ions were eliminated	[80]
20–40	None					[81]

(Continued)

Table 3 (Continued)

Size (nm)	Surface coating	Model	Concentration tested	Exposure duration	Outcome	References
		Japanese medaka (<i>O. latipes</i>) at early-life stages	0.5–8 µg/ml fish 0.5–4 µg/ml eggs 0.1–1 µg/ml embryos	48 h 168 h 60 days	Developmental retardation and morphological defects in embryonic larvae, toxicity in larval–juvenile medaka, histopathological changes in the larval eye were evaluated	
10, 35, > 600	None	Rainbow trout (<i>Oncorhynchus mykiss</i>)	10, 100 µg/ml	240 h	Smallest AgNPs induced expression of cyp1a2 in the gills	[82]
35	None	Carp (<i>Cyprinus carpio</i>)	0.01 and 0.1 µg/ ml	21 days	AgNP uptake via gastrointestinal route	[10]
3, 10, 50, 100	None	Zebrafish (<i>D. rerio</i>) embryos	100 µM	24–120 h	Dose-dependent toxicity and a variety of embryonic morphological malformations	[83]

31–50	None	Fathead minnow (<i>Pimephales promelas</i>)	0.625–25 µg/ml	96 h	Toxicity	[84]
50 Ag ⁺	None	Japanese medaka (<i>O. latipes</i>)	1 and 25 ng/ml	24–240 h	Genotoxicity, carcinogenic, and oxidative stresses, induction of genes related with metal detoxification/ metabolism regulation, and radical scavenging action	[85]
10–20	None	Zebrafish (<i>D. rerio</i>) embryos	10, 20 ng/ml	48 h	Toxicity and a variety of embryonic morphological malformations, induction of antioxidant enzymes, changes in gene expression	[86]
26 44 and 216 in medium	None	Zebrafish (<i>D. rerio</i>) adults	1 µg/ml	48 h	Toxicity, changes in gills morphology and gene expression	[87,88]
5–20	BSA and starch coated	Zebrafish (<i>D. rerio</i>) embryos	5–100 µg/ml	24, 48, 72 h postfertilization	Dose-dependent toxicity and a variety of embryonic morphological malformations	[89]

(Continued)

Table 3 (Continued)

Size (nm)	Surface coating	Model	Concentration tested	Exposure duration	Outcome	References
5–46	None	Zebrafish (<i>D. rerio</i>) embryos	0.04–0.71 nM	24–120 h	Dose-dependent mortality and developmental abnormality in embryos	[90]
<i>Crustaceans</i> 60 and 300	None	<i>Daphnia magna</i>	N/A	48 h	EC ₅₀ 1.0 and 1.4 µg Ag/l for 60 and 300 nm AgNP, respectively. No toxicity if Ag ⁺ ions were eliminated	[80]
26 44 and 216 in medium	None	<i>Daphnia pulex</i>	1 µg/ml	48 h	Toxicity	[88]
26 44 and 216 in medium	None	<i>Ceriodaphnia dubia</i> (juveniles)	1 µg/ml	48 h	Toxicity	[88]
35 <i>Bivalves</i>	None	<i>D. magna</i>	0.1 µg/ml	96 h	60% toxicity	[10]

15	None	Oyster (<i>Crassostrea virginica</i>) embryos, adults	0.0016–1.6 ng/ ml	48 h	Inhibition of embryo development, lysosomal destabilization, changes in metallothionein gene expression	[91]
<i>Worms</i>						
7, 21, 75	PVP, citrate	<i>Caenorhabditis elegans</i> (wild type and mutant)	50, 104 µg/ml	24 h	Growth inhibition and toxicity, partially due to the Ag ⁺	[92]
20	None	<i>C. elegans</i>	0.1, 0.5 µg/ml	24–72 h	Decreased reproductive potential. Changes in gene expression	[93]
<i>Insects</i>						
10	Polysaccharide	<i>Drosophila melanogaster</i> (larvae)	50, 100 µg/ml	Ingestion, 24 and 48 h	Oxidative stress, induction of <i>hsp70</i> , <i>p38</i> and <i>p53</i> and activity of caspase 3 and 9	[94]
10	Polysaccharide versus bare	<i>D. melanogaster</i> (adult)	50, 100 µg/ml	Inhalation, 24 and 48 h	Oxidative stress, induction of <i>hsp70</i>	[95]

aquatic species as this is considered to be an important environmental compartment for AgNPs in the environment. This is not surprising, since AgNPs are released from fabrics during washing [96], and under certain conditions, AgNPs may stay largely dispersed in freshwater and slightly salty water of environmental relevance [97]. The number of publications reporting toxicity of AgNPs for nonaquatic species is very limited and even smaller than those for aquatic species (Table 3).

3.3.1. Nonmammalian vertebrates

Most data for AgNPs are available for a variety of fish species including larval and adult life stages. AgNPs affect the early development of zebrafish (*Danio rerio*) embryos [86,90]. Developmental retardation, increased heart rates, neurodevelopmental effects, sluggish circulation, pericardial edema, tube heart, and eye malformations were observed resulting from embryonic exposure to AgNPs [81,86]. Edema was also the most prominent malformation in fathead minnows (*Pimephales promelas*) after larval exposure [84]. The effects were ascribed both to the actual AgNP exposure and to the toxicity of Ag ions formed during AgNP dissolution, as uptake of AgNPs has been reported for fish embryos [62] and Ag^+ in culture media was reported [84].

In adult zebrafish, there was evidence of uptake of AgNPs via the gills that caused AgNP-specific changes in gene expression [87] and resulted in increased mortality [88]. Increased mortality upon treatment with AgNPs was also observed in adult Japanese medaka (*Oryzias latipes*) [81], accompanied by induction of DNA damage [85]. Treatment of rainbow trout (*Oncorhynchus mykiss*) with AgNPs caused an increase in expression of *cyp1a2* in the gills [82].

It cannot be excluded that AgNPs are partly decomposed *in vivo*, thus causing exposure to Ag^+ [83]. Interestingly, gene expression profiles in fish after exposure to Ag^+ ion and AgNP showed little similarity, providing distinguishable toxicity fingerprints of Ag ions compared to AgNPs [10,85]. The result adds further evidence that AgNPs can directly induce harm in exposed organisms and that those biological responses are induced not only by dissolved silver ions [45,85,88,98], as sometimes suggested [99].

3.3.2. Invertebrates

AgNPs were more toxic to *Daphnia magna* in a 96 h acute exposure study than the bulky counterparts [10]. The LC_{50} for survival in *Daphnia pulex* (adults) and *Ceriodaphnia dubia* (juveniles) was in the same range, whereas the susceptibility of both species to the identical AgNPs was higher than that of zebrafish. The higher susceptibility of crustaceans is explained by the fact that filter feeders may be exposed to more than 190 million NPs per hour under these experimental conditions [88]. While it was recognized some time ago that lethality of *Daphnia* sp. may not be a sensitive endpoint and

that therefore sublethal effects need to be studied [88,100], data for subchronic and sublethal effects of AgNPs are still missing.

AgNPs affected the embryonic development of oysters (*Crassostrea virginica*) and decreased lysosomal integrity in adult hepatopancreas tissue, thus giving evidence for potential threats to bivalve embryos and adults [91]. Similarly, growth of the terrestrial nematode *Caenorhabditis elegans* was reduced following exposure to AgNPs, and only some toxic effects could be related to the release of free silver species, again giving evidence for “nano-specific” toxicity [92]. Recent results of functional genomic studies by Roh *et al.* [93] revealed that AgNPs-induced dramatic reproductive failure in *C. elegans* likely associated with oxidative stress.



4. INFLAMMATORY RESPONSE

Inflammation is fundamental in a range of homeostatic and pathophysiological processes, such as in protection against invading pathogens and in the repair of damaged tissue. In several *in vivo* studies, inflammatory responses have been investigated, using different concentrations and different sizes of particles, with and without coating in acute or chronic treatment regimes. Inflammatory changes after inhalation exposure to AgNP have been reported in some instances [58]. In some studies, no such changes have been reported [57,61,67], but it is not always clear to what extent inflammatory changes have been monitored. After oral exposure, a focal lymphocytic infiltration was observed in the liver portal tracts of both nano- and micron-size particle-fed mice, suggesting the induction of inflammation. Further, in the NP-fed mice, focal lymphocytic infiltration was also found in the intestine. From a microarray analysis of the RNA from the livers, the expression of genes related to inflammation was observed [101].

Subchronic oral toxicity study of AgNPs in rats by Kim *et al.* [63] confirmed the liver as a target organ for AgNPs toxicity after ingestion. An increase in necrotic cells in liver was observed, in particular, in the male rats. At the high dose, multiple foci of inflammatory cell infiltrates, including eosinophils, were found especially around the central vein and portal areas. No, or only negligible, signs of inflammation were observed in other tissues. When AgNPs were applied dermally, macroscopic observations showed no gross irritation in the porcine skin; however, microscopic and ultrastructural examination revealed areas of focal dermal inflammation and with no difference for the washed and unwashed particles. Importantly, this study indicates that toxicity of the AgNPs is due to residual contaminants in the silver NPs solution, and conceivably this is also the case for the inflammatory responses [5].

Interestingly, direct anti-inflammatory effects are also shown for AgNPs. Thus, in a porcine contact dermatitis model, lower levels of proinflammatory Tgfb1 and Tnf and increased expression of the anti-inflammatory cytokine Il4 were detected after treatment with nanocrystalline silver, compared to an Ag-nitrate-treated group [73,102]. Further, Bhol *et al.* [76] demonstrated, using a murine dermatitis model, decreased expression of the inflammatory cytokines Tnf and Il12 after treatment with nanocrystalline silver cream. Moreover, in a thermal injury animal model, faster wound recovery was observed when wound dressings were coated with nanosilver, and levels of proinflammatory cytokines were decreased both locally and systemically [103]. The same group has also used a postoperative peritoneal adhesion model, in which nanosilver decreased adhesion formation, implying decreased Infg or Il12 production [104]. In line with this, another study using a model of bladder inflammation observed significantly decreased lymphocyte and mast cell recruitment as well as decreased Tnf expression after treatment with nanosilver [105].

Taken together, the bioactivity of AgNPs seems to be a double-edged sword. Several reports emphasize the beneficial anti-inflammatory effects, whereas other research is highlighting the possibilities of proinflammatory responses that may lead to adverse effect. Possibly, the anti-inflammatory responses emerge in a prestimulated state and/or at high concentration of AgNPs, whereas the proinflammatory responses appear under homeostatic conditions and/or at lower concentrations.

5. THE ROLE OF OXIDATIVE STRESS IN AGNP-INDUCED TOXICITY AND DNA DAMAGE

Many studies have demonstrated that the generation of reactive oxygen species (ROS) is a key mechanism by which airborne ultrafine particles exert their proinflammatory and proatherogenic effects on the respiratory and cardiovascular systems [106–108]. Similarly, overproduction of ROS is proposed as a crucial mechanism for engineered NP-toxicity [56]. Under normal physiological conditions, ROS are generated in low concentrations during cell respiration in the mitochondrial electron transport chain and have important roles in cell signaling. However, the presence of NPs could increase the ROS formation by interfering with the mitochondria or other enzymes producing ROS, such as NADPH-oxidase [109]. Further, the surface chemistry of particles can lead to direct ROS formation [107,108]. Additionally, the natural property for many NPs to bind transition metals is believed to enhance ROS-induced toxicity. Under normal physiological conditions, ROS are easily neutralized by antioxidant defenses such as

glutathione (GSH) and several antioxidant enzymes. However, upon NPs exposure, an excess of ROS production can occur and the antioxidant defenses available may be overwhelmed, which may lead to a damage in cellular components [110].

Toxicity of AgNPs has been associated with oxidative damage to the cell by many authors [43,51,106]. Several studies have reported the mitochondria as a sensitive target of AgNP-mediated cytotoxicity. A reduced mitochondrial membrane potential and a leakage of ROS have been reported in the study of Hussain *et al.* [51], but the mechanism of AgNPs action on mitochondria has not been resolved. Interestingly, Ag ions have been found to bind with high affinity to cysteine residues contained in the *Escherichia coli* homolog of mitochondrial NADH:ubiquinone oxidoreductase, resulting in an inefficient passage of electrons leading to a production of large quantities of ROS, thereby causing toxicity to *E. coli* [111]. It would be of interest if such a mechanism could be extrapolated to AgNPs action in eukaryotic cells.

Hussain *et al.* have also reported a significant depletion of GSH in BRL3A cells following exposure to AgNPs, which could be due to the direct binding of AgNPs by GSH or to the inhibition of enzymes involved in GSH synthesis. GSH depletion in liver cells exposed to AgNPs is strongly correlated with an increase in ROS. It is speculated that the loss of GSH may compromise the cellular antioxidant defense and lead to the accumulation of ROS generated as by-products of normal cellular function [51].

Endogenous overproduction of ROS is commonly considered the major source of genotoxicity that has been observed after exposure to many types of engineered NPs that have been found to cause DNA-strand breaks, point mutations, oxidative DNA adducts, and chromosomal fragmentation [56]. AgNPs are no exception. Extensive and dose-dependent damage to DNA and/or alterations in DNA-damage response has been observed after AgNPs treatment in studies *in vitro* as well as *in vivo* (Table 4). Double-strand breaks (DSB), if not repaired, are considered one of the most biologically lethal forms of lesion to cells among the different DNA-damage types. Several studies on AgNP exposure clearly demonstrate the induction of this particular damage type [42,79]. Chromosomal aberrations and formation of micronuclei often occur as a direct consequence of DSB formation. Chromosomal aberrations have been observed in AgNP-treated IMR-90 and U251 cells. Interestingly, the chromosomal abnormalities were more pronounced in the cancer cell (U251) when compared to the fibroblasts (IMR-90) [21]. AgNP-exposed HepG2 human hepatoma cells also demonstrated an increased frequency of micronucleus formation. The results suggested more severe chromosome damage with AgNPs compared to ionic Ag⁺ and polystyrene NP [38]. Interestingly, bulky DNA adducts have also been detected by ³²P-postlabeling in the human lung cancer cell line (A549) exposed to AgNP [28].

Table 4 Induction of DNA damage by AgNP

Size (nm)	Surface coating	Model	Dose and exposure	Methods	Endpoints	Outcomes	References
69 (spherical)	0.2% polyvinylpyrrolidone	A549 human lung carcinoma epithelial-like cell line	0–15 µg/ml, 24 h	³² P-postlabeling	DNA adduct formation	Dose-dependent increase in the level of bulky DNA adducts inhibited by antioxidant treatment 1 h prior to Ag exposure	[28]
20–25	None	THP-1 monocytes	3.5 µg/ml, 24 h	Alkaline comet assay	DNA-strand breaks	No significant DNA damage was observed	[112]
5–20	None	Zebrafish (<i>Danio rerio</i>)	0–120 mg/l, 24 h	Western blot γH2AX foci	Double-strand breaks, DNA repair	Induction of DNA damage was found at highest dose. Increased <i>tp53</i> expression	[79]
30 (spherical)	None	Japanese medaka (<i>Oryzias latipes</i>) OLHNI2 cell line	0.05–5 µg/cm ² , 24 h	Chromosomal aberrations	Chromosome breaks	Induction of chromosomal aberrations and aneuploidy	[34]
8 (spherical)	None	Human Mono Mac 6 cells, rat alveolar macrophages	0.5–10 µg/cm ² for 10 min	Alkaline comet assay	DNA-strand breaks	Induction of DNA damage. After exposure to NPs cells were incubated for 24 h in cell culture medium	[113]

10 (stock) 48 (suspension)	Polysaccharide	Wild-type <i>Drosophila melanogaster</i>	0–100 µg/ml, 24 h	Western blot	DNA damage repair	Induction of both cell cycle checkpoint <i>tp53</i> and cell signaling protein p38	[114]
7–10 Ag ₂ CO ₃ (Ag ⁺)	Polyethylenimine	Human hepatoma HepG2 cells	AgNP/Ag ⁺ , 1 mg/l, 24 h	Micronucleus test	Chromosomal abnormalities	Highly increased frequency of micronuclei after exposure to AgNP. The effect was not seen after exposure to Ag ⁺	[38]
5–10 (spherical) 100–300 in media. AgNO ₃ (Ag ⁺)	None	Human hepatoma HepG2 cells	AgNP/Ag ⁺ , 1– 2 µg/ml, 24 h	γH2AX foci	Double-strand breaks	Induction of DNA damage after exposure to AgNP or Ag ⁺ The effect was inhibited by 2 h pretreatment with antioxidant	[39]
6–20	Starch	Human glioblastoma cells (U251), human fibroblasts (IMR-90)	0–400 µg/ml, 48 h	Alkaline comet assay, micronucleus test	Double-strand breaks, chromosomal abnormalities	Extensive and dose- dependent damage to DNA (both cell types). Significant numbers of micronuclei were formed, but the number was higher in cancer cells as opposed to fibroblasts	[24]

(Continued)

Table 4 (Continued)

Size (nm)	Surface coating	Model	Dose and exposure	Methods	Endpoints	Outcomes	References
30 (spherical and nanoprisms) AgNO ₃ (Ag ⁺)	Citrate	Human skin HaCaT keratinocytes	100 µg/ml, 24 h	Alkaline comet assay	DNA-strand breaks	Negative for colloidal AgNPs. Positive results for AgNps powder	[11]
25	Polysaccharide versus uncoated	Mouse embryonic stem cells and mouse embryonic fibroblasts	50 µg/ml, 4–72 h	Western blot γH2AX/ Rad51 foci	Double-strand breaks, DNA repair	Increased level of γH2AX/Rad51 Coated AgNP exhibited more severe damage than uncoated AgNP	[42]
7–20 (spherical)	None	Human skin carcinoma (A431)/ fibrosarcoma (HT-1080)	6.25 µg/ml, 24 h	Agarose gel electrophoresis	DNA fragmentation	DNA laddering	[6]



6. SUMMARY

To the broad public, the benefits of nanotechnology development are doubtless, but on the other hand, clear scientific evidence has been gained of AgNPs toxicity to both humans and the environment. Responsible and sustained development of nanotechnology requires attention to possible risks to human health and environment along with other public concerns about social and ethical issues. Public awareness of nanotechnologies is now increasing rapidly, largely as a consequence of nonspecifically regulated introduction of products containing nanomaterials into the market.

It is hard to generalize from the already available data because new NPs are continuously synthesized with different shapes, coatings, sizes, etc. Further, the experimental conditions between different studies are quite different with the use of nanomaterials that are vastly diverse concerning their physicochemical properties. At this stage, it is not possible to draw conclusions about the drawbacks of AgNPs in biological systems, since the studies are still quite limited [41] and the materials are not always adequately characterized. There is a need for some kind of standardization concerning experimental conditions, toxicity methods, and NPs used (reference NPs) as well as adequate characterization of the materials under study in order to be able to make comparisons across studies. In addition, it is questionable whether the existing conventional testing strategies are adequate for nanotoxicology. Therefore, it has been proposed that the use of toxicogenomics and proteomics may provide a good alternative that could also give more insight in new mechanisms of NPs action [115].

There is a clear lack of ecotoxicological data for AgNPs; hence, more research especially on relevant test species is needed as the potential uptake of AgNPs was already shown for a variety of species. The observed differences in acute toxicity for AgNPs of similar size classes can probably be attributed to other components present on the NP surface, chemical mixtures, or to interspecies differences. This aspect needs a more thorough research and reporting in the scientific literature. Further, the methods used for preparation of AgNPs suspension for testing in aquatic environments need a discussion in the future, as the applied rigid and sophisticated suspension procedures may not be realistic for AgNPs in the natural environment with factors in the water such as pH, salinity, or dissolved organic carbon (DOC) constantly changing and influencing AgNPs stability [9,94].

Given that there is a paucity of information, persistent long-term exposure to NPs requires understanding their impact on living organisms, which is essential for toxicological and ecotoxicological hazard and risk estimation [116,117]. Such information is necessary in order to facilitate the development of any future regulations based on robust scientific information and

evidence enabling an informed risk assessment. Such a requirement must make use of studies that provide a holistic, interdisciplinary approach that permits the use of existing methodologies and technologies. At the same time, development is necessary of more novel *fit for purpose* regulatory tools that are robust and reproducible.

ACKNOWLEDGMENTS

The contribution of A. C. G. and A. G. was in part made possible within NanEAU (FNR/08/SR/07—Fonds National de la Recherche Luxembourg). The other authors were supported fulltime or in part by Polish-Norwegian Research Fund Grant PNRF122-AI.

REFERENCES

- [1] N. Silvestry-Rodriguez, E.E. Sicairos-Ruelas, C.P. Gerba, K.R. Bright, Silver as a disinfectant, *Rev. Environ. Contam. Toxicol.* 191 (2007) 23–45.
- [2] C. Marambio-Jones, E.M.V. Hoek, A review of the antibacterial effects of silver nanomaterials and potential implications for human health and the environment, *J. Nanopart. Res.* 12 (2010) 1531–1551.
- [3] N.R. Panyala, E.M. Pena-Mendez, J. Havel, Silver or silver nanoparticles: A hazardous threat to the environment and human health? *J. Appl. Biomed.* 6 (2008) 117–129.
- [4] X. Chen, H.J. Schluesener, Nanosilver: A nanoproduct in medical application, *Toxicol. Lett.* 176 (2008) 1–12.
- [5] M.E. Samberg, S.J. Oldenburg, N.A. Monteiro-Riviere, Evaluation of silver nanoparticle toxicity in skin in vivo and keratinocytes in vitro, *Environ. Health Perspect.* 118 (2010) 407–413.
- [6] S. Arora, J. Jain, J.M. Rajwade, K.M. Paknikar, Cellular responses induced by silver nanoparticles: In vitro studies, *Toxicol. Lett.* 179 (2008) 93–100.
- [7] F.F. Larese, F. D’Agostin, M. Crosera, G. Adami, N. Renzi, M. Bovenzi, G. Maina, Human skin penetration of silver nanoparticles through intact and damaged skin, *Toxicology* 255 (2009) 33–37.
- [8] B. Karn, T. Kuiken, M. Otto, Nanotechnology and in situ remediation: A review of the benefits and potential risks, *Environ. Health Perspect.* 117 (2009) 1813–1831.
- [9] J. Gao, S. Youn, A. Hovsepyan, V.L. Llaneza, Y. Wang, G. Bitton, J.C. Bonzongo, Dispersion and toxicity of selected manufactured nanomaterials in natural river water samples: Effects of water chemical composition, *Environ. Sci. Technol.* 43 (2009) 3322–3328.
- [10] B.K. Gaiser, T.F. Fernandes, M. Jepson, J.R. Lead, C.R. Tyler, V. Stone, Assessing exposure, uptake and toxicity of silver and cerium dioxide nanoparticles from contaminated environments, *Environ. Health* 8 (Suppl. 1) (2009) S2.
- [11] W. Lu, D. Senapati, S. Wang, O. Tovmachenko, A.K. Singh, H. Yu, P.C. Ray, Effect of surface coating on the toxicity of silver nanomaterials on human skin keratinocytes, *Chem. Phys. Lett.* 487 (2010) 92–96.
- [12] M. Mahmood, D.A. Casciano, T. Mocan, C. Iancu, Y. Xu, L. Mocan, D.T. Iancu, E. Dervishi, Z. Li, M. Abdalmuhsen, A.R. Biris, N. Ali, *et al.*, Cytotoxicity and biological effects of functional nanomaterials delivered to various cell lines, *J. Appl. Toxicol.* 30 (2010) 74–83.

- [13] N.M. Sirimuthu, C.D. Syme, J.M. Cooper, Monitoring the uptake and redistribution of metal nanoparticles during cell culture using surface-enhanced Raman scattering spectroscopy, *Anal. Chem.* 82 (2010) 7369–7373.
- [14] W. Lesniak, A.U. Bielinska, K. Sun, K.W. Janczak, X. Shi, J.R. Baker Jr., L.P. Balogh, Silver/dendrimer nanocomposites as biomarkers: Fabrication, characterization, in vitro toxicity, and intracellular detection, *Nano Lett.* 5 (2005) 2123–2130.
- [15] M.K. Gregas, F. Yan, J. Scaffidi, H.N. Wang, T. Vo-Dinh, Characterization of nanoprobe uptake in single cells: Spatial and temporal tracking via SERS labeling and modulation of surface charge, *Nanomedicine* 7 (1) (2010) 115–122.
- [16] M. Geiser, B. Rothen-Rutishauser, N. Kapp, S. Schurch, W. Kreyling, H. Schulz, M. Semmler, H. Im, V.J. Heyder, P. Gehr, Ultrafine particles cross cellular membranes by nonphagocytic mechanisms in lungs and in cultured cells, *Environ. Health Perspect.* 113 (2005) 1555–1560.
- [17] M. Kirkham, R.G. Parton, Clathrin-independent endocytosis: New insights into caveolae and non-caveolar lipid raft carriers, *Biochim. Biophys. Acta* 1746 (2005) 349–363.
- [18] B.M. Rothen-Rutishauser, S. Schurch, B. Haenni, N. Kapp, P. Gehr, Interaction of fine particles and nanoparticles with red blood cells visualized with advanced microscopic techniques, *Environ. Sci. Technol.* 40 (2006) 4353–4359.
- [19] L. Hu, Z.W. Mao, C.Y. Gao, Colloidal particles for cellular uptake and delivery, *J. Mater. Chem.* 19 (2009) 3108–3115.
- [20] V. Mailander, K. Landfester, Interaction of nanoparticles with cells, *Biomacromolecules* 10 (2009) 2379–2400.
- [21] P.V. AshaRani, M.P. Hande, S. Valiyaveetil, Anti-proliferative activity of silver nanoparticles, *BMC Cell Biol.* 10 (2009) 65.
- [22] C. Greulich, J. Diendorf, T. Simon, G. Eggeler, M. Eppler, M. Koller, Uptake and intracellular distribution of silver nanoparticles in human mesenchymal stem cells, *Acta Biomater.* 7 (1) (2010) 347–354.
- [23] H.J. Yen, S.H. Hsu, C.L. Tsai, Cytotoxicity and immunological response of gold and silver nanoparticles of different sizes, *Small* 5 (2009) 1553–1561.
- [24] P.V. AshaRani, G.L.K. Mun, M.P. Hande, S. Valiyaveetil, Cytotoxicity and genotoxicity of silver nanoparticles in human cells, *ACS Nano* 3 (2009) 279–290.
- [25] B.A. Vanwinkle, K.L. de Mesy Bentley, J.M. Malecki, K.K. Gunter, I.M. Evans, A. Elder, J.N. Finkelstein, G. Oberdorster, T.E. Gunter, Nanoparticle (NP) uptake by type I alveolar epithelial cells and their oxidant stress response, *Nanotoxicology* 3 (2009) 307–318.
- [26] Y.C. Chung, I.H. Chen, C.J. Chen, The surface modification of silver nanoparticles by phosphoryl disulfides for improved biocompatibility and intracellular uptake, *Biomaterials* 29 (2008) 1807–1816.
- [27] P.V. AshaRani, S. Sethu, S. Vadukumpully, S. Zhong, C.T. Lim, M.P. Hande, S. Valiyaveetil, Investigations on the structural damage in human erythrocytes exposed to silver, gold, and platinum nanoparticles, *Adv. Funct. Mater.* 20 (2011) 1233–1242.
- [28] R. Foldbjerg, D.A. Dang, H. Autrup, Cytotoxicity and genotoxicity of silver nanoparticles in the human lung cancer cell line, A549, *Arch. Toxicol.* (2011) Apr 29. [Epub ahead of print].
- [29] P. Gopinath, S.K. Gogoi, P. Sanpui, A. Paul, A. Chattopadhyay, S.S. Ghosh, Signaling gene cascade in silver nanoparticle induced apoptosis, *Colloid Surf. B* 77 (2010) 240–245.
- [30] S. Kokura, O. Handa, T. Takagi, T. Ishikawa, Y. Naito, T. Yoshikawa, Silver nanoparticles as a safe preservative for use in cosmetics, *Nanomedicine* 6 (2010) 570–574.
- [31] P.W. Li, T.H. Kuo, J.H. Chang, J.M. Yeh, W.H. Chan, Induction of cytotoxicity and apoptosis in mouse blastocysts by silver nanoparticles, *Toxicol. Lett.* 197 (2010) 82–87.

- [32] S. Love, C. Haynes, Assessment of functional changes in nanoparticle-exposed neuroendocrine cells with amperometry: Exploring the generalizability of nanoparticle-vesicle matrix interactions, *Anal. Bioanal. Chem.* (2010) 1–12.
- [33] E.J. Park, E. Bae, J. Yi, Y. Kim, K. Choi, S.H. Lee, J. Yoon, B.C. Lee, K. Park, Repeated-dose toxicity and inflammatory responses in mice by oral administration of silver nanoparticles, *Environ. Toxicol. Pharmacol.* 30 (2010) 162–168.
- [34] S. Wise, B.C. Goodale, S.S. Wise, G.A. Craig, A.F. Pongan, R.B. Walter, W.D. Thompson, A.K. Ng, A.M. Aboueissa, H. Mitani, M.J. Spalding, M.D. Mason, Silver nanospheres are cytotoxic and genotoxic to fish cells, *Aquatic Toxicol.* 97 (2010) 34–41.
- [35] S. Arora, J. Jain, J.M. Rajwade, K.M. Paknikar, Interactions of silver nanoparticles with primary mouse fibroblasts and liver cells, *Toxicol. Appl. Pharmacol.* 236 (2009) 310–318.
- [36] C. Greulich, S. Kittler, M. Eppler, G. Muhr, M. Koller, Studies on the biocompatibility and the interaction of silver nanoparticles with human mesenchymal stem cells (hMSCs), *Langenbecks Arch. Surg.* 394 (2009) 495–502.
- [37] K. Kalishwaralal, E. Banumathi, S.R.K. Pandian, V. Deepak, J. Muniyandi, S.H. Eom, S. Gurunathan, Silver nanoparticles inhibit VEGF induced cell proliferation and migration in bovine retinal endothelial cells, *Colloid Surf. B* 73 (2009) 51–57.
- [38] K. Kawata, M. Osawa, S. Okabe, In vitro toxicity of silver nanoparticles at non-cytotoxic doses to HepG2 human hepatoma cells, *Environ. Sci. Technol.* 43 (2009) 6046–6051.
- [39] S. Kim, J.E. Choi, J. Choi, K.H. Chung, K. Park, J. Yi, D.Y. Ryu, Oxidative stress-dependent toxicity of silver nanoparticles in human hepatoma cells, *Toxicol. In Vitro* 23 (2009) 1076–1084.
- [40] N. Miura, Y. Shinohara, Cytotoxic effect and apoptosis induction by silver nanoparticles in HeLa cells, *Biochem. Biophys. Res. Commun.* 390 (2009) 733–737.
- [41] H. Rosas-Hernández, S. Jiménez-Badillo, P.P. Martínez-Cuevas, E. Gracia-Espino, H. Terrones, M. Terrones, S.M. Hussain, S.F. Ali, C. González, Effects of 45-nm silver nanoparticles on coronary endothelial cells and isolated rat aortic rings, *Toxicol. Lett.* 191 (2009) 305–313.
- [42] M. Ahamed, M. Karns, M. Goodson, J. Rowe, S.M. Hussain, J.J. Schlager, Y. Hong, DNA damage response to different surface chemistry of silver nanoparticles in mammalian cells, *Toxicol. Appl. Pharmacol.* 233 (2008) 404–410.
- [43] C. Carlson, S.M. Hussain, A.M. Schrand, L.K. Braydich-Stolle, K.L. Hess, R.L. Jones, J.J. Schlager, Unique cellular interaction of silver nanoparticles: Size-dependent generation of reactive oxygen species, *J. Phys. Chem. B* 112 (2008) 13608–13619.
- [44] Y.H. Hsin, C.F. Chen, S. Huang, T.S. Shih, P.S. Lai, P.J. Chueh, The apoptotic effect of nanosilver is mediated by a ROS- and JNK-dependent mechanism involving the mitochondrial pathway in NIH3T3 cells, *Toxicol. Lett.* 179 (2008) 130–139.
- [45] N. Lubick, Nanosilver toxicity: Ions, nanoparticles—Or both? *Environ. Sci. Technol.* 42 (2008) 8617.
- [46] A.M. Schrand, L.K. Braydich-Stolle, J.J. Schlager, L. Dai, S.M. Hussain, Can silver nanoparticles be useful as potential biological labels? *Nanotechnology* 19 (2008) 235104.
- [47] S. Park, Y.K. Lee, M. Jung, K.H. Kim, N. Chung, E.K. Ahn, Y. Lim, K.H. Lee, Cellular Toxicity of various inhalable metal nanoparticles on human alveolar epithelial cells, *Inhal. Toxicol.* 19 (2007) 59–65.
- [48] K.F. Soto, L.E. Murr, K.M. Garza, Cytotoxic responses and potential respiratory health effects of carbon and carbonaceous nanoparticulates in the Paso del Norte airshed environment, *Int. J. Environ. Res. Public Health* 5 (2008) 12–25.

- [49] S.M. Hussain, A.K. Javorina, A.M. Schrand, H.M. Duhart, S.F. Ali, J.J. Schlager, The interaction of manganese nanoparticles with PC-12 cells induces dopamine depletion, *Toxicol. Sci.* 92 (2006) 456–463.
- [50] L.K. Braydich-Stolle, B. Lucas, A. Schrand, R.C. Murdock, T. Lee, J.J. Schlager, S.M. Hussain, M.C. Hofmann, Silver nanoparticles disrupt GDNF/Fyn kinase signaling in spermatogonial stem cells, *Toxicol. Sci.* 116 (2010) 577–589.
- [51] S.M. Hussain, K.L. Hess, J.M. Gearhart, K.T. Geiss, J.J. Schlager, In vitro toxicity of nanoparticles in BRL 3A rat liver cells, *Toxicol. In Vitro* 19 (2005) 975–983.
- [52] K.F. Soto, A. Carrasco, T.G. Powell, K.M. Garza, L.E. Murr, Comparative *in vitro* cytotoxicity assessment of some manufactured nanoparticulate materials characterized by transmission electron microscopy, *J. Nanopart. Res.* 7 (2005) 145–169.
- [53] E.J. Park, J. Yi, Y. Kim, K. Choi, K. Park, Silver nanoparticles induce cytotoxicity by a Trojan-horse type mechanism, *Toxicol. In Vitro* 24 (2010) 872–878.
- [54] J.D. Brain, M.A. Curran, T. Donaghey, R.M. Molina, Biologic responses to nanomaterials depend on exposure, clearance, and material characteristics, *Nanotoxicology* 3 (2009) 174–180.
- [55] A. Dhawan, V. Sharma, D. Parmar, Nanomaterials: A challenge for toxicologists, *Nanotoxicology* 3 (2009) 1–9.
- [56] A. Nel, T. Xia, L. Madler, N. Li, Toxic potential of materials at the nanolevel, *Science* 311 (2006) 622–627.
- [57] J.H. Ji, J.H. Jung, S.S. Kim, J.U. Yoon, J.D. Park, B.S. Choi, Y.H. Chung, I.H. Kwon, J. Jeong, B.S. Han, J.H. Shin, J.H. Sung, *et al.*, Twenty-eight-day inhalation toxicity study of silver nanoparticles in Sprague-Dawley rats, *Inhal. Toxicol.* 19 (2007) 857–871.
- [58] J.H. Sung, J.H. Ji, J.U. Yoon, D.S. Kim, M.Y. Song, J. Jeong, B.S. Han, J.H. Han, Y.H. Chung, J. Kim, T.S. Kim, H.K. Chang, *et al.*, Lung function changes in Sprague-Dawley rats after prolonged inhalation exposure to silver nanoparticles, *Inhal. Toxicol.* 20 (2008) 567–574.
- [59] Y.S. Kim, J.S. Kim, H.S. Cho, D.S. Rha, J.M. Kim, J.D. Park, B.S. Choi, R. Lim, H.K. Chang, Y.H. Chung, I.H. Kwon, J. Jeong, *et al.*, Twenty-eight-day oral toxicity, genotoxicity, and gender-related tissue distribution of silver nanoparticles in Sprague-Dawley rats, *Inhal. Toxicol.* 20 (2008) 575–583.
- [60] M.F. Rahman, J. Wang, T.A. Patterson, U.T. Saini, B.L. Robinson, G.D. Newport, R.C. Murdock, J.J. Schlager, S.M. Hussain, S.F. Ali, Expression of genes related to oxidative stress in the mouse brain after exposure to silver-25 nanoparticles, *Toxicol. Lett.* 187 (2009) 15–21.
- [61] J.S. Hyun, B.S. Lee, H.Y. Ryu, J.H. Sung, K.H. Chung, I.J. Yu, Effects of repeated silver nanoparticles exposure on the histological structure and mucins of nasal respiratory mucosa in rats, *Toxicol. Lett.* 182 (2008) 24–28.
- [62] H.Y. Lee, Y.J. Choi, E.J. Jung, H.Q. Yin, J.T. Kwon, J.E. Kim, H.T. Im, M.H. Cho, J.H. Kim, H.Y. Kim, B.H. Lee, Genomics-based screening of differentially expressed genes in the brains of mice exposed to silver nanoparticles via inhalation, *J. Nanopart. Res.* 12 (2010) 1567–1578.
- [63] Y.S. Kim, M.Y. Song, J.D. Park, K.S. Song, H.R. Ryu, Y.H. Chung, H.K. Chang, J.H. Lee, K.H. Oh, B.J. Kelman, I.K. Hwang, I.J. Yu, Subchronic oral toxicity of silver nanoparticles, *Part. Fibre Toxicol.* 7 (2010) 20.
- [64] S. Takenaka, E. Karg, C. Roth, H. Schulz, A. Ziesenis, U. Heinzmann, P. Schramel, J. Heyder, Pulmonary and systemic distribution of inhaled ultrafine silver particles in rats, *Environ. Health Perspect.* 109 (Suppl. 4) (2001) 547–551.
- [65] G.N. Jeong, U.B. Jo, H.Y. Ryu, Y.S. Kim, K.S. Song, I.J. Yu, Histochemical study of intestinal mucins after administration of silver nanoparticles in Sprague-Dawley rats, *Arch. Toxicol.* 84 (2010) 63–69.

- [66] J.H. Sung, J.H. Ji, J.D. Park, J.U. Yoon, D.S. Kim, K.S. Jeon, M.Y. Song, J. Jeong, B.S. Han, J.H. Han, Y.H. Chung, H.K. Chang, *et al.*, Subchronic inhalation toxicity of silver nanoparticles, *Toxicol. Sci.* 108 (2009) 452–461.
- [67] J.H. Sung, J.H. Ji, K.S. Song, J.H. Lee, K.H. Choi, S.H. Lee, I.J. Yu, Acute inhalation toxicity of silver nanoparticles, *Toxicol. Ind. Health* 27 (2011) 149–154.
- [68] J. Tang, L. Xiong, S. Wang, J. Wang, L. Liu, J. Li, Z. Wan, T. Xi, Influence of silver nanoparticles on neurons and blood-brain barrier via subcutaneous injection in rats, *Appl. Surf. Sci.* 255 (2008) 502–504.
- [69] J. Tang, L. Xiong, S. Wang, J. Wang, L. Liu, J. Li, F. Yuan, T. Xi, Distribution, translocation and accumulation of silver nanoparticles in rats, *J. Nanosci. Nanotechnol.* 9 (2009) 4924–4932.
- [70] D.P. Lankveld, A.G. Oomen, P. Krystek, A. Neigh, J.A. Troost-de, C.W. Noorlander, J.C. Van Eijkeren, R.E. Geertsma, W.H. De Jong, The kinetics of the tissue distribution of silver nanoparticles of different sizes, *Biomaterials* 31 (2010) 8350–8361.
- [71] H.S. Sharma, S. Hussain, J. Schlager, S.F. Ali, A. Sharma, Influence of nanoparticles on blood-brain barrier permeability and brain edema formation in rats, *Acta Neurochir.* 106 (Suppl.) (2010) 359–364.
- [72] M. Fondevila, R. Herrero, M.C. Casallas, L. Abecia, J.J. Duchá, Silver nanoparticles as a potential antimicrobial additive for weaned pigs, *Anim. Feed Sci. Technol.* 150 (2009) 259–269.
- [73] P.L. Nadworny, J. Wang, E.E. Tredget, R.E. Burrell, Anti-inflammatory activity of nanocrystalline silver in a porcine contact dermatitis model, *Nanomedicine* 4 (2008) 241–251.
- [74] M.E. McAuliffe, M.J. Perry, Are nanoparticles potential male reproductive toxicants? A literature review, *Nanotoxicology* 1 (2010) 204–210.
- [75] W.Y. Kim, J. Kim, J.D. Park, H.Y. Ryu, I.J. Yu, Histological study of gender differences in accumulation of silver nanoparticles in kidneys of Fischer 344 rats, *J. Toxicol. Environ. Health A* 72 (2009) 1279–1284.
- [76] K.C. Bhol, P.J. Schechter, Topical nanocrystalline silver cream suppresses inflammatory cytokines and induces apoptosis of inflammatory cells in a murine model of allergic contact dermatitis, *Br. J. Dermatol.* 152 (2005) 1235–1242.
- [77] Z. Yang, Z.W. Liu, R.P. Allaker, P. Reip, J. Oxford, Z. Ahmad, G. Ren, A review of nanoparticle functionality and toxicity on the central nervous system, *J.R. Soc. Interface* 7 (Suppl. 4) (2010) S411–S422.
- [78] K. Bilberg, H. Malte, T. Wang, E. Baatrup, Silver nanoparticles and silver nitrate cause respiratory stress in Eurasian perch (*Perca fluviatilis*), *Aquatic Toxicol.* 96 (2010) 159–165.
- [79] J.E. Choi, S. Kim, J.H. Ahn, P. Youn, J.S. Kang, K. Park, J. Yi, D.Y. Ryu, Induction of oxidative stress and apoptosis by silver nanoparticles in the liver of adult zebrafish, *Aquatic Toxicol.* 100 (2010) 151–159.
- [80] J. Kim, S. Kim, S. Lee, Differentiation of the toxicities of silver nanoparticles and silver ions to the Japanese medaka (*Oryzias latipes*) and the cladoceran *Daphnia magna*, *Nanotoxicology* (2011) 5:208–214.
- [81] Y. Wu, Q. Zhou, H. Li, W. Liu, T. Wang, G. Jiang, Effects of silver nanoparticles on the development and histopathology biomarkers of Japanese medaka (*Oryzias latipes*) using the partial-life test, *Aquatic Toxicol.* 100 (2010) 160–167.
- [82] T.M. Scown, E.M. Santos, B.D. Johnston, B. Gaiser, M. Baalousha, S. Mitov, J.R. Lead, V. Stone, T.F. Fernandes, M. Jepson, R. van Aerle, C.R. Tyler, Effects of aqueous exposure to silver nanoparticles of different sizes in rainbow trout, *Toxicol. Sci.* 115 (2010) 521–534.
- [83] O. Bar-Ilan, R.M. Albrecht, V.E. Fako, D.Y. Furgeson, Toxicity assessments of multi-sized gold and silver nanoparticles in zebrafish embryos, *Small* 5 (2009) 1897–1910.

- [84] G. Laban, L. Nies, R. Turco, J. Bickham, M. Sepulveda, The effects of silver nanoparticles on fathead minnow (*Pimephales promelas*) embryos, *Ecotoxicology* 19 (2010) 185–195.
- [85] Y.J. Chae, C.H. Pham, J. Lee, E. Bae, J. Yi, M.B. Gu, Evaluation of the toxic impact of silver nanoparticles on Japanese medaka (*Oryzias latipes*), *Aquatic Toxicol.* 94 (2009) 320–327.
- [86] M.-K. Yeo, M. Kang, Effects of nanometer sized silver materials on biological toxicity during zebrafish embryogenesis, *Bull. Korean Chem. Soc.* 29 (2008) 1179–1184.
- [87] R.J. Griffitt, K. Hyndman, N.D. Denslow, D.S. Barber, Comparison of molecular and histological changes in zebrafish gills exposed to metallic nanoparticles, *Toxicol. Sci.* 107 (2009) 404–415.
- [88] R.J. Griffitt, J. Luo, J. Gao, J.C. Bonzongo, D.S. Barber, Effects of particle composition and species on toxicity of metallic nanomaterials in aquatic organisms, *Environ. Toxicol. Chem.* 27 (2008) 1972–1978.
- [89] P.V. AshaRani, Y.L. Wu, Z. Gong, S. Valiyaveetil, Toxicity of silver nanoparticles in zebrafish models, *Nanotechnology* 19 (2008) 255102.
- [90] K.J. Lee, P.D. Nallathamby, L.M. Browning, C.J. Osgood, X.H. Xu, In vivo imaging of transport and biocompatibility of single silver nanoparticles in early development of zebrafish embryos, *ACS Nano* 1 (2007) 133–143.
- [91] A.H. Ringwood, M. McCarthy, T.C. Bates, D.L. Carroll, The effects of silver nanoparticles on oyster embryos, *Marine Environ. Res.* 69 (2010) S49–S51.
- [92] J.N. Meyer, C.A. Lord, X.Y. Yang, E.A. Turner, A.R. Badireddy, S.M. Marinakos, A. Chilkoti, M.R. Wiesner, M. Auffan, Intracellular uptake and associated toxicity of silver nanoparticles in *Caenorhabditis elegans*, *Aquatic Toxicol.* 100 (2010) 140–150.
- [93] J.Y. Roh, S.J. Sim, J. Yi, K. Park, K.H. Chung, D.Y. Ryu, J. Choi, Ecotoxicity of silver nanoparticles on the soil nematode *Caenorhabditis elegans* using functional ecotoxicogenomics, *Environ. Sci. Technol.* 43 (2009) 3933–3940.
- [94] M. Ahamed, R. Posgai, T.J. Gorey, M. Nielsen, S.M. Hussain, J.J. Rowe, Silver nanoparticles induced heat shock protein 70, oxidative stress and apoptosis in *Drosophila melanogaster*, *Toxicol. Appl. Pharmacol.* 242 (2010) 263–269.
- [95] H.R. Siddique, K. Mitra, V.K. Bajpai, R.K. Ravi, D.K. Saxena, D.K. Chowdhuri, Hazardous effect of tannery solid waste leachates on development and reproduction in *Drosophila melanogaster*: 70 kDa heat shock protein as a marker of cellular damage, *Ecotoxicol. Environ. Saf.* 72 (2009) 1652–1662.
- [96] T.M. Benn, P. Westerhoff, Nanoparticle silver released into water from commercially available sock fabrics, *Environ. Sci. Technol.* 42 (2008) 7025–7026.
- [97] S.A. Cumberland, J.R. Lead, Particle size distributions of silver nanoparticles at environmentally relevant conditions, *J. Chromatogr. A* 1216 (2009) 9099–9105.
- [98] E. Navarro, F. Piccapietra, B. Wagner, F. Marconi, R. Kaegi, N. Odzak, L. Sigg, R. Behra, Toxicity of silver nanoparticles to *Chlamydomonas reinhardtii*, *Environ. Sci. Technol.* 42 (2008) 8959–8964.
- [99] S.W.P. Wijnhoven, W.J.G.M. Peijnenburg, C.A. Herberths, W.I. Hagens, A.G. Oomen, E.H.W. Heugens, B. Roszek, J. Bisschops, I. Gosens, D. Van De Meent, S. Dekkers, W.H. De Jong, *et al.*, Nano-silver—A review of available data and knowledge gaps in human and environmental risk assessment, *Nanotoxicology* 3 (2009) 109–138.
- [100] G. Oberdörster, V. Stone, K. Donaldson, Toxicology of nanoparticles: A historical perspective, *Nanotoxicology* 1 (2007) 2–25.
- [101] K. Cha, H.W. Hong, Y.G. Choi, M.J. Lee, J.H. Park, H.K. Chae, G. Ryu, H. Myung, Comparison of acute responses of mice livers to short-term exposure to nano-sized or micro-sized silver particles, *Biotechnol. Lett.* 30 (2008) 1893–1899.

- [102] P.L. Nadworny, J. Wang, E.E. Tredget, R.E. Burrell, Anti-inflammatory activity of nanocrystalline silver-derived solutions in porcine contact dermatitis, *J. Inflamm. (Lond.)* 7 (2010) 13.
- [103] J. Tian, K.K. Wong, C.M. Ho, C.N. Lok, W.Y. Yu, C.M. Che, J.F. Chiu, P.K. Tam, Topical delivery of silver nanoparticles promotes wound healing, *ChemMedChem* 2 (2007) 129–136.
- [104] K.K. Wong, S.O. Cheung, L. Huang, J. Niu, C. Tao, C.M. Ho, C.M. Che, P.K. Tam, Further evidence of the anti-inflammatory effects of silver nanoparticles, *ChemMedChem* 4 (2009) 1129–1135.
- [105] W. Boucher, J.M. Stern, V. Kotsinyan, D. Kempuraj, D. Papaliodis, M.S. Cohen, T.C. Theoharides, Intravesical nanocrystalline silver decreases experimental bladder inflammation, *J. Urol.* 179 (2008) 1598–1602.
- [106] N. Li, C. Sioutas, A. Cho, D. Schmitz, C. Misra, J. Sempf, M. Wang, T. Oberley, J. Froines, A. Nel, Ultrafine particulate pollutants induce oxidative stress and mitochondrial damage, *Environ. Health Perspect.* 111 (2003) 455–460.
- [107] A. Nel, Air pollution-related illness: Effects of particles, *Science* 308 (2005) 804–806.
- [108] G. Oberdorster, A. Maynard, K. Donaldson, V. Castranova, J. Fitzpatrick, K. Ausman, J. Carter, B. Karn, W. Kreyling, D. Lai, S. Olin, N. Monteiro-Riviere, *et al.*, Principles for characterizing the potential human health effects from exposure to nanomaterials: Elements of a screening strategy, *Part. Fibre Toxicol.* 2 (2005) 8.
- [109] Y. Mo, R. Wan, S. Chien, D.J. Tollerud, Q. Zhang, Activation of endothelial cells after exposure to ambient ultrafine particles: The role of NADPH oxidase, *Toxicol. Appl. Pharmacol.* 236 (2009) 183–193.
- [110] B. Halliwell, Antioxidant defence mechanisms: From the beginning to the end (of the beginning), *Free Radic. Res.* 31 (1999) 261–272.
- [111] K.B. Holt, A.J. Bard, Interaction of silver(I) ions with the respiratory chain of *Escherichia coli*: An electrochemical and scanning electrochemical microscopy study of the antimicrobial mechanism of micromolar Ag^+ , *Biochemistry* 44 (2005) 13214–13223.
- [112] F. Martinez-Gutierrez, P.L. Olive, A. Banuelos, E. Orrantia, N. Nino, E.M. Sanchez, F. Ruiz, H. Bach, Y. Av-Gay, Synthesis, characterization, and evaluation of antimicrobial and cytotoxic effect of silver and titanium nanoparticles, *Nanomedicine* 6 (2010) 681–688.
- [113] J. Grigg, A. Tellabati, S. Rhead, G.M. Almeida, J.A. Higgins, K.J. Bowman, G.D. Jones, P.B. Howes, DNA damage of macrophages at an air-tissue interface induced by metal nanoparticles, *Nanotoxicology* 3 (2009) 348–354.
- [114] M. Ahamed, R. Posgai, T.J. Gorey, M. Nielsen, S.M. Hussain, J.J. Rowe, Silver nanoparticles induced heat shock protein 70, oxidative stress and apoptosis in *Drosophila melanogaster*, *Toxicol. Appl. Pharmacol.* 242 (2010) 263–269.
- [115] J.M. Balbus, A.D. Maynard, V.L. Colvin, V. Castranova, G.P. Daston, R.A. Denison, K.L. Dreher, P.L. Goering, A.M. Goldberg, K.M. Kulinowski, N.A. Monteiro-Riviere, G. Oberdörster, *et al.*, Meeting report: Hazard assessment for nanoparticles—Report from an interdisciplinary workshop, *Environ. Health Perspect.* 115 (2007) 1654–1659.
- [116] R. Owen, M. Depledge, Nanotechnology and the environment: Risks and rewards, *Mar. Pollut. Bull.* 50 (2005) 609–612.
- [117] M.N. Moore, Do nanoparticles present ecotoxicological risks for the health of the aquatic environment? *Environ. Int.* 32 (2006) 967–976.

CARBOXYMETHYLATION OF DNA INDUCED BY *N*-NITROSO COMPOUNDS AND ITS BIOLOGICAL IMPLICATIONS

Jianshuang Wang *and* Yinsheng Wang*

Contents

1. Introduction	220
2. The Chemistry of DNA Carboxymethylation	221
2.1. Human exposure to NOCs	221
2.2. DNA carboxymethylation induced by NOCs	222
2.3. Diverse carboxymethylated DNA adducts and carboxymethylating agents	224
3. Detection of Carboxymethylated DNA Adducts	227
3.1. Radioisotope-labeled DNA-binding assay	228
3.2. Antibody-based immunoassay	229
3.3. Mass spectrometry	229
4. Chemical Synthesis of Carboxymethylated Nucleosides and Their Incorporation into DNA	230
4.1. Synthesis of carboxymethylated nucleosides	230
4.2. Site-specific incorporation of carboxymethylated nucleosides into oligodeoxyribonucleotides	234
5. Biological Implications	236
5.1. Relevance between carboxymethylating NOCs and gastrointestinal cancers	236
5.2. Mutagenicity and repair of carboxymethylated DNA adducts	237
References	239

Abstract

Chemical modifications of DNA are of interest in toxicology and in evaluating human health risks associated with exposure to chemical carcinogens. In this chapter, focus was placed on a specific type of DNA modification, namely DNA carboxymethylation, where a carboxymethyl moiety is covalently bonded to an

Department of Chemistry, University of California, Riverside, California, USA

*Corresponding author. Tel.: +1 (951) 827-2700; Fax: +1 (951) 827-4713

E-mail address: Yinsheng@ucr.edu

Advances in Molecular Toxicology, Volume 5

ISSN 1872-0854, DOI: 10.1016/B978-0-444-53864-2.00006-2

© 2011 Elsevier B.V.

All rights reserved.

oxygen or nitrogen atom at various positions of nucleobases. This modification is induced mainly upon exposure to endogenous and exogenous sources of *N*-nitroso compounds. We also described various carboxymethylated DNA lesions and diverse carboxymethylating agents that have been uncovered since the 1980s. In addition, we reviewed analytical methods for detecting carboxymethylated DNA lesions and synthetic strategies for the preparation of authentic carboxymethylated DNA lesions and their incorporation into oligodeoxyribonucleotides. Further, we discussed the cytotoxic and mutagenic properties of the carboxymethylated DNA lesions and the implications of these DNA lesions in the early stage of gastrointestinal cancer development.

1. INTRODUCTION

Chemical modification of DNA is of interest in toxicology and in evaluating human health risks associated with exposure to chemical carcinogens. Formation of various DNA adducts is considered an initial step for chemical species to exert their genotoxicity. In this chapter, we focus on a specific type of DNA modification, namely, carboxymethylation, where a carboxymethyl moiety is covalently bonded to an oxygen or nitrogen atom at various positions of nucleobases.

DNA carboxymethylation is mainly induced upon exposure to endogenous and exogenous sources of *N*-nitroso compounds (NOCs) [1,2], and it was hypothesized as a potential etiological factor for gastrointestinal carcinogenesis [3]. NOCs are characterized by a nitroso group ($-N=O$) being bonded to a nitrogen atom and are capable of inducing a diverse array of DNA adducts [4]. NOCs that can be considered as *N*-carboxymethyl-*N*-nitroso derivatives are potential carboxymethylating agents. Since the 1980s, a series of carboxymethylated DNA adducts have been shown to be formed *in vitro* and *in vivo*, and in the mean time, a number of carboxymethylating agents have been uncovered.

Initial toxicological and biological studies have concentrated on O^6 -carboxymethyl-2'-deoxyguanosine (O^6 -CMdG) since alkylation at the O^6 position of guanine is known to give rise to mutations by polymerase misinsertions. O^6 -Methyl-2'-deoxyguanosine (O^6 -MdG) is a highly mutagenic DNA adduct and subject to repair by O^6 -methylguanine methyltransferase (MGMT) [1]; however, O^6 -CMdG cannot be repaired by MGMT [1,5]. In addition, the cytotoxicity of azaserine (AS), a model carboxymethylating agent, is thought to be elicited by its effect on carboxymethylation, but not on methylation [5]. Moreover, replication of potassium diazoacetate (KDA, a carboxymethylating agent)-treated, human *p53* gene-containing plasmid in yeast cells gave rise to a mutation spectrum that is distinct from that induced by *N*-methyl-*N*-nitrosourea (MNU, a

methylating agent) [3]. Importantly, the types and frequencies of non-CpG mutations in human *p53* gene induced by KDA are strikingly similar to those found in stomach and colorectal cancers. Therefore, this study suggests that DNA carboxymethylation might be potentially involved in the early stage of gastrointestinal cancer development.

Although DNA carboxymethylation has been known for almost three decades, we are still in the relatively early stage of studies about chemistry of this modification and about the replication and repair of these carboxymethylated DNA lesions. The goal of this chapter is to introduce readers with our current understanding about DNA carboxymethylation.

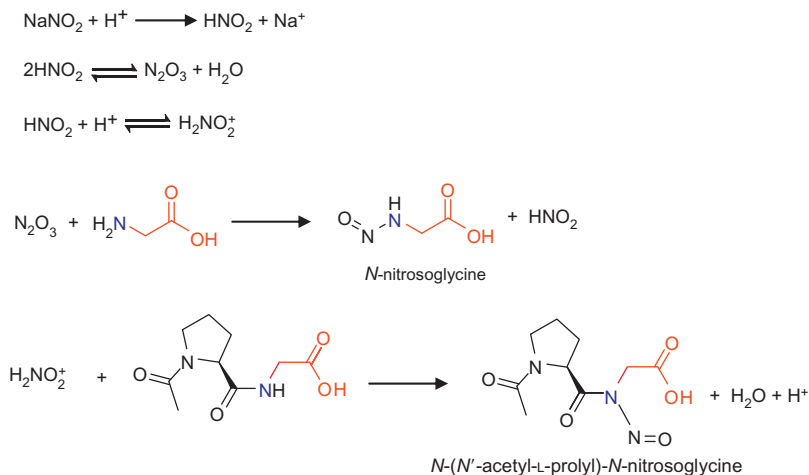
2. THE CHEMISTRY OF DNA CARBOXYMETHYLATION

2.1. Human exposure to NOCs

NOCs are ubiquitously present in the human environment, although at a very low level. Humans are exposed to NOCs and their precursors in tobacco smoke, as well as from occupational, dietary, and other environmental sources. For example, NOCs are found in tanneries and plants manufacturing pesticides, rubber products, and tires [6,7]. The most abundant NOCs present in the diet are nonvolatile *N*-nitrosated amino acids and amino acid derivatives such as *N*-nitrosated glycine [8], and they are mainly found in smoked and nitrate-cured meats, dried and smoked fish, seafood, and smoked cheese [9]. Other sources of NOCs are pharmaceuticals, toiletry and cosmetic products, and other household products such as detergents and pesticides [8].

In addition to exogenous sources, *in vivo* formation of NOCs was estimated to account for 45–75% of total human NOC exposure [8]. The endogenous transformation of amines to NOCs in laboratory animals and humans is well known. Many nitrogenous dietary precursors can be converted to NOCs through nitrite-derived nitrosation [4]. The principal reactions involved in this process are shown in Scheme 1. For nitrite to induce nitrosation, it must be acidified to form nitrous acid (HNO_2). On one hand, HNO_2 dimerizes to form N_2O_3 with the loss of water, and the resulting N_2O_3 reacts with amines to give NOCs; on the other hand, HNO_2 can be protonated to yield H_2NO_2^+ which preferentially reacts with amides to yield nitrosamides [4]. Owing to the importance of acidic environment in the generation of NOCs from nitrite, the acidic gastric compartment is expected to be the major site for nitrite-derived nitrosation in humans [10,11].

Other than nitrite-induced nitrosation, mammalian cell-mediated nitrosation and bacterial nitrosation are two other major pathways for endogenous generation of NOCs. Many types of mammalian cells produce NO via a common biochemical pathway involving oxidation of an ω -nitrogen of



Scheme 1 Formation of NOCs through nitrite-derived nitrosation.

L-arginine by NO synthase (NOS) in the presence of O_2 and coenzyme NADPH [12,13]. Being a signaling molecule, NO formed *in vivo* has important biological functions [14]. However, under certain conditions such as intense physical activity and immunostimulation, cells exhibit elevated endogenous NO synthesis, which may stimulate the generation of nitrosating species [15–17].

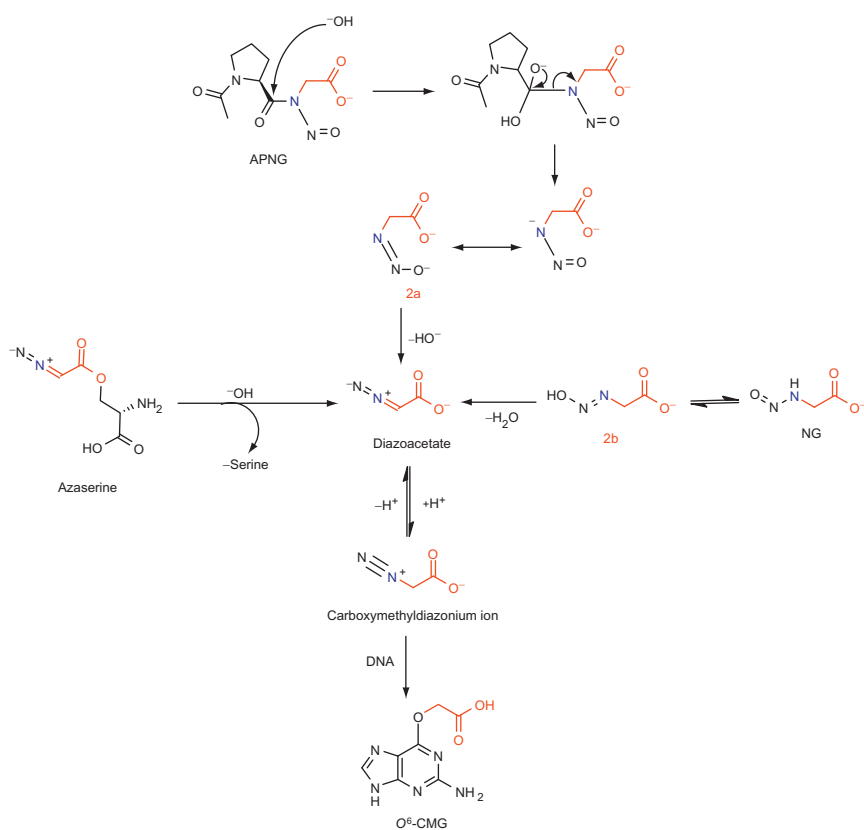
Some bacteria inhabiting the gastrointestinal tract can also evoke the nitrosation of secondary amines at neutral pH [18], where the cytochrome *cd*₁-nitrite reductase may catalyze nitrosation through the production of NO or NO-like species [19]. Bacterial nitrosation at neutral pH is inhibited by ascorbic acid [20] and cysteine [21], suggesting that the nitrosating species are most likely N_2O_3 or N_2O_4 produced via an NO intermediate. For example, *Escherichia coli* reduces nitrite to NO and a small amount of N_2O under anaerobic conditions; under aerobic conditions, nitrosating agents are produced and they are presumably N_2O_3 and N_2O_4 [22].

Several reviews summarized the mechanism by which NOCs exert their biological effects and their relevance to human cancers [23,24]. NOCs exhibit wide tissue specificity, and chemical modification of DNA induced by NOCs is thought to be the initial step of carcinogenesis [4].

2.2. DNA carboxymethylation induced by NOCs

NOCs are known alkylating agents, and O^6 -MdG is a characteristic mutagenic and toxic adduct induced by *N*-methyl-*N*-nitroso compounds. As described above, NOCs that can be considered as *N*-carboxymethyl-*N*-nitroso derivatives are potential carboxymethylating agents. Scheme 1

illustrates an example of *in vivo* formation of NOCs that are carboxymethylating agents. Once *N*-carboxymethyl-*N*-nitroso compounds are generated, they can undergo decomposition in stomach or move to other organs. The diffusion is mediated by a combined effect of their stability and surrounding pH [11]. It is well known that *N*-nitrosamines (as alkylating agents) require metabolic activation by cytochrome P450 enzyme to give α -hydroxynitrosamines as the initial step of alkylation, and nitrosamides are converted to alkylating species by chemical, nonenzymic reactions. However, the detailed mechanism of carboxymethylation remains largely unknown, and it was hypothesized that carboxymethylation occurs through a highly reactive intermediate, diazoacetate [2,25]. A representative mechanism based on nitrosamide and nitrosated primary amine is displayed in Scheme 2. The intermediates are proposed structures and have not been formally



Scheme 2 Formation of diazoacetate and its induction of DNA carboxymethylation.

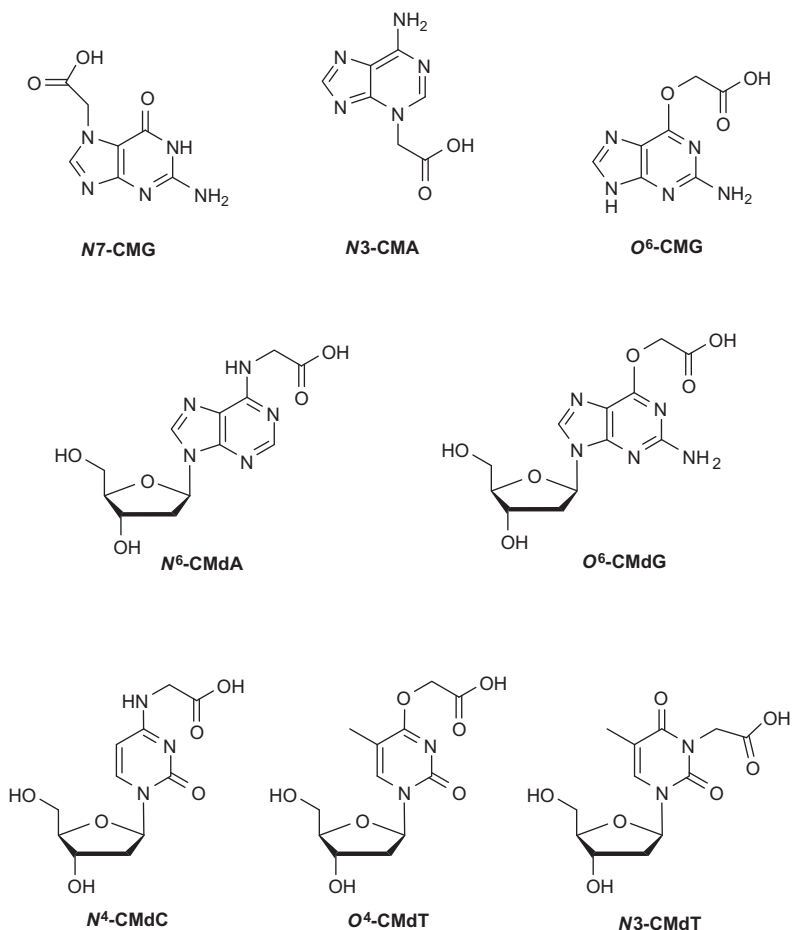
characterized, and other type of carboxymethylating agents may also require metabolic activation to initiate the decomposition.

It is of note that intermediates 2a and 2b in Scheme 2 are diazoates which possess a *Z* or *E* conformation. Fishbein *et al.* [26] previously demonstrated that in general simple (*E*)-alkanediazoates decompose with rate-limiting N–O bond heterolysis yielding diazonium ions that are diffusionally equilibrated intermediates. Decomposition of (*Z*)-diazoates requires acid catalysis to enable proton transfer to oxygen that is concerted with N–O bond heterolysis to yield diazonium ions. *Z* and *E* isomers usually have different decomposition rates, and in a case of trifluoroethanediazoic acid, the *Z* isomer decomposes 2600 times faster than the *E* isomer. Although the intermediates generated from decomposition of carboxymethylating agents have not been characterized, it is reasonable to extend the aforementioned generation mechanism of diazonium ions from alkanediazoates to carboxymethyl diazoates (intermediates 2a and 2b).

It should be pointed out that most carboxymethylating agents can also induce methylation to a lesser extent, and different compounds yield different ratios of methyl and carboxymethyl adducts upon reaction with DNA. This observation appears to rule out a possibility that the intermediate such as carboxymethyldiazonium ion is not the only source giving rise to both carboxymethyl and methyl adducts. It suggests that, during the decomposition of carboxymethylating agents, intermediates other than carboxymethyldiazonium ion may also arise from the precursors; however, these intermediates are not in rapid equilibria with each other. As a result, the partition between carboxymethylation and methylation varies among different carboxymethylating agents [2,25]. The proposed mechanism for diazoacetate-mediated carboxymethylation, as illustrated in Scheme 2, is based on the alkylation mechanism of simple NOCs, though other mechanisms are also possible.

2.3. Diverse carboxymethylated DNA adducts and carboxymethylating agents

Many carboxymethylated DNA adducts emanating from exposure to NOCs have been identified, and the structures of known carboxymethylated DNA adducts are summarized in Scheme 3. In 1982, Longnecker *et al.* [27] identified the first carboxymethylated DNA adduct, N7-carboxymethylguanine (N7-CMG) in pancreatic acinar cells treated with AS. Shuker *et al.* [28] subsequently carried out a large body of work about DNA carboxymethylation. In 1987, they found that the incubation of calf thymus DNA with *N*-nitrosoglycocholic acid (NOGC) *in vitro* gave rise to N7-CMG, N3-carboxymethyladenine (N3-CMA), and O⁶-carboxymethylguanine (O⁶-CMG). Later in 1997, they reported the synthesis of O⁶-CMdG and detected, by using an immunochemical method, this adduct in calf thymus

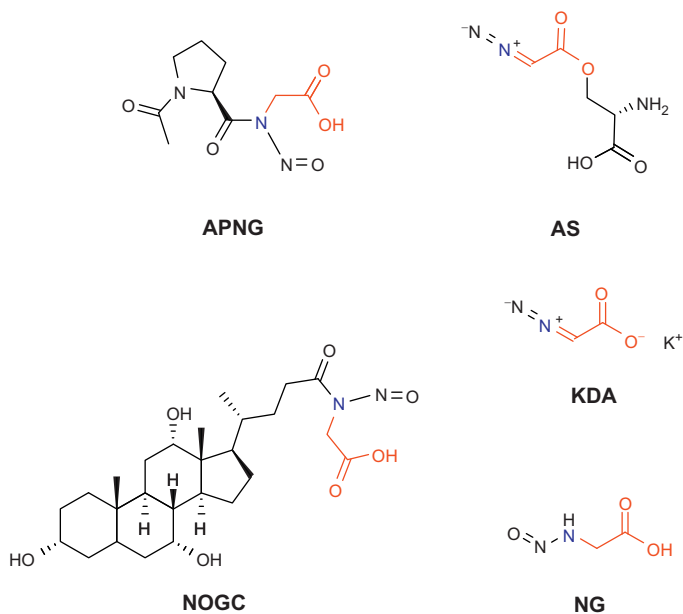


Scheme 3 Carboxymethylated DNA adducts induced by NOCs.

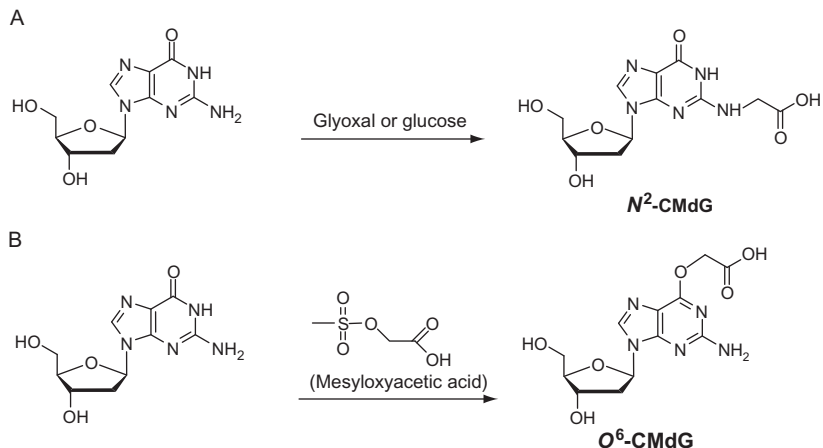
DNA treated *in vitro* with three different carboxymethylating agents encompassing *N*-(*N*⁷-acetyl-L-prolyl)-*N*-nitrosoglycine (APNG), AS, and KDA [29]. In 2004, they discovered that *O*⁶-CMdG can be produced in calf thymus DNA treated with a reaction mixture of nitric oxide (NO) and glycine, which was the first time that *O*⁶-CMdG was found to arise from NO exposure [30]. Very recently, several carboxymethylated DNA adducts including *N*⁴-carboxymethyl-2'-deoxycytidine (*N*⁴-CMdC), *N*3-carboxymethylthymidine (*N*3-CMdT), *O*⁴-carboxymethylthymidine (*O*⁴-CMdT), and *N*⁶-carboxymethyl-2'-deoxyadenosine (*N*⁶-CMdA) were chemically synthesized and their formation in calf thymus DNA upon treatment with KDA was confirmed by LC-MS/MS [31,32].

DNA carboxymethylation is largely induced by NOCs. Among the many *N*-alkyl-*N*-nitroso compounds that are known to be carcinogenic, many are carboxymethylating agents that share a common feature of being an *N*-carboxymethyl-*N*-nitroso derivative. Some examples of carboxymethylating agents are shown in Scheme 4. Strictly speaking, AS and KDA are not true NOCs, but they can be considered as the decomposition intermediates of their corresponding NOCs. Thus, we do not exclude them when discussing NOCs as carboxymethylating agents.

Aside from NOCs, other chemicals are also capable of inducing DNA carboxymethylation. As a toxic chemical present in the environment and a degradation product of glucose under physiological conditions, glyoxal was frequently observed to be present at elevated levels in the plasma of patients with diabetes, peritoneal dialysis, and uremia [33–35]. An earlier study by Kronberg *et al.* [36] demonstrated that treatment of 2'-deoxyguanosine or calf thymus DNA with glyoxal could give rise to *N*²-carboxymethyl-2'-deoxyguanosine (*N*²-CMdG) as well as some other adducts, but *N*²-CMdG was found to be the only stable adduct formed during this treatment. In addition, Wang *et al.* [37] recently observed that incubation of calf thymus DNA with glucose or glyoxal led to a dose-dependent formation of *N*²-CMdG (Scheme 5A), and exposure of HEK 293T cells to glyoxal further stimulated the formation of this adduct. It was also found that



Scheme 4 Examples of NOCs that are carboxymethylating agents.



Scheme 5 Formation of carboxymethylated DNA adducts by non-NOC species: (A) glyoxal or glucose; (B) mesyloxyacetic acid.

mesyloxyacetic acid (MAA) can induce both carboxymethylation and methylation at O⁶ position of 2'-deoxyguanosine in calf thymus DNA (Scheme 5B) [2], and the ratio of O⁶-CMdG to O⁶-MdG was found to be 18 upon treatment with 5 mM of MAA [2].

3. DETECTION OF CARBOXYMETHYLATED DNA ADDUCTS

Detection of DNA adducts remains one of the core tasks for research in DNA damage. Various methods for DNA adduct detection have been developed over the past few decades [38]. Except for immunohistochemical methods which can facilitate the detection of DNA adducts in intact tissues, other detection methods normally require sample preparation, where DNA extraction and adduct isolation constitute two major steps.

Several methods are available for extracting DNA from tissues of laboratory animals and patients as well as from cultured cells that are treated with genotoxic agents. Phenol–chloroform extraction is a classic DNA isolation method that has been used for many decades. In order to avoid using toxic phenol, a simple high salt method was developed in which cellular proteins were first precipitated from a solution containing high concentrations of inorganic salts and DNA was subsequently isolated by ethanol precipitation [39]. If operated properly, both methods can afford high-quality DNA. Since the amount of DNA adducts is typically many orders of magnitude

lower than unmodified DNA bases in biological samples, enrichment of DNA adducts of interest is sometimes necessary prior to the measurement. During the enrichment process, DNA adducts, in the form of nucleobases, 2'-deoxyribonucleosides or 2'-deoxyribonucleotides, are first liberated from DNA chain by hydrolysis or enzymatic digestion. The mild enzymatic digestion method has the least likelihood in the artificial generation or decomposition of DNA adduct(s) under investigation. However, neutral thermal hydrolysis is also effective in releasing N7-guanine and N3-adenine derivatives; the formation of the latter two modified nucleobases renders the N-glycosidic linkage labile. Adducts of interest are subsequently enriched from the mixtures by various separation techniques including column purification, HPLC, solid-phase extraction, and extraction of hydrophobic adducts into butanol. The accumulated DNA adducts are then subject to analysis.

A variety of analytical methods are available for DNA adduct detection, and the choice of a method depends on the form of DNA available for analysis and the type of DNA adduct under investigation. Next, we discuss several methods that have been used for detecting carboxymethylated DNA adducts.

3.1. Radioisotope-labeled DNA-binding assay

By dosing experimental animals, culturing cells or treating isolated DNA with radioisotope-labeled genotoxic compounds, radioisotope-labeled DNA adducts can be generated. This is probably the most reliable method to reveal all adducts that may be induced by a genotoxic agent. Owing to their long half-lives, ^3H - and ^{14}C -labeled compounds are most commonly used in such studies. The disadvantages of this method lie in two aspects: first, not all genotoxic agents are available in the radiolabeled form; second, under certain experimental conditions or in specific biological tissues, the relatively rapid and easy exchange of ^3H with the nonradioactive ^1H results in false-positive identification and inaccurate quantification of DNA adducts [40].

After treatment with the radiolabeled compound, DNA is isolated, purified, and the labeled adducts are detected by scintillation counting to quantify the total amount of bound radioactivity. In order to confirm the adduct formation and elucidate the chemical structure of adduct, the radioactively labeled DNA is usually digested to 2'-deoxynucleosides and separated by HPLC to reveal whether the radiolabel is from a covalently bound adduct or other nonadduct species such as metabolites of radiolabeled compounds or noncovalent adduct. In addition, by comparison with the chromatogram of authentic compounds, certain DNA adducts can be identified [41,42]. Along this line, Longnecker *et al.* [27] cultured pancreatic acinar cells with ^{14}C -labeled AS and subsequently employed neutral thermal

hydrolysis to liberate the unstable *N*-alkylated purines. One component in the purine mixture coeluted with authentic *N*7-CMG on three different HPLC systems, thereby establishing *N*7-CMG as a DNA adduct induced by AS. Radioisotope-labeled DNA-binding assay is capable of detecting one adduct in up to 10^8 nucleotides, but requires submilligram to several milligrams of DNA sample.

3.2. Antibody-based immunoassay

Immunoassay for DNA adduct detection is based on the specific interaction between an antibody and a DNA adduct of interest [43,44]. Among the various DNA adduct detection techniques, immunohistochemistry is unique in that it can detect DNA adducts in intact tissues. Intact DNA or digested DNA can be analyzed by competitive immunoassays, and antibodies to DNA adducts may also be used to prepare immunoaffinity columns. Although specific antibodies for adducts of interest are often not available, antibodies against some methyl and carboxymethyl adducts were developed. Along this line, Shuker *et al.* [2] established a combined immunoaffinity/HPLC method to assess the concomitant formation of *O*⁶-CMdG and *O*⁶-MdG in calf thymus DNA upon exposure to nitrosated glycine derivatives.

It is worth noting that, in addition to the limitation of antibodies, some antibodies may not be highly specific to the adduct of interest and they may cross-react with adduct(s) of similar structure. Antibody-based immunoassay requires less DNA sample (normally 1–200 µg) than what is needed for radioisotope-labeled DNA-binding assay. The sensitivity of immunoassay depends on the binding affinity of the antibody for the adduct of interest; thus, it is variable among different biological samples, but could reach one adduct per 10^8 nucleotides.

3.3. Mass spectrometry

Today, mass spectrometry has become the most powerful bioanalytical tool in many fields of research and continues to improve and achieve greater application and sensitivity. Among all the detection methods for DNA adducts in cellular or tissue DNA, mass spectrometry provides the most structural information especially when tandem mass spectrometry is employed [45,46]. Along this line, the elimination of 2-deoxyribose is frequently observed upon the collisionally induced dissociation (CID) of 2'-deoxynucleosides and their derivatives, and this loss is reflected by a mass difference of 116 Da between the fragment and precursor ions in tandem mass spectra. This fragmentation pathway is commonly employed for the LC-MS/MS analysis of modified 2'-deoxyribonucleosides. In this vein, this method was recently used for the successful identification of four

carboxymethylated DNA adducts including N^3 -CMdT, O^4 -CMdT, N^6 -CMdA, and N^4 -CMdC [31,32].

The great success of the LC-MS/MS method is attributed to the development of electrospray ionization (ESI) which allows direct introduction of HPLC effluent into a mass spectrometer. If stable isotope-labeled internal standards are available, accurate quantitation can be achieved. The sensitivity of mass spectrometry has continued to improve, and it already reached the level of one adduct per 10^9 – 10^{10} nucleosides.

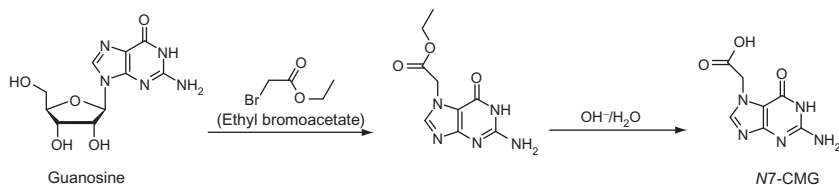
4. CHEMICAL SYNTHESIS OF CARBOXYMETHYLATED NUCLEOSIDES AND THEIR INCORPORATION INTO DNA

4.1. Synthesis of carboxymethylated nucleosides

Although many methods for DNA adduct analysis have been developed, most of them rely on the availability of structurally defined DNA lesions as standards. Viewing that direct treatment of nucleosides with a chemical carcinogen often results in the formation of the adduct of interest in a relatively low yield and it is frequently difficult to isolate pure and sufficient modified nucleosides from the reaction mixture, synthesis of authentic compounds is often necessary.

The introduction of an ester form of the carboxymethyl functionality into nucleobases has been recognized as a key step toward the synthesis of carboxymethylated DNA adducts, and the desired carboxymethylated adduct can be obtained from simple alkaline hydrolysis of the ester derivative. For instance, treatment of 2'-deoxyguanosine with ethyl bromoacetate yielded 7-ethoxycarbonylmethylguanine which, upon alkaline hydrolysis, rendered N^7 -CMG (Scheme 6) [47].

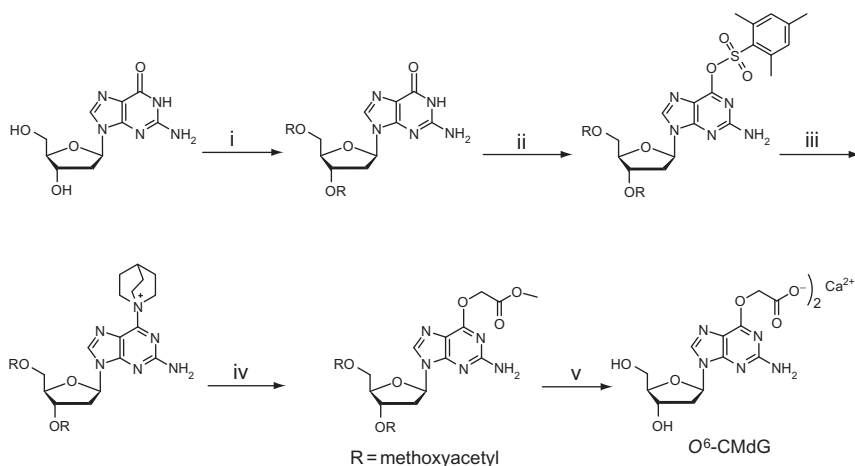
Since the 1990s, synthesis of authentic carboxymethylated DNA adducts has been extended to 2'-deoxyribonucleoside derivatives. Although proper protection and deprotection are sometimes required for deoxyribose hydroxyl groups, this approach offers several obvious advantages. (1)



Scheme 6 Synthesis of N^7 -carboxymethylguanine.

As described above, stable carboxymethylated nucleobase lesions can be released from DNA as nucleosides upon enzymatic digestion. The availability of the authentic nucleoside derivatives makes it feasible to identify carboxymethylated lesion(s) in the nucleoside mixture. (2) Upon appropriate nucleobase protection, 2'-deoxyribonucleoside derivatives can be converted to phosphoramidite building blocks, which are amenable for the incorporation of the modified nucleosides into DNA by automated solid-phase DNA synthesis. This aspect will be discussed further in Section 4.2. Since modification on O^6 position of guanine is known to be mutagenic, efforts were first made toward synthesizing O^6 -CMdG (Scheme 7) [29].

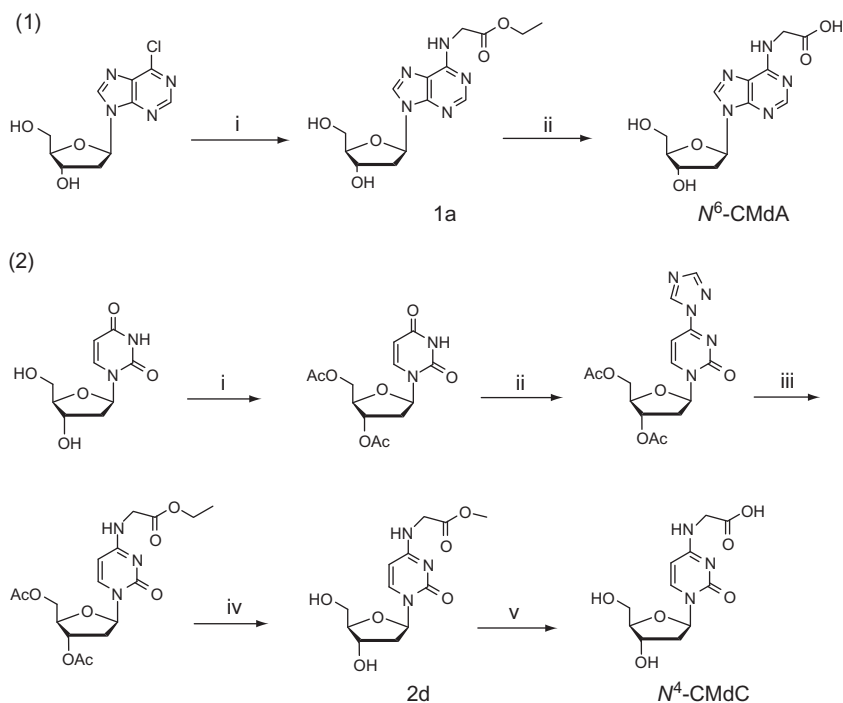
The synthetic route for O^6 -CMdG was based on an approach developed by Gaffney and Jones [48]. In this regard, the 3',5'-hydroxyl groups were first protected with readily hydrolyzable H_3COCO -functionalities, and the O^6 -arylsulfonate is subsequently replaced with a trialkylamine, quinuclidine, with the resulting trialkylammonium intermediate reacting with methyl glycolate to give the corresponding ester derivative of O^6 -CMdG. It is of note that intermediate trimethylammonium or *N*-methylpyrrolidinium ion in Gaffney's and Jones' reaction is not suitable for preparing O^6 -CMdG, and these two intermediates gave rise to the formation of substantial amounts of 6-(dimethylamino)- and 6-pyrrolidino-dG products, respectively. The introduction of quinuclidine overcame this problem and afforded a 65% conversion yield.



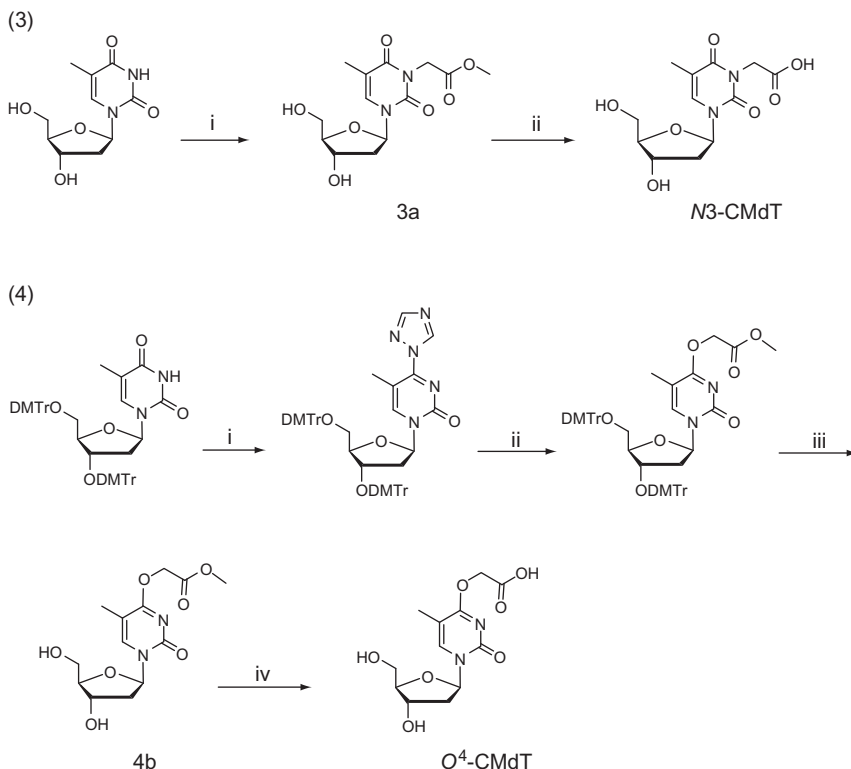
Scheme 7 Synthesis of O^6 -carboxymethyl-2'-deoxyguanosine. Conditions: (i) methoxyacetic anhydride, *N,N*-dimethylformamide (DMF); (ii) mesitylenesulfonyl chloride, triethylamine (TEA), *N,N*-dimethyl-4-aminopyridine (DMAP); (iii) quinuclidine, tetrahydrofuran (THF); (iv) methyl glycolate, 1,8-diazabicyclo[5.4.0]undec-7-ene (DBU), THF, 65 °C; (v) 1, TEA, MeOH; 2, $Ca(OH)_2/H_2O$.

In the recent couple of years, we synthesized authentic carboxymethylated derivatives of 2'-deoxyadenosine, 2'-deoxycytidine and thymidine (see synthetic procedures in Schemes 8 and 9) [31,32]. In this respect, we introduced the ethoxycarbonylmethyl functionality to the N^6 position of 2'-deoxyadenosine by substitution of the chlorine atom in 6-Cl-dA with glycine ethyl ester, and the resulting compound was hydrolyzed under alkaline conditions to render N^6 -CMdA. The chemical synthesis of N^4 -CMdC was inspired by the previous synthesis of O^4 -methylthymidine [49]. In this vein, the 1,2,4-triazolyl moiety was replaced with glycine ethyl ester in the presence of triethylamine to give ester derivative of N^4 -CMdC, which was again hydrolyzed under alkaline conditions to yield the desired N^4 -CMdC.

We also introduced the methyl ester derivative of the carboxymethyl functionality to the N^3 position of thymidine by alkylation with methyl bromoacetate, and treated the resulting compound with 0.5 M NaOH



Scheme 8 Synthesis of N^6 -carboxymethyl-2'-deoxyadenosine and N^4 -carboxymethyl-2'-deoxycytidine. Conditions: (1): (i) glycine ethyl ester, TEA, acetonitrile (ACN); (ii) 0.5 M NaOH/MeOH. (2): (i) acetic anhydride, DMAP, ACN; (ii) 1,2,4-triazole, phosphorus oxychloride, TEA, ACN; (iii) glycine ethyl ester, TEA, ACN; (iv) 0.4 M TEA/MeOH; (v) 0.5 M NaOH/MeOH.



Scheme 9 Synthesis of *N*3-carboxymethylthymidine and *O*⁴-carboxymethylthymidine. Conditions: (3): (i) methyl bromoacetate, potassium carbonate, MeOH; (ii) 0.5 M aqueous NaOH. (4): (i) 1,2,4-triazole, phosphorus oxychloride, TEA, CH₃CN; (ii) methyl glycolate, DBU, CH₃CN; (iii) trichloroacetic acid, CH₂Cl₂; (iv) 0.1 M aqueous NaOH.

to give the desired *N*3-CMdT. *O*⁴-CMdT was synthesized by using a nucleoside conversion strategy similar to the synthesis of *N*⁴-CMdC. The 1,2,4-triazolyl moiety was incorporated into the C4 carbon atom of 3',5'-*O*-di-DMTr-protected thymidine, which, upon treatment with methyl glycolate in the presence of 1,8-diazabicycloundec-7-ene (DBU), renders the corresponding methyl ester of *O*⁴-CMdT. The DMTr groups in the latter derivative was removed by using 3% trichloroacetic acid (TCA) in CH₂Cl₂, and the resulting product was incubated with 0.1 M NaOH to give the corresponding carboxylic acid derivative, *O*⁴-CMdT.

We used two-dimensional NMR methods to confirm the structures of carboxymethylated DNA adducts. In particular, the heteronuclear multiple-bond correlation (HMBC) experiment allowed us to assign unambiguously the sites of carboxymethylation in the modified nucleosides. In this respect,

the two methylene protons in the carboxymethyl functionality exhibit strong correlation with the C6 atom in N^6 -CMdA, the C4 atom in N^4 -CMdC, both the C2 and C4 atoms in $N3$ -CMdT, and the C4 atom (but not the C2 atom) in O^4 -CMdT (Figure 1). These distinct spectral features confirm the sites where the carboxymethyl moiety is introduced [31,32].

4.2. Site-specific incorporation of carboxymethylated nucleosides into oligodeoxyribonucleotides

The availability of oligodeoxyribonucleotides (ODNs) bearing a site-specifically incorporated carboxymethylated adduct constitutes a crucial step toward examining the biological implications of these adducts at the molecular level. Solid-phase DNA synthesis makes use of phosphoramidite derivatives of four nucleosides with nucleobase amino groups being properly protected. If a phosphoramidite derivative of a DNA adduct is available, this adduct can be site-specifically inserted into a certain ODN sequence by using automated solid-phase ODN synthesis.

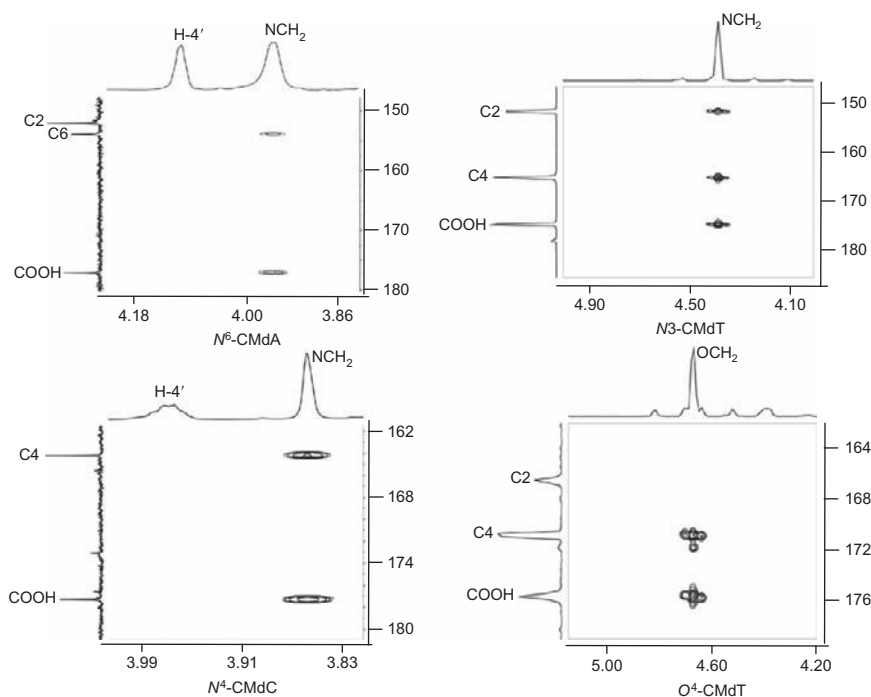
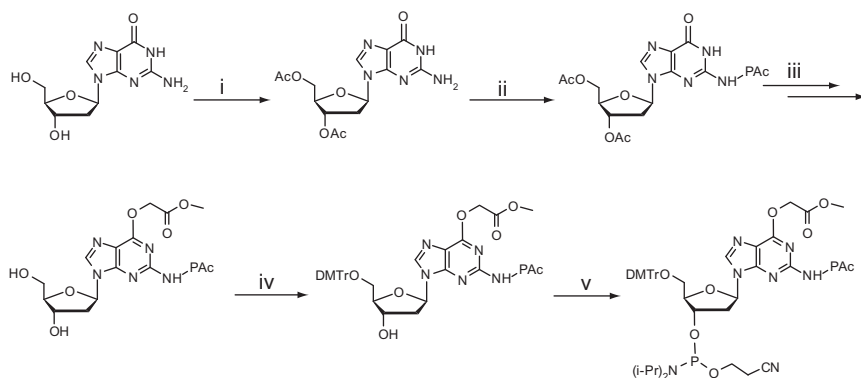


Figure 1 ^1H - ^{13}C HMBC Spectra of N^6 -CMdA, N^4 -CMdC, $N3$ -CMdT, and O^4 -CMdT. Correlations indicate the positions where the carboxymethyl moiety is covalently bonded.

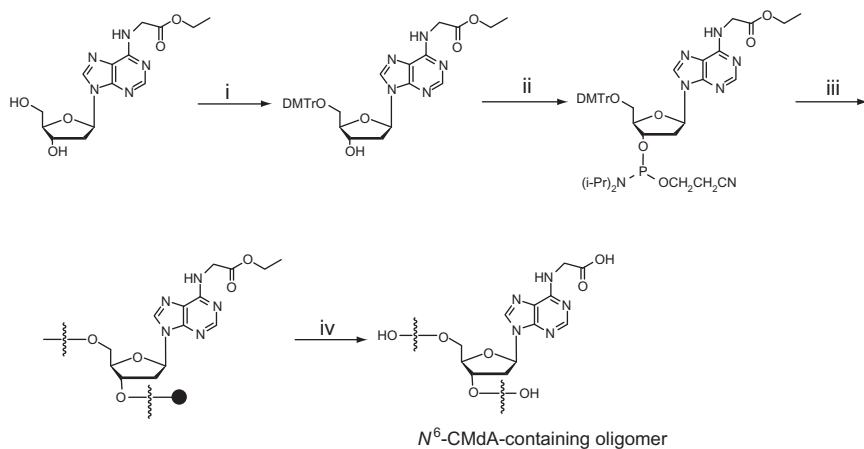
In 2000, Xu [50] developed the first synthetic route to incorporate the O^6 -CMdG into a 12-mer ODN. It was found that an acyl group at the N^2 -position of an O^6 -substituted guanine is much more resistant to removal by ammonia than that at N^2 -position of an unmodified guanine [51–53]; therefore, the isobutyryl group that is frequently used for protecting the amino group in 2'-deoxyguanosine is no longer suitable for amino protection in O^6 -CMdG. For this reason, a base-labile functionality, phenoxyacetyl (Pac) group was chosen for N^2 protection in O^6 -CMdG phosphoramidite synthesis [50]. Xu's synthetic pathway is summarized in Scheme 10.

After ODN assembly, the amino-protecting groups on nucleobases need to be removed. However, since the carboxymethyl moiety is in its ester form, common deprotection procedures with the concentrated ammonium hydroxide cannot be used, as this will result in partial conversion of ester to amide. Nevertheless, aqueous NaOH at low concentration satisfactorily produced oligomers containing O^6 -CMdG. Risks that one needs to be aware of are that alkaline solution might lead to the conversion of N^6 -substituted adenine and N^4 -substituted cytosine into hypoxanthine and uracil, respectively, but this can be largely avoided by using NaOH solution at low concentration [50].

In our synthesis of ODNs containing carboxymethylated DNA adducts, certain precursors such as 1a, 2d, 3a, and 4b in Schemes 8 and 9 were readily converted to the corresponding phosphoramidites. After ODN assembly, simple alkaline hydrolysis rendered ODNs containing the desired



Scheme 10 Synthesis of O^6 -CMdG-containing phosphoramidite building block. Conditions: (i) acetic anhydride, pyridine, DMF; (ii) phenoxyacetic anhydride, pyridine; (iii) see corresponding conditions in Scheme 7; (iv) 4,4'-dimethoxytrityl chloride, DMAP, pyridine; (v) 2-cyanoethyl-*N,N*-diisopropylchlorophosphoramidite, diisopropylethylamine (DIPEA), CH_2Cl_2 .



Scheme 11 Synthesis of N^6 -CMda-containing phosphoramidite building block and its insertion into DNA. Conditions: (i) 4,4'-dimethoxytrityl chloride, DMAP, pyridine; (ii) 2-cyanoethyl- N,N -diisopropylchlorophosphoramidite, DIPEA, CH_2Cl_2 ; (iii) automated solid-phase DNA synthesis; (iv) 0.5 M aqueous NaOH, 6 h, followed by neutralization with 1.0 M aqueous HCl.

carboxymethylated adducts. Scheme 11 depicts a general protocol used for assembly and deprotection of ODNs containing N^6 -CMda [31,32].

5. BIOLOGICAL IMPLICATIONS

5.1. Relevance between carboxymethylating NOCs and gastrointestinal cancers

A number of studies have suggested the implications of human exposure to NOCs in the etiology of gastrointestinal cancer. The gastrointestinal tract tends to suffer long-term NOC exposure under a wide range of pH. The maximum total NOC level was observed at pH 1.0–2.5 and 6.0–8.5, which was attributed to chemical nitrosation at low pH and bacterial nitrosation at high pH. At pH 2–6, the NOC level decreases, but it is still higher than 3 μM in many individuals' gastric juice samples [54,55]. These endogenously produced NOCs are known to cause damage to DNA, and the resulting DNA adducts can be both mutagenic and carcinogenic.

Gastric infection with *Helicobacter pylori* contributes to the etiology of gastric cancer [56]. Intestinal metaplasia of the stomach, a precursor lesion for gastric cancer, is associated with *H. pylori* infection, elevated bile acid levels and other factors [57]. Earlier studies by Wogan *et al.* [58] revealed that the treatment of male Fischer rats with nitrosated bile acid conjugates

NOGC and *N*-nitrosotaurocholic acid (NOTC) could induce significant levels of hepatocarcinoma in 54–70% of the treated animals, and 12–13% of the treated rats developed gastric tumors. Forward mutation assay in *Salmonella typhimurium* and in TK6 diploid human lymphoblasts showed that NOGC and NOTC are both mutagenic, with NOGC being more effective in inducing mutations in TK6 cells.

By using the Comet assay, Shuker *et al.* [59] observed a dose-dependent DNA lesion formation upon KDA treatment in three different types of mammalian cells including human peripheral lymphocytes, human adenocarcinoma colon Caco-2 cells, and rat primary colon cells. This finding confirmed that KDA is genotoxic in a range of mammalian cells; however, the relative contributions of carboxymethylation and methylation remained unclear. Later, the same group demonstrated that red meat consumption enhances the colonic formation of O^6 -CMG [60]. Red meat is known to be associated with the endogenous formation of NOCs and increased risk for developing colorectal cancers. The percentage of positive staining for the NOC-specific DNA adduct, O^6 -CMG was significantly ($P < 0.001$) higher in colonic exfoliated cells of individuals on high-red-meat diet. O^6 -CMG was also found in intact small intestine from rats treated with the APNG and in HT-29 cells treated with diazoacetate. Since NOGC, APNG, and diazoacetate can all give rise to carboxymethylation of nucleobases in DNA, the above studies suggest that DNA carboxymethylation induced by NOCs could be involved in pathology of gastrointestinal cancers.

5.2. Mutagenicity and repair of carboxymethylated DNA adducts

Mutation in *p53* tumor suppressor gene is a hallmark for many human tumors. An earlier work by Greenblatt *et al.* [61], who reviewed more than 2500 *p53* mutations, revealed a high frequency of G:C → A:T transition mutations in human cancers which is accompanied by G → T and G → C transversion mutations. Simple alkylating NOCs may produce at least some of these G:C → A:T transitions, especially those occurring at non-CpG sites through the generation of O^6 -alkyl adducts of dG. However, Shuker *et al.* [3] recently observed that the passage of KDA-treated, human *p53* gene-containing plasmid in yeast cells can result in substantial single-base substitutions. Distinct from the high frequency of G:C → A:T transition mutations (>80%) induced by methylating agent MNU, KDA elicited almost equal distributions of transition and transversion mutations, and strikingly the mutation spectrum induced by KDA at non-CpG site is very similar to the corresponding mutation spectra found in stomach and colorectal cancers (Figure 2). In addition to carboxymethylated DNA lesions, KDA can also induce, to a lesser extent, methylated DNA adducts.

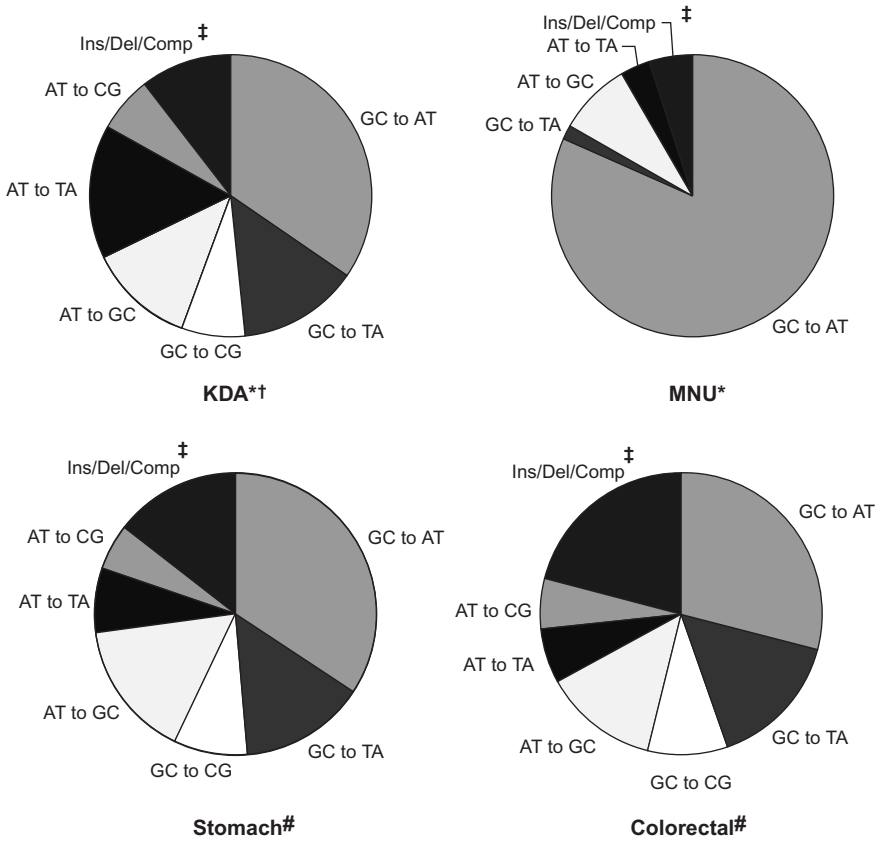


Figure 2 Comparison of mutation spectra of human *p53* gene induced by KDA and MNU in yeast cells with those found in stomach and colorectal cancers (reprint with permission from Oxford University Press).

The above findings suggest that carboxymethylation may contribute significantly to *p53* mutations in gastrointestinal cancers, and diazoacetate may constitute the major etiological agent in the development of gastrointestinal cancers. This conclusion was also consistent with a previous observation that the cytotoxicity of a model carboxymethylating agent AS is due to DNA carboxymethylation, but not methylation [5].

Another important aspect of this study highlighted a substantial frequency of single-base substitutions at A:T base pairs that are comparable to those observed in human gastrointestinal tumors. The percentages of mutations occurring at A:T base pairs account for 43% and 28% of all observed mutations, while the human *p53* gene-containing plasmid was treated with KDA in PBS and Tris-EDTA, respectively. Additionally, the observation of a significant proportion of mutations at A:T base pairs

supports that KDA can also induce promutagenic lesions at adenine and/or thymine. In this respect, our unpublished mutagenesis study showed that N3-CMdT and O⁴-CMdT are highly mutagenic in *E. coli* cells [62].

The high frequency of G:C → A:T mutations in *p53* in human cancers reduces the usefulness of this mutation in identifying the responsible carcinogens; however, the unique mutation spectra found in stomach and colorectal cancers suggest that carboxymethylating agents could contribute significantly to the etiology of these cancers, and carboxymethylated DNA adducts may serve as potential biomarkers for early diagnosis of these diseases.

To counteract the deleterious effects of DNA lesions, cells are equipped with an intricate DNA repair system. Some initial studies have been carried out for carboxymethylated DNA lesions, particularly for O⁶-CMdG. Despite the fact that O⁶-MdG is subject to repair by MGMT, O⁶-CMdG appears not to be repaired by MGMT. Along this line, Karran *et al.* [5] demonstrated that the AS-mediated cell killing cannot be rescued by the overexpression of MGMT, which agrees with a previous study by Shuker *et al.* [1] showing that O⁶-CMdG is not subject to repair by MGMT *in vitro*. Likewise, S⁶-CMdG, a structure analog of O⁶-CMdG, was found not to be a substrate for mismatch repair (MMR) system. However, lymphoblastoid cells deficient in nucleotide excision repair (NER) were significantly more sensitive to AS than the control repair-proficient cells, suggesting that O⁶-CMdG can be repaired by NER factors [5].

Although many human cancers have been linked to NOC exposure, DNA carboxymethylation arising from NOCs might be an important initial step toward the development of gastrointestinal cancers. The chemical synthesis of authentic carboxymethylated nucleosides and their incorporation into DNA facilitate the assessment of the formation and biological consequences of the carboxymethylated DNA lesions *in vivo*. We hope that future studies on how these DNA lesions perturb the fidelity and efficiency of DNA replication and how they are repaired in mammalian cells will improve further our understanding of the implications of these lesions in the development of gastrointestinal cancers.

REFERENCES

- [1] D.E.G. Shuker, G.P. Margison, Nitrosated glycine derivatives as a potential source of O⁶-methylguanine in DNA, *Cancer Res.* 57 (1997) 366–369.
- [2] K.L. Harrison, R. Jukes, D.P. Cooper, D.E.G. Shuker, Detection of concomitant formation of O⁶-carboxymethyl- and O⁶-methyl-2'-deoxyguanosine in DNA exposed to nitrosated glycine derivatives using a combined immunoaffinity/HPLC method, *Chem. Res. Toxicol.* 12 (1999) 106–111.
- [3] E. Gottschalg, G.B. Scott, P.A. Burns, D.E.G. Shuker, Potassium diazoacetate-induced *p53* mutations *in vitro* in relation to formation of O⁶-carboxymethyl- and O⁶-methyl-2'-

- deoxyguanosine DNA adducts: Relevance for gastrointestinal cancer, *Carcinogenesis* 28 (2007) 356–362.
- [4] S.S. Mirvish, Role of *N*-nitroso compounds (NOC) and *N*-nitrosation in etiology of gastric, esophageal, nasopharyngeal and bladder cancer and contribution to cancer of known exposures to NOC, *Cancer Lett.* 93 (1995) 17–48.
- [5] M. O'Driscoll, P. Macpherson, Y.Z. Xu, P. Karran, The cytotoxicity of DNA carboxymethylation and methylation by the model carboxymethylating agent azaserine in human cells, *Carcinogenesis* 20 (1999) 1855–1862.
- [6] A. Raj, J.F. Mayberry, T. Podas, Occupation and gastric cancer, *Postgrad. Med. J.* 79 (2003) 252–258.
- [7] W.J. Lee, W. Lijinsky, E.F. Heineman, R.S. Markin, D.D. Weisenburger, M.H. Ward, Agricultural pesticide use and adenocarcinomas of the stomach and oesophagus, *Occup. Environ. Med.* 61 (2004) 743–749.
- [8] A.R. Tricker, *N*-Nitroso compounds and man: Sources of exposure, endogenous formation and occurrence in body fluids, *Eur. J. Cancer Prev.* 6 (1997) 226–268.
- [9] J.E. Stuff, E.T. Goh, S.L. Barrera, M.L. Bondy, M.R. Forman, Construction of an *N*-nitroso database for assessing dietary intake, *J. Food Compos. Anal.* 22 (2009) S42–S47.
- [10] C.D. Leaf, J.S. Wishnok, S.R. Tannenbaum, Mechanisms of endogenous nitrosation, *Cancer Surv.* 8 (1989) 323–334.
- [11] S.S. Mirvish, Formation of *N*-nitroso compounds: Chemistry, kinetics, and *in vivo* occurrence, *Toxicol. Appl. Pharmacol.* 31 (1975) 325–351.
- [12] U. Forstermann, H.H.H.W. Schmidt, J.S. Pollock, H. Sheng, J.A. Mitchell, T.D. Warner, M. Nakane, F. Murad, Isoforms of nitric-oxide synthase: Characterization and purification from different cell-types, *Biochem. Pharmacol.* 42 (1991) 1849–1857.
- [13] D.J. Stuehr, N.S. Kwon, C.F. Nathan, O.W. Griffith, P.L. Feldman, J. Wiseman, *N*-omega-hydroxy-L-arginine is an intermediate in the biosynthesis of nitric-oxide from L-arginine, *J. Biol. Chem.* 266 (1991) 6259–6263.
- [14] E. Anggard, Nitric oxide: Mediator, murderer, and medicine, *Lancet* 343 (1994) 1199–1206.
- [15] S. Tamir, R.S. Lewis, T.D. Walker, W.M. Deen, J.S. Wishnok, S.R. Tannenbaum, The influence of delivery rate on the chemistry and biological effects of nitric oxide, *Chem. Res. Toxicol.* 6 (1993) 895–899.
- [16] S. Burney, J.L. Caulfield, J.C. Niles, J.S. Wishnok, S.R. Tannenbaum, The chemistry of DNA damage from nitric oxide and peroxynitrite, *Mutat. Res.* 424 (1999) 37–49.
- [17] M. Feelisch, T. Rassaf, S. Mnaimneh, N. Singh, N.S. Bryan, D. Jourdain, M. Kelm, Concomitant S-, N-, and heme-nitros(yl)ation in biological tissues and fluids: Implications for the fate of NO *in vivo*, *FASEB J.* 16 (2002) 1775–1785.
- [18] S.A. Leach, M. Thompson, M. Hill, Bacterially catalyzed *N*-nitrosation reactions and their relative importance in the human stomach, *Carcinogenesis* 8 (1987) 1907–1912.
- [19] S. Calmels, H. Ohshima, Y. Henry, H. Bartsch, Characterization of bacterial cytochrome cd(1)-nitrite reductase as one enzyme responsible for catalysis of nitrosation of secondary amines, *Carcinogenesis* 17 (1996) 533–536.
- [20] C.W. Mackerness, S.A. Leach, M.H. Thompson, M.J. Hill, The inhibition of bacterially mediated *N*-nitrosation by Vitamin C: Relevance to the inhibition of endogenous *N*-nitrosation in the achlorhydric stomach, *Carcinogenesis* 10 (1989) 397–399.
- [21] C.M. Odonnell, C. Edwards, J. Ware, Nitrosamine formation by clinical isolates of enteric bacteria, *FEMS Microbiol. Lett.* 51 (1988) 193–197.
- [22] X.B. Ji, T.C. Hollocher, Mechanism for nitrosation of 2,3-diaminonaphthalene by *Escherichia coli*: Enzymatic production of NO followed by O₂-dependent chemical nitrosation, *Appl. Environ. Microbiol.* 54 (1988) 1791–1794.

- [23] M.C. Archer, Mechanisms of action of *N*-nitroso compounds, *Cancer Surv.* 8 (1989) 241–250.
- [24] P.N. Magee, The experimental basis for the role of nitroso compounds in human cancer, *Cancer Surv.* 8 (1989) 207–239.
- [25] M.M. Kreevoy, Dennis E. Konasewich, The mechanism of hydrolysis of diazoacetate ion, *J. Phys. Chem.* 74 (26) (1970) 4464–4472.
- [26] J. Ho, J.C. Fishbein, Rate-limiting formation of diazonium ions in the aqueous decomposition of primary alkanediazoates, *J. Am. Chem. Soc.* 116 (1994) 6611–6621.
- [27] J. Zurlo, T.J. Curphey, R. Hiley, D.S. Longnecker, Identification of 7-carboxymethyl-guanine in DNA from pancreatic acinar cells exposed to azaserine, *Cancer Res.* 42 (1982) 1286–1288.
- [28] D.E.G. Shuker, J.R. Howell, B.W. Street, Formation and fate of nucleic acid and protein adducts from *N*-nitroso bile acid conjugates. In relevance of *N*-nitroso compounds for human cancer: Exposures and mechanisms, *IARC Sci. Publ.* 84 (1987) 187–190.
- [29] K.L. Harrison, N. Fairhurst, B.C. Challis, D.E.G. Shuker, Synthesis, characterization, and immunochemical detection of *O*⁶-carboxymethyl-2'-deoxyguanosine: A DNA adduct formed by nitrosated glycine derivatives, *Chem. Res. Toxicol.* 10 (1997) 652–659.
- [30] B.C. Cupid, Z.T. Zeng, R. Singh, D.E.G. Shuker, Detection of *O*⁶-carboxymethyl-2'-deoxyguanosine in DNA following reaction of nitric oxide with glycine and in human blood DNA Using a quantitative immunoslot blot assay, *Chem. Res. Toxicol.* 17 (2004) 294–300.
- [31] J. Wang, Y. Wang, Chemical synthesis of oligodeoxyribonucleotides containing N³- and *O*⁴-carboxymethylthymidine and their formation in DNA, *Nucleic Acids Res.* 37 (2009) 336–345.
- [32] J. Wang, Y. Wang, Synthesis and characterization of oligodeoxyribonucleotides containing a site-specifically incorporated *N*⁶-carboxymethyl-2'-deoxyadenosine or *N*⁴-carboxymethyl-2'-deoxycytidine, *Nucleic Acids Res.* 38 (2010) 6774–6784.
- [33] A. Lapolla, R. Flamini, A.D. Vedova, A. Senesi, R. Reitano, D. Fedele, E. Basso, R. Seraglia, P. Traldi, Glyoxal and methylglyoxal levels in diabetic patients: Quantitative determination by a new GC/MS method, *Clin. Chem. Lab. Med.* 41 (2003) 1166–1173.
- [34] Y. Ueda, T. Miyata, E. Goffin, A. Yoshino, R. Inagi, Y. Ishibashi, Y. Izuhara, A. Saito, K. Kurokawa, C.V. de Strihou, Effect of dwell time on carbonyl stress using icodextrin and amino acid peritoneal dialysis fluids, *Kidney Int.* 58 (2000) 2518–2524.
- [35] D.S.C. Raj, D. Choudhury, T.C. Welbourne, M. Levi, Advanced glycation end products: A nephrologist's perspective, *Am. J. Kidney Dis.* 35 (2000) 365–380.
- [36] D. Pluskota-Karwatka, A.J. Pawlowicz, M. Tomas, L. Kronberg, Formation of adducts in the reaction of glyoxal with 2'-deoxyguanosine and with calf thymus DNA, *Bioorg. Chem.* 36 (2008) 57–64.
- [37] H. Wang, H. Cao, Y. Wang, Quantification of *N*²-Carboxymethyl-2'-deoxyguanosine in calf thymus DNA and cultured human kidney epithelial cells by capillary high-performance liquid chromatography-tandem mass spectrometry coupled with stable isotope dilution method, *Chem. Res. Toxicol.* 23 (2010) 74–81.
- [38] M.W. Himmelstein, P.J. Boogaard, J. Cadet, P.B. Farmer, J.H. Kim, E.A. Martin, R. Persaud, D.E.G. Shuker, Creating context for the use of DNA adduct data in cancer risk assessment: II. Overview of methods of identification and quantitation of DNA damage, *Crit. Rev. Toxicol.* 39 (2009) 679–694.
- [39] S.A. Miller, D.D. Dykes, H.F. Polesky, A simple salting out procedure for extracting DNA from human nucleated cells, *Nucleic Acids Res.* 16 (1988) 1215.

- [40] R.T. Riley, B.W. Kemppainen, W.P. Norred, Quantitative tritium exchange of ^3H aflatoxin-B1 during penetration through isolated human skin, *Biochem. Biophys. Res. Commun.* 153 (1988) 395–401.
- [41] M. Stiborova, M. Miksanova, M. Sulc, H. Rydlova, H.H. Schmeiser, E. Frei, Identification of a genotoxic mechanism for the carcinogenicity of the environmental pollutant and suspected human carcinogen *o*-anisidine, *Int. J. Cancer* 116 (2005) 667–678.
- [42] P.J. Boogaard, K.P. de Kloe, E.D. Booth, W.P. Watson, DNA adducts in rats and mice following exposure to $[4-^{14}\text{C}]$ -1,2-epoxy-3-butene and to $[2,3-^{14}\text{C}]$ -1,3-butadiene, *Chem. Biol. Interact.* 148 (2004) 69–92.
- [43] U. Nair, H. Bartsch, J. Nair, Lipid peroxidation-induced DNA damage in cancer-prone inflammatory diseases: A review of published adduct types and levels in humans, *Free Radic. Biol. Med.* 43 (2007) 1109–1120.
- [44] M.C. Poirier, R.M. Santella, A. Weston, Carcinogen macromolecular adducts and their measurement, *Carcinogenesis* 21 (2000) 353–359.
- [45] R. Singh, P.B. Farmer, Liquid chromatography-electrospray ionization-mass spectrometry: The future of DNA adduct detection, *Carcinogenesis* 27 (2006) 178–196.
- [46] P.B. Farmer, R. Singh, Use of DNA adducts to identify human health risk from exposure to hazardous environmental pollutants: The increasing role of mass spectrometry in assessing biologically effective doses of genotoxic carcinogens, *Mutat. Res. Rev. Mutat. Res.* 659 (2008) 68–76.
- [47] B.W. Stewart, P.F. Swann, J.W. Holsman, P.N. Magee, Cellular injury and carcinogenesis: Evidence for alkylation of rat liver nucleic acids *in vivo* by *N*-nitrosomorpholine, *Z. Krebsforsch.* 82 (1974) 1–12.
- [48] B.L. Gaffney, R.A. Jones, Synthesis of O^6 -alkylated deoxyguanosine nucleosides, *Tetrahedron Lett.* 23 (1982) 2253–2256.
- [49] Y.Z. Xu, P.F. Swann, A simple method for the solid-phase synthesis of oligodeoxynucleotides containing O^4 -alkylthymine, *Nucleic Acids Res.* 18 (1990) 4061–4065.
- [50] Y.Z. Xu, Synthesis and characterization of DNA containing O^6 -carboxymethylguanine, *Tetrahedron* 56 (2000) 6075–6081.
- [51] B.F.L. Li, P.F. Swann, Synthesis and characterization of oligodeoxynucleotides containing O^6 -methylisopropylguanine, O^6 -ethylisopropylguanine, and O^6 -isopropylguanine, *Biochemistry* 28 (1989) 5779–5786.
- [52] C.A. Smith, Y.Z. Xu, P.F. Swann, Solid-phase synthesis of oligodeoxynucleotides containing O^6 -alkylguanine, *Carcinogenesis* 11 (1990) 811–816.
- [53] H. Borowyborowski, R.W. Chambers, A study of side reactions occurring during synthesis of oligodeoxynucleotides containing O^6 -alkyldeoxyguanosine residues at preselected sites, *Biochemistry* 26 (1987) 2465–2471.
- [54] G.P. Xu, P.I. Reed, Method for group determination of total *N*-nitroso compounds and nitrite in fresh gastric juice by chemical denitrosation and thermal energy analysis, *Analyst* 118 (1993) 877–883.
- [55] G.P. Xu, P.I. Reed, *N*-Nitroso compounds in fresh gastric juice and their relation to intragastric pH and nitrite employing an improved analytical method, *Carcinogenesis* 14 (1993) 2547–2551.
- [56] R.M. Peek, M.J. Blaser, *Helicobacter pylori* and gastrointestinal tract adenocarcinomas, *Nat. Rev. Cancer* 2 (2002) 28–37.
- [57] G.M. Sobala, B. Pignatelli, C.J. Schorah, H. Bartsch, M. Sanderson, M.F. Dixon, S. Shires, R.F.G. King, A.T.R. Axon, Levels of nitrite, nitrate, *N*-nitroso compounds, ascorbic acid and total bile acids in gastric juice of patients with and without precancerous conditions of the stomach, *Carcinogenesis* 12 (1991) 193–198.
- [58] W.F. Busby Jr., D.E. Shuker, G. Chamley, P.M. Newberne, S.R. Tannenbaum, G.N. Wogan, Carcinogenicity in rats of the nitrosated bile acid conjugates *N*-nitrosoglycocholic acid and *N*-nitrosotaurocholic acid, *Cancer Res.* 45 (1985) 1367–1371.

- [59] D. Anderson, R.J. Hambly, T.W. Yu, F. Thomasoni, D.E.G. Shuker, The effect of potassium diazoacetate on human peripheral lymphocytes, human adenocarcinoma colon Caco-2 cells, and rat primary colon cells in the Comet assay, *Teratogen. Carcin. Mut.* 19 (1999) 137–146.
- [60] M.H. Lewin, N. Bailey, T. Bandaletova, R. Bowman, A.J. Cross, J. Pollock, D.E.G. Shuker, S.A. Bingham, Red meat enhances the colonic formation of the DNA adduct *O*⁶-carboxymethyl guanine: Implications for colorectal cancer, *Cancer Res.* 66 (2006) 1859–1865.
- [61] M.S. Greenblatt, W.P. Bennett, M. Hollstein, C.C. Harris, Mutations in the *p53* tumor-suppressor gene: Clues to cancer etiology and molecular pathogenesis, *Cancer Res.* 54 (1994) 4855–4878.
- [62] B. Yuan, J. Wang, H. Cao, R. Sun, Y. Wang, High-throughput analysis of the mutagenic and cytotoxic properties of DNA lesions by next-generation sequencing, *Nucleic Acids Res.* 39 (2011) doi: 10.1093/nar/gkr159.

This page intentionally left blank

Subject Index

Page numbers followed by *f* indicate figures, *sch* indicate schemes and *t* indicate tables

A

Acetylcholinesterase (AChE)
 non-AChE mechanism
 gene expression profiling, 123–124
 oxidative stress, 124–125
 VX poisoning, 123
 OP nerve agents, 114–115
 sarin interaction, 115*f*
 AChE. *See* Acetylcholinesterase
 AgNPs. *See* Silver nanoparticles
 Algal toxins action mechanism
 AZAs
 AZA-1, 66
 SILAC procedure, 65–66
 toxicity cellular mechanisms, 64–65
 ciguateroxins
 ciguatera symptoms, 69–70
 P-CTX-1, 70
 gambierol, 71
 marine microalgae, 51
 MCs
 amnion cells, 59
 cellular responses, proteins, 57
 MC-LR, 56–57
 MC-RR, 59
 molecular mechanism, 56
 p44 ERK expression, 58
 p53 protein expression, 58–59
 protein spots, 58
 toxicity, molecular mechanism, 57–58
 tumor promoting activity, 56
 mixtures, 73–75
 molecular processes, 52
 OA, MCF-7 human breast cancer
 ATP metabolism, 63–64
 gene ontology (GO) database, 60–61
 hsp 27 isoforms, 61–63, 62*f*
 molecular responses, 64
 oxidative stress, cellular responses, 64
 omics technology, 55
 palytoxin
 Ostreopsis, 71–72
 PITX, MCF-7 cells, 72–73, 74*f*
 potency and molecular targets, 51–52, 52*t*
 receptors/targets and action mechanism,
 53–54

 toxicity and biomarkers, 54–55, 54*f*
 YTX, 67, 68–69
 Apoptosis
 BCL-2, 126
 Bcl-2-related genes, 127
 human neuronal cells gene expression, 127
 metal oxide nanoparticles, 152–153
 necrotic mechanism, 127–128
 nerve agent poisoning neurotoxic mechanism,
 126–127
 Azaspiracids (AZAs)
 algal toxins action mechanism
 AZA-1, 66
 SILAC procedure, 65–66
 toxicity cellular mechanisms, 64–65
 contamination, algal toxins
 DGs, 80
 Dinophysis species, 80–81
 P-ring proteins, 80

B

Blood-brain barrier (BBB) dysfunction
 break down mechanism, 130–131
 proinflammatory cytokines, 131
 sarin and soman, 130
 Bronchoalveolar lavage fluid (BALF), 150

C

Calf thymus (CT), 10
 Carboxymethylated nucleosides
 site-specific incorporation, ODNs
 alkaline hydrolysis, 235–236
 amino group protection, 235
 *N*⁶-CMdA, 236*sch*
 *O*⁶-CMdG phosphoramidite synthesis,
 235, 235*sch*
 solid-phase DNA synthesis, 234
 synthesis
 deoxyribose hydroxyl groups, 230–231
 HMBC, 233–234
 *N*⁶-CMdA and *N*⁴-CMdC, 232, 232*sch*
 *N*3-CMdT and *O*⁴-CMdT, 232–233,
 233*sch*
 *N*7-CMG, 230, 230*sch*
 *O*⁶-CMdG, 231, 231*sch*

- Cellular uptake, AgNPs
 intracellular, 182–183
 kinetics, 181
 mechanisms, *in vitro*, 182
- Chemical warfare nerve agent molecular toxicology
 acute toxic response, 137
 animal models, 135
 Chemical Weapons Convention, 113–114
 cholinergic and non-cholinergic mechanisms, 136, 136f
 exposure route, 114
 gene expression profiling, 137
 G-series and V-series organophosphorus, 49f, 112
 medical countermeasures
 OP, 116
 poisoning survivors, 116–117
 mitochondria, 137
 non-AChE mechanism, OP and exposure
 secondary effects
 apoptosis, 126–128
 BBB dysfunction, 130–131
 gene expression profiling, 123–124
 inflammation, 128–130
 mitochondrial dysfunction, 125–126
 oxidative stress, 124–125
 repair and recovery, 132–134
 VX poisoning, 123
 “omics” technologies, 134–135
 OP acute toxicity
 AChE, 114, 115f
 symptoms, 116
 screening, exposure
 bioinformatic tools, 120–121
 genomics, 117–118
 metabolomics, 120
 OP, 117
 proteomics, 118–120
 tabun, 112
 three-phase model
 oligonucleotide microarrays, 122
 sarin exposure, 122–123
 seizure, brain damage, 121–122
- Chloranilic acid
 formation, 15
 Lossen-type rearrangement, 35
 TCBQ conversion, 32, 33f
- Chlorinated phenol/quinone toxicity and bioaccumulation, 4
 carcinogenesis
 cancer risk, 5–6
 PCP, 5, 6
 carcinogenic polyhalogenated and hydroxamic acids
 BHA, TCBQ hydrolysis, 32, 34f
 cancer/iron-overload diseases, 31
 DTPA, 31–32
 phenyl isocyanate production, 33–34
 TCBQ to DDBQ, 32, 33f
 DFO protection, TCHQ-induced DNA damage
 cyto- and genotoxicity, human fibroblasts, 16–17
 TCSQ, 13–15
 PCP. *See* Pentachlorophenol
 regulation, 3
 structures, 2–3, 2f
 Ciguatoxins, 69–70
 Comet assay
 DNA
 damage, 9–10
 lesion formation, KDA treatment, 59
 PCP metabolites cyto- and genotoxic effects, 16–17
 CT. *See* Calf thymus
- ## D
- Desferal. *See* Desferrioxamine
 Desferrioxamine (DFO)
 iron-chelating property and TCSQ
 DTPA chemical structure, 14f
 and Fe(III) complex structure, 14f
 Fenton reaction, 13–15
 hydrolysis, chloranilic acid, 15
 TCHQ-induced cyto- and genotoxicity, human fibroblasts, 16–17
 MTT and “comet” assay, 16–17
 TCSQ radical inhibition, 16f
 2,5-Dichloro-3,6-dihydroxy-1,4-benzoquinone (DDBQ). *See* Chloranilic acid
 Diesel exhaust particles, 151–152
 Differential expression proteomics
 bioinformatic tools and databases
 computational, 95–96
 GO, 96–97
 MS techniques, 96
 hsp 27, 92
 microalgal toxins, 56, 68–69, 84
 proteins, biological systems, 85t
 quantitative issues, 81–84
 tools, 55
 toxicity pathways, 73
 toxin contamination, natural samples, 80
 DNA adduct detection
 analytical methods, 228
 antibody-based immunoassay, 229
 mass spectrometry
 LC-MS/MS method, 230
 structural information, 229–230
 phenol-chloroform extraction, 227–228
 radioisotope-labeled DNA-binding assay
³H- and ¹⁴C-labeled compounds, 228

scintillation counting, 228–229
DNA carboxymethylation, NOCs
adducts and
decomposition intermediates, 226
glyoxal, 226–227
mesyloxyacetic acid (MAA), 226–227, 227*sch*
N7-CMG and O⁶-CMdG, 224–225
adducts formation, 220
carboxymethylated nucleosides
site-specific incorporation, 234–236
synthesis, 230–234
carboxymethyldiazonium ion, 224
detection, DNA adducts
analytical methods, 228
antibody-based immunoassay, 229
mass spectrometry, 229–230
phenol-chloroform extraction, 227–228
radioisotope-labeled DNA-binding assay,
228–229
diazoacetate formation, 223
endogenous and exogenous sources, 220
gastrointestinal cancers
comet assay, 237
Helicobacter pylori, 236–237
pH range, 236
human exposure
bacterial nitrosation, 222
cancers, 222
dietary precursors, 221
nitrite-induced nitrosation, 221–222, 222*sch*
mutagenicity and repair, adducts
A:T base pairs, 238–239
comparison, human *p53* gene mutation
spectra, 238*f*
G:C→A:T transition, 237–238
human cancers, 239
O⁶-CMdG, 239
O⁶-CMdG, 220–221, 222–224
Z and E isomers, 224
DNA microarray-based gene expression profiling,
165–166, 167–169

E

Electron spin resonance (ESR) trapping
method, 23–24

F

Fenton reaction, 8–9, 17, 19–20

G

Gambierol, 71
Gastrointestinal cancers, 236–237
Gene expression profiling, nanomaterials
DNA microarray-based analysis
cellular responses assessment, 165–166
in vivo studies, 167–169

pulmonary fibrosis, 166
in vivo studies
C₆₀ fullerenes, 167
CNTs, 166–167
German nerve agent (G-agent), 112

H

Haber–Weiss reaction, 8
Heteronuclear multiple-bond correlation
(HMBC), 233–234, 234*f*
Hydrogen peroxide (H₂O₂)
DCBQ, 28–29
DMPO-157 adduct, 28
HRP/H₂O₂-mediated PCP oxidation, 11–12
metal-independent production, OH, 17–24
remediation, environmental pollutants, 31
TCHQ genotoxicity, 9–10
Hydroxyl radical
DNA damage, 9, 13–15
metal-independent production, 17–24
scavenger, 16–17

I

Inflammation

gene expression
proinflammatory, 129
sarin-induced, 128
neurodegenerative disorders, 128
proinflammatory cytokines, 130
response
cytokines, 153
iron oxide, 153
NiO, 154
solubility, 154
Y₂O₃ and ZnO, 153
soman intoxication, 129–130

L

Lossen rearrangement mechanism, 31–36

M

Material safety data sheet (MSDS), 160, 162
MCs. *See* Microcystins
Mechanisms of toxicity
gene expression profiling, 123–124
global profiling technique, 137
nerve agents, 118–119
OP exposure, 117
proteomics, 54*f*
Metal oxides nanoparticles toxicity, biological
effects
adsorption, 160
apoptosis, 152–153
biological influences evaluation, 169–170, 171*f*
cellular influence factors, 169–170, 170*f*

- Metal oxides nanoparticles toxicity, biological effects (*cont.*)
- evaluation methods
 - adsorption, *in vitro* testing, 162
 - cultured cells, *in vitro* experiments, 162–164
 - dosage, 165
 - fetus effects, 164–165
 - gene expression profiling, nanomaterials, 165–169
 - in vitro* vs. *in vivo* experiments, 164
 - markers, 163*t*
 - NOAEL, 165
 - noncellular system, 162
 - solubility, 162
 - in vivo* and *in vitro* characterization, 161
 - inflammation response
 - cytokines, 153
 - iron oxide, 153
 - NiO, 154
 - solubility, 154
 - Y₂O₃ and ZnO, 153
 - long-term effects
 - carcinogenesis, 155
 - lungs, 154–155
 - oxidative stress
 - CeO₂ biological effects, 151–152
 - glutathione and heme oxygenase, 147–148
 - homeostasis, 147–148
 - intracellular inducement, 149–151
 - markers, 148–149
 - particle shape and crystalline phase, 161
 - primary particle, aggregate and agglomerate
 - anatase TiO₂, 156–157
 - cosmetics, 156
 - definition, 156
 - loose bonding, 155–156
 - phagocytosis, 157
 - solubility
 - metal ions elution, 159
 - MSDS, 160
 - NiO nano and fine particles, 159
 - surface area and activity
 - functional group and adsorbed materials, 159
 - NH₂, –OH and –COOH, 158
 - physical and chemical, 157
 - physicochemical properties, 158
 - ROS production, 157–158
 - zeta potential, 160–161
- Microalgal toxins
- differential expression proteomics, 81, 82*t*
 - MCs, 84
 - molecular targets, 52*t*
 - palytoxin, 71–73
 - protein staining and image analysis, 81–84
 - proteomic, 54–55, 54*f*
 - seafood contamination, 53–54
- Microarray
- DNA based analysis, gene expression profiling
 - cellular responses assessment, 165–166
 - in vivo* studies, 167–169
 - pulmonary fibrosis, 166
 - nerve agent-induced BBB, 130–131
 - oligonucleotide, 122, 133*f*
 - RNA, 205
 - sarin and soman, 137
- Microcystins (MCs)
- algal toxins action mechanism
 - ammon cells, 59
 - cellular responses, proteins, 57
 - MC-LR, 56–57
 - MC-RR, 59
 - molecular mechanism, 56
 - p44 ERK expression, 58
 - p53 protein expression, 58–59
 - protein spots, 58
 - toxicity, molecular mechanism, 57–58
 - tumor promoting activity, 56
 - contamination, algal toxins
 - biomarkers, 76
 - C. fluminea*, 77–78
 - medaka fishes, MC-LR, 76
 - zebrafish, 78
- Microcystis, 56–60
- Mitochondrial dysfunction
- ATP levels, intracellular, 126
 - CNS, 125
 - intracellular calcium sequestration, 125
 - stress, 125–126
- Molecular screening, toxicant exposure
- bioinformatic tools
 - microarray technology, 120–121
 - software programs, 121
 - genomics, 117–118
 - metabolomics, 120
 - OP, 117
 - proteomics
 - gene expression, 118–119
 - protein microarrays, 120
 - technologies, 119
- MSDS. *See* Material safety data sheet
- N**
- Nanoparticles (NPs)
- definition, 180
 - detection, 183
 - silver. *See* Silver nanoparticles
 - surface modification, 182
- Nanosilver
- medical products, 180–181
 - NPs, 181
 - release, 198
- N7-carboxymethylguanine (N7-CMG)
- pancreatic acinar cells, 224–225
 - synthesis, 230*sch*
- Nerve agent toxicity

- exposure, 114
medical countermeasures, 116–117
non-AChE mechanism, OP
 apoptosis, 126–128
 BBB dysfunction, 130–131
 inflammation, 128–130
 mitochondrial dysfunction, 125–126
 oxidative stress, 124–125
 repair and recovery, 132–134
 three-phase model, 121–123
N-nitroso compounds (NOCs)
 DNA carboxymethylation. *See* DNA
 carboxymethylation, NOCs
 gastrointestinal cancers, 236–237
 human exposure, 221–222
NPs. *See* Nanoparticles
- O**
- Okadaic acid (OA)
 algal toxin contamination
 digestive gland (DG), *Mytilus galloprovincialis*, 79
 and proteomic analysis, 78–79
MCF-7 human breast cancer
 ATP metabolism, 63–64
 gene ontology (GO) database, 60–61
 hsp 27 isoforms, 61–63, 62f
 molecular responses, 64
 oxidative stress, cellular responses, 64
Organophosphate, 113
Oxidative stress
 AgNP-induced toxicity
 GSH depletion, 207
 induction, DNA damage, 208t
 mitochondria, 207
 reactive oxygen species (ROS), 206–207
 CeO₂ biological effects
 BEAS-2B, 151
 Nrf2, 152
 and Y₂O₃, 151–152
 enzymes hyperactivation, 124–125
 homeostasis, 147–148
 intracellular inducement
 A549 cells, 149
 BEAS-2B cells, 150
 CuO and ZnO, 149
 induction, 150–151
 RAW264.7 cells, 150
 ROS level, 149
 SiO₂ and ZnO, 149–150
 TiO₂, 150
 markers, 148–149
 nerve agent poisoning, 125
- P**
- Palytoxin (PITX)
 description, 71–72
- effect, hsp 27, 83f
MCF-7 cell line, 72–73
OA and, 92
toxicity pathway, 88f, 89f
PCP. *See* Pentachlorophenol
PCP quinoid metabolite-induced genotoxicity
 molecular mechanism, OH and H₂O₂
 Carassius auratus liver, 23–24
 chlorinated quinones, chemical
 structures, 20f
 DNA sensor, DNA damage, 22–23
 Fenton reaction, 19–20
 TCBQ, 22, 23f
 TCSQ, 20–21, 21f
 TrCBQ-OH, 22
OH production and H₂O₂
 DMPO/OH and DMPO/CH₃, 17–19
 ESR spin trapping methods, 18f
 Fenton reaction, 17
 salicylate hydroxylation method, 17
organic hydroperoxides and alkoxyl radicals
 DCBQ, 24
 ROOH, 24
 t-BuOOH and DCBQ interaction, 24–25, 25f, 26f
quinone ketoxy radical intermediate
 CBQ(OH)-O-*t*-Bu, 27
 DMPO, 27
 DMPO-157 adduct, 27–28, 29f
 H₂O₂, 31
 HPLC method, 26–27
 NMR and IR, 27
Pentachlorophenol (PCP)
 carcinogenic quinoid metabolites
 description, 6–7
 DNA, 9
 malignant lymphoma and leukemia, 7
 redox cycling, 8–9
 TCBQ, 8
 TCHQ, 7–8
 DNA damage, molecular mechanisms
 adducts and TCBQ, 10–11
 CT treatment, 10
 dG and duplex DNA (CT), 12
 leukemia, 11–12
 OH, 9
 8-OH-dG, 9
 TCHQ to H₂O₂ genotoxicity, 9–10
 pro-oxidant *vs.* antioxidant equilibrium, 12–13
 quinoid metabolite-induced genotoxicity
 ketoxy radical intermediate, 26–31
 OH and H₂O₂, 17–24
 organic hydroperoxides and alkoxyl radicals, 24–26
Phagocytosis, 157
Proteomics
 algal toxins action mechanism
 AZAs, 64–67

Proteomics (*cont.*)

- ciguatoxins, 69–70
- gambierol, 71
- marine microalgae, 51
- microcystins, 56–60
- mixtures, 73–75
- molecular processes, 52
- OA, 53
- okadaic acid, 60–64
- omics technology, 55
- palytoxin, 71–73
- potency and molecular targets, 51–52, 52*t*
- receptors/targets and action mechanism, 53–54
- toxicity and biomarkers, 54–55, 54*f*
- yessotoxins, 67–69
- biological element characterization, 47
- noxious agent, 46–47
- predictive toxicology and algal toxin contamination
 - AZAs, 80–81
 - MCs, 76–78
 - OA, 78–80
- toxicity pathways
 - artifacts and biomarkers, 91–94
 - bioinformatic tools and databases, 95–97
 - characterization, 84–91
 - expression, quantitative issues, 81–84
 - mechanistic interpretations, 94–95
 - model systems, 81
- toxins, biological systems
 - description, 48
 - experimental design, 48
 - generic experiment characterization, 49–50, 49*f*
 - human genome project, 47–48
 - “omics” approaches, 50
 - “proteomic pipeline”, 48–49
 - toxicsants, 50

Q

Quinone toxicity

- chlorinated. *See* Chlorinated phenol/quinone toxicity
- PCP's genotoxicity, 7
- protein adducts, 8

R

Reactive oxygen species (ROS), 147–148

Reductionistic studies

- microalgal toxins, 95
- toxicity pathways, 84

ROS. *See* Reactive oxygen species

S

Sarin

- BBB breakdown, 130
- detoxification, 36

exposure

- BBB breakdown, 131
- behavioral abnormalities, 116–117
- gene expression profiles, 129
- microarray analysis, 122
- multiple gene alteration, 133–134
- purinergic signaling, 126
- gene expression, 123–124
- induced seizure onset, 129
- interaction, acetylcholinesterase, 115*f*
- terrorist attack, 113–114, 132
- volatility, 114
- V-series agents, toxicity, 113
- SILAC procedure, 65–66, 81–84
- Silver nanoparticles (AgNPs)
 - antimicrobial effects, 180–181
 - cellular uptake
 - intracellular distribution, 182–183
 - kinetics, 181
 - mechanisms, 182
 - environment, release, 181
 - inflammatory response
 - anti-inflammatory effects, 206
 - in vivo* studies, 205
 - liver, 205
 - oxidative stress
 - GSH depletion, 207
 - induction, DNA damage, 208*t*
 - mitochondria, 207
 - reactive oxygen species (ROS), 206–207
 - toxicity
 - in vitro*, 184–191
 - in vivo*, 191–198
 - nonmammalian eukaryotes, 198–205
- Single cell gel electrophoresis assay. *See* Comet assay
- Solubility
 - CuO and NiO, 160
 - metal ion elution, 159
 - metal oxide
 - lung inflammation, 154
 - nanoparticles, 162
 - NiO nanoparticles, 159
- Soman
 - BBB, 130
 - brain ChE inhibition, 121–122
 - intoxication, 129–130
 - synthesise, 112
- Spin-trapping method, 18*f*, 20–21, 29
- System-level analysis
 - biological, proteomics, 47–50
 - molecular responses, toxin mixtures, 71, 91
 - PLTX, MCF-7 cell line, 72–73
 - proteins quantification, 97–98

T

Tabun. *See* German nerve agent

TCBQ. *See* Tetrachloro-1,4-benzoquinone

TCHQ-induced DNA damage, DFO

- cyto- and genotoxicity, human fibroblasts
 - MTT and “comet” assay, 16–17
 - TCSQ radical inhibition, 16*f*
 - iron-chelating property and TCSQ
 - DTPA chemical structure, 14*f*
 - and Fe(III) complex structure, 14*f*
 - Fenton reaction, 13–15
 - hydrolysis, chloranilic acid, 15
 - TCSQ. *See* Tetrachlorosemiquinone
 - Tetrachloro-1,4-benzoquinone (TCBQ)
 - vs.* DDBQ molecule, 15
 - deoxyguanosine (dG) and, 10–11
 - Tetrachlorosemiquinone (TCSQ)
 - decay, 15*f*
 - desferrioxamine protection, TCHQ-induced
 - DNA damage, 13–15
 - inhibition, 16*f*
 - OH production, 21*f*
 - Toxicity, AgNPs
 - humans, *in vivo*, 198, 198*f*
 - in vitro*
 - cell line-based models, 184
 - cellular uptake and biological response, 191
 - embryonic development, mouse blastocysts, 191
 - models, assessment, 185*t*
 - polyvinylacetate- and starch-coated AgNPs, 184–191
 - in vivo*, mammalian animal models
 - accumulation, organs, 196–198
 - assessment, 192*t*
 - blood-brain barrier, 198
 - dose and size, 196
 - dose-dependent liver lesions, 197
 - gastrointestinal tract, 197
 - genes expression, 196
 - routes, exposure, 191–196
 - nonmammalian eukaryotes
 - invertebrates, 204–205
 - models, assessment, 199*t*
 - vertebrates, 204
 - Toxicity networks, 94–95, 97–98
 - Toxicity pathways, proteomics
 - bioinformatic tools and database
 - computational, 95–96
 - GO, 96–97
 - MS techniques, 96
 - biomarkers, artifacts
 - cellular protein, 91–92
 - characterization, 91
 - DJ-1 protein, 93–94
 - hsp 27, 92, 93*f*
 - proteins, 91
 - characterization
 - Bcl-2 family and DJ-1, 86
 - GB, 87–88
 - MCs, 84
 - MCs, OA and palytoxin, 89–90, 89*f*
 - OA and PITX, 86–87
 - PITX, 87
 - proteins, affected, 85*t*
 - SOD, MC-LR and OA, 90–91
 - toxic responses, 91
 - expression, quantitative issues
 - MCF-7 and SH-SY5Y cell hsp 27, 83*f*
 - microalgal toxins action, 81, 82*t*
 - protein staining and image analysis, 81–84
 - mechanistic interpretations
 - characterization, 95
 - complexity, 94–95
 - ecotoxicological issues, 95
 - proteomes description, 94
 - model system, 81
 - Toxicoproteomics, 84
 - Toxin mixtures, 73–75
 - Transcriptomics
 - BAX, BID, and Bcl-2, 56–57
 - molecular domains, living organisms, 47–48
- V**
- VX poisoning, 123
- Y**
- Yessotoxins (YTX)
 - effects, cellular systems, 67
 - health risk, 67
 - hnRNPs, 68
 - and molecular responses, 67
 - pathway analysis, 68–69
 - Ras superfamily proteins, 69